State of Oregon
Oregon Department of Geology and Mineral Industries
Brad Avy, State Geologist

GEOLOGICAL MAP 126

GEOLOGIC MAP OF THE DOG RIVER AND NORTHERN PART OF THE BADGER LAKE 7.5' QUADRANGLES, HOOD RIVER COUNTY, OREGON

by Jason D. McClaughry[1], William E. Scott[2], Carlie J.M. Duda[3], and Richard M. Conrey[4]

2020

[1] Oregon Department of Geology and Mineral Industries, Baker City Field Office, Baker County Courthouse, 1995 3rd Street, Suite 130, Baker City, Oregon 97814
[2] U.S. Geological Survey, Cascades Volcano Observatory, 1300 SE Cardinal Court, Vancouver, Washington 98683
[3] Oregon Department of Geology and Mineral Industries, 800 NE Oregon Street, Suite 965, Portland, Oregon 97232
[4] Hamilton Analytical Laboratory, Taylor Science Center, Hamilton College, 198 College Hill Road, Clinton, New York 13323

NOTICE

Cover photograph: View west towards Mount Hood volcano and the north-flowing East Fork Hood River, which bisects the Dog River–Badger Lake area (45.35401, -121.53569 WGS84 geographic coordinates; 614697mE, 5023320mN WGS84 UTM Zone 10 coordinates). Photo credit: Jason McClaughry, 2019.

Expires: 12/1/2021

Oregon Department of Geology and Mineral Industries Geologic Map 126
Published in conformance with ORS 516.030.

For additional information:
Administrative Offices
800 NE Oregon Street, Suite 965
Portland, OR 97232
Telephone (971) 673-1555
Fax (971) 673-1562
https://www.oregongeology.org
https://www.oregon.gov/dogami

TABLE OF CONTENTS

LIST OF FIGURES

LIST OF TABLES

GEODATABASE

DRBL2020_GeMS_v10.7.gdb

See the Appendix for geodatabase description. See the digital publication folder for files. Geodatabase is Esri® version 10.7 format. Metadata is embedded in the geodatabase and shapefiles and is also provided as separate .xml format files.

SHAPEFILES AND SPREADSHEETS

Shapefiles
Orientation Points: DRBL2020_OrientationPoints.shp
Geochemistry: DRBL2020_GeochemPoints.shp
Geochronology: DRBL2020_GeochronPoints.shp
Magnetics: DRBL2020_MagneticPoints.shp
Stations: DRBL2020_StationsPoints.shp
Wells: DRBL2020_WellPoints.shp
Reference map: DRBL2020_RefMap.shp
Cross Section Lines: DRBL2020_XSectionLines.shp

Spreadsheets (Microsoft® Excel®)

DRBL2020_DATA.xlsx master file contains sheets:
Orientation Points: DRBL2020_OrientationPoints
Geochemistry: DRBL2020_GeochemPoints
Geochronology: DRBL2020_GeochronPoints
Magnetics: DRBL2020_MagneticPoints
Wells: DRBL2020_WellPoints

MAP PLATE

Plate 1. Geologic map of the Dog River and northern part of the Badger Lake 7.5' quadrangles, Hood River County, Oregon, scale 1:24,000.

1.0 INTRODUCTION

The Dog River and northern part of the Badger Lake 7.5′ quadrangles encompasses an area of ~201 km^2 (77.6 mi^2) of the High Cascades of north-central Oregon, lying across the eastern slopes of Mount Hood volcano (**Figure 1-1**; Plate 1; referred to herein as Dog River–Badger Lake area). Mount Hood, known as Wy'east to Native Americans, is Oregon's tallest peak (3,427 m [11,241 ft]). The volcano has erupted episodically for the past 500,000 years, experiencing two major eruptive periods during the last 1,500 years (Scott and others, 1997a; Scott and others, 2003; Scott and Gardner, 2017). Cascade Range volcanism and structural development in the area dates back longer, with eruptive activity dating from latest Miocene to recent time; part of that volcano-tectonic record is detailed by new high-resolution geologic mapping presented here.

The geology of the Dog River–Badger Lake area was mapped by the Oregon Department of Geology and Mineral Industries (DOGAMI) between 2017 and 2020, in collaboration with geoscientists from the U. S. Geological Survey Cascade Volcano Observatory (USGS CVO) and Hamilton College, New York. The primary objective of this investigation is to provide an updated and spatially accurate geologic framework for the Dog River–Badger Lake area as part of a multi-year study of the geology of the larger Middle Columbia Basin (**Figure 1-1**, **Figure 1-2**). Additional key objectives of this project are to: 1) determine the geologic history of volcanic rocks in this part of the northern Oregon Cascade Range, including lava flows and volcaniclastic deposits erupted from Middle Pleistocene to Holocene Mount Hood volcano; 2) provide significant new details about the structure and fault history along the northern segment of the High Cascades intra-arc graben (Hood River graben); and 3) better understand geologic hazards in the region, related to earthquakes, volcanoes, and landslides. New detailed geologic data presented here also provides a basis for future geologic, geohydrologic, and geohazard studies in the greater Middle Columbia Basin. Detailed geologic mapping in this part of the Middle Columbia Basin is a high priority of the Oregon Geologic Map Advisory Committee (OGMAC), supported in part by grants from the STATEMAP component of the USGS National Cooperative Geologic Mapping Program (G17AC00210, G19AC00160). Additional funds were provided by the State of Oregon.

The core products of this study are this report, an accompanying geologic map and cross sections (Plate 1), an Esri ArcGIS™ geodatabase, and Microsoft Excel® spreadsheets tabulating point data for geochemistry, geochronology, magnetic polarity, orientation points, and well data. The geodatabase presents the new geologic mapping in a digital format consistent with the USGS National Cooperative Geologic Mapping Program Geologic Map Schema (GeMS) (U.S. Geological Survey National Cooperative Geologic Mapping Program, 2020). This geodatabase contains spatial information, including geologic polygons, contacts, structures, geochemistry, geochronology, magnetic observation, orientation points, and well data, as well as data about each geologic unit such as age, lithology, mineralogy, and structure. Digitization at scales of 1:8,000 or better was accomplished using a combination of high-resolution lidar topography and imagery. Surficial and bedrock geologic units contained in the geodatabase are depicted on the Plate 1 at a scale of 1:24,000. Both the geodatabase and geologic map are supported by this report describing the geology in detail.

Figure 1-1. Location of the Dog River-Badger Lake study area in the Middle Columbia Basin of north-central Oregon. The study area is shown by a black outline. The solid orange line corresponds to the watershed boundary of the Middle Columbia Basin. The Columbia River, flowing from east to west, in the upper part of the figure, separates Oregon on the south from Washington State on the north. The Deschutes River marks the boundary between Wasco County on the west and Sherman County on the east.

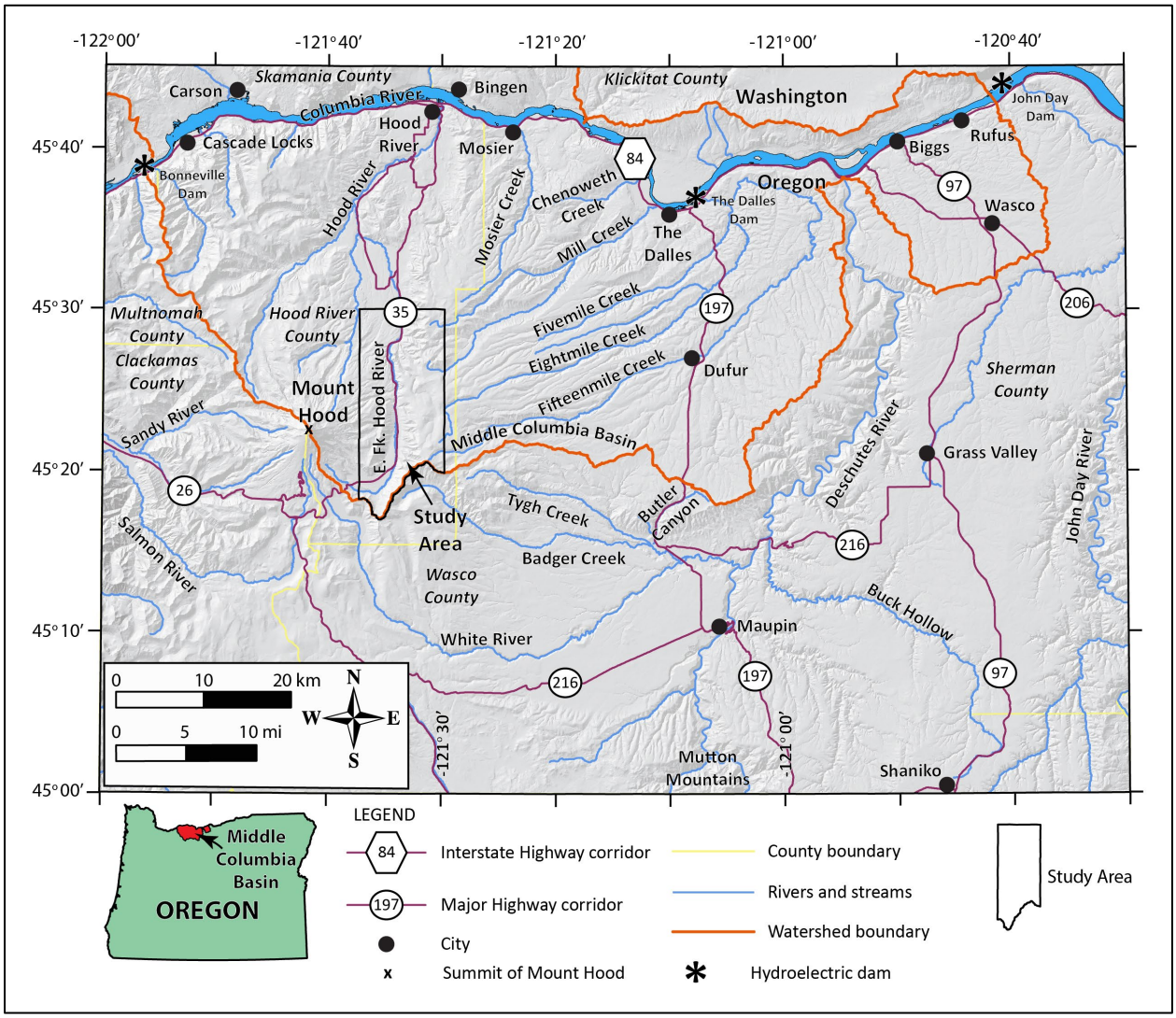

Figure 1-2. Status map of geologic mapping completed, in progress, and planned in the Middle Columbia Basin. The yellow-shaded area encompasses geologic mapping in the Dog River–Badger Lake area completed for this report. Blue-shaded quadrangles include areas where geologic mapping is currently being conducted by the USGS (FEDMAP). Orange-shaded quadrangles include areas that have been mapped by DOGAMI with funding from OWRD and STATEMAP between 2011 and 2020. Purple-shaded quadrangles include targets of future geologic mapping by DOGAMI. Label abbreviations are as follows: B—Bingen; BD—Bonneville Dam; C—Carson; CL—Cascade Locks; D—Dufur; GV—Grass Valley; HR—Hood River; JDD—John Day Dam; R—Rufus; TD—The Dalles; TDD—The Dalles Dam; W—Wasco.

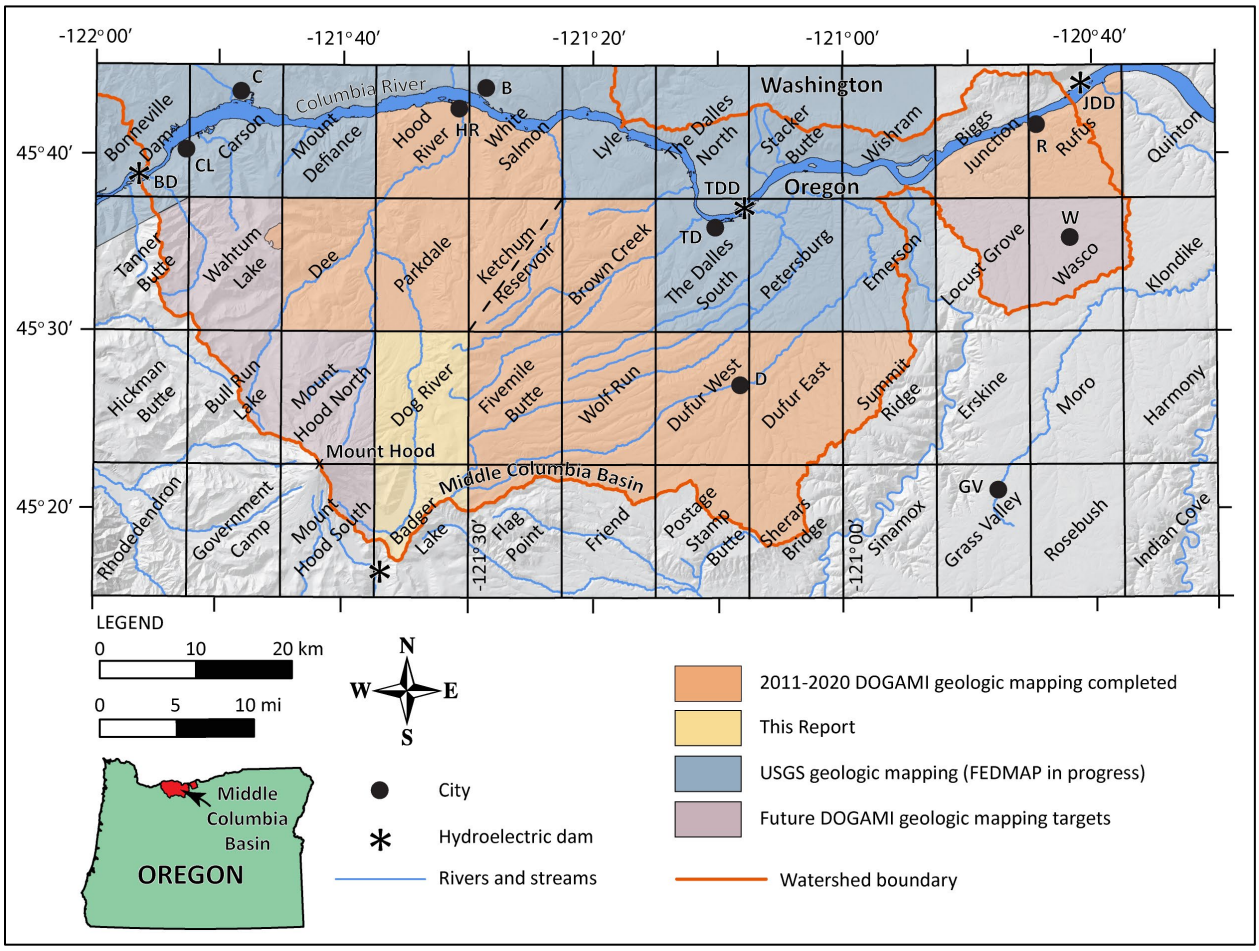

2.0 GEOGRAPHY

The Dog River–Badger Lake area of the north-central Oregon Cascades is rugged, mountainous terrain characterized by densely forested, sharp ridges and steep canyons (**Figure 2-1, Figure 2-2**). The north-flowing East Fork Hood River and its tributaries drain the area (**Figure 1-1**, **Figure 2-1**, **Figure 2-2**; Plate 1). Topographic relief in the area is substantial ranging from a high of 1,990 m (6,525 ft) at the summit of Lookout Mountain to a low of 552 m (1,812 ft) where the East Fork Hood River exits the northern part of the map area (**Figure 2-1**; Plate 1). Bluegrass Ridge forms a prominent, north-trending narrow topographic spine along the southwestern edge of the map area, extending from Elk Mountain north to Tamanawas Falls (**Figure 2-1**, **Figure 2-2**; Plate 1). Climate in the Dog River–Badger Lake area is heavily influenced by the wet marine airflow of western Oregon, averaging ~85 cm (34 in) of precipitation annually (NOAA, 2020). The rain shadow of the Cascade Range reduces annual precipitation eastward sharply to <40 cm (15.8 in) across the semi-arid eastern part of the Middle Columbia Basin (**Figure 1-1**). Heavy winter snowfall in this part of the Cascade Range seasonally blocks access to most parts of the area, exclusive of OR Highway 35, which remains open year-round (**Figure 2-1**; Plate 1).

Much of the map area is public national forest (NF) land managed by the US Forest Service (USFS); private parcels are scattered across the northern part of the map area in the Upper Hood River Valley (**Figure 2-1**; Plate 1). The western edge of the area includes part of the Mount Hood Wilderness, while the Badger Lake Wilderness bounds the southeastern edge of the map area (**Figure 2-1**; Plate 1). Roads in the Dog River–Badger Lake area are few. OR Highway 35, a major transportation corridor in this part of Oregon, bisects the project area from south to north, paralleling East Fork Hood River (**Figure 1-1**, **Figure 2-1**; Plate 1). The east side of the map area can be accessed by Brooks Meadow-Dufur Valley Road (NF Road 44), connecting OR Highway 35 to Dufur in the eastern part of the Middle Columbia Basin (**Figure 2-1**; Plate 1). Two main graveled NF roads connect from NF Road 44, providing north-south access to the high ridgeline of the eastern part of the map area. Lookout Mountain Road (NF Road 4410) and Hood River-Barlow Road (NF Road 3550) extend south to Bennett Pass; Long Prairie Road (NF Road 17) extends north through the Dog River 7.5′ quadrangle (**Figure 2-1**; Plate 1). A number of short seasonal access roads, originally built for logging operations, branch off main traffic corridors. Many of these roads have been subsequently closed by the USFS. Roadless parts of the map area can be accessed by a network of designated NF trails.

Figure 2-1. Geographic overview of the study area showing key locations referenced in the text. The base image is an oblique landscape view from Google Earth Pro™ looking north. The white outline is the Dog River-Badger Lake study area. Abbreviated labels CSC – Crystal Springs Creek; CSR – Cooper Spur Road; DC – Doe Creek; LJ – Little John Sno-Park; LGT – Lookout-Gumjuwac Saddle Trail; PC – Polallie Campground; TJC – Tilly Jane Creek; WC – Weygant Canyon.

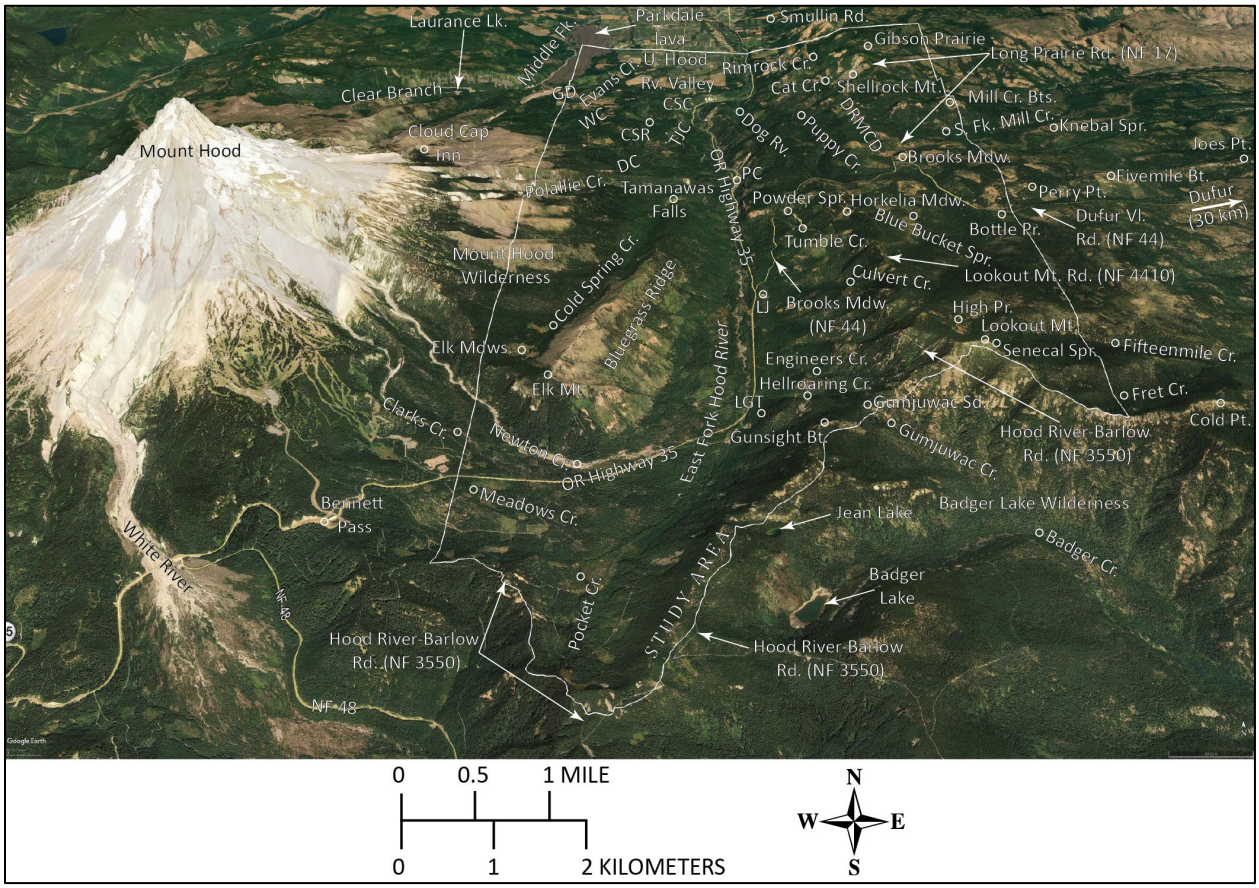

Figure 2-2. Photographs showing the typical landscape of the Dog River–Badger Lake area. (a) View west across the East Fork Hood River Valley (45.35401, -121.53569 WGS84 geographic coordinates; 614697mE, 5023320mN WGS84 UTM Zone 10 coordinates). The East Fork Hood River runs from south to north (left to right) through the valley. A white arrow shows the approximate location of the river and the direction of flow. The north-south ridge holding the west side of East Fork Hood River Valley is Bluegrass Ridge. Elk Mountain forms the high southern end of Bluegrass Ridge. Farther west, the skyline is dominated by glacier-clad Mount Hood volcano. Photo credit: Jason McClaughry, 2019. (b) View southwest towards Mount Hood and the northern part of Bluegrass Ridge (45.42444, -121.56529 WGS84 geographic coordinates; 612238mE, 5031102mN WGS84 UTM Zone 10 coordinates). The East Fork Hood River and Oregon Highway 35 are visible downslope from the observer in the middle part of the photograph. The white arrow indicates the north-flowing direction of East Fork Hood River. Photo credit: Jason McClaughry, 2017.

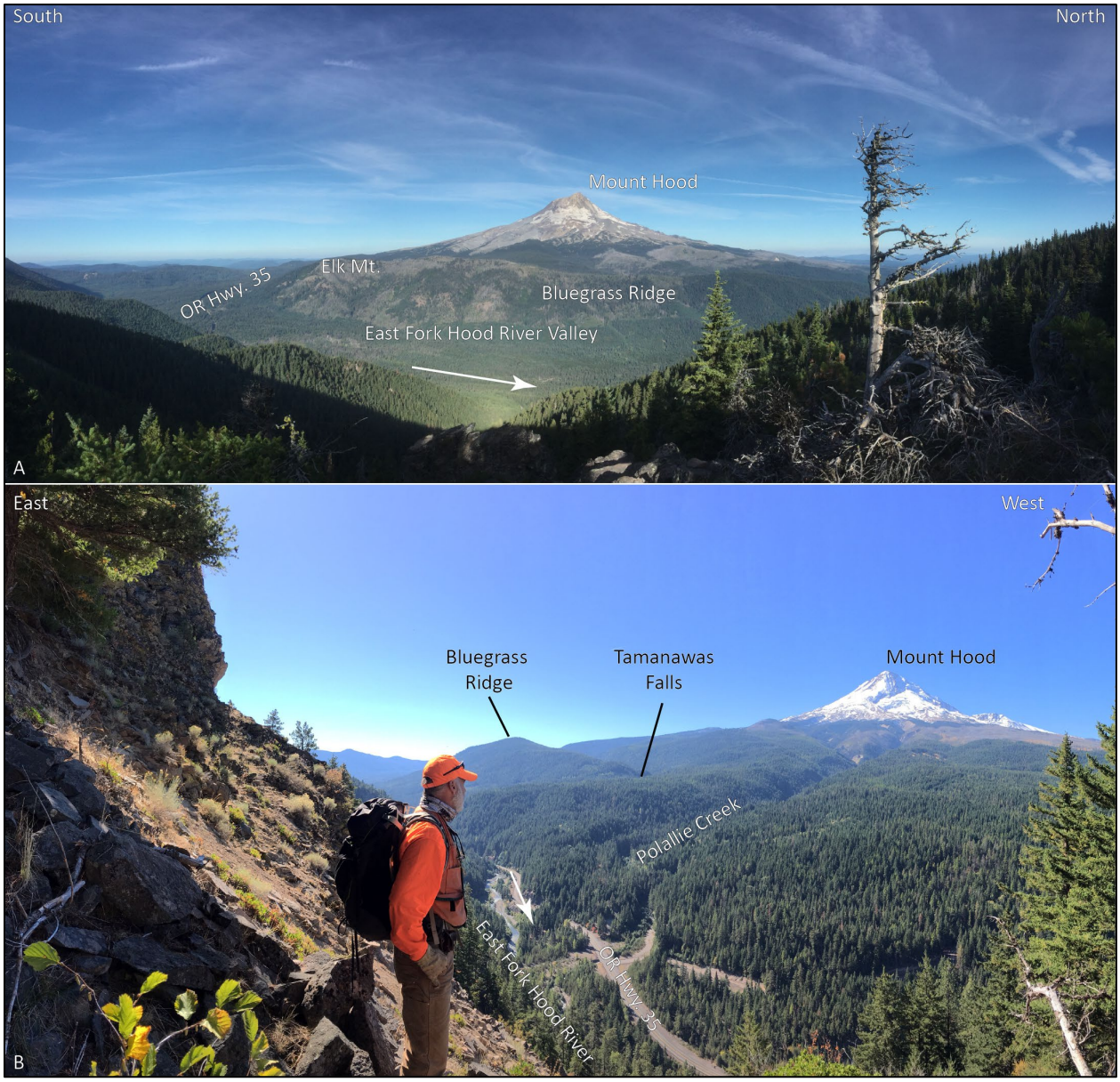

3.0 METHODOLOGY

The suite of Columbia River Basalt Group (CRBG) and Cascade Range volcanic rocks exposed in the Dog River–Badger Lake area is stratigraphically complex, reflecting the variable processes of deposition and reworking of volcanic and volcaniclastic units in a structurally active subaerial volcanic arc environment. The area is characterized by dozens of small overlapping and intricately interbedded volcanic flows, which are often difficult to trace over significant distance. Additional complications in mapping in this volcanic terrain arise from a lack of sufficient outcrop, paucity of distinctive or widespread marker units, burial by glacial till, colluvium, or alluvial deposits, and characteristic steep and densely forested terrain. Thus, reliable map correlations, even of similar appearing stratigraphic sequences, benefits greatly from the use of detailed digital lidar-based geologic mapping combined with numerous direct field observations. Conventional lithologic criteria, in combination with geochemical analyses, corroborating isotopic ages, and measurements of natural remanent magnetization were used to assign rocks and deposits to geologic map units. Comparative visual analysis of unanalyzed rocks with analyzed rocks, in the context of stratigraphic position, allowed for wider correlation of map units.

Mapping presented in this report was collected digitally using a GPS-enabled Apple® iPad® 4, loaded with Esri™ Collector, following standard DOGAMI procedures outlined in Duda and others (2018, 2019). Field mapping used 1-m lidar DEMs (8 pts/m^2), USGS digital raster graphics (DRGs) of traditional topographic maps, and digital Esri™ imagery as basemaps. Fieldwork conducted during this study consisted of data collection along OR Highway 35, forest roads, and the NF trail network, combined with numerous down-ridge traverses mapping lithologic contacts and faults across lands managed by the USFS and the City of The Dalles Municipal Watershed.

Geologic linework portrayed on the geologic map is based upon detailed observations at more than 2200 field stations visited by the authors between 1991 and 2019, and observations at additional sites by D.R. Sherrod (unpublished field notes; Sherrod and Scott, 1995), Wise (1969), Shearer (2002), Darr (2006), and Westby (2014) (see Stations Map inset on Plate 1). Supplementary lithologic information was obtained from comparison of more than 1000 rock samples collected from field sites visited by J.D. McClaughry and C.J.M. Duda between 2017 and 2019. Lithologic map correlations also rely on 496 new and 209 compiled X-ray fluorescence (XRF) whole-rock geochemical analyses, 39 new and compiled $^{40}Ar/^{39}Ar$ and K-Ar isotopic ages, petrographic analysis of 102 thin-sections, 445 field measurements of natural remanent magnetization, and 149 field and remotely collected orientation measurements (Plate 1; Appendix). Surficial units within the project area were delineated on the basis of geomorphology as interpreted from a combination of field observations, 1-m lidar DEMs, 2018 NAIP orthophotos, USGS 7.5′ topographic maps, and NRCS soils maps (Green, 1981).

In this report, volcanic rocks with fine-grained (<1 mm [0.04 in]; Mackenzie and others, 1997; Le Maitre and others, 2004), average crystal or particle size in the groundmass are characterized in the following manner:

- A “coarse groundmass” if the average crystal or particle size is <1 mm (0.04 in) and can be determined using the naked eye (>~0.5 mm [0.02 in]).
- A “medium groundmass” if crystals of average size cannot be determined by eye but can be distinguished by using a hand lens (>~0.05 mm [0.02 in]).
- A “fine groundmass” if crystals or grains of average size can be determined only by using a microscope (or by hand lens recognition of sparkle or sheen in reflected light, indicating the presence of crystalline groundmass).

- A "glassy groundmass" if the groundmass has (fresh), or originally had (altered), groundmass with the characteristics of glass (conchoidal fracture; sharp, transparent edges; vitreous luster; etc.).
- Mixtures of crystalline and glassy groundmass are described as intersertal; ratios of glass to crystalline materials may be indicated by textural terms including holocrystalline, hypocrystalline, hyalophitic, and hyalopilitic.
- Microphenocrysts are defined as crystals larger than the overall groundmass and <1 mm across (0.04 in).

Intrusive igneous rocks are described as being coarse-grained if crystal diameters are >5 mm (0.2 in); as being medium-grained if the range of crystal diameters is between 1 and 5 mm (0.04 in and 0.2 in); and fine-grained if the range of crystal diameters is <1 mm (0.04 in) (Mackenzie and others, 1997; Le Maitre and others, 2004).

Grain size of clastic sedimentary rocks is described following the Wentworth (1922) scale. Hand samples of unconsolidated sediments and clastic sedimentary rocks were compared in the field and or in the laboratory to graphical representations (comparator) of the Wentworth scale to determine average representative grain size in various parts of a respective sedimentary geologic unit. Colors given for hand-sample descriptions are from the Geological Society of America Rock-Color Chart Committee (1991).

Whole-rock XRF geochemical data are essential for separating difficult-to-distinguish lavas and pyroclastic rocks into eruptive units in the volcanic-dominated terrain of the Cascade Range. Many lavas are too fine grained and glassy to be adequately characterized by mineralogical criteria alone and lithologically and mineralogically similar appearing units can have meaningfully different chemical signatures. Descriptive rock unit names for volcanic rocks are based in part on the online British Geological Survey classification schemes (Gillespie and Styles, 1999; Robertson, 1999; Hallsworth and Knox, 1999), and normalized major element analyses plotted on the total alkali ($Na_2O + K_2O$) versus silica (SiO_2) diagram (TAS) of Le Bas and others (1986), Le Bas and Streckeisen (1991), and Le Maitre and others (1989, 2004). Whole-rock geochemical samples were prepared and analyzed by XRF at the Washington State University GeoAnalytical Lab, Pullman, Washington, and at the USGS Geology, Geophysics, and Geochemistry Science Center, Denver, Colorado and Menlo Park, California (Appendix). Analytical procedures for the Washington State University GeoAnalytical Lab are described by Johnson and others (1999) and are available online at https://environment.wsu.edu/facilities/geoanalytical-lab/technical-notes/; USGS analytical procedures are described by Taggart (2002) and are available online at https://www.usgs.gov/energy-and-minerals/mineral-resources-program/science/analytical-chemistry?qt-science_center_objects=0#qt-science_center_objects. Major element determinations are normalized to a 100-percent total on a volatile-free basis and recalculated with total iron expressed as FeO*. Further details of this process are described in the Appendix under the heading *Geochemistry*.

Our mapping presents 11 new $^{40}Ar/^{39}Ar$ ages (Plate 1; Appendix). Samples for age determinations were prepared and analyzed by Dr. Dan Miggins at the College of Oceanic and Atmospheric Sciences, Oregon State University, Corvallis (OSU). The methodology for $^{40}Ar/^{39}Ar$ geochronology at OSU is summarized in Duncan and Keller (2004) and the OSU laboratory website http://geochronology.coas.oregonstate.edu/. One $^{40}Ar/^{39}Ar$ age was determined by Dr. Matt Heizler at the New Mexico Geochronological Research Laboratory (NMGRL) administered by the New Mexico Bureau of Geology and Mineral Resources at the New Mexico Institute of Mining and Technology in Socorro, New Mexico. The general operational details for the NMGRL can be found at internet site https://geoinfo.nmt.edu/labs/argon/home.cfml. The map also includes 8 K-Ar and $^{40}Ar/^{39}Ar$ ages of Pliocene and younger lavas, originally published by Scott and others (1997a, 2003) and Scott and Gardner

(2017) (Plate 1; Appendix). Rock samples for age determinations reported by Scott and Gardner (2017) were prepared and analyzed at the U.S. Geological Survey (USGS) laboratory in Menlo Park, California, under the direction of Marvin Lanphere; many of the previously determined K-Ar ages have been redated by higher precision $^{40}Ar/^{39}Ar$ methods at the USGS laboratory in Menlo Park under the direction of Andrew Calvert (Scott and Gardner, 2017). Twenty-two additional K-Ar ages in the area come from studies by Wise (1969), Hull and Riccio (1979), Bela (1982), P.E. Hammond in Fiebelkorn and others (1983), Keith and others (1985), Sherrod and Scott (1995), and Conrey and others (1996) (Plate 1; Appendix). Numerical ages assigned to dated units are described using standard conventions in reporting age in millions of years ago (mega-annum, abbreviated Ma) for units >1 m.y. old; for units <1 m.y. old, ages are reported in thousands of years ago (kilo-annum, abbreviated ka). Further details of this process are described in the Appendix under the heading *Geochronology*.

The magnetic polarity of strongly magnetized lavas was determined at numerous outcrops in the Dog River–Badger Lake area using a handheld digital fluxgate magnetometer (Appendix). Magnetic polarity reversals, commonly preserved by volcanic rocks and readily measured in the field, provide for 1) distinguishing between flow units with normal and reversed magnetic polarity, 2) a check on the permissible age of isotopically-dated samples, when compared to the paleomagnetic time scale (Cande and Kent, 1992), and 3) another way to constrain possible depositional ages for some undated strata. Further details of this process are described in the Appendix under the heading *Natural Remanent Magnetization*.

Orientation measurements of geological planes (e.g., inclined bedding) were obtained in the field area by traditional compass and clinometer methods and compiled from data published by previous workers. Additional bedding measurements were generated using a routine and model developed by DOGAMI in Esri ArcGIS™ Model Builder to calculate three-point solutions from lidar bare-earth DEMs. Further details of this process are described in the Appendix under the heading *Orientation Points*.

Subsurface geology shown in the geologic cross sections incorporates lithologic interpretations from water-well drill records available through the Oregon Water Resources Department (OWRD) GRID system (Plate 1; Appendix). An attempt was made to locate water wells and other drill holes that have well logs archived by OWRD. Approximate locations were estimated using a combination of sources, including internal OWRD databases of located wells, Google Earth™, tax lot maps, street addresses, and aerial photographs. The accuracy of the locations ranges widely, from errors up to 0.8 km (0.5 mi) for wells located only by Township/Range/Section (2.6 km^2 [1 mi^2]) and plotted at the section centroid to a few tens of meters for wells located by address or tax lot number on a city lot with bearing and distance from a corner. For each well, the number of the well log is indicated in the database. This number can be combined with the first four letters of the county name (e.g., HOOD 5473), to retrieve an image of the well log from the OWRD web site (https://apps.wrd.state.or.us/apps/gw/well_log/). Water wells in the map area are sparse; a database of 60 located water-well logs with interpreted subsurface geologic units is provided in the Appendix. Further details of this process are described in the Appendix under the heading *Water Wells*.

Microsoft Excel® spreadsheets tabulating geochemical and geochronological analyses, magnetic polarity, orientation measurements, and well points are provided as part of this publication. The Appendix contains a more detailed summary of data collection methods and a list of the data fields for the spreadsheets mentioned above.

New mapping was compiled with published and unpublished data and converted into digital format using Esri ArcGIS™ ArcMAP™ GIS software. On-screen digitizing was performed through heads-up digitizing using georeferenced 1-m lidar DEMs, 1:24,000-scale USGS digital raster images (DRGs) of

traditional topographic maps, hillshade derivative of USGS 10-m DEMs, and 2018 National Agriculture Imagery Program (NAIP) digital orthophotos. Remote sensing of the locations of both contacts and faults is improved through the use of enhanced 1-m lidar DEMs, processed using the Sky-View Factor computation tool (Zakšek and others, 2011). The Sky-View Factor computation tool is part of the Relief Visualization Toolbox (RVT), open-source processing software produced by the Institute of Anthropological and Spatial Studies at the Research Centre of the Slovenian Academy of Sciences and Arts (ZRCSAZU), to help visualize raster elevation model datasets (https://iaps.zrc-sazu.si/en/rvt#v). Sky-View visualizes hillshade models using diffuse illumination, overcoming the common problem of direct illumination, which can obscure linear objects that lie parallel to the direction of the light source and saturation of shadow areas. Digitization and the final digital Esri ArcGIS™ format geodatabase was completed at a minimum scale of 1:8,000, supported by 3D visualization of lidar topographic data in Quick Terrain Modeler™ (Duda and others, 2018, 2019). The geologic time scale used is the 2020 (v2020/01), version of the International Stratigraphic Commission on chronostratigraphic chart (https://stratigraphy.org/chart) revised from Gradstein and others (2004), Ogg and others (2008), and Cohen and others (2013).

4.0 PREVIOUS WORK

The Dog River–Badger Lake area was mapped in this study as part of a larger effort to construct an updated geologic framework for the Middle Columbia Basin (**Figure 1-2**). Several sources of previously published mapping (**Figure 4-1**) were consulted during the preparation of our geologic map and this report. Earlier maps depicting the geology in the map area are few; the most detailed geologic map covering the area is a 100,000-scale map by Sherrod and Scott (1995). Other geologic maps and research studies covering the area, include works by Wise (1969), Swanson and others (1981), Williams and others (1982), Bela (1982), Beeson and others, 1982, Sherrod and Smith (2000), and Shearer (2002). McClaughry and others (2012) produced a detailed geologic map of the Hood River Valley, directly to the north of the Dog River–Badger Lake area (**Figure 4-1**).

Figure 4-1. Sources of regional geologic mapping reviewed and consulted during the preparation of the Dog River-Badger Lake geologic map (Plate 1) and this report. See DataSourcePolys feature class in the geodatabase. Dog River–Badger Lake area shown by black outline.

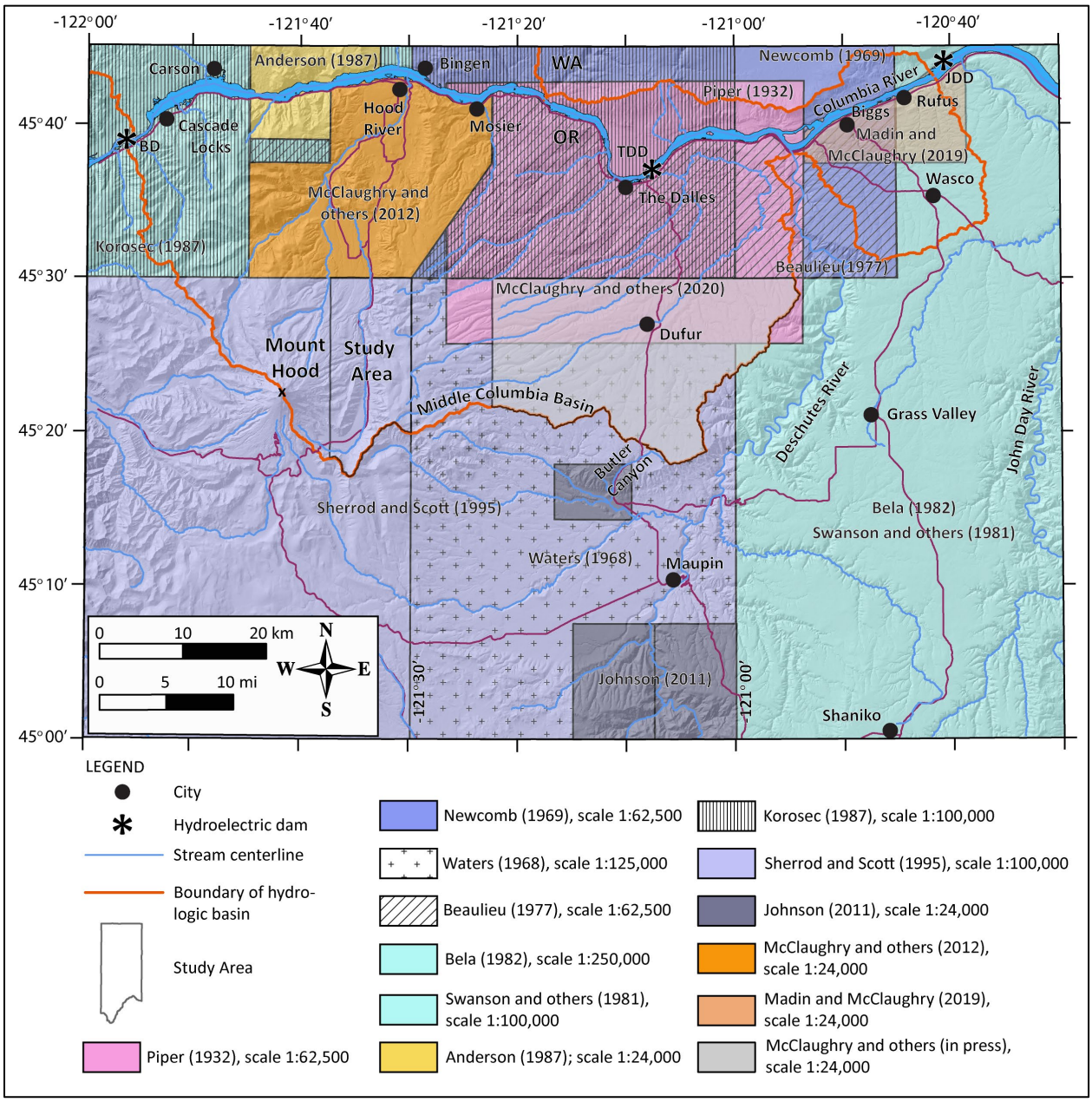

5.0 GEOLOGIC AND TECTONIC SETTING

The Dog River–Badger Lake area lies across the lower eastern slopes of Mount Hood, along the eastern side the Cascade Range in northern Oregon (**Figure 5-1**, **Figure 5-2**). The Cascade Range is a north-south-trending volcanic arc stretching for ~1,300 km (800 mi) between northern California and southern British Columbia. Volcanoes making up the range and their eroded remnants are the observable magmatic expression of oblique convergence since ~40 Ma along the Cascadia subduction zone, where the offshore Juan de Fuca tectonic plate is subducted beneath North America (**Figure 5-1**; Lux, 1982; Phillips and others, 1986; Verplanck and Duncan, 1987; Conrey and others, 2002; Sherrod, 2019). The Cascade Range in Oregon is traditionally separated into two subprovinces on the basis of this ~40 m.y. geologic history: the Western Cascades and High Cascades (**Figure 5-2**; Dicken, 1965). The Western Cascades subprovince is a deeply eroded area of Pliocene to Eocene volcanic and sedimentary rocks, while the High Cascades encompasses the Pliocene to Holocene active volcanic arc. The High Cascades subprovince contains the major Pleistocene to Holocene volcanoes, including Mount Hood.

Figure 5-1. Tectonic setting of the northwest United States and southwest Canada showing regional plate boundaries, the Cascadia subduction zone, and volcanoes of the Cascade Range. The surface projection of the Cascadia megathrust (red line) is defined by bathymetry where the abyssal plain meets the continental slope. The study area is shown by a red polygon in north-central Oregon. Modified from Nelson and others (2006).

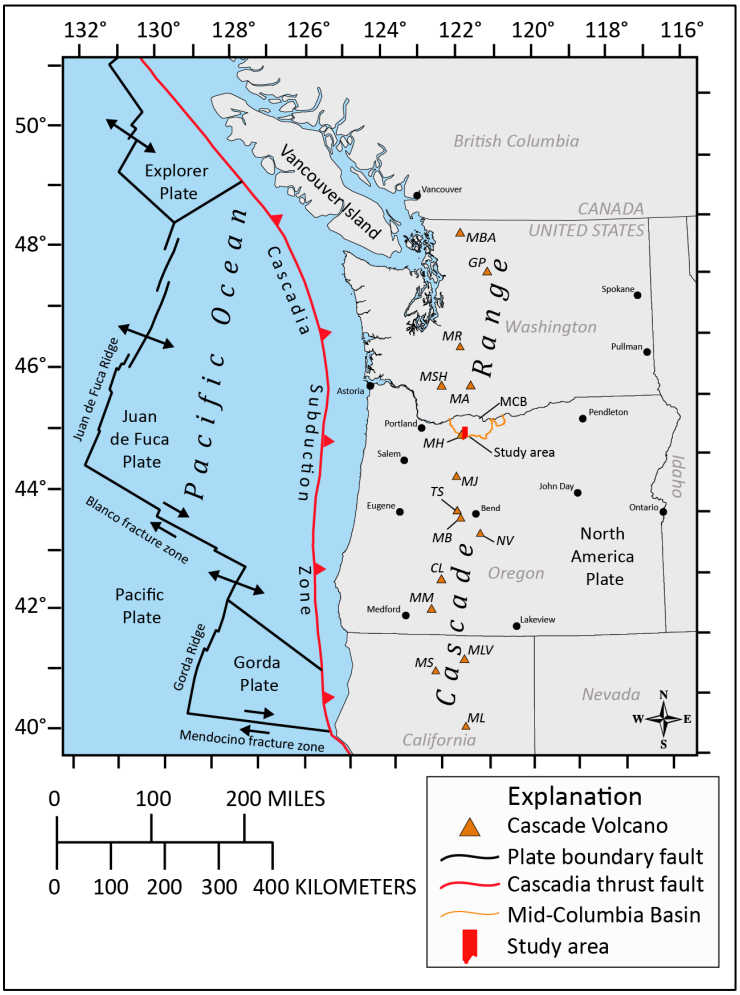

Figure 5-2. Map of the Cascade Range in the Pacific Northwest showing geographic locations, approximate extent of Western (tan) and High Cascades (purple), and the spatial relationships of some major structural features in Oregon. Note that the names Western Cascades and High Cascades are not used in Washington or south of Mount Shasta in California. The study area is shown by a red polygon in north-central Oregon. The numerals 1, 2, and 3 refer to the three segments of the High Cascades graben from south to north: 1) southern segment, 2) central segment, and 3) Hood River graben segment. Labels: BFZ – Brothers fault zone; BV – Boring Volcanic Field; EDFZ – Eugene-Denio fault zone; HRF – Hood River fault zone; HCF – Horse Creek fault zone; GCF – Gales Creek fault; GRF – Green Ridge fault zone; PB – Portland Basin; PHF – Portland Hills fault; MCB – Middle Columbia Basin (orange outline); MHFZ – Mount Hood fault zone; MFZ – Mount McLoughlin fault zone; OWL – Olympic-Wallowa Lineament; SFZ – Sisters fault zone; SV – Simcoe Mountains; TB – Tualatin Basin; VFZ – Vale fault zone. Oregon physiographic provinces after Dicken (1965). Geologic provinces of Washington from the Washington Geological Survey (https://www.dnr.wa.gov/programs-and-services/geology/explore-popular-geology/geologic-provinces-washington).

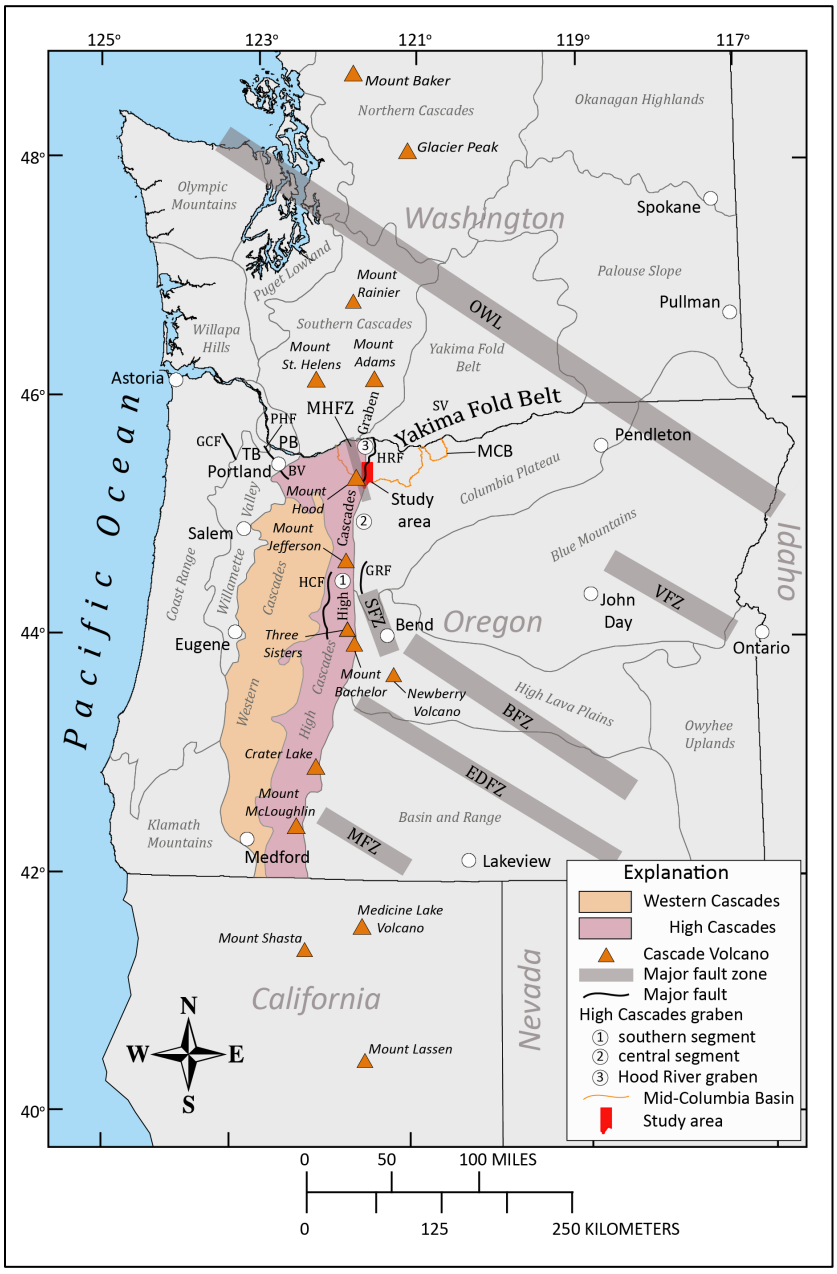

5.1 Yakima Fold Belt

The axis of the High Cascades in north-central Oregon is superimposed across the Yakima Fold Belt, a series of northeast-southwest-trending, asymmetric, locally overturned and faulted anticlinal ridges separated by broad synclinal valleys (**Figure 5-2**; Swanson and others, 1979, 1981; Anderson, 1987; Watters, 1989; Reidel and Campbell, 1989; Tolan and Reidel, 1989; Anderson and others, 2013). The Yakima Fold Belt occurs over much of the western and west-central Columbia Plateau (OR) and Yakima Fold Belt (WA) physiographic provinces (Tolan and others, 2009a) and continues westward through the Cascade Range (**Figure 5-2**). Structural deformation associated with the Yakima Fold Belt may occur as far west as the Oregon Coast Range, where Siletz River and younger rocks are broadly folded along north-east-trending fold axes (McClaughry and others, 2010; **Figure 5-2**). Folds in the Yakima Fold Belt are generally east-west-striking across eastern Oregon and Washington, while across the Cascade Range, fold axes strike more consistently to the southwest-northeast (Swanson and others, 1981; Bela, 1982; Reidel and others, 1989; Tolan and others, 2009a). East-west-striking Yakima folds east of the Cascades are inferred to have formed in response to a general north-south compressional regime (Reidel and others, 1989; Beeson and Tolan, 1990), while northeast-striking folds in the northern Oregon Cascade Range indicate a stress regime with the major compressive stress oriented northwest-southeast (Venkatakrishnan and others, 1980; Williams and others, 1982).

Northeast-striking folds in the Hood River and Dog River–Badger Lake areas of the Cascade Range are locally segmented by northwest-striking cross faults (N. 20°W. to N. 30°W.; **Figure 5-3**). Previous workers in the Columbia River Gorge and on the Columbia Plateau have referred to these faults as wrench faults (Anderson, 1987). Spatial and crosscutting relationships between folds, thrust faults, and strike-slip faults indicate a mutual development of all three components during progressive deformation occurring in the Yakima Fold Belt from the middle Miocene to late Pliocene (Anderson, 1987).

Deformation in the Yakima Fold Belt has persisted since at least the middle Miocene, with a majority of the present structural relief developing since ~10.5 Ma (Reidel and others, 1989; Tolan and others, 2009a). Structural warping in the western part of the Yakima Fold Belt during the middle Miocene is inferred to have increasingly restricted the distribution of the younger parts of the Grande Ronde, Wanapum, and Saddle Mountains Basalts to structural lows in the Columbia River Gorge and Willamette Valley (Vogt, 1981; Beeson and others, 1985; Anderson and Tolan, 1986). Successively younger lavas, most notably flows in the Priest Rapids and Pomona Members, were partially or wholly confined to paleocanyons, possibly structurally controlled by the Yakima Fold Belt. The thickness and distribution of these CRBG units through the Columbia River Gorge locally show evidence of restricted distribution and thinning across anticlines, although these ancient channel remnants do not precisely correspond to present-day structural highs and lows (Anderson, 1987; Anderson and Vogt, 1987; Beeson and Tolan, 1990). Folds continued to develop in post-CRBG time, as large accumulations of volcaniclastic and sedimentary detritus shed from the late Miocene Cascades (e.g., Dalles Formation) preferentially accumulated in basins along synclinal troughs. Thrust faults associated with the growth of anticlinal ridges in the Yakima Fold Belt regionally remained active following deposition of the 9 to 5 Ma Dalles Formation. Along East Fork Hood River, the Hellroaring Creek thrust fault was active in Pliocene or later time as it juxtaposes late Miocene Dalles Formation intrusions against rocks of early to late Pliocene age (**Figure 2-1**; Plate 1). Compressional deformation in the Hood River area continued into the Pliocene and Pleistocene. Lavas as young as 3.05 Ma, are broadly folded and are structurally dismembered by fold-associated, north-northwest-striking strike-slip or oblique-slip faults in the Hood River Valley (**Figure 5-3**; McClaughry and others, 2012). Similarly oriented normal or oblique-slip faults in the Dog River–

Badger Lake area show significant lateral and vertical offset of geologic units as young as 1.87 Ma (Plate 1). Other evidence for recent activity on north-northwest-striking faults in the wider Middle Columbia Basin is found where these structures are redirecting modern drainages (McClaughry and others, 2012).

Figure 5-3. Map of the Dog River–Badger Lake area and greater Mount Hood region, highlighting structural features. Red outline is the study area. Mapped faults are shown as black lines. Fold axes are shown as magenta lines. Label abbreviations are as follows: BB – Badger Butte; BH – Booth Hill; BR – Bluegrass Ridge; BRFZ – Blue Ridge Fault Zone; CCT – Cat Creek thrust fault; CF – Chenoweth reverse fault; CL – Clear Lake; DRMF – Dog River-Mill Creek divide; EF – East Fork Hood River; FM – Fifteenmile Creek; GCWF – Gate Creek-Wyeth fault; GP – Grasshopper Point; GPF – Gibson Prairie fault; HCT – Hellroaring Creek thrust fault; HRF – Hood River fault zone; HRV – Hood River Valley; MM – Middle Mountain; MMF – Multorpor Mountain fault; NFMT – North Fork Mill Creek thrust fault; PL – Parkdale lava flow; PCFZ – Pocket Creek fault zone; RPF – Rocky Prairie thrust fault; TLF – Twin Lakes fault; UHRV – Upper Hood River Valley; WCF – Whiskey Creek thrust fault. Question mark over dashed line identifies the location of an inferred concealed thrust fault underlying the Upper Hood River Valley.

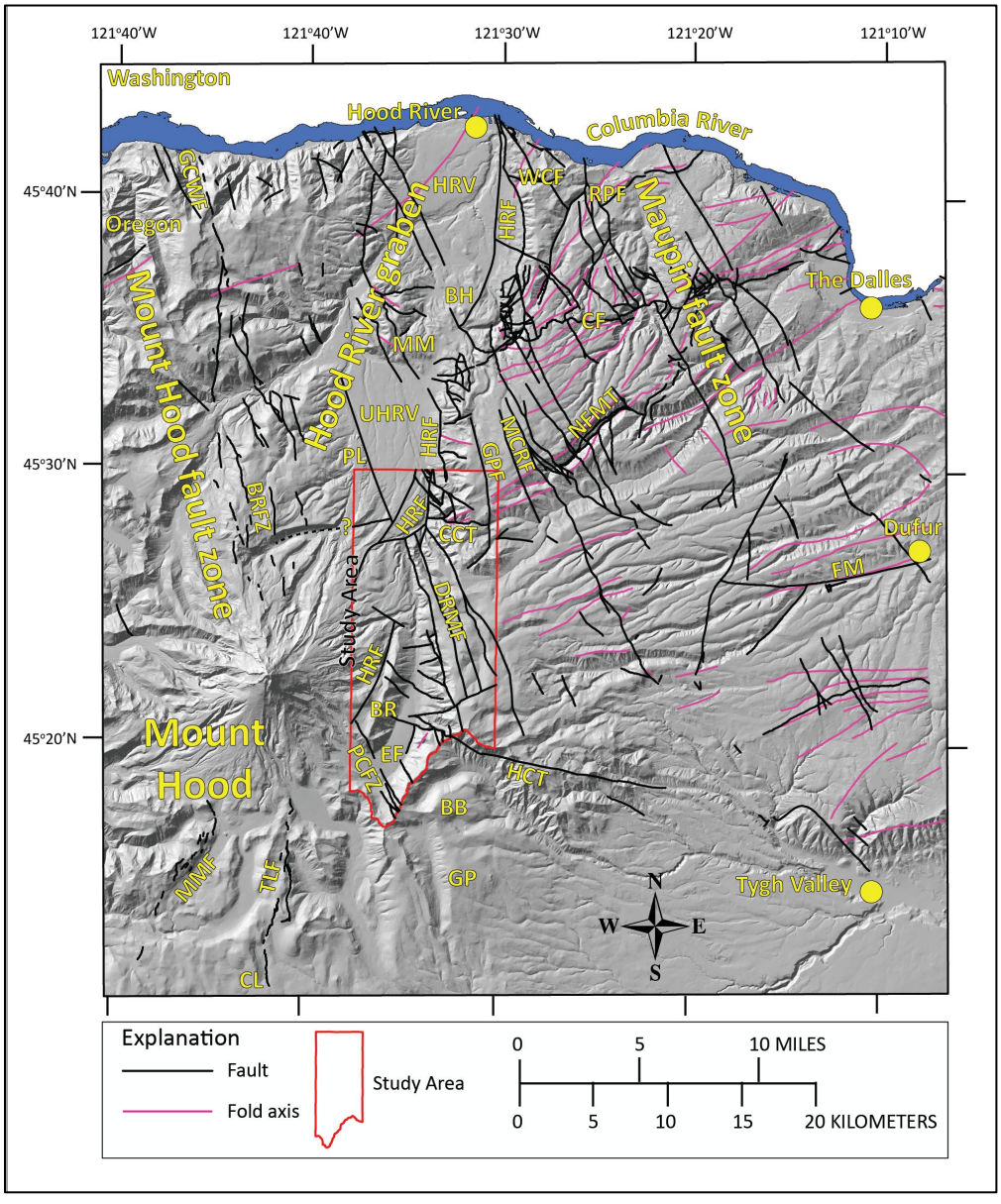

5.2 High Cascades graben

Since ~3.7 Ma, compressional deformation in the north-central Oregon part of the Yakima Fold Belt has been accompanied by and overprinted by extension and intra-arc graben formation along the axis of the High Cascades (**Figure 5-1**, **Figure 5-2**). From the Three Sisters (Oregon) north to Mount Adams (Washington State), the High Cascades occupy an ~30-km-wide (18.6 mi) structural graben formed by a northward propagating rift (**Figure 5-2**; Allen, 1966; Taylor, 1981; Williams and others, 1982; Smith and Taylor, 1983; Smith and others, 1987; Conrey and others, 2002; McClaughry and others, 2012). The High Cascades graben is segmented into three northward younging parts, including a "southern" segment between the Three Sisters and Mount Jefferson, a "central" segment between Mount Jefferson and Mount Hood, and a northern segment between Mount Hood and Mount Adams known as the Hood River graben (segments are numbered in **Figure 5-2**; Conrey and others, 2002; Conrey and others, 2019). Older rocks, which along strike are foundered within the graben, crop out near the range crest in the vicinity of Mount Jefferson and Mount Hood, thus precluding the presence of a significant through-going rift or graben as originally proposed by Allen (1966). All segments of the graben are defined by significant offset along eastern boundary normal faults and asymmetric uplift of the western graben margin (**Figure 5-2**). Paleo-drainages west of the graben are elevated 600 to 800 m (1,969 to 2,625 ft) above modern base levels, suggesting broad uplift of the Western Cascades concurrent with rifting (Conrey and others, 2002). Tilted fault blocks invariably dip eastward off the structural high.

The segmented and structurally discontinuous High Cascades graben is time-transgressive, propagating northward from central Oregon (Green Ridge) since 5.3 Ma to Mount Adams (Washington State) at an overall rate of 4 cm/yr (1.6 in/yr) (**Figure 5-2**; Smith and others, 1987; Sherrod and Smith, 2000; Conrey and others, 2002). Geothermal drill-core data suggest a total subsidence of 3 km (1.9 mi) in the southern segment and 1 km (0.6 mi) in the central segment (Conrey and others, 2002), while the northern Hood River graben segment exhibits subsidence <1.2 km (0.7 mi) (**Figure 5-2**). The High Cascades graben corresponds to the area with the greatest production of Quaternary volcanic material (Williams and others, 1982). Subsidence developed along each graben segment as eruptions declined, typically after ~2 m.y. of elevated eruption rates. Pre-graben eruptions are notable for the presence of MORB-like low-K tholeiites, Fe-rich intermediate lavas, rhyolites, and ash-flow tuffs (Conrey and others, 2002; McClaughry and others, 2012; Conrey and others, 2019).

5.3 Hood River graben

Between Mount Hood and Mount Adams (Washington State), the northernmost segment of the High Cascades graben is known as the Hood River graben, a complex tectonic depression that forms the Hood River and Upper Hood River valleys (**Figure 5-2**, **Figure 5-3**). The graben occurs from an area just south of Mount Hood, north ~50 km (31 mi) at least to Underwood Mountain along the north side of the Columbia River in Washington State. It is defined by an ~20- to 25-km-wide (12.4 to 15.5 mi) zone of distributed north-south striking normal faults and complex graben subsidence, bounded by north-northwest-striking right-lateral normal-oblique slip master faults, including the Mount Hood fault zone on the west and Maupin fault zone on the east (**Figure 5-3**). Middle Mountain, a partially fault-bounded structural block composed of Columbia River Basalt divides the Hood River graben into two rhombohedral-shaped segments identified as the Hood River and Upper Hood River valleys (**Figure 5-3**). The southern part of the Hood River graben in the Dog River–Badger Lake area is largely infilled by <500 ka lava flows and clastic units erupted from Mount Hood volcano.

The timing of initial graben formation in the Hood River area was contemporaneous with a major pulse of mafic volcanism in the northern Oregon Cascade Range, between 4.4 and 2.1 Ma (Conrey and others, 1996; Gray and others, 1996). This pulse of mafic volcanism was distinctly younger than a similar episode that had culminated in the southern segment of the High Cascades graben of central Oregon by ~5 Ma (**Figure 5-2**). It contrasts with the preceding ten m.y., when andesitic eruptions dominated the northern Oregon Cascade Range (~14 to 5 Ma; Wise, 1969; Priest and others, 1983; Keith and others, 1985; Conrey and others, 1996). Subsidence may be time transgressive at the scale of the Hood River graben, chiefly post 3.7 Ma on the south end at Mount Hood versus <3.05 Ma on the north at Hood River (**Figure 5-3**).

The Hood River graben shares structural characteristics and a tectonic setting consistent with formation as a complex, transtensional fault-bounded pull-apart basin across the north-central part of the High Cascades. Classic pull-apart basins, described elsewhere and in theoretical models, are characterized as rhombic- to spindle-shaped basins, forming between two or more bounding strike-slip faults and bounded on their ends by diagonal transfer faults (Burchfiel and Stewart, 1966; Crowell, 1974; Wu and others, 2009). Relative motion of crustal blocks in a pull-apart basin can be either parallel to bounding displacement zones (pure strike-slip) or occur along faults oblique (transtensional) to the bounding displacement zones (Wu and others, 2009). The spindle- to rhombic-shape, association with middle Miocene to recent Yakima Fold Belt deformation, and geographic position between two master north-northwest-trending right-lateral normal-oblique fault slip fault zones (Mount Hood fault zone on the west and Maupin fault zone on the east), suggests the Hood River graben's probable origin as a pull-apart basin (**Figure 5-3**). The transtensional nature of the Hood River graben is suggested by both oblique slip on bounding master faults and an eastern margin bounded longitudinally by a transverse system of oblique-slip faults (Hood River fault zone) linking (?) with bounding master faults (**Figure 5-3**). This interpretation of the Hood River graben is consistent with characteristics described in the Tualatin basin of the northern Oregon Coast Range, which shares a similar tectonic setting along the western edge of the Cascade volcanic arc, ~80 km (50 mi) west of Mount Hood (McPhee and others, 2014; **Figure 5-2**). Bennett and others (2019) suggested that the Hood River graben may accommodate both intra-arc rifting as well as the northward translation of rotating crustal blocks in the upper plate of the Cascadia subduction zone (**Figure 5-1**).

5.3.1 Hood River graben, eastern boundary

The eastern boundary of the Hood River graben is defined by the prominent west-facing escarpment of the Hood River fault zone (**Figure 5-3**; McClaughry and others, 2012). The Hood River fault zone is ~50 km (31 mi) long, mapped from an area just north of Underwood Mountain in Washington State, south to Bluegrass Ridge and Pocket Creek along the east flank of Mount Hood (**Figure 5-3**). The fault zone may continue farther to the south of Mount Hood where it joins more southern strands of the eastern boundary fault of the more extensive High Cascades graben, but its presence or precise location in that area is not well constrained (Sherrod and Pickthorn, 1989).

The Hood River fault zone is a 1- to 3-km-wide (0.6 to 2.0 mi) zone of generally north-striking and west-dipping, en echelon, down-on-the-west normal faults that run obliquely and link to the north-northwest-striking right-lateral normal-oblique fault slip faults (Plate 1). North-south-striking fault strands occur as discontinuous right-stepping en echelon faults that progressively shift the location of the Hood River fault zone to the east, moving north from Mount Hood to the Columbia River (e.g., East Fork Hood River at the mouth of Crystal Springs Creek; Booth Hill area) (**Figure 5-3**; Plate 1). The Hood River fault zone has accommodated a significant amount of vertical offset (hundreds of meters) along the

eastern graben margin since Pliocene and latest Pleistocene time, with cumulative displacement apparently progressively decreasing to the north. The Hood River graben shallows to the north, with local subsidence of at least 1,220 m (4,000 ft) on the south, in contrast to ~130 m (426 ft) at Hood River (McClaughry and others, 2012).

5.3.2 Hood River graben, western boundary

The western boundary of the Hood River graben is notably obscure, but appears to be crudely defined by the ~55 km-long (35 mi) north-northwest-trending Mount Hood fault zone (Madin and others, 2017), extending from the Columbia River south through the summit of Mount Hood volcano to Clear Lake (**Figure 5-3**). Components of the Mount Hood fault zone from north to south include the Gate Creek-Wyeth fault, Blue Ridge fault zone, and the Twin Lakes fault (Sherrod and Scott, 1995; McClaughry and others, 2012; Madin and Ma, 2012; Madin and others, 2017; Bennett and others, 2019). The Pocket Creek fault zone, striking northwest along the southern end of the Dog River–Badger Lake area, lies along the southern end of the Mount Hood fault zone (Plate 1; **Figure 5-3**). Bennett and others (2019) recognized a protracted history of right-lateral normal-oblique fault slip along the 10- to 20-km-long (6 to 12.5 mi), north-northwest-striking and east-northeast-dipping Gate Creek-Wyeth fault. The east-dipping Gate Creek-Wyeth fault is antithetic to offset along the Hood River fault zone, and has accommodated ~100 to 200 m (328 to 656 ft) cumulative down-on-the-east vertical offset. The Blue Ridge fault zone on the northern flank of Mount Hood is a 12-km-long (7.5 mi) and 4.5-km-wide (2.8 mi) zone of normal faults (**Figure 5-3**; McClaughry and others, 2012; Madin and Ma, 2012; Madin and others, 2017). All but one segment in the Blue Ridge fault zone has west-side-down displacement (Madin and others, 2017), while Mount Hood fault zone strands between Gate Creek and Blue Ridge have variable senses of vertical offset, both to the west and east. The Twin Lakes fault at the southern end of the Mount Hood fault zone, extends for more than 12 km (7.5 mi) from Clear Lake to OR Highway 35, and consists of two en echelon, west-dipping normal fault segments (**Figure 5-3**).

Quaternary activity is indicated on several of these faults, including the west-dipping Blue Ridge and east-dipping Gate Creek faults, as they locally offset late Pleistocene and/or Holocene glacial moraines (Madin and others, 2017; Bennett and others, 2019). Isotopic ages (^{14}C) obtained from organic material within the Blue Ridge fault zone shows evidence for a single earthquake event, which occurred between ~13,540 and 9,835 years before present (B.P.) (Madin and others, 2017).

5.4 Stratigraphic and structural synopsis

The following synopsis summarizes the distribution, composition, lithology, and age of map units and structural development of the Dog River–Badger Lake area since the late Oligocene. It is divided on the basis of the broad periods of time used in the Explanation of Map Units starting on page 33 and shown in **Figure 5-4** and on Plate 1: ~26 Ma Ancestral Cascades; ~16 Ma Columbia River Basalt Group (CRBG); 9 to 5 Ma Dalles Formation; ~5 to 4 Ma Gunsight Butte volcanics; 4.2 to 2.7 Ma Pliocene to early Pleistocene volcanics; 2.7 to 2.3 Ma Lookout Mountain volcanics; 2.5 Ma to 7 ka products of regional volcanoes; ~1.5 Ma products of pre-Mount Hood and <500 ka products of Mount Hood volcano; and Late Pleistocene glacial deposits and Late Pleistocene to Holocene alluvial and colluvial deposits. Broad geochemical compositions of the Dog River–Badger Lake area volcanic units are depicted in the total alkali-silica diagram (TAS) in **Figure 5-5**. Isotopic ages obtained on geologic map units from the study area are summarized in **Table 5-1**. Most of the geographic names mentioned in the synopsis are shown in **Figure 2-1** and on **Figure 5-2**.

Figure 5-4. Distribution of the broad geologic units exposed in the Dog River–Badger Lake area. (a) CRBG; (b) Dalles Formation; (c) Gunsight Butte volcanics; (d) Pliocene to early Pleistocene volcanics; (e) Badger Butte and Lookout Mountain volcanics; (f) Quaternary regional volcanoes; (g) pre-Mount Hood and products of Mount Hood; (h) glacial deposits; (i) alluvial and colluvial deposits. Oligocene volcanic rocks are not exposed in the map area and thus are not portrayed in the figure.

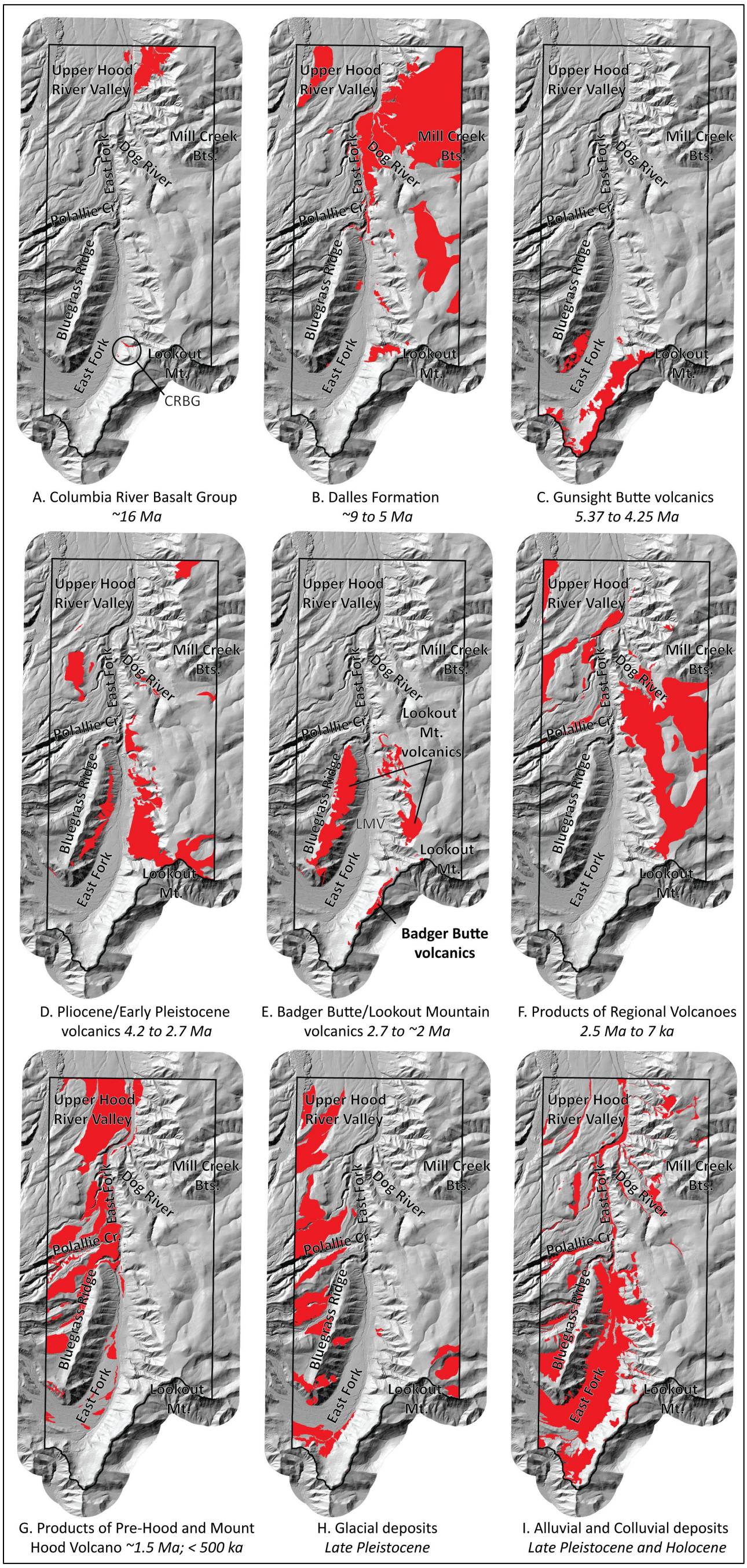

Figure 5-5. Total alkalis ($Na_2O + K_2O$) vs. silica (SiO_2) (TAS) classification of whole-rock XRF analyses (*n* = 600) on volcanic rocks from the Dog River–Badger Lake area (normalized to 100 percent anhydrous). Fields are from Le Bas and others (1986) and Le Maitre and others (1989). Red-dashed line is the dividing line between alkaline (above) and subalkaline/tholeiitic (below) fields of Cox and others (1979).

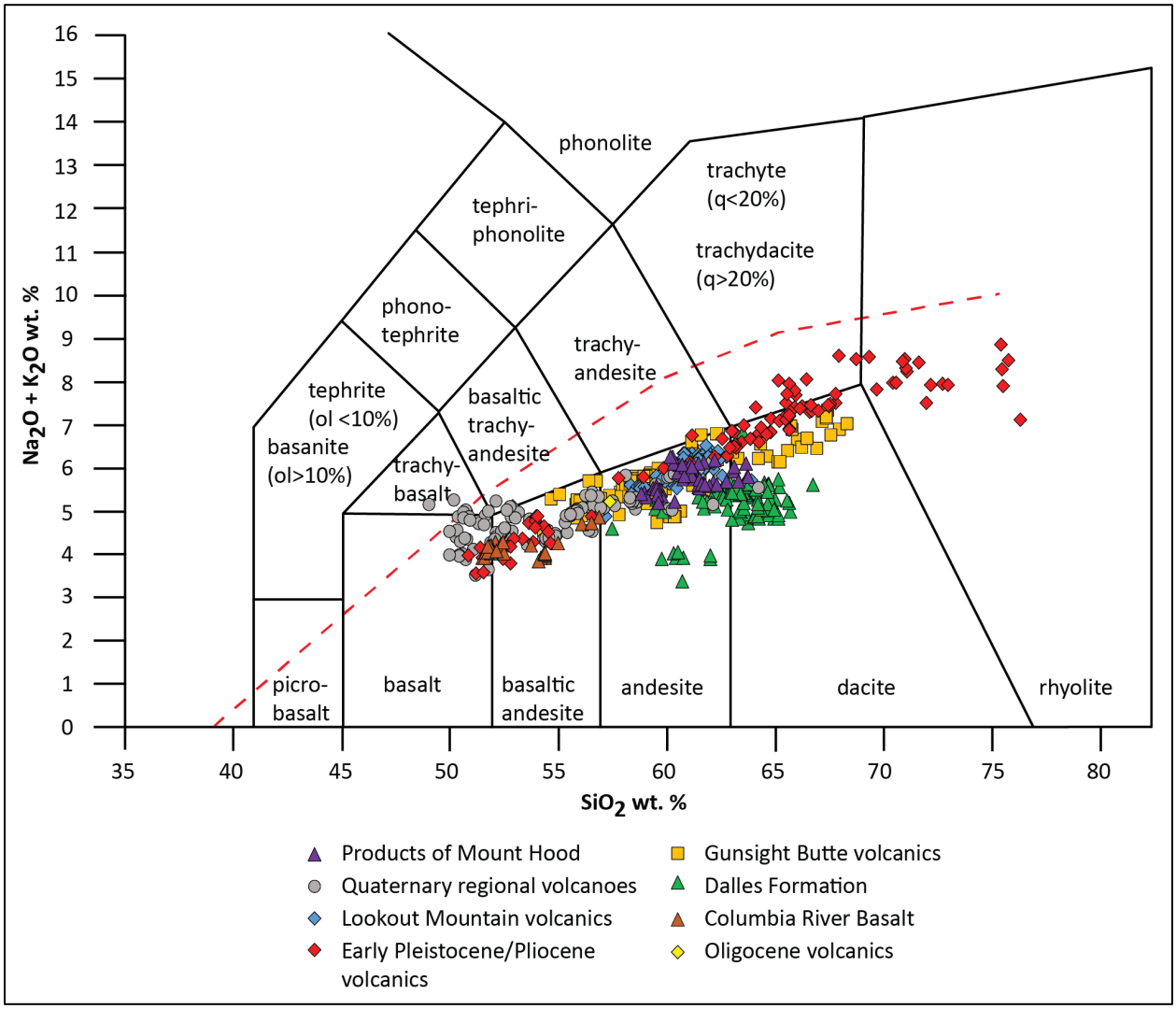

Table 5-1. Summary of isotopic ages for Oligocene to Late Pleistocene volcanic rocks in the Dog River–Badger Lake area.

Map Unit	Age	Sample	Method	Material Analyzed	Source	UTM N (NAD 83)	UTM E (NAD 83)
Qh3lc	29 ± 11 ka	920820-1	K/Ar	Whole Rock	Scott and Gardner (2017)	5028706	610560
Qh3lc	44 ± 9 ka	950705-2	K/Ar	Whole Rock	Scott and Gardner (2017)	5028390	608303
Qh3lc	46.1 ± 2.2 ka[1]	920820-1	$^{40}Ar/^{39}Ar$	Whole Rock	Scott and Gardner (2017)	5028706	610560
Qh3lc	56.7 ± 3 ka[1]	950705-2	$^{40}Ar/^{39}Ar$	Whole Rock	Scott and Gardner (2017)	5028390	608303
Qh4cp	180 ± 16 ka	940707-1	K/Ar	Whole Rock	Scott and Gardner (2017)	5027243	608871
Qh4tj	475 ± 14 ka	931029-6	K/Ar	Whole Rock	Scott and Gardner (2017)	5031397	610599
Qphd	931 ± 15 ka	91T-84	K/Ar	Whole Rock	Scott and Gardner (2017)	5030333	608846
Qrab	1.18 ± 0.01 Ma	51 MCB-DRJ 17	$^{40}Ar/^{39}Ar$	Groundmass	This study	5030887	614577
Qrab	1.91 ± 0.22 Ma	51 MCB-DRJ 17	$^{40}Ar/^{39}Ar$	Amphibole	This study	5030887	614577
Qrai	1.83 ± 0.02 Ma	89a MCB-DRJ 18	$^{40}Ar/^{39}Ar$	Groundmass	This study	5037045	612470
Qr5dr	1.51 ± 0.08 Ma	178 DFWJ 15	$^{40}Ar/^{39}Ar$	Plagioclase	This study	5032481	614681
Qr5dr	1.87 ± 0.01 Ma	178 DFWJ 15	$^{40}Ar/^{39}Ar$	Groundmass	This study	5032481	614681
QTab2	1.68 ± 0.06 Ma[2]	79TF0004	K/Ar	Whole Rock	Keith and others (1985)	5028454	610683
QTab2	1.88 ± 0.05 Ma[2]	79TF0004	K/Ar	Whole Rock	Keith and others (1985)	5028454	610683
Qrbb	2.06 ± 0.08 Ma	S92-H265	K/Ar	Whole Rock	Conrey and others (1996)	5032151	613725
Qrai	2.1 ± 0.2 Ma	Bela-19	K/Ar	Whole Rock	Bela (1982)	5037045	612470
Qrbb	2.26 ± 0.08 Ma	S92-H269	K/Ar	Whole Rock	Conrey and others (1996)	5031022	612245
QTab3	2.36 ± 0.03 Ma	375 MCB-DRJ 17	$^{40}Ar/^{39}Ar$	Plagioclase	This study	5025673	610751
QTbt	2.43 ± 0.14 Ma	S91-H47	K/Ar	Whole Rock	Conrey and others (1996)	5027895	612670
Qbau	2.10 ± 0.09 Ma	RC01-126/84 DRBLJ 19	$^{40}Ar/^{39}Ar$	Plagioclase	This study	5017915	611574
Qbau	2.44 ± 0.02 Ma	RC01-126/84 DRBLJ 19	$^{40}Ar/^{39}Ar$	Groundmass	This study	5017915	611574
QTbt	2.5 ± 0.026 Ma	940616-1	K/Ar	Whole Rock	Scott and Gardner (2017)	5031352	609425
Qrbh	2.52 ± 0.13 Ma	S91-H197	K/Ar	Whole Rock	Conrey and others (1996)	5027457	614228
Qr5tj	2.63 ± 0.01 Ma	380 MCB-DRJ 17	$^{40}Ar/^{39}Ar$	Groundmass	This study	5025723	611173
QTat	2.7 ± 0.2 Ma	Bela-18	K/Ar	Whole Rock	Bela (1982)	5027835	612618
QTat	2.74 ± 0.3 Ma	79SWC0010A	K/Ar	Whole Rock	Keith and others (1985)	5027835	612618
Qrbl1	2.35 ± 0.03 Ma[3]	S92-H271a/Wise-104	K/Ar	Whole Rock	Conrey and others (1996)	5022475	614601
Tpds	3.14 ± 0.2 Ma	70-Wise	K/Ar	Whole Rock	Wise (1969)	5022006	615432
Tpdc	3.68 ± 0.07 Ma	RC14-9/22 DRBLJ 19	$^{40}Ar/^{39}Ar$	Plagioclase	This study	5025306	613074
Tpdc	3.77 ± 0.02 Ma	RC14-9/22 DRBLJ 19	$^{40}Ar/^{39}Ar$	Groundmass	This study	5025306	613074
Tpbr	4.19 ± 0.01 Ma	184 MCB-DRJ 17	$^{40}Ar/^{39}Ar$	Groundmass	This study	5038579	615311
Tpag	4.25 ± 0.6 Ma	Wise-49	K/Ar	Whole Rock	Wise (1969)	5018456	611980
Tmdei	5.37 ± 0.06 Ma	34 DRBLJ 19	$^{40}Ar/^{39}Ar$	Groundmass	This study	5021158	612500
Tmdei	8.78 ± 0.29 Ma	34 DRBLJ 19	$^{40}Ar/^{39}Ar$	Plagioclase	This study	5021158	612500
Tmdy	6.2 ± 1.3 Ma	PH-MCB-1	K/Ar	Hornblende	Fiebelkorn and others (1983)	5033920	614612
Tmdm	6.83 ± 0.01 Ma	660 MCBJ 16	$^{40}Ar/^{39}Ar$	Groundmass	This study	5033208	616253
Tmde	7.15 ± 0.8 Ma	40-Wise	K/Ar	Whole Rock	Wise (1969)	5030959	612189
Tmdi	7.5 ± 0.4 Ma	HD-64	K/Ar	Whole Rock	Hull and Riccio (1979)	5033598	615490
Tmde	8.18 ± 0.06 Ma	79EF0016A	K/Ar	Whole Rock	Keith and others (1985)	5032718	611353
Toav	26.29 ± 0.03 Ma[4]	1111-3-1	$^{40}Ar/^{39}Ar$	Groundmass	This study	5042056	613125

[1]Newer $^{40}Ar/^{39}Ar$ age of same sample; [2]Two ages reported for the same sample; [3]Weighted average age of two ages of 2.91 ± 0.12 and 2.31 ± 0.03.; [4]Sample from an outcrop in the Hood River graben escarpment, ~2 km (1.2 mi) north of map area.

5.4.1 Oligocene volcanic rocks

5.4.1.1 Ancestral Cascades

5.4.1.1.1 Distribution, composition, and lithology

Ancestral Cascades rocks >18 m.y. old are poorly known east of Mount Hood, typically buried by regionally widespread lava flows of the early to middle Miocene CRBG (**Figure 5-6**). The only known exposure of ancestral Cascade rocks in the Middle Columbia Basin, is found along the eastern escarpment of the Hood River graben in the area of Smullin Road, ~2 km (1.2 km) north of the Dog River–Badger Lake area (**Figure 2-1**, **Figure 5-2, Figure 5-6**). Subsidence of the Hood River graben and relative uplift of the horst escarpment in the Smullin Road area has revealed older abundantly plagioclase-phyric andesite (**Toav**) (SiO_2 = 57.40 weight percent; K_2O = 1.47 weight percent, *n* = 1; **Figure 5-5**) beneath the Grouse Creek member (**Tggc**), the oldest part of the CRBG in the Dog River–Badger Lake area.

5.4.1.1.2 Age

Isotopic dating of the plagioclase-phyric andesite (**Toav**) from the Smullin Road locality has returned an $^{40}Ar/^{39}Ar$ age of 26.29 ± 0.03 Ma (groundmass; sample 1111-3-1; **Figure 2-1**; **Table 5-1**; Appendix). Isotopic age of the Smullin Road area outcrop is consistent with correlation of these rocks with the 40 to 18 Ma early Western Cascade episode of Priest and others (1983).

5.4.2 Lower to middle Miocene volcanic rocks

5.4.2.1 Columbia River Basalt Group

5.4.2.1.1 Distribution, composition, and lithology

The oldest rocks exposed in the Dog River–Badger Lake area are part of the early to middle Miocene CRBG, an extensive succession of tholeiitic basalt and basaltic andesite lavas covering more than 210,000 km^2 (130,488 mi^2) in parts of Washington, Oregon, and Idaho (**Figure 5-7**; Tolan and others, 1989; Reidel and others, 2013). Members of the CRBG exposed in the map area include the Frenchman Springs Member (**Twfs**, **Twfh**) of the Wanapum Basalt and Sentinel Bluffs (**Tgsb**), Winter Water (**Tgww**), Ortley (**Tgo**), and Grouse Creek (**Tggc**) members of the Grande Ronde Basalt (Plate 1). CRBG exposures in the map area are limited to the northern part of the Dog River 7.5′ quadrangle and the east-central part of the Badger Lake 7.5′ quadrangle, where these older rocks have been exhumed from depth along east-west striking thrust faults and north-striking normal fault strands of the Hood River fault zone (**Figure 5-4a**). CRBG units commonly form distinctive bench and slope topography, resulting from differential erosion within and between flows. More easily erodible interflow zones are often marked by bands of trees, while more resistant flow interiors typically form continuous cliffs with grass-topped benches. Aggregate thickness of the CRBG in the map area is ≤549 m (1,800 ft).

CRBG lavas were erupted from north-northwest-striking linear fissure systems in the eastern part of the Columbia Plateau ~16 Ma and flowed westward through the Columbia Trans-Arc Lowland toward the low-relief topography of western Oregon (**Figure 5-7;** Tolan and Beeson, 1984; Beeson and others, 1985, 1989; Tolan and others, 1989; Wells and others, 1989, 2009; Kasbohm and Schoene, 2018). The Columbia Trans-Arc Lowland was a generally southwest-northeast-directed, ~60-km-wide (37 mi) topographic low that extended across the ancestral Cascade Range during the early to middle Miocene (**Figure 5-7**; Beeson and others, 1989; Beeson and Tolan, 1990). The lowland was likely structural in origin and related to fold-

deformation of Eocene to middle Miocene rocks underlying north-central Oregon; it was likely not related to the development of the early Cascades volcanic arc (Beeson and Tolan, 1990). The position of the lowland, however, may have influenced later development and growth of the volcanic arc in this area (Beeson and Tolan, 1990).

Figure 5-6. Generalized geology of north-central Oregon. Geology is from OGDC-6, compiled by Smith and Roe (2015). Study area shown by black outline. Solid orange line corresponds to the watershed hydrologic boundary of the Middle Columbia Basin. Label abbreviations are as follows: BD—Bonneville Dam; JDD—John Day Dam; TDD—The Dalles Dam.

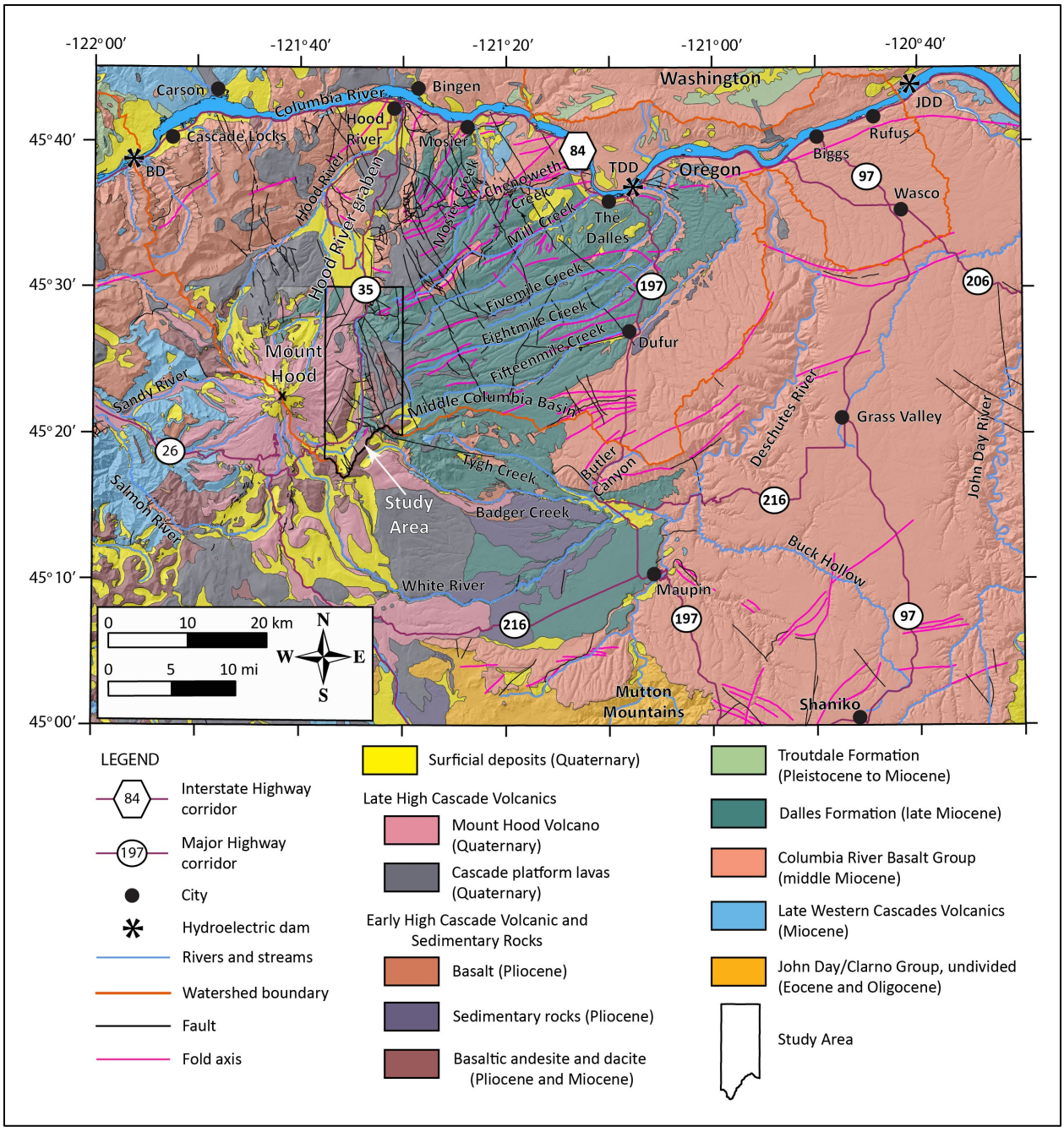

Figure 5-7. Sketch map showing the outcrop distribution of the CRBG (orange fill). The extent of flows includes areas from which the lavas have been eroded, in addition to areas where lavas are concealed by younger units. Modified from Reidel and others (2013) and Ferns and McClaughry (2013). Label abbreviations are as follows: CJD – Chief Joseph Dike Swarm; PDG – Picture Gorge Dike Swarm; SD – Steens Dike Swarm; SM – Strawberry Mountain; ST – Steens Mountain.

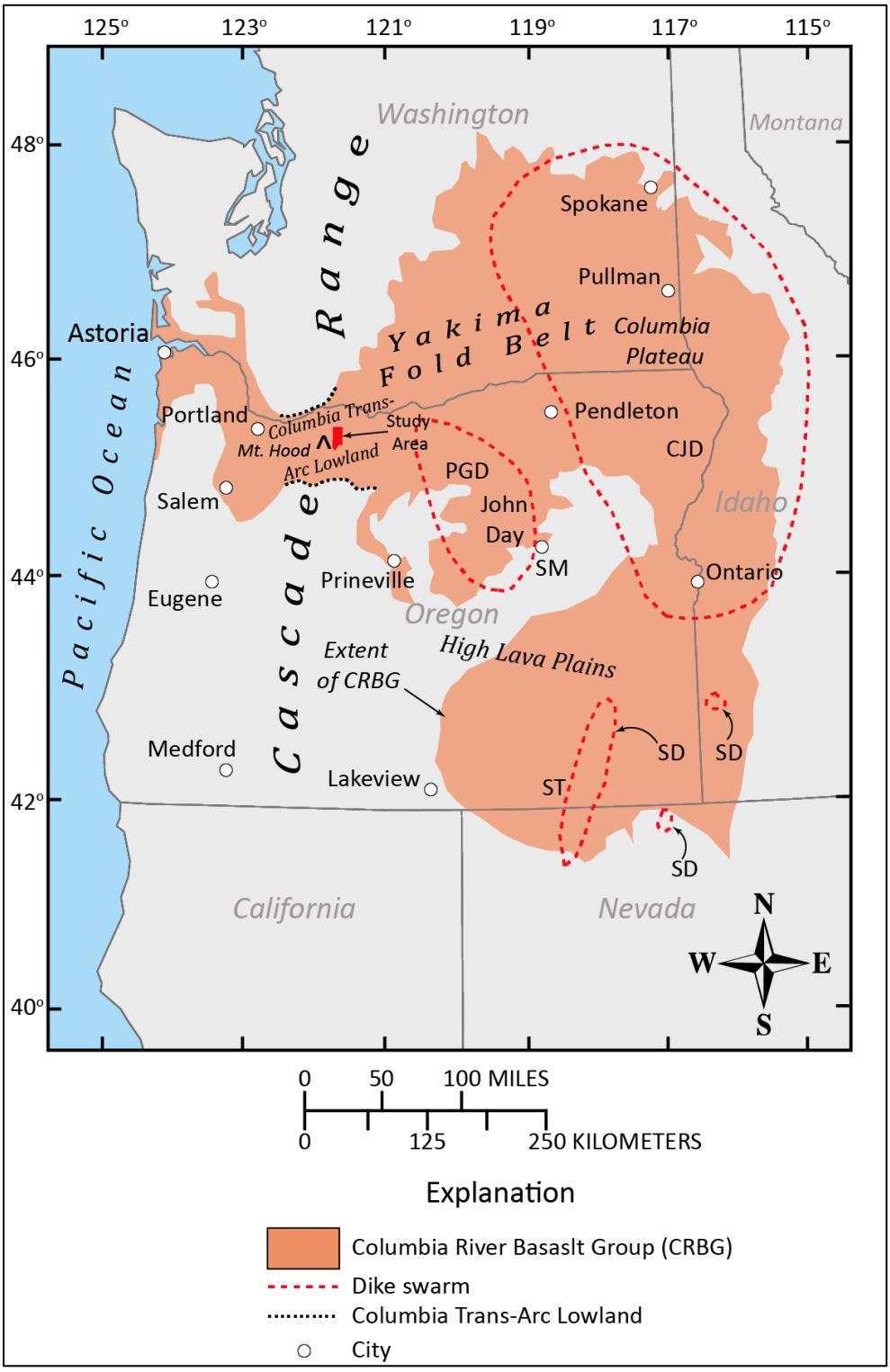

5.4.2.1.2 Age

Isotopic dating of CRBG flows has struggled with accuracy and precision issues, complicating the development of an unambiguous chronology for the timing and duration of CRBG volcanism (Baksi and Farrar, 1990; Baksi, 2013; Barry and others, 2013). Isotopic dating of basaltic lavas by $^{40}Ar/^{39}Ar$ and K-Ar techniques suggests main-phase eruptions of the Grande Ronde Basalt occurred over a 0.4 m.y. interval, between ~16.0 and 15.6 Ma. The eruption of younger Wanapum Basalt is considered to span a time period between ~15.6 and <15 Ma (Barry and others, 2010, 2013). Work by Kasbohm and Schoene (2018) has established a more accurate and precise age model for the CRBG, improving understanding of the eruption timing of Wanapum and Grande Ronde flows that traversed the Columbia Trans-Arc Lowland (**Figure 5-7**). Kasbohm and Schoene (2018) examined silicic tuff interbeds between basalt flows in central and eastern parts of the Columbia Plateau, U-Pb dating single zircon crystals (**Figure 5-7**). High precision U-Pb zircon dates of interbedded tuffs indicate slightly older ages for CRBG units across the Columbia Plateau, including those present in the Dog River–Badger Lake area. The age of the Frenchman Springs Member (**Twfs**, **Twfh**) is now bracketed by U-Pb dates of 15.895 ± 0.019 Ma for ash between the overlying Basalt of Rosalia and Basalt of Lolo (Priest Rapids Member, Wanapum Basalt) and 16.066 ± 0.04 Ma for ash from the Vantage Horizon between the Basalt of Ginkgo and the Sentinel Bluffs Member (**Tgsb**). Upper Grande Ronde units, including the Sentinel Bluffs (**Tgsb**), Winter Water (**Tgww**), Ortley (**Tgo**), and Grouse Creek (**Tggc**) members are bracketed by U-Pb dates of 16.066 ± 0.04 Ma for ash from the overlying Vantage Horizon and 16.254 ± 0.034 Ma for ash between the Wapshilla Ridge and Meyer Ridge Members of the underlying R2 magnetostratigraphic unit. U-Pb ages place an end to Grande Ronde volcanism at ~16 Ma, while a majority (>77 percent) of Wanapum Basalt completed eruption prior to ~15.9 Ma.

5.4.3 Upper Miocene and lower Pliocene volcanic and sedimentary rocks of the early High Cascades

5.4.3.1 Dalles Formation

5.4.3.1.1 Distribution, composition, and lithology

Regional CRBG units in this part of the north-central Oregon Cascade Range are unconformably overlain by volcanic and sedimentary rocks of the late Miocene and early Pliocene Dalles Formation. The Dalles Formation was emplaced across a broad constructional volcanic highland along the east side of the Dog River–Badger Lake area and in areas underlying present day Mount Hood; correlative strata form a broad northeast-sloping arc-adjacent volcanic plain stretching ~40 km (25 mi) from the Dog River–Badger Lake area, northeast to the Columbia River (**Figure 5-4b**, **Figure 5-6**; Plate 1). In the Dog River–Badger Lake area, the Dalles Formation is characterized by interlayered vent-proximal lava flows and domes, hypabyssal intrusions, block-and-ash flow deposits, and ash-flow tuff (Plate 1). Distal deposits exposed eastward to The Dalles and Dufur, become increasingly rich in thick sections of block-and-ash-flow deposits, volcanogenic debris flow (lahar) deposits, hyperconcentrated flood-flow deposits, and ash-flow tuff, interbedded with horizons of fluvial conglomerate, sandstone, and siltstone (**Figure 5-6**; McClaughry and others, in press). Intracanyon lavas are inset into volcaniclastic rocks forming the arc-adjacent volcanic plain along several northeast-directed drainages. These lithologic associations indicate a transition from proximal volcanic dominated highlands in the Dog River–Badger Lake area on the west to a more distal broad volcaniclastic apron on the east, characterized by an east-northeast-directed axial stream drainage system (**Figure 5-6**). Generation and distal runout of Dalles Formation lahars eastward into the Dufur area and beyond (>25 km [15.5 mi] from source areas in the Dog River–Badger Lake area

requires 1) an adequate water source, 2) abundance of unconsolidated debris (e.g., pyroclastic-flow and -fall deposits), 3) steep slopes and substantial relief in the source area, and 4) a triggering mechanism (e.g., volcanic eruptions or other process such as torrential rains or melting of snow and ice) (Vallance, 1999). At the extreme distal edge of the volcanic apron, Cascade-derived Dalles Formation units interfinger with sediment of Deschutes River provenance (Cannon and O'Connor, 2019). During periods of voluminous volcanic and sediment production, Dalles Formation facies may have dominated even the ancestral Deschutes River system.

Geochemical analyses of Dalles Formation volcanic and intrusive units in the Dog River–Badger Lake area indicate low- to medium-K_2O calc-alkaline lava flows and domes with SiO_2 ranging between 57.47 and 66.72 weight percent (**Figure 5-5**) and K_2O ranging between 0.72 and 1.65 weight percent (an average of 1.17 weight percent K_2O at 63.30 weight percent SiO_2; *n* =105 samples). Mineralogy of Dalles rocks includes plagioclase, pyroxene (orthopyroxene ≥ clinopyroxene), and ± hornblende. The thickness of the Dalles Formation in the map area ranges between 457 to 610 m (1,500 to 2,000 ft; Plate 1, cross sections).

Late Miocene and early Pliocene rocks in the map area are equivalent to the Dalles Formation as defined by previous workers (Condon, 1874; Cope, 1880; Piper, 1932; Newcomb, 1966, 1969; Gannett, 1982; Korosec, 1987; Luttrell and others, 1991; Gray and others, 1996; **Figure 5-2**). Farooqui and others (1981a,b) suggested substituting the name "Chenoweth" in place of Dalles Formation in this area and the promotion of "Dalles" to group status. Their "Dalles Group" was considered to include all late Miocene and early Pliocene volcanogenic and epiclastic sedimentary rocks, pyroclastic rocks, and basaltic lavas that unconformably overlie the early to middle Miocene CRBG east of the Cascade Range in Oregon. Five mappable formations were assigned to the "Dalles Group" by Farooqui and others (1981a,b), including the "Chenoweth" (previously Dalles), Deschutes, Alkali Canyon, McKay, and Tygh Valley formations. Several workers in the northern Oregon Cascade Range have adopted usage of the "Chenoweth Formation" and "Dalles Group" (Farooqui and others, 1981a,b; Tolan and Beeson, 1984; Lite and Grondin, 1988; Burns and others, 2012). However, usage of the term "Dalles Group" is inappropriate as the terminology combines geographically separated, lithologically diverse, and genetically unrelated geologic formations (e.g., intra-Cascade arc and rift related Deschutes and Tygh Valley Formations versus the pre-rift Dalles Formation or epiclastic sedimentary rocks of the Alkali Canyon and McKay Creek Formations; Conrey and others, 1996; McClaughry and others, 2012). We therefore retain the conventional name Dalles Formation as established by earlier workers (Condon, 1874).

5.4.3.1.2 Age

Rocks of the Dalles Formation represent part of the early High Cascade episode in this part of the High Cascades of north-central Oregon. They were chiefly erupted between 8.8 and ~5 Ma as determined on the basis of a number of isotopic ages (**Figure 5-6**; Plate 1). Several $^{40}Ar/^{39}Ar$ ages have been obtained on Dalles Formation rocks, both from proximal volcanic units in the Dog River–Badger Lake area and from distal volcaniclastic apron deposits in the Dufur area (**Table 5-1**; **Figure 5-6**). $^{40}Ar/^{39}Ar$ ages in vent-proximal areas include 6.83 ± 0.01 Ma on a microdiorite dome (**Tmdm**) (groundmass; sample 660 MCBJ 16) forming part of Mill Creek Buttes and 5.37 ± 0.06 Ma (groundmass; sample 34 DRBLJ 19) on a hypabyssal intrusion (**Tmdei**) exposed along East Fork Hood River in the southern part of the map area (**Table 5-1**; **Figure 2-1**; Plate 1; Appendix). Broadly similar ages, determined on distal apron deposits in the Dufur area (east of map area), include 8.75 ± 0.05 Ma) (hornblende; sample 212 DFWJ 14) obtained from a lahar clast near the base of the formation at the intersection of Fifteenmile Creek and Rail Hollow, 8.07 ± 0.10 Ma (hornblende; sample 29 DFWJ 14) on a section-capping ash-flow tuff in the upper reaches

of Rail Hollow, and 7.91 ± 0.08 Ma (plagioclase; sample 291 DFWJ 14) on a section-capping dacitic lava flow along Eightmile Creek (**Figure 5-6**; McClaughry and others, in press)

Previously published K-Ar analyses have returned similar, but typically less precise, ages of 7.15 ± 0.8 Ma (whole rock; 40-Wise; Wise, 1969) and 8.18 ± 0.06 Ma (whole rock; sample 79EF0016A; Keith and others, 1985) for the andesite and dacite of East Fork (**Tmde**) (**Table 5-1**; Plate 1; Appendix), 7.74 ± 0.16 Ma obtained from a lahar clast in Fifteenmile Creek (plagioclase; sample S88-24; Gray and others, 1996; east of study area), 7.71 ± 0.17 Ma from flows on Fivemile Butte (plagioclase; sample RC S88-23; **Figure 2-1**; Gray and others, 1996; east of the study area), 7.5 ± 0.4 Ma from domes forming Mill Creek Buttes (whole rock; sample HD-64; **Table 5-1**; **Figure 2-1**; Plate 1; Appendix; Hull and Riccio, 1979), 5.87 ± 0.6 Ma (plagioclase; sample 10574) and 5.7 ± 0.6 Ma (feldspar concentrate; 110-WB) obtained from lahar clasts on Chenoweth Creek (northeast of study area), and 5.28 ± 0.5 Ma (whole rock; sample 106-WB) and 5.1 ± 0.5 Ma (sample 109-WB) for flows at Jordan Butte (southeast of study area) (Farooqui and others, 1981a,b; Bunker and others, 1982. A basalt flow interbedded in the Dalles Formation at Fulton Ridge, near the mouth of the Deschutes River has returned an $^{40}Ar/^{39}Ar$ age of 5.4 Ma (Cannon and O'Connor, 2019). Vertebrate and leaf fossil data reported by Buwalda (1929), Buwalda and Moore (1929, 1930), and Newcomb (1966) also are consistent with a late Miocene and early Pliocene age for the formation.

5.4.3.2 Gunsight Butte volcanics

5.4.3.2.1 Distribution, composition, and lithology

The Gunsight Butte volcanics are chiefly composed of a flow-on-flow succession of basaltic andesite, andesite, and dacite lavas and minor breccia overlying the Dalles Formation in the southern part of the map area (**Figure 5-4c**; Plate 1). The best exposures of the unit are beneath the early Pleistocene Badger Butte volcanics at Gunsight Butte, south of the Hellroaring Creek thrust fault (**Figure 2-1**; Plate 1). Although slopes west of Gunsight Butte are largely mantled by Quaternary glacial deposits (**Qgsp**, **Qgot**), talus (**Qt**), and colluvium (**Qc**), flows crop out discontinuously in a number of distinct benches visible in 1-m lidar topography. Correlative units **Tpmv** and **Tpml** form the base of the southern end of Bluegrass Ridge (**Figure 2-1**; **Figure 5-4c**; Plate 1). Basaltic andesite and andesite flows (SiO_2 = 54.7 and 63.48 weight percent, avg = 59.14; K_2O 0.92 to 2.05 weight percent, avg = 1.54; *n* = 53) dominate the sequence (~80 percent), with the remainder being interbedded dacite lavas (SiO_2 = 62.34 to 68.35 weight percent, avg = 65.84; K_20 = 1.59 to 2.41 weight percent, avg = 2.05; *n* = 22; **Figure 5-5**). Mineralogy of Gunsight Butte lavas includes plagioclase, pyroxene (orthopyroxene ≥ clinopyroxene), and ± olivine (Shearer, 2002). The dacite of Bennett Pass Road (**Tpmu**) and tuff breccia of Bennett Pass Road (**Tpmt**) form some of the oldest part of the Gunsight Butte volcanics and include hornblende as a primary phenocryst phase. Thickness of the Gunsight Butte volcanics in the map area is ≤610 m (2,000 ft) south of Mine Creek (**Figure 2-1**; Plate 1).

Reconnaissance mapping and geochemical sampling by Shearer (2002) showed that no Gunsight Butte lavas occur east of Badger Lake (east of map area; **Figure 2-1**). Shearer (2002) suggested the possibility of a north-northeast trending, down-on-the west normal fault in the proximity of Badger Lake that generated fault-controlled paleotopography in the area, against which Gunsight lavas may have ponded. If present, this postulated structure could be related to north-south trending, down-on-the west tear faults that developed in conjunction with the Hellroaring thrust fault and significantly offset CRBG, Dalles, and Gunsight units at Gumjuwac Saddle.

5.4.3.2.2 Age

The Gunsight Butte volcanics underlie the 2.44 Ma and younger Badger Butte volcanics at Gunsight Butte. An isotopic age at the top of the Gunsight Butte volcanics sequence southwest of Gunsight Butte and northwest of Badger Lake is 4.25 ± 0.6 Ma (**Tpa**g; K-Ar; whole rock; sample Wise-49; Wise, 1969) (**Figure 2-1**; **Table 5-1**; Plate 1). The oldest part of the Gunsight Butte volcanic sequence (**Tpml**; **Tpmn**; **Tpmb1**; **Tpmb2**) onlaps 5.37 Ma intrusive rocks of Dalles Formation unit **Tmdei** along Mine Creek (Plate 1).

5.4.3.3 Pliocene and Lower Pleistocene volcanic rocks along East Fork Hood River

5.4.3.3.1 Distribution, composition, and lithology

Pliocene and early Pleistocene and volcanics exposed within the Dog River–Badger Lake form a generally north-dipping, flow-on-flow succession of basalt, basaltic andesite, andesite, trachyandesite and trachydacite, dacite, rhyolite and tuff breccia, exposed above the Dalles Formation, north of the Hellroaring Creek fault and largely west of the Dog-River Mill Creek divide (**Figure 2-1**; **Figure 5-4d**; Plate 1). Rocks of this age also overlie the Gunsight Butte volcanics and older Dalles Formation along Elk Mountain and Bluegrass Ridge (**Figure 5-4d**; Plate 1). A number of generally north-striking dikes and intrusions related to some of these flows (**Tpdf**; **Tprc**) are present in the vicinity of Culvert Creek, adjacent to the Hood River graben-bounding Powder Springs and Dog River faults (**Figure 2-1**; Plate 1). Mafic lavas of unit **Tpbc** erupted from a cinder cone vent mapped along the north side of Culvert Creek (**Figure 2-1**; Plate 1). Composition of early Pleistocene and Pliocene volcanics ranges from primitive olivine basalt (50.89 weight percent SiO_2) to rhyolite (76.30 weight percent SiO_2). The full range of silica is present with all units having an average low-SiO_2 dacite composition (SiO_2 = 63.08; K_2O = 2.38 weight percent; *n* = 101; **Figure 5-5**). Mineralogy of silicic to intermediate composition early Pleistocene and Pliocene volcanics is dominated by plagioclase and pyroxene (orthopyroxene ≥ clinopyroxene); olivine is a primary component of mafic rocks in the sequence. The composite thickness of early Pleistocene and Pliocene volcanics in the map area is ≥762-m-thick (2,500 ft), west of Lookout Mountain (**Figure 2-1**).

The Pliocene and early Pleistocene interval between 4.2 and 2.5 Ma signaled a key period in the volcanic and structural evolution of the late High Cascades of north-central Oregon. Intra-arc faulting initiated during the Pliocene and early Pleistocene along north-northwest-striking normal or normal oblique-slip faults and north-south-striking normal faults led to the formation of the north-striking Hood River graben along the axis of the High Cascades volcanic arc (**Figure 5-2**, **Figure 5-3**; McClaughry and others, 2012). Development of the southern part of the Hood River graben in the Dog River–Badger Lake area was temporally and spatially associated with the eruption of a compositionally diverse suite of volcanic rocks (basalt to rhyolite). In contrast to the relatively wide regional distribution of Early High Cascades rocks of the Dalles Formation (**Figure 5-6**), younger Pliocene and early Pleistocene volcanics were increasingly confined to areas west of the Dog River-Mill Creek Divide (**Figure 2-1**; **Figure 5-4d**). Distribution of Pliocene and early Pleistocene volcanics was controlled by a combination of constructional volcanic topography on remnant Dalles volcanoes, northeast-striking stream channels incised into the Dalles Formation arc-adjacent volcaniclastic apron, and structural relief created along active faults. Pliocene and early Pleistocene volcanics erupted along the structural margins of the Hood River graben in the Dog River–Badger Lake area, and largely filled the accommodation spaces created by active extensional and transtensional structures. Few lava flows of this age, with the exception of 3.69 trachydacite of Fivemile Creek (**Tpdv**), the andesite of Fret Creek (**Tpaf**), and the 3.02 Ma dacite of Fifteenmile Creek (**Tpdf**), escaped the developing graben (**Figure 5-4d**). Those lavas that did exit the graben to the east were confined within channels incised into the older Dalles arc-adjacent plain,

approximately paralleling modern-day canyon patterns and gradient. The trachydacite of Fivemile Creek (**Tpdv**) entered the upper parts of Fivemile Creek, south of Mill Creek Buttes, and descended that drainage for a distance of ~24 km (15 mi) nested as an intracanyon lava within older Dalles Formation strata (**Tmdl**). Likewise, both the andesite of Fret Creek (**Tpaf**) and the dacite of Fifteenmile Creek (**Tpdf**) flowed east into the northeast-striking Fifteenmile Creek drainage as intracanyon lavas (**Figure 2-1**); the farther traveled dacite of Fifteenmile Creek (**Tpdf**) flowed ~13.6 km (8.5 mi) to the east-northeast of the map area inset into the volcaniclastic strata of the Dalles Formation (**Tmdl**).

Large fault displacement of several key "marker" units (**Tpdv**; **Tpaf**; **Tpdf**) in the Pliocene and early Pleistocene volcanic section indicates that initiation of Hood River graben subsidence in the Dog River–Badger Lake area began after 3.69 Ma. The 3.69 Ma trachydacite of Fivemile Creek (**Tpdv**) is a widely exposed flow unit mapped overlying the Dalles Formation (**Tmdl**, **Tmde**) along East Fork Hood River at and elevation of ~1,098 m (3,600 ft) and at higher elevations of 1,291 m (4,234 ft) in the headwaters of South Fork Mill Creek, south of Mill Creek Buttes (**Figure 2-1**, Plate 1). Following emplacement, unit **Tpdv** was progressively downdropped west into the developing Hood River graben across three major north-northwest-trending normal faults, including the Puppy Creek, Dog River, and Powder Springs faults (Plate 1). Cumulative down-on-the west vertical offset of unit **Tpdv** across these faults, between outcrops in the headwaters of South Fork Mill Creek along East Fork Hood River is >270 m (885 ft). Similar fault offsets are mapped for the andesite of Fret Creek (**Tpaf**) and the 3.14 Ma andesite and dacite of Senecal Spring (**Tpds**), along southern segments of the Powder Springs fault. Vertical down-on-the west offset of the andesite of Fret Creek (**Tpaf**) along the Powder Springs fault, west of Horkelia Meadow, is ~256 m (840 feet). The andesite and dacite of Senecal Spring (**Tpds**) is offset ~290 m (950 ft) in a vertical, down-on-the-west sense along the southern strand of the Powder Springs fault. Vertical, down-on-the west offset of the 3.02 Ma dacite of Fifteenmile Creek (**Tpdf**) across the Powder Springs fault is less at ~45 m (150).

Compositionally diverse Pliocene and early Pleistocene volcanics in the Dog River–Badger Lake area contrast with the dominantly low-K_2O andesite and dacites characterizing the older Dalles Formation, and are unique for this part of the northern Oregon Cascades volcanic arc due to the conspicuous presence of rhyolite units (**Tprn**, **Tpre**, **Tprc**, **Tprd**; **Figure 5-5**; Plate 1). Rhyolites are not present in either preceding or subsequent volcanic episodes marking the Mount Hood region (**Figure 5-5**). Rhyolites were erupted contemporaneously with 3.7 Ma trachyandesite and trachydacite lavas (**Tpdv**, **Tpdc**) in the Dog River–Badger Lake area (Plate 1) as well as 3.68 Ma trachydacitic ash-flow and ~3.71 Ma trachydacite-clast block-and-ash flows cropping out in the Friend and Dufur areas (**Figure 5-6**; J.D. McClaughry unpublished geologic mapping). These rocks are temporally equivalent to a similar suite of silicic volcanic rocks emplaced outside the map area at nearby Gordon Butte (8.6 km [5.4 mi] southeast of Lookout Mt.) and Graveyard Buttes (28 km [17.4 mi] southeast of Lookout Mt.) between 3.8 and 3.6 Ma (Westby, 2014). Westby (2014) considered early-phase silicic volcanism in the Gordon and Graveyard Buttes areas to share geochemical and mineralogical traits consistent with petrogenesis in an intra plate or extensional setting, while late phase silicic rocks appear to be more arc related. Intermediate to silicic volcanism between Gordon Butte and East Fork Hood River was also contemporaneous with a more widespread pulse of high-MgO mafic volcanism in the northern Oregon Cascade Range dated between 4.4 Ma and 2.1 Ma (Conrey and others, 1996; McClaughry and others, 2012). Extrusion of mafic lavas during the late Pliocene was accompanied by Yakima Fold Belt deformation, inception of rifting along the axis of this part of the Cascade arc, and formation of the Hood River graben after 3.7 Ma (**Figure 5-2**; McClaughry and others, 2012). Foundering of the Cascade volcanic arc into a half graben during the early to late Pliocene was accompanied by regional uplift or upwarp of the Cascade Range and formation of the modern Columbia River Gorge after 3 Ma (Tolan and Beeson, 1984; Beeson and Tolan, 1990).

5.4.3.3.2 Age

Pliocene and early Pleistocene volcanics in the Dog River–Badger Lake area chiefly erupted between 4.2 and 2.5 Ma on the basis of isotopically dated units in the section (**Figure 5-4d**). The lowest part of the Pliocene and early Pleistocene interval is marked by the 4.19 ± 0.01 Ma ($^{40}Ar/^{39}Ar$; groundmass; sample 184 MCB-DRJ 17) basalt and basaltic andesite of Rimrock (**Tpbr**) which directly overlies the Dalles Formation (**Tmdl**) in the northeastern part of the map area (**Table 5-1**, **Figure 2-1;** Plate 1). South of Mill Creek Buttes and in exposures along East Fork Hood River, the trachydacite of Fivemile Creek (**Tpdv**) forms a conspicuous stratigraphic marker at the base of the sequence, directly overlying late Miocene Rocks of the Dalles Formation (**Tmdl**; **Tmde**). The trachydacite of Fivemile Creek (**Tpdv**) has an $^{40}Ar/^{39}Ar$ plateau age of 3.69 ± 0.02 Ma (groundmass; sample 173 DFWJ 15; McClaughry and others, in press) and an older K-Ar age of 3.7 ± 0.2 Ma (whole rock; sample JA85022; Anderson, 1987) obtained for outcrops in the type exposure along Fivemile Creek (northeast of map area; **Figure 5-6**). Several units overlying the trachydacite of Fivemile Creek (**Tpdv**) between East Fork Hood River and Lookout Mountain have isotopic ages, including the porphyritic trachydacite of Culvert Creek (**Tpdc**) (3.68 ± 0.07 Ma; $^{40}Ar/^{39}Ar$; plagioclase; 3.77 ± 0.02 Ma; $^{40}Ar/^{39}Ar$; groundmass; RC14-9/22 DRBLJ 19; **Table 5-1**; Plate 1), the andesite and dacite of Senecal Spring (**Tpds**) (3.14 ± 0.2 Ma; K-Ar; whole rock; sample 70-Wise; **Table 5-1**; Plate 1), and the dacite of Fifteenmile Creek (**Tpdf**) (3.02 ± 0.02 Ma; $^{40}Ar/^{39}Ar$; groundmass; sample 146 DFWJ 15; McClaughry and others, in press; 2.86 ± 0.06 Ma; K-Ar; plagioclase; sample RCS88-25; Gray and others, 1996). The uppermost part of the early Pleistocene and Pliocene volcanic section in the Dog River–Badger Lake area is defined by the andesite of Tumble Creek (**QTat**), a hornblende-bearing andesite with a K-Ar age of 2.74 ± 0. 3 Ma (whole rock; sample 79WC0010A; Keith and others, 1985) and High-TiO_2 lavas of unit **QTbt** with ages of 2.43 ± 0.14 Ma (K-Ar; whole rock; sample S91-H47; Conrey and others, 1996), 2.5 ± 0.026 Ma (K-Ar; whole rock; sample 940616-1; Scott and Gardner, 2017, basalt of Tilly Jane), and 2.63 ± 0.01 Ma ($^{40}Ar/^{39}Ar$; groundmass; sample 380 MCB-DRJ 17) (**Table 5-1**, **Figure 2-1**; Plate 1).

Isotopic ages in the Dog River–Badger Lake area correspond closely to $^{40}Ar/^{39}Ar$ plateau age results for stratigraphically and temporally equivalent sections in eastern parts of the Middle Columbia Basin, including: 1) 3.68 ± 0.02 Ma (plagioclase; sample 154 DFWJ 15) on the tuff of Friend, exposed just west of the ghost-town of Friend, and 2) 3.72 ± 0.01 Ma (groundmass; sample 172 DFWJ 15) on a basaltic lava flow, exposed directly beneath the trachydacite of Fivemile Creek (**Tpdv**) along Fivemile Creek (**Figure 5-6**; east of map area; McClaughry and others, in press). A tuff exposed at the base of a block- and ash-flow deposit near Dufur, OR has returned an $^{40}Ar/^{39}Ar$ plateau age of 3.83 ± 0.01 Ma (plagioclase; sample 373 DFWJ 14), while a single clast obtained from breccia directly overlying the tuff has an $^{40}Ar/^{39}Ar$ age of 3.71 ± 0.02 Ma (plagioclase; sample 265 DFWJ 14; **Figure 5-6;** east of map area, McClaughry and others, in press). Westby (2014) reported similar $^{40}Ar/^{39}Ar$ plateau ages of 3.86 ± 0.07 Ma for andesite (groundmass; sample S12-6) and 3.67 ± 0.01 (feldspar; sample X3) and 3.65 ± 0.01 (feldspar; sample CC14) for rhyolite at Graveyard Butte and 3.64 ± 0.03 for rhyolite (feldspar; sample GB4-3) at Gordon Butte, southeast of the map area.

5.4.3.4 Lookout Mountain volcanics

5.4.3.4.1 Distribution, composition, and lithology

The Lookout Mountain volcanics are chiefly composed of a flow-on-flow succession of two-pyroxene andesite and low-SiO_2 dacite (SiO_2 = 58.33 to 63.92 weight percent, avg = 60.61; K_2O = 1.41 to 2.33 weight percent, avg = 1.81; *n* = 82) and minor rhyodacite (SiO_2 = 69.23 weight percent; K_2O = 3.17 weight percent *n* = 1 analysis) exposed in north-dipping sections underlying Lookout Mountain and Bluegrass Ridge

(**Figure 2-1**, **Figure 5-4e**, **Figure 5-5**; Plate 1). East of East Fork Hood River, the lowest part of the sequence (**QTal1**) overlies inclusion-rich lavas of unit **Tpdf**. On Bluegrass Ridge, the sequence rests directly on High-TiO_2 lavas (**QTbt**) forming the top of the older Pliocene volcanic rocks exposed along East Fork Hood River. Mineralogy of Lookout Mountain lavas includes plagioclase and pyroxene (orthopyroxene ≥ clinopyroxene); the uppermost flows capping the northern part of Bluegrass Ridge (**QTab6**) and a dike cutting across Elk Mountain (**QTai**) contain hornblende as a primary phenocryst phase. Thickness of the Lookout Mountain volcanics is ≤305 m (1,000 ft) northwest of High Prairie (**Figure 2-1;** Plate 1).

Similar to the majority of older Pliocene and early Pleistocene lavas, the distribution of the Lookout Mountain volcanics is confined to areas west of the Dog River fault (**Figure 5-4e**; Plate 1). The geologic map pattern suggests that sheetlike lavas were emplaced across a complexly faulted and active volcanic terrain and largely infilled and ponded against a pre-existing Hood River graben structure. A singular north-south striking dike correlated with unit **QTal2** is mapped in the headwaters of Culvert Creek, just east of the Powder Springs fault (**Figure 2-1**; Plate 1). Continued fault activity along the Powder Springs and Dog River faults in Pleistocene time has further faulted the Lookout Mountain volcanics.

5.4.3.4.2 Age

The age of the Lookout Mountain volcanics ranges from 2.7 to 2.3 Ma, indicating emplacement across the Pliocene-Quaternary boundary. On Bluegrass Ridge the lowest andesite lavas (**QTab1**) in the sequence directly overlie 2.63 Ma High-TiO_2 basaltic lavas (**QTbt**) (**Figure 2-1**; Plate 1). The top of the Bluegrass Ridge sequence is undated. East of East Fork Hood River, basal Lookout Mountain lavas (**QTal1**) overlie the 3.02 Ma dacite of Fifteenmile Creek (**Tpdf**) (**Figure 2-1**; Plate 1). North of Tumble Creek andesite lavas of unit **QTal2** sit above both High-TiO_2 basaltic lavas (**QTbt**) and the 2.74 Ma andesite of Tumble Creek (**QTat**) (Keith and others, 1985; **Figure 2-1**; Plate 1). Upper age constraints on the Lookout Mountain volcanics come from K-Ar ages on overlying olivine basalt flows with ages of 2.52 Ma at Horkelia Meadow (**Qrbh**) and 2.35 beneath Lookout Mountain (**Qrbp**) (Conrey and others, 1996; **Figure 2-1**; Plate 1).

5.4.3.5 Badger Butte volcanics

5.4.3.5.1 Distribution, composition, and lithology

The Badger Butte volcanics are chiefly composed of a flow-on-flow succession of reversed-polarity, two-pyroxene basaltic andesite and andesite (SiO_2 = 54.37 to 62.05 weight percent, avg = 58.65; K_2O = 0.78 to 2.21 weight percent, avg = 1.57; *n* = 36 [*n* = 18 outside map area]) disconformably overlying the 4.25 to 5.37 Ma Gunsight Butte volcanics in the southeast part of the map area. Flows of the Badger Butte volcanics also form Badger Butte east of the map area and crop out in the canyons of Crane Creek, Badger Creek, and Pine Creek further east. The geologic map pattern, portrayed by Sherrod and Scott (1995), shows intracanyon Badger Butte flows reach as far east as Happy Ridge. Lava flows forming the Badger Butte volcanics were erupted from Badger Butte (Wise, 1969; Sherrod and Scott, 1995; Conrey and others, 1996; Shearer , 2002); andesite of unit **Qbla** corresponds to a NE.-striking dike cutting older flows, west of Badger Lake. Badger Butte lavas are highly plagioclase-phyric (>15 percent vol.) and contain phenocrysts of pyroxene (orthopyroxene ≥ clinopyroxene) and olivine (Conrey and others, 1996; Shearer (2002). Plagioclase-pyroxene glomerocrysts ≤7 mm (0.3 in) are common. Several flows in the sequence, including unit **Qbba**, contain microdiorite inclusions ranging from 5 mm to 2 cm (0.2 to 0.8 in) across. Thickness of the Badger Butte volcanics is ≤91 m (300 ft) below Gunsight Butte (**Figure 2-1;** Plate 1). At Badger Butte, the sequence is ≥182 m (600 ft) thick.

5.4.3.5.2 Age

The Badger Butte volcanics are comparable in age and similar in composition to the Lookout Mountain volcanics underlying Lookout Mountain and Bluegrass Ridge. An $^{40}Ar/^{39}Ar$ plateau age from the Badger Butte volcanic sequence, west of Badger Lake, is 2.44 ± 0.6 Ma (groundmass; sample RC01-126/84 DRBLJ 19) (**Figure 2-1**; **Table 5-1**; Plate 1). Conrey and others (1996) reported a similar K-Ar age of 2.1 ± 0.04 Ma (whole rock; Wise-55) for basaltic andesite forming the southwest slope of Badger Butte, ~0.75 km (0.5 mi) east of the map area (**Figure 2-1**). Basaltic andesite capping the ridge between Gunsight Butte and Gumjuwac Saddle is of similar composition and stratigraphic position to basaltic andesite dated at site W-55 and may be of similar age (~2 Ma) (**Figure 2-1**; Plate 1; Wise, 1969; Conrey and others, 1996).

5.4.4 Quaternary and/or upper Pliocene volcanic and sedimentary rocks of the late High Cascades

5.4.4.1 Products of regional Quaternary volcanoes

5.4.4.1.1 Distribution, composition, and lithology

Pliocene and older rocks are locally disconformably overlain in the Dog River–Badger Lake area by a series of latest Pliocene and Quaternary olivine-phyric basalt, basaltic andesite, and andesite lava flows erupted from small volcanoes situated along the High Cascades crest (**Figure 5-2**, **Figure 5-4f**). We refer to these basaltic to andesitic vents of Quaternary age surrounding Mount Hood as products of regional Quaternary volcanoes (Plate 1). In the Mount Hood region, Quaternary volcanism spans across an ~160 km-wide (99 mi) west to east region, from the forearc Boring Volcanic Field in the Portland Basin, through the Cascade Range, and eastward to the back-arc Simcoe Mountains (WA) (**Figure 5-2**; Hildreth, 2007). More than 300 vents of Quaternary age lie within an ~ 50 km-wide (31 mi) region north and south of the Columbia River, including the large composite volcanoes of Mount St. Helens, Mount Adams, and Mount Hood (**Figure 5-2**).

Mafic to intermediate volcanism was predominant in the Dog River–Badger Lake area during Quaternary time, with basalt, basaltic andesite, and andesite lavas erupting from a north-south trending belt of extant vents situated between Mill Creek Buttes and Lookout Mountain, along the broad eastern escarpment of the Hood River graben (**Figure 2-1**, **Figure 5-3**; Plate 1). Vent alignments were spatially associated with north-northwest trending fault strands (Plate 1). Basalt and basaltic andesite (SiO_2 = 49.06 and 54.88 weight percent, avg = 52.04; K_2O = 0.24 to 1.43 weight percent, avg = 0.91; *n* = 64) compositions dominate in Quaternary lavas erupted prior to 1.87 Ma in the Dog River–Badger Lake area (**Figure 5-5**). Post-1.87 Ma lavas have basaltic andesite to andesite compositions (SiO_2 = 55.34 to 59.50 weight percent, avg = 57.03; K_2O = 0.63 to 1.69, avg = 1.01; *n* = 45; **Figure 5-5**). Mineralogy of Regional Quaternary lavas includes plagioclase and olivine ± pyroxene. At least two domes of andesitic composition (SiO_2 = 58.13 to 62.16 weight percent, avg = 57.03; K_2O = 1.03 to 1.57; *n* = 4; **Figure 5-5**) were also emplaced along the eastern escarpment of the Hood River graben in the Middle Pleistocene (**Qrab**; **Qras**) (Plate 1). Mineralogy of Middle Pleistocene domes includes plagioclase and hornblende.

Lavas erupted high along the eastern escarpment of the Hood River graben in the Dog River–Badger Lake area flowed eastward away from source vents down an east-sloping landscape, confined to north-northeast-directed drainages carved into older late Miocene and Pliocene rocks (**Figure 5-4f**, **Figure 5-6**). These drainages were of similar location and orientation to those followed by older Pliocene intracanyon lavas (**Tpdv**, **Tpaf**, **Tpdf**). Regional Quaternary lava flows also moved northwest, down into the low, fault-controlled topography of the Hood River graben along a wide drainage paralleling modern Dog River and

Puppy Creek (**Figure 5-4f**). The 1.87 Ma basaltic andesite of Dog River (**Qr5dr**), erupted from a fault-controlled cinder cone–capped fissure along the Dog River-Mill Creek divide at an altitude of 1,391 m (4,565 ft), ~5.7 km (3.5 mi), and was the farthest traveled of Quaternary lavas (**Figure 2-1**; Plate 1). Dog River lavas (**Qr5dr**) descended northeast into South Fork Mill Creek, flowing at least 26 km (16 mi) downstream to Oak Flat, near The Dalles (**Figure 2-1**, **Figure 5-6**; McClaughry and others, in press). An additional lobe of the basaltic andesite of Dog River (**Qr5dr**) was also directed west and northwest into the structural low of the Hood River graben. This western lobe extended at least 6 km (3.7 mi) from the vent area to now down-faulted exposures, outcropping at an elevation of 716 m (2,350 ft) in the canyon of the modern East Fork Hood River.

The western edge of the map area includes two younger lavas included as products of regional Quaternary volcanoes (**Figure 5-4f**; Plate 1). The basaltic andesite and andesite of Cloud Cap (**Qr4cc**), erupted at ~424 ka from a now obscure shield volcano lying ~5 km (2.5 mi) northeast of the summit of Mount Hood, near Cloud Cap Inn (**Figure 2-1**; Scott and Gardner, 2017). Lavas flowed northeast extending into the map area, forming three distal tongues down ancestral valleys of Polallie Creek, Tilly Jane Creek, and Crystal Springs Creek (**Figure 2-1;** Plate 1). The ~7.7 ka andesite of Parkdale (**Qr1pk**), exposed in the northwest corner of the map area, is the youngest lava of a Cascade regional volcano erupted between Mount Adams and Mount Jefferson (**Figure 2-1**, **Figure 5-2**; Plate 1). The flow erupted from a linear vent, situated about 12 km (7.5 mi) from the summit of Mount Hood and moved down the ancestral Middle Fork Hood River valley about 7 km (4.3 mi) (Wise, 1969; Sherrod and Scott, 1995; **Figure 2-1**).

5.4.4.1.2 Age

Lavas capping the eastern escarpment of the Hood River graben are assigned a latest Pliocene or Quaternary age on the basis of plateau-capping or intracanyon stratigraphic relationships, spatial and temporal association with still present cinder cones and domes, and isotopic ages (**Figure 5-4f**; Plate 1). Isotopic ages include 2.52 ± 0.13 Ma (K-Ar) for the basalt of Horkelia Meadow (**Qrbh**), 2.35 ± 0.13 Ma (K-Ar) for the basalt of Bennett Pass Road (**Qrbp**), and 2.06 ± 0.08 Ma and 2.26 ± 0.08 Ma (K-Ar) for the basaltic andesite of Blue Bucket Springs (**Qrbb**) (**Table 5-1**; Plate 1). The basaltic andesite of Dog River (**Qr5dr**) has an $^{40}Ar/^{39}Ar$ plateau age of 1.87 ± 0.01 Ma (groundmass; sample 178 DFWJ 15); Anderson (1987) reported a K-Ar age of 1.7 ± 0.4 Ma (whole-rock; sample JA85022) for this unit for a sample collected along South Fork Mill Creek (northeast of the map area). The microdiorite of Brooks Meadow (**Qrab**) has an $^{40}Ar/^{39}Ar$ plateau age of 1.18 ± 0.01 Ma and a single crystal hornblende age of 1.91 ± 0.22 Ma (groundmass, hornblende; sample 51 MCB-DRJ 17; **Table 5-1**; Plate 1).

Younger lavas assigned as products of regional Quaternary volcanoes include the basaltic andesite and andesite of Cloud Cap (**Qr4cc**) with a K-Ar age of 424 ± 19 ka (Scott and Gardner, 2017), and the Holocene andesite of Parkdale (**Qr1pk**). There is no direct age for the andesite of Parkdale (**Qr1pk**), but charcoal collected below the flow (Harris, 1973; 6,890 ± 130) has a calibrated radiocarbon age of 7,510–7,970 cal yr BP (2-σ uncertainty). The relationship between the Parkdale lava and the 7,700-yr-old Mazama ash, whose original fallout thickness across the northern part of Mount Hood was at least several centimeters, is uncertain.

5.4.4.2 Products of Mount Hood and pre-Mount Hood composite volcanoes

5.4.4.2.1 Distribution, composition, and lithology

Mount Hood is a Middle Pleistocene to Holocene stratovolcano composed of a sequence of lava flows, domes, and fragmental deposits. Its summit is located 5.7 km (3.5 mi) west of the Dog River–Badger Lake

area (**Figure 2-1**, **Figure 2-2**, **Figure 5-2**). Throughout its ~500,000-year history, Mount Hood has erupted in two basic modes: 1) andesitic lava flows that extend up to 12 km (7.5 mi) from now obscured vents or 2) andesitic and dacitic lava domes in the summit area that produced large volumes of fragmental debris from pyroclastic flows and lahars (**Figure 5-4g**). Lahars generated by pyroclastic flows that swiftly melted snow and ice, as well as lahars generated by large landslides, have surged tens of kilometers farther down valleys (Crandell, 1980; Cameron and Pringle, 1986, 1987; Scott and others, 1997a,b; Scott and others, 2003; Pierson and others, 2011; Scott and Gardner, 2017). Tephra-fall deposits of latest Pleistocene and late Holocene age, derived chiefly from ash clouds of pyroclastic flows and minor explosive eruptions are not mapped, but mantle broad areas in the western part of map to thicknesses of as much as 50 cm (19.7 in); in the eastern part of the map area, tephra is much thinner and mostly admixed into soil by surficial processes. Products of Mount Hood volcano and its earlier Quaternary predecessors are similar in mineralogy, texture, and chemical composition. Lavas are mostly 58.8 to 64.5 weight percent SiO_2 and range through about one percent K_2O at a given silica content (**Figure 5-5**); all are crystal-rich with plagioclase dominating a variable mafic mineral content of orthopyroxene or orthopyroxene>clinopyroxene, iron-titanium oxides, and, in some samples, amphibole; olivine is rare. Light-colored, rounded, mafic enclaves of mostly basaltic andesite composition consisting of plagioclase, pyroxene, and occasionally amphibole, but not olivine, are present in variable proportions in most units.

Eruptions of pre-Hood composite volcanoes were similar in style and composition to products of Mount Hood during the past 500,000 years (Scott and Gardner, 2017). Pre-Hood lavas are found scattered on west, north, and east flanks of Mount Hood in small valley-bottom exposures or forming ridges roughly radial to, but distant from, the current edifice (**Figure 5-4g**). Vent areas for pre-Hood lavas are unknown but probably lay within a couple of kilometers of the summit of Mount Hood. In the map area, these flows are found as intracanyon lavas (**Qphe**, **Qphm**) banked against the southern end of Bluegrass Ridge, north of Newton Creek, and as ridge-capping exposures along Doe Creek (**Qphd**) (**Figure 2-1**).

5.4.4.2.2 Age

Pre-Mount Hood lava flows in the map area have reported K-Ar ages of 931 ± 15 ka (whole rock; sample 91T-84) on the andesite of Doe Creek (**Qphd**) in the northwest part of the map area and ~1.5 Ma on the andesite of Elk Meadows Trail (**Qphm**) exposed along the southern end of Bluegrass Ridge (Scott and Gardner, 2017; **Figure 2-1**; **Table 5-1**; Plate 1).

Scott and Gardner (2017) reported on a selection of ~80 K-Ar and $^{40}Ar/^{39}Ar$ isotopic ages that have been obtained from Mount Hood volcano. The volcano has erupted episodically for the past 500,000 years, including the Polallie eruptive period from ~30 to 15 ka and two late Holocene eruptive periods at 1.5 ka and events in the late 18th century. The distal ends of at least eight Mount Hood lavas extend eastward into the Dog River–Badger Lake area spanning the first three time periods. The oldest is the 475 ± 14 ka (K/Ar; whole rock; sample 931029-6) andesite of Tilly Jane Creek (**Qh4tj**); the youngest is the andesite of Langille Crags (**Qh3lc**) with ages of 56.7 ± 3 ka ($^{40}Ar/^{39}Ar$; whole rock; sample 950705-2), 46.1 ± 2.23 ka ($^{40}Ar/^{39}Ar$; whole rock; sample 920820-1), 44 ± 9 ka (K/Ar; whole rock; sample 950705-2), and 29 ± 11 ka (K/Ar; whole rock; sample 920820-1) (**Figure 5-4g**; **Table 5-1**). The latter time period between ~30 and 15 ka corresponds to the Polallie eruptive episode (Crandell, 1980), which spans both the maximum extent and recession of valley glaciers during the last ice age. During Polallie time lava domes and stubby lava flows built much of the upper 600 m (1968) of Mount Hood volcano (Scott and Gardner, 2017). Activity primarily consisted of the collapse of near-summit domes and flows to produce extensive fragmental pyroclastic-flow and lahar deposits **(Qh2pc)** emplaced in broad fans or thick channel fills. Some of this material was emplaced on ridge tops flanked by extensive glaciers or directly on glaciers and

transported to end moraines or left as hummocky stagnant-ice deposits. Coeval ash clouds of the flows deposited thick, fine-grained tephra on the flanks of Mount Hood and in the Upper Hood River Valley (**Figure 2-1**).

5.4.5 Upper Cenozoic surficial deposits

5.4.5.1 Alluvial, colluvial, and glacial deposits

5.4.5.1.1 Distribution, composition, and lithology

Much of the Dog River–Badger Lake area is covered by unconsolidated or only slightly indurated sedimentary units, including glacial deposits, alluvial-plain deposits, and valley fringing landslide, colluvial, fan deposits, and modern fill and construction material (**Figure 5-4h-i**; Plate 1).

Mapped glacial deposits consist chiefly of till and minor outwash, forming belts of end moraines and thick ground moraines that obscure underlying lava flows (**Figure 5-4h**; Plate 1). Till deposited during the Suttle Lake advance is separated into two units. Unit **Qgsp**, mapped chiefly along Tilly Jane Creek and East Fork Hood River, is rich in clasts of dome lava of Polallie eruptive period (**Figure 2-1**; Plate 1). Pyroclastic debris shed from growing Mount Hood summit lava domes of Polallie age accumulated on glaciers, was transported as superglacial drift, and deposited as end moraines or as hummocky ground moraine as debris-covered glacier ice downwasted and stagnated. Other Suttle Lake advance till (**Qgst**) consists chiefly of clasts of dense andesite derived from Mount Hood lava flows, but also include minor dome lava and basaltic andesite and andesite of regional volcanoes, and older rocks (Plate 1). Outwash deposits (**Qgso**) forms stratified gravel deposits in valleys downstream from coeval till deposits (Plate 1). In many valleys draining Mount Hood, outwash is interbedded with lahar deposits generated by lava dome growth and collapse during the Polallie eruptive period. Undifferentiated till (**Qgot**), older than the Suttle Lake advance, is also present in parts of the map area, forming muted moraines, filling small valleys and cirques, and capping older bedrock (Plate 1). These tills were chiefly deposited in ground or lateral moraines. Older till deposits (**Qgot**) are typically poorly exposed and may include till of several glaciations.

The major rivers draining Mount Hood transport sediment derived from glacier and snow melt, storm- and landslide-generated debris flows, and post-eruptive erosion. The rivers also convey syneruptive lahars and related sediment, but we map those under Products of Mount Hood volcano. Alluvium occurs along most small to large stream channels in the map area (**Qa**) and at the mouths of channels (**Qaf**) (**Figure 5-4i**; Plate 1). Major streams in the area, such as East Fork Hood River, Meadows Creek, Clarks Creek, and Newton Creek, draining the southeast sector of Mount Hood volcano, are characterized by a complex network of channels that we map showing intricate areas of older to recent alluvial, terrace, and debris flow deposits (**Qalr**, **Qaly**, **Qalo**) (**Figure 2-1**, **Figure 5-4h**; Plate 1). Pond and marsh deposits are mapped in Elk Meadows (**Qafg**) (**Figure 2-1**, **Figure 5-4i**; Plate 1). Most slopes in the area are mantled by thick wedges of colluvium (**Qc**), active talus (**Qt**), and landslide deposits (**Qls**) which locally, partially to fully obscure underlying bedrock (**Figure 5-4i**; Plate 1). Lidar topography reveals that many colluvial mantled slopes in the area are characterized by distinct tongues, lobes, and lobate terraces that may be the result of solifluction, the slow flowage of saturated soils downslope in areas that were underlain by permanently frozen ground during past ice ages.

5.4.5.1.2 Age

During the last glacial maximum about 25 to 20 ka, glaciers radiated outward from Mount Hood up to 15 km (9.3 mi) along major valleys and deposited till of the Suttle Lake advance (**Qgst**), which is broadly

equivalent to glacial deposits of Evans Creek age in the Washington Cascade Range (**Figure 2-1**, **Figure 5-4h**; Plate 1). Recessional till deposits are probably as young as 15 ka. Age constraints on older tills (**Qgot**) are few. Between Crystal Spring Creek and Evans Creek, older till forms a bulky lateral moraine that is banked against the 424-ka basaltic andesite and andesite of Cloud Cap (**Qr4cc**) (**Figure 2-1**, **Figure 5-4h**; Plate 1). On the basis of comparison to glacial sequences elsewhere in the Pacific Northwest, parts of the unit **Qgot** could be as young as marine oxygen isotope stage 6 (about 150 ka).

Alluvial deposits are largely Holocene in age with older deposits extending back into the late Pleistocene. Age constraints are few. Gravelly alluvium and bouldery debris-flow deposits forming terraces and fans along Clark and Newton Creeks (**Qalo**) have radiocarbon ages of about 1,500 cal yr BP and are mantled by tephra of the 1.5-ka Timberline and late 18th century Old Maid eruptive periods. Stream alluvium (**Qaly**) mapped along East Fork Hood River and those draining Mount Hood is inset into ~30 to 15 ka deposits of the Polallie eruptive episode (**Qh2pc**) unit **Qalo** (**Figure 2-1**; Plate 1). Although not formed directly by eruptive processes, some debris-flow deposits may record rock avalanches from older parts of the volcano generated by earthquakes or edifice deformation related to magma intrusion.

6.0 EXPLANATION OF MAP UNITS

The Explanation of Map Units describes the basis for subdividing rocks into stratigraphic units on the geologic map shown on Plate 1. A time-rock chart graphically displaying age ranges and relationships for the 128 late Cenozoic bedrock and surficial units is shown in **Figure 6-1** and on Plate 1. Unit names follow formal stratigraphic names or local stratigraphic nomenclature when available; informal names are given on the basis of composition or sites of good exposure when formal rock names are lacking.

Formal stratigraphic names have been established only for the CRBG; those rocks are assigned to units following conventions established by Tolan and others (1989, 2009a) and Reidel and others (2013). The Dalles Formation is formally named, but separate strata within the formation are only informally named. Few Cascade Range units have been formally named, and none in the map area. Late Miocene to Holocene Cascade volcanic rocks in the Dog River–Badger Lake area are subdivided here on the basis of conventions established by Peck and others (1964), Priest and others (1983), Priest (1990), and Conrey and others (1997) for rocks of the Cascade Range. Priest and others (1983) divided rocks of the Western Cascades into four time-stratigraphic units on the basis of apparent time breaks that generally correspond to regional compositional changes. These time- stratigraphic intervals include: 1) an early Western Cascade episode between 40 and 18 Ma; 2) a late Western Cascade episode between 18 and 9 Ma; 3) an early High Cascade episode between 9 and 4 Ma; and 4) a late High Cascade episode from 4 Ma to present. Rocks of the late Miocene to early Pliocene Dalles Formation correspond to volcanism during an early High Cascades episode from 9 to 4 Ma, while younger Pliocene to Holocene volcanic rocks are considered part of the 4 Ma to present late High Cascades episode. CRBG lavas are temporally correlative with the late Western Cascade episode, but are not included within this stratigraphic interval, as they were erupted from distant vents located in northeast Oregon and southeast Washington (**Figure 5-7**). Ancestral Cascades rocks (**Toav**), exposed beneath the CRBG a short distance north of the map area, are equivalent to the early Western Cascade episode of Priest and others (1983).

6.1 Overview of map units

UPPER CENOZOIC SURFICIAL DEPOSITS

COLLUVIAL DEPOSITS

Qf modern fill and construction material (upper Holocene)
Qt talus (Holocene and Upper Pleistocene [?])
Qc colluvium (Holocene and Upper Pleistocene [?])
Qls landslide deposits (Holocene and Upper Pleistocene [?])

ALLUVIAL DEPOSITS

Qalr prominent recent debris-flow deposits (upper Holocene)
Qaly younger alluvium and debris-flow deposits (upper Holocene)
Qalo older alluvium and debris-flow deposits (upper Holocene)
Qafg fine-grained alluvium, pond, and marsh deposits (Holocene)
Qa gravelly alluvium (Holocene and Upper Pleistocene [?])
Qaf fan deposits (Holocene and Upper Pleistocene [?])
Qtu upper fluvial terrace deposits (Upper Pleistocene)

GLACIAL DEPOSITS

Qgsp Till of Suttle Lake advance (of Cabot Creek glaciation of Scott, 1977) rich in clasts of dome lava of Polallie eruptive period (Upper Pleistocene)

Qgst Till of Suttle Lake advance (of Cabot Creek glaciation of Scott, 1977) with no or minor dome lava (Upper Pleistocene)

Qgso outwash of Suttle Lake advance (of Cabot Creek glaciation of Scott, 1977) (Upper Pleistocene)

Qgot older till (Middle Pleistocene [?])

Unconformity

UPPER CENOZOIC VOLCANIC AND SEDIMENTARY ROCKS

QUATERNARY AND/OR UPPER PLIOCENE VOLCANIC AND SEDIMENTARY ROCKS OF THE LATE HIGH CASCADES

PRODUCTS OF MOUNT HOOD VOLCANO

Qh2pc diamicts of Polallie eruptive period (Upper Pleistocene)

Qh3lc andesite of Langille Crags (Upper Pleistocene) 29 ± 11 ka (K-Ar), 46.1 ± 2.2 ka ($^{40}Ar/^{39}Ar$); 44 ± 9 ka (K-Ar), 56.3 ± 3 ka ($^{40}Ar/^{39}Ar$)

Qh3cf andesite of Coe Falls (Upper Pleistocene) ~90 ka (K-Ar)

Qhcwl lahar deposits of Whiskey Creek (Upper and Middle Pleistocene)

Qh4cs andesite of Cold Spring Creek (Middle Pleistocene) ~150 to 200 ka (K-Ar)

Qh4cp andesite of Cold Spring-Polallie divide (Middle Pleistocene) 180 ± 16 ka (K-Ar)

Qh4lb andesite of Lamberson Butte (Middle Pleistocene) ~150-200 ka ($^{40}Ar/^{39}Ar$, K-Ar)

Qh4gc andesite of lower Gnarl Ridge and North Fork Cold Spring Creek (Middle Pleistocene) 238 ka (K-Ar)

Qh4tj andesite of Tilly Jane Creek (Middle Pleistocene) 475 ± 14 ka (K-Ar)

Qhcgr diamict of Griswell Creek (Middle or lower Pleistocene)

Qhcu undifferentiated clastic deposits of Mount Hood (Pleistocene)

PRODUCTS OF PRE-MOUNT HOOD COMPOSITE VOLCANO

Qphd pre-Mount Hood andesite of Doe Creek (lower Pleistocene) 931 ± 15 ka (K-Ar)

Qphe pre-Mount Hood andesite of Elk Mountain (lower Pleistocene)

Qphm pre-Mount Hood andesite of Elk Meadows Trail (lower Pleistocene) ~1.5 Ma (K-Ar)

PRODUCTS OF REGIONAL QUATERNARY VOLCANOES

Qr1pk andesite of Parkdale (Holocene)

Qr4cc basaltic andesite and andesite of Cloud Cap (Middle Pleistocene) 424 ± 19 ka (K-Ar), 590 ± 30 ka (K-Ar)

Qrab microdiorite of Brooks Meadow (lower Pleistocene) 1.18 ± 0.01 Ma ($^{40}Ar/^{39}Ar$; groundmass); 1.91 ± 0.22 Ma ($^{40}Ar/^{39}Ar$; amphibole)

Qras microdiorite of Shellrock Mountain (lower Pleistocene)

Qrbv basalt and basaltic andesite vents (lower Pleistocene)

Qrai basaltic andesite intrusive rocks (lower Pleistocene) 1.83 ± 0.02 Ma ($^{40}Ar/^{39}Ar$)

Qr5dr basaltic andesite of Dog River (lower Pleistocene) 1.87 ± 0.01 Ma ($^{40}Ar/^{39}Ar$; groundmass); 1.51 ± 0.08 Ma ($^{40}Ar/^{39}Ar$; plagioclase); 1.7 ± 0.4 Ma (K-Ar)

Qrbhp basaltic andesite of High Prairie (lower Pleistocene)

Qrba basalt of Agnes Spring (lower Pleistocene)

Qrbw basaltic andesite of Ward Creek (lower Pleistocene)

Qrbc basalt of Cooks Meadow (lower Pleistocene)

Qrbb basaltic andesite of Blue Bucket Springs (lower Pleistocene) 2.06 ± 0.08 Ma (K-Ar); 2.26 ± 0.08 Ma (K-Ar)

Qrbp basalt of Bennett Pass Road (lower Pleistocene) 2.35 ± 0.03 Ma (K-Ar)

Qrbi gabbro norite intrusion (lower Pleistocene)

Qrbh basalt of Horkelia Meadow (lower Pleistocene or upper Pliocene) 2.52 ± 0.13 Ma (K-Ar)

Qrbu basalt, undifferentiated (lower Pleistocene or upper Pliocene [?])

Qr5ll basalt and basaltic andesite of Laurance Lake (lower Pleistocene [?] or upper Pliocene [?])

QTbk glomeroporphyritic basalt of Knebal Springs (lower Pleistocene [?] or upper Pliocene [?])

Disconformity

LOWER PLEISTOCENE AND PLIOCENE VOLCANIC AND SEDIMENTARY ROCKS OF THE LATE HIGH CASCADES

BADGER BUTTE VOLCANICS

Qbba basaltic andesite (lower Pleistocene)

Qbua andesite (lower Pleistocene)

Qbla andesite (lower Pleistocene) 2.44 ± 0.02 Ma ($^{40}Ar/^{39}Ar$; groundmass); 2.10 ± 0.09 Ma ($^{40}Ar/^{39}Ar$; plagioclase)

LOOKOUT MOUNTAIN VOLCANICS

Bluegrass Ridge area

QTai andesite intrusive rocks (lower Pleistocene)

QTdi dacite intrusive rocks (lower Pleistocene)

QTab6 andesite of Bluegrass Ridge, flow sequence 6 (lower Pleistocene)

QTab5 andesite of Bluegrass Ridge, flow sequence 5 (lower Pleistocene)

QTab4 andesite of Bluegrass Ridge, flow sequence 4 (lower Pleistocene)

QTab3 dacite of Bluegrass Ridge, flow sequence 3 (lower Pleistocene) 2.36 ± 0.03 Ma ($^{40}Ar/^{39}Ar$)

QTab2 andesite of Bluegrass Ridge, flow sequence 2 (lower Pleistocene)

QTab1 andesite of Bluegrass Ridge, flow sequence 1 (lower Pleistocene)

Lookout Mountain area

QTrl porphyritic rhyolite (lower Pleistocene or upper Pliocene)

QTal4 andesite of Lookout Mountain, flow sequence 4 (lower Pleistocene or upper Pliocene)

QTal3 andesite of Lookout Mountain, flow sequence 3 (lower Pleistocene or upper Pliocene)

QTal2 andesite of Lookout Mountain, flow sequence 2 (lower Pleistocene or upper Pliocene)

QTal1 andesite of Lookout Mountain, flow sequence 1 (lower Pleistocene or upper Pliocene)

QTa andesite (lower Pleistocene or upper Pliocene)

LOWER PLEISTOCENE AND PLIOCENE VOLCANIC ROCKS ALONG EAST FORK HOOD RIVER

QTbt High-TiO_2 basalt and basaltic andesite (lower Pleistocene and/or upper Pliocene [?]) 2.63 ± 0.01 Ma ($^{40}Ar/^{39}Ar$); 2.5 ± 0.026 Ma (K-Ar); 2.43 ± 0.14 Ma (K-Ar)

QTat andesite of Tumble Creek (lower Pleistocene or upper Pliocene) 2.74 ± 0.3 Ma (K-Ar)

QTpi intrusive rocks (lower Pleistocene or upper Pliocene)

Tpdf dacite of Fifteenmile Creek (upper Pliocene) 3.02 ± 0.02 Ma ($^{40}Ar/^{39}Ar$); 2.86 ± 0.06 Ma (K-Ar)

Tpds andesite and dacite of Senecal Spring (upper Pliocene) 3.14 ± 0.2 Ma (K-Ar)

Tprd rhyolite and volcaniclastic rocks (upper Pliocene)

Tpat andesite (upper Pliocene)

Tpre rhyolite of Elk Mountain (upper Pliocene)

Tpba basaltic andesite of Bluegrass Ridge (upper Pliocene)

Tptb tuff breccia (upper Pliocene)

Tprc porphyritic rhyolite of Culvert Creek (upper Pliocene)

Tpbb basaltic andesite (upper Pliocene)

Tpaf andesite of Fret Creek (upper Pliocene)

Tpdc porphyritic trachydacite of Culvert Creek (upper Pliocene) 3.77 ± 0.02 Ma ($^{40}Ar/^{39}Ar$; groundmass); 3.68 ± 0.07 Ma ($^{40}Ar/^{39}Ar$; plagioclase)

Tpda trachyandesite (upper Pliocene)

Tpbe basaltic andesite (upper Pliocene)

Tpbc basalt (upper Pliocene)

Tpdd tuff breccia of Engineers Creek (lower Pliocene)

Tpal andesite and dacite of Lunch Creek (lower Pliocene)

Tpdv trachydacite of Fivemile Creek (lower Pliocene) 3.69 ± 0.01 Ma ($^{40}Ar/^{39}Ar$); 3.7 ± 0.2 Ma (K-Ar)

Tpbl basalt (lower Pliocene)

Tpde dacite of Engineers Creek (lower Pliocene)

Tprn rhyolite of Engineers Creek (lower Pliocene)

Tpdu trachydacite (lower Pliocene)

Tpbr basalt and basaltic andesite of Rimrock Creek (lower Pliocene) 4.19 ± 0.01 Ma ($^{40}Ar/^{39}Ar$)

Disconformity

LOWER PLIOCENE AND UPPER MIOCENE VOLCANIC AND SEDIMENTARY ROCKS OF THE EARLY HIGH CASCADES

GUNSIGHT BUTTE VOLCANICS

Tpag andesite of Gumjuwac Saddle (lower Pliocene) 4.25 ± 0.6 Ma (K-Ar)

Tpms dacite (lower Pliocene)

Tpmj andesite (lower Pliocene)
Tpmp andesite (lower Pliocene)
Tpmc andesite (lower Pliocene)
Tpmb3 basaltic andesite, upper flows (lower Pliocene)
Tpmb2 basaltic andesite, middle flows (lower Pliocene)
Tpmb1 basaltic andesite, lower flows (lower Pliocene)
Tpmh basaltic andesite, undifferentiated (lower Pliocene)
Tpmn andesite (lower Pliocene)
Tpmd dacite (lower Pliocene)
Tpmi andesite dikes (lower Pliocene)
Tpmu dacite of Bennett Pass Road (lower Pliocene)
Tpmt tuff breccia of Bennett Pass Road (lower Pliocene)
Tpml dacite of Pocket Creek (lower Pliocene)
Tpma andesite (lower Pliocene)
Tpmv Gunsight Butte volcanics, undivided (lower Pliocene or upper Miocene [?])

Disconformity to nonconformity

DALLES FORMATION

Tmdl Dalles Formation, undivided (lower Pliocene [?] and upper Miocene)
Tmdei microdiorite of East Fork (lower Pliocene [?] or upper Miocene) 5.37 ± 0.06 Ma ($^{40}Ar/^{39}Ar$; groundmass); 8.78 ± 0.29 Ma ($^{40}Ar/^{39}Ar$; plagioclase)
Tmda plagioclase-microporphyritic dacite of Surveyors Ridge Road (upper Miocene)
Tmdy hornblende-porphyritic dacite of Surveyors Ridge Road (upper Miocene) 6.2 ± 1.3 Ma (K-Ar)
Tmde andesite and dacite of East Fork (upper Miocene) 7.15 ± 0.8 Ma (K-Ar), 8.18 ± 0.06 Ma (K-Ar)

Mill Creek Buttes

Tmdm plagioclase- and hornblende-porphyritic dacite of Mill Creek Buttes (upper Miocene) 6.83 ± 0.01 Ma ($^{40}Ar/^{39}Ar$)
Tmdh hornblende-porphyritic microdiorite of Mill Creek Buttes (upper Miocene)
Tmdi hornblende-porphyritic microdiorite of Mill Creek Buttes Lookout (upper Miocene) 7.5 ± 0.4 Ma (K-Ar)
Tmdf dacite of Fivemile Butte, upper flow (upper Miocene)
Tmdv dacite of Fivemile Butte, lower flows and domes (upper Miocene) 7.71 ± 0.17 Ma (K-Ar)
Tmdw dacite of Wolf Run (upper Miocene) 7.91 ± 0.01 Ma ($^{40}Ar/^{39}Ar$)
Tmdp hornblende-porphyritic dacite of Puppy Creek (upper Miocene)
Tmdc andesite (upper Miocene)
Tmdr tuff of Rim Rock (upper Miocene)

Angular unconformity to disconformity

MIDDLE AND LOWER MIOCENE VOLCANIC ROCKS

COLUMBIA RIVER BASALT GROUP

Wanapum Basalt

Frenchman Springs Member

Twfs Basalt of Sentinel Gap (middle or lower Miocene)

Twfh Basalt of Sand Hollow (middle or lower Miocene)

Disconformity — Vantage Member of the Ellensburg Formation

Grande Ronde Basalt

Normal-polarity (N2) magnetostratigraphic unit

Tgsb Sentinel Bluffs Member (lower Miocene)

Tgww Winter Water Member (lower Miocene)

Tgo Ortley member (lower Miocene)

Reversed-polarity (R2) magnetostratigraphic unit

Tggc Grouse Creek member (lower Miocene)

Unconformity

OLIGOCENE VOLCANIC ROCKS

Toav Oligocene volcanic rocks, undivided (upper Oligocene) (cross section only) 26.29 ± 0.03 Ma ($^{40}Ar/^{39}Ar$)

OTHER ROCKS

QTfb fault breccia (Pleistocene [?] to upper Miocene [?])

Figure 6-1. Time-rock chart showing the 128 geologic units shown on the geologic map and geologic cross sections on Plate 1. Note that depth of exposure in the map area does not extend beneath the Grouse Creek Member (Tggc).

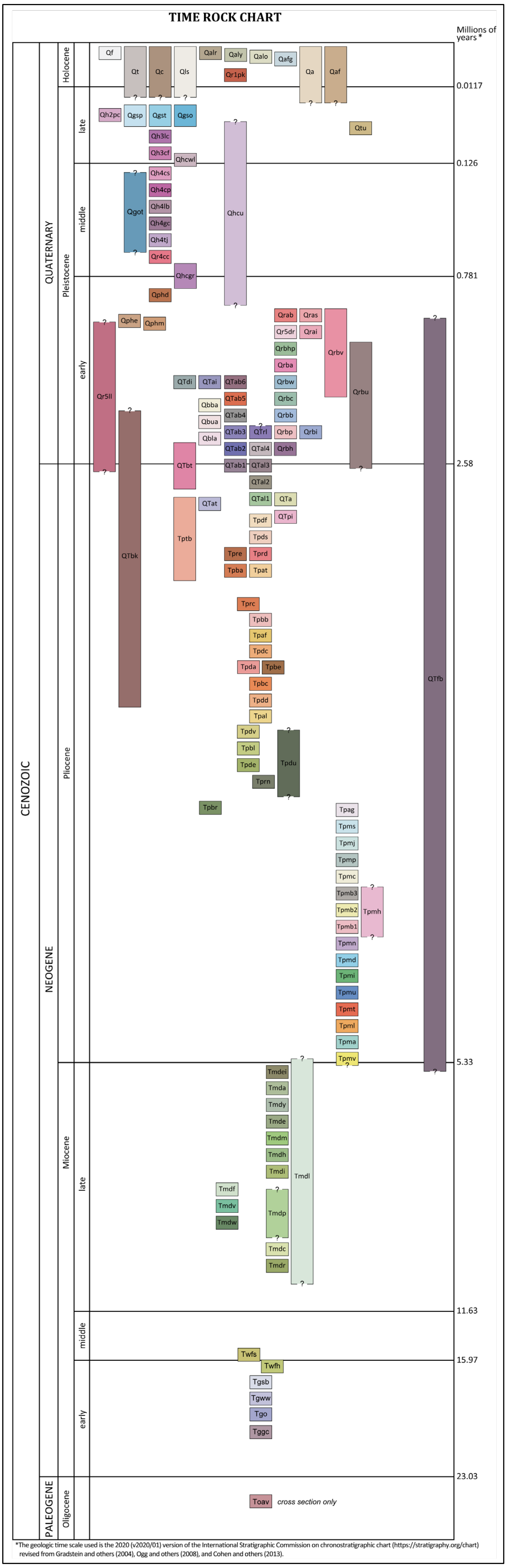

6.2 Upper Cenozoic surficial deposits

6.2.1 Colluvial deposits

Qf **modern fill and construction material (upper Holocene)**—Artificial or constructed fill deposits of poorly sorted and crudely layered mixed gravel, sand, clay, and other engineered fill (Plate 1). These deposits usually contain rounded to angular clasts ranging from small pebbles up to several meters across. The orientation of clasts is typically less uniform than is found in naturally occurring imbricated or bedding-parallel gravel. Older fills are likely uncompacted versus newer fills, which are likely engineered and reinforced using geotextiles or retaining structures. Deposits mapped as modern fill and construction material in the map area are generally associated with road embankments, causeways, culvert fills, and mined land (Plate 1). The thickness of fill-deposits may exceed 30 m (98 ft). Unit **Qf** is assigned a late Holocene age.

Qt **talus (Holocene and Upper Pleistocene [?])—**Blocky to platy, open-work detritus typically forming broad aprons below steep cliff-forming outcrops. The unit includes unvegetated areas of active talus intermixed with areas partially stabilized by local soil development and encroaching vegetation. Talus deposits are often associated with frost-heaved outcrops at higher elevations or on south- or west-facing slopes (Plate 1). Unit **Qt** is assigned a Late Pleistocene and Holocene age on the basis of stratigraphic position.

Qc **colluvium (Holocene and Upper Pleistocene [?])—**Unconsolidated poorly sorted deposits of rock and soil deposited along valley walls and as fans and aprons of debris at the foot of steep slopes (Plate 1). Unit **Qc** locally includes now completely vegetated talus deposits, debris-flow deposits, and coarse-grained alluvium. Thickness of colluvial deposits is highly varied; maximum thickness is several meters. Unit **Qc** is assigned a Late Pleistocene and Holocene age on the basis of stratigraphic position.

Qls **landslide deposits (Holocene and Upper Pleistocene [?])—**Unconsolidated, chaotically mixed masses of rock and soil deposited by landslides, including slumps, slides, earthflows, debris flows, and rock avalanches (Plate 1). Landslides in the area are chiefly derived from rocks of late Miocene and Pliocene age with failures along dip-slopes underlain by strata of contrasting lithologies. Landslide terrain is characterized by irregular sloping hummocky surfaces, closed depressions, springs, and wet seeps. Toes to more recent deposits retain convex-up, fan-shaped morphologies. Slides are often traceable uphill to head scarps or failure surfaces. In deeper landslides, these head scarps commonly expose bedrock. Deposits in the map area typically consist of simple slump or shallowly-seated earthflow-type features covering areas ≤6 hectares (<15 acres) and up to 32 hectares (77 acres). Thickness of landslide deposits is highly varied, but may be more than several tens of meters in larger deposits. Landslide deposits range in age from Late Pleistocene, to those that have been recurrently active in the Holocene.

6.2.2 Alluvial deposits

The major rivers draining Mount Hood transport sediment derived from normal glacier and snow melt, storm- and landslide-generated debris flows, and post-eruptive erosion. The rivers also convey syneruptive lahars and related sediment, but we map those under products of Mount Hood volcano.

Qalr **prominent recent debris-flow deposits (upper Holocene)—**Bouldery debris-flow deposits preserved along Newton Creek and generated by intense rainstorms since 2000, chiefly November 2006 (**Figure 2-1**; Plate 1).

Qaly **younger alluvium and debris-flow deposits (upper Holocene)—**Chiefly gravel and sand that forms valley fills, terraces, and fans along streams heading on Mount Hood, in particular East Fork Hood River (**Figure 2-1**; Plate 1). Deposits range from well-stratified alluvial gravel and sand, to glacial outwash, to massive, non stratified bouldery deposits of debris flows. Unit **Qaly** includes extensive incised terraces of unstratified, poorly sorted, muddy, sandy gravels and gravelly, muddy sands deposited along Polallie Creek by a flood and debris flow occurring on Christmas Day 1980 (Gallino and Pierson, 1985; Scott and Gardner, 2017; **Figure 2-1**, Plate 1). The debris flow terminated at the mouth of Polallie Creek and temporarily dammed East Fork Hood River. Distal deposits of the Christmas Day 1980 flood are also found along East Fork Hood River, north of the mouth of Polallie Creek, partly resulting from the breakout of the temporary debris flow dam that blocked East Fork Hood River (Gallino and Pierson, 1985). Unit **Qaly** is assigned a late Holocene age on the basis of stratigraphic position, inset into unit **Qalo;** parts of the unit have been deposited in historic times (Gallino and Pierson, 1985). The unit may include deposits containing man-made debris or artifacts.

Qalo **older alluvium and debris-flow deposits (upper Holocene)—**Gravelly alluvium and bouldery debris-flow deposits that form terraces and fans along Clarks and Newton Creeks (**Figure 2-1**; Plate 1). Unit **Qalo** is distinguished by a mantle of late Holocene tephra of Old Maid and(or) Timberline eruptive periods, weak soil development, and radiocarbon ages of about 1,500 cal yr BP. The age is roughly coincident with the Timberline eruptive period of Mount Hood, which did not directly affect these valleys with pyroclastic flows or lahars related to lava-dome growth. Some debris-flow deposits are rich in hydrothermally altered material that originated as landslides from near-Mount Hood summit areas of hydrothermal alteration.

Qafg **fine-grained alluvium, pond, and marsh deposits (Holocene)—**Chiefly sand and mud, locally rich in organic matter, and minor fine gravel in depressions or poorly drained alpine wetlands, such as Elk Meadows along the southwest edge of the map area (**Figure 2-1**; Plate 1). In Elk Meadows, unit **Qafg** includes interbedded and laminated Old Maid and Timberline tephras of latest Holocene age (Scott and Gardner, 2017).

Qa **gravelly alluvium (Holocene and Upper Pleistocene [?])—**Unconsolidated, poorly- to moderately-stratified gravel and sand along streams preserved in uplands south and east of East Fork Hood River (**Figure 2-1**; Plate 1). Unit **Qa** includes gravelly alluvium preserved in the headwaters of Cold Spring Creek, west of Bluegrass Ridge, and two isolated gravel patches, of unknown age, preserved above unit **Qr4cc** in the northwest part of the map area. Thickness of unit **Qa** is generally <10 m (33 ft); bedrock units may be locally exposed in the base of stream channels within areas

mapped as unit **Qa**. Unit **Qa** is assigned a Late Pleistocene and Holocene age on the basis of stratigraphic position and a lack of more precise age indicators.

Qaf **fan deposits (Holocene and Upper Pleistocene [?])—**Unconsolidated, poorly sorted, poorly graded deposits of boulders, cobbles, pebbles, granules, sand, silt, and clay in upland drainages and as fan-shaped accumulations at the transition between low-gradient valley floodplains and steeper uplands (Plate 1). Individual fans generally cover less than 2 hectares (5 acres). The local thickness of alluvial fan deposits is variable but is probably <15 m (50 ft). Unit **Qaf** includes fan deposits of Late Pleistocene and Holocene age.

Qtu **upper fluvial terrace deposits (Upper Pleistocene)—**Dissected, unconsolidated deposits of gravel and sand, with subordinate amounts of silt and clay forming an upper terrace ~27 to >30 m (90 to >100 ft) above the modern floodplain of East Fork Hood River, south of the mouth of Cold Springs Creek (**Figure 2-1**; Plate 1). The terrace is visible on 1-m lidar DEMs as a planar to very gently sloping, equal-elevation surface (tread) on both sides of the modern channel. Steeper descending slopes (risers) define the streamside edges of the terrace deposits. Unit **Qtu** is considered to be older than ~30 to 15 ka Polallie eruptive deposits, which infill streamside edges along East Fork Hood River (**Figure 2-1**; Plate 1). Distribution of the terrace exclusively to the south of the mouth Cold Spring Creek suggests formation at ~46 Ma when the andesite of Langille Crags (**Qh3lc**) filled the ancestral valley of East Fork Hood River to a depth of 50 to 80 m (164 to 262 ft), terminated against the ancestral east valley wall, and blocked the north-flowing East Fork Hood River (**Figure 2-1**, Plate 1; Scott and Gardner, 2017). The Langille Crags (**Qh3lc**) lava flow dam caused aggradation upstream (south) as flanking fans graded to East Fork; it may have persisted for some time before East Fork Hood River cut through to a lower base level.

6.2.3 Glacial deposits

Mapped glacial deposits consist chiefly of till and minor outwash. During the last glacial maximum about 25 to 20 ka, glaciers radiated outward from Mount Hood up to 15 km (9 mi) along major valleys. Deposits of pre-last glacial maximum age are mapped locally beyond the last maximum glacial limit.

Qgsp **Till of Suttle Lake advance (of Cabot Creek glaciation of Scott, 1977) rich in clasts of dome lava of Polallie eruptive period (Upper Pleistocene)—**Very poorly sorted, angular to sub-rounded pebbles, cobbles, and boulders in a silty sand matrix. Many clasts are faceted into crude pentagonal shapes and some are striated. The unit chiefly forms belts of end moraines and thick ground moraines that obscure underlying lava flows. Unit **Qgsp** till is distinguished by a high content (tens of percent to essentially all) of low-density clasts of andesite and dacite dome lava of the Polallie eruptive period (**Qh2pc**; SiO_2 = 60.6 to 63.9 weight percent; *n* = 22 analyses). We infer that these deposits represent pyroclastic debris shed from a growing Mount Hood summit lava domes of Polallie age that accumulated on glaciers, were transported as superglacial drift, and deposited as end moraines or as hummocky ground moraine as debris-covered glacier ice downwasted and stagnated. Unit **Qgsp** is mapped chiefly along Tilly Jane Creek and East Fork Hood River (**Figure 2-1**; Plate 1). The degree of soil development and weathering is similar to that described for unit **Qgst**.

Qgst **Till of Suttle Lake advance (of Cabot Creek glaciation of Scott, 1977) with no or minor dome lava (Upper Pleistocene)—**Unconsolidated, very poorly sorted, angular to sub-rounded pebbles, cobbles, and boulders in a silty sand matrix. Many clasts are faceted into crude pentagonal shapes and some are striated. Unit **Qgst** chiefly forms belts of forested end moraines and thick ground moraines that obscure underlying lava flows. Moraines mark the extent of glaciers during the last glacial maximum and recessional stages (Plate 1). Clasts are chiefly dense andesite derived from Mount Hood lava flows, but also include minor dome lava and basaltic andesite and andesite of regional volcanoes, and older rocks. Typical soils formed in till and mantle of fine-grained eolian and ash-cloud deposits of Polallie age consist of oxidized B horizons about 25 to 40 cm thick (9.8 to 15.7 in) that locally contain pods of Mazama ash (~7.7 ka) and display no clay accumulation; weathering rinds ≤0.2 mm thick (0.008 in) on fine-grained clasts from B horizon.

Qgso **outwash of Suttle Lake advance (of Cabot Creek glaciation of Scott, 1977) (Upper Pleistocene)—**Unconsolidated, subrounded to rounded cobbles and pebbles in a sandy matrix. Unit **Qgso** forms stratified gravel deposits in valleys downstream from coeval till deposits (Plate 1). In many valleys draining Mount Hood, outwash is interbedded with lahar deposits generated by lava dome growth and collapse during the Polallie eruptive period; such deposits are mapped as diamicts of Polallie eruptive period (**Qh2pc**).

Qgot **older till (Middle Pleistocene [?])—**Unconsolidated, very poorly sorted, angular to sub-rounded pebbles, cobbles, and boulders in a fine-grained silty sand matrix. Many clasts are faceted into crude pentagonal shapes and some are striated. Unit **Qgot** forms muted moraines, fills small valleys and cirques, and forms caps above older bedrock of well-weathered deposits displaying argillic B horizons tens of centimeters thick with weathering rinds 1 mm (0.04 in) or thicker on fine-grained clasts. Deposits are typically poorly exposed and may include tills of several glaciations. Age constraints are few. In the Dog River–Badger Lake area, unit **Qgot** includes poorly-exposed till capping Elk Mountain and till found within cirque basins along the southeast flank of Bluegrass Ridge and in the headwaters of Fifteenmile and Fret creeks (**Figure 2-1**; Plate 1). One of the largest and best preserved moraines mapped as part of unit **Qgot** is a bulky lateral moraine in the northwest part of the map area between Crystal Spring Creek and Evans Creek that is banked against ~424-ka basaltic andesite and andesite of Cloud Cap (**Qr4cc**) (**Figure 2-1**; Plate 1). On the basis of comparison to glacial sequences elsewhere in the Pacific Northwest, parts of unit could be as young as marine oxygen isotope stage 6 (about 150 ka). Unit **Qgot** till was chiefly deposited in ground or lateral moraines. The map label on plate 1 is queried for possible glacial deposits of unknown age mapped on the north-side of Lunch Creek (Plate 1).

Unconformity

6.3 Upper Cenozoic volcanic and sedimentary rocks

6.3.1 Quaternary and/or upper Pliocene volcanic and sedimentary rocks of the late High Cascades

6.3.1.1 Products of Mount Hood volcano

Qh2pc **diamicts of Polallie eruptive period (Upper Pleistocene)—**Sequences of bouldery, gravelly, non-sorted, massive 1- to >3 m-thick (3.3 to >6.3 ft) beds with a sandy matrix. Prismatically jointed blocks sampled from deposits are andesite and dacite lava (SiO_2 = 61.94 to 63.73 weight percent; K_2O = 1.27 to 1.68 weight percent; *n* = 9 analyses). Unit **Qh2pc** deposits primarily formed by pyroclastic flows and related lahar and colluvial deposits from growing lava domes at and near the summit of Mount Hood (**Figure 2-1**). Eruptions during the last ice age are recorded in the map area chiefly by till and outwash rich in dome lava (see Glacial Deposits, unit **Qgsp**), whereas dome growth during glacial retreat formed thick fills of fragmental deposits, now incised, along Polallie Creek, East Fork Hood River, and upper White River (**Figure 2-1**, Plate 1). Unit **Qh2pc** is assigned a Late Pleistocene age on the basis of association with the ~30 to 15 ka Polallie eruptive episode (Crandell, 1980; Scott and Gardner, 2017).

Qh3lc **andesite of Langille Crags (Upper Pleistocene)—**Andesite lava flows (SiO_2 = 60.16 to 62.19 weight percent; K_2O = 1.40 to 1.88 weight percent; *n* = 14 analyses) exposed widely on the north flank of Mount Hood and forming conspicuous valley-filling lobes south of Polallie Creek and between the main and South Fork of Polallie Creek (**Figure 2-1**; Plate 1; **Table 6-1**; Appendix; Scott and Gardner, 2017). Lava flows forming the unit are typically characterized by high K_2O (1.7 to 1.8 weight percent) and Sr (830 to 1050 ppm), but flows exposed between the forks of Polallie Creek have moderate K_2O (1.4 to 1.5 weight percent) and Sr (about 700 ppm). The unit is up to 95 m thick (312 ft) in the vicinity of Tamanawas Falls (**Figure 2-1**; Plate 1). Typical hand samples of the andesite are very light gray (N8) to medium gray (N5) with 5 to 15 percent (vol.) clear, blocky to prismatic plagioclase microphenocrysts and phenocrysts to 3 to 5 mm (0.1 to 0.2 in), 6 percent (vol.) greenish black (5GY2/1) to dusky red (5R 3/4) weathered, blocky pyroxene microphenocrysts ≤1 mm (0.04 in) (orthopyroxene > clinopyroxene), and 3 percent microphenocrysts of amphibole (replaced by Fe-Ti oxides), contained within a fine-grained holocrystalline groundmass. The valley-filling lava flow dammed East Fork Hood River, which has since incised a narrow canyon between the flow and upper Neogene rocks exposed on the east; about 75 m (246 ft) of the lava is well exposed near Tamanawas Falls (**Figure 2-1**; Plate 1). Unit **Qh3lc** lava flows are locally thickly mantled by till of the Suttle Lake advance (**Qgst**) and diamicts of the Polallie eruptive period (**Qh2pc**). Unit **Qh3lc** has normal magnetic polarity and is assigned a Late Pleistocene age. The valley-filling lava flow has an $^{40}Ar/^{39}Ar$ age of 46.1 ± 2.2 ka (whole rock; sample 920820-1) and a less precise K-Ar age of 29 ± 11 ka (whole rock; sample 920820-1); the lava flow exposed between the forks of Polallie Creek yielded K-Ar ages of 56.7 ± 3 ka (whole rock; sample 950705-2; Thouret, 2005) and 44 ± 9 ka (whole rock; sample 950705-2) (**Figure 2-1**; Plate 1; **Table 5-1**; Appendix).

Table 6-1. Select XRF geochemical analyses for Mount Hood and pre-Mount Hood lavas in the Dog River–Badger Lake area.

Sample	920820-1	950705-2	950706-2	970820-1	980903-1	940707-1	970806-2	931029-6	91T-84	393 DRBLJ 19	130801-3
Geographic Area	Tamanaw as Falls	Polallie Creek	Polallie Creek	North Fork Spring Creek	North Fork Spring Creek	North Fork Spring Creek	North Fork Spring Creek	Cooper Spur Road	Doe Creek	Newton Creek	Newton Creek
Formation	Mount Hood	Mount Hood	Mount Hood	Mount Hood	Mount Hood	Mount Hood	Mount Hood	Mount Hood	Pre-Mount Hood	Pre-Mount Hood	Pre-Mount Hood
Map Unit	Qh3lc	Qh3lc	Qh3cf	Qh4cs	Qh4cs	Qh4cp	Qh4lb	Qh4tj	Qphd	Qphe	Qphm
UTM N (NAD 83)	5028705	5028390	5028517	5025960	5025340	5027243	5024219	5031397	5030334	5021484	5021322
UTM E (NAD 83)	610559	608302	607685	608587	608050	608870	607942	610598	608848	607964	607737
Age (Ma, ka)	46.1 ka	56.7 ka	~90 ka	~150-200 ka	~150-200 ka	180 ka	~150-200 ka	475 ka	931 ka	na	~1.5 Ma
Map No.	G378	G356	G372	G293	G270	G323	G240	G464	G140	G134	G125
Oxides, weight percent											
SiO_2	60.89	61.24	62.18	61.48	61.54	61.64	61.62	59.66	60.83	60.37	58.65
Al_2O_3	17.05	17.35	16.99	17.38	17.53	17.28	17.15	18.22	17.38	17.96	17.75
TiO_2	0.94	0.92	0.89	0.88	0.90	0.89	0.86	1.03	0.930	0.89	1.13
FeO*	5.54	5.50	5.41	5.41	5.33	5.44	5.41	6.29	5.63	5.99	6.63
MnO	0.10	0.09	0.10	0.09	0.10	0.09	0.09	0.11	0.101	0.10	0.11
CaO	6.23	5.94	5.66	5.87	5.64	5.75	5.88	5.77	6.12	6.37	6.71
MgO	2.92	2.99	2.84	2.99	3.01	3.04	3.15	3.29	3.21	2.99	3.35
K_2O	1.71	1.40	1.54	1.39	1.40	1.37	1.37	1.29	1.38	1.20	1.41
Na_2O	4.31	4.32	4.16	4.18	4.35	4.25	4.26	4.09	4.17	3.96	4.07
P_2O_5	0.30	0.23	0.23	0.32	0.21	0.24	0.21	0.24	0.232	0.17	0.18
LOI	na	na	na	na	na	na	na	na	na	0.38	na
Total_I	na	na	na	na	na	na	na	na	na	99.11	na
Trace Elements, parts per million											
Ni	22	23	33	29	30	25	33	22	28	21	19
Cr	na	25	38	34	37	27	38	31	17	15	30
Sc	na	26	24	14	15	na	14	na	na	14	17
V	na	103	115	102	101	na	112	na	na	114	145
Ba	445	322	342	338	344	350	349	340	200	225	276
Rb	23	18	24	18	20	19	19	20	17	15	18
Sr	900	683	516	611	587	620	654	620	641	693	606
Zr	192	164	183	164	165	176	157	164	137	144	173
Y	13	16	18	15	15	12	16	20	26	19	21
Nb	0.0	11.7	13.4	9.8	9.9	0.0	9.2	10.0	9	5.8	9.8
Ga	na	19	20	20	26	na	19	na	na	19	21
Cu	44	31	39	22	16	48	61	34	50	42	46
Zn	74	77	71	70	68	47	75	64	59	62	71
Pb	na	8	4	6	2	na	7	na	na	3	4
La	44	na	na	66	23	0	18	0	<30	18	19
Ce	86	na	na	46	52	59	40	45	<30	35	36
Th	na	3	4	1	4	na	4	na	na	2	4
Nd	na	na	na	na	na	na	19	na	na	18	20
U	na	na	na	na	na	na	0	na	na	3	0

Major element determinations have been normalized to a 100-percent total on a volatile-free basis and recalculated with total iron expressed as FeO*; nd - no data or element not analyzed; na - not applicable or no information. LOI, Loss on Ignition; Total_I, original analytical total.

Qh3cf **andesite of Coe Falls (Upper Pleistocene)—**Andesite lava flow (SiO_2 = 62.18 weight percent; K_2O = 1.54 weight percent; *n* = 1 analysis) exposed on the floor of Polallie Creek valley, near the west edge of the map area (**Figure 2-1**; Plate 1; **Table 6-1**; Appendix). Unit **Qh3cf** has normal magnetic polarity and is assigned a Late Pleistocene age on the basis of provisional correlation with a chemically similar, extensive unit on the north flank of Mount Hood that has a K-Ar age of ~90 ka (Scott and Gardner, 2017).

Qhcwl **lahar deposits of Whiskey Creek (Upper and Middle Pleistocene)—**Massive, matrix-supported, poorly sorted, boulder-cobble lahar deposits exposed covering a broad flat in Upper Hood River Valley (**Figure 2-1**; Plate 1). Distal facies extend northward of the Columbia River into Washington State, where deposits >10 m thick (32.8 ft) are exposed at least 4 km (2.5 mi) up the White Salmon River drainage (Scott and others, 1997a; Vallance, 1999; McClaughry and others, 2012; Scott and Gardner, 2017). Unit **Qhcwl** comprises deposits of a variety of ages that are difficult to differentiate in low-relief areas of the Upper Hood River Valley. Chief among them is a voluminous fines-rich lahar deposit inferred to have been generated by a Mount Hood north-flank debris avalanche; the deposit contains fresh to variably hydrothermally altered clasts of Mount Hood lava, intraclasts of Mount Hood pyroclastic-flow deposits, a matrix clay of hydrothermal origin, as well as exotic clasts of older rocks (Vallance, 1999). Two clasts sampled in the map area are andesite, with 59.95 to 59.62 weight percent SiO_2 and 1.12 to 1.32 weight percent K_2O (*n* = 2 analyses) (Plate 1). The avalanche lahar is locally interbedded in sandy lahar deposits related to lava dome growth and collapse both before and following debris avalanche. Analyses of boulders of Mount Hood andesite and dacite from the avalanche lahar suggest multiple source units. In near-surface exposures, deposits bear a mantle of Latest Pleistocene ash-cloud deposits of Polallie age (unmapped) overlying a reddish-brown soil with argillic B-horizon, a degree of soil development that likely represents a time period of roughly 100,000 yr. Unit **Qhcwl** is assigned a Late Pleistocene age on the basis of stratigraphic position and isotopic ages; the deposit contains wood fragments with radiocarbon ages >38 k.y. B.P. (Vallance, 1999). K-Ar ages of 61 ± 21, 109 ± 9, and 120 ± 11 ka, obtained from fresh andesitic boulders within avalanche and dome-derived lahar deposits in the Hood River Valley north of the map area, are consistent with eruption and debris avalanche happening in the early part of the Late Pleistocene (Scott and Gardner, 2017). Several north-flank lava-flow sequences now fill the avalanche scar. Unit **Qhcwl** is equivalent to the Hood River lahar of Scott and others (1997a,b), Vallance (1999), and McClaughry and others (2012).

Qh4cs **andesite of Cold Spring Creek (Middle Pleistocene)—**Andesite lava flows (SiO_2 = 61.48 to 61.72 weight percent; K_2O = 1.37 to 1.41 weight percent; *n* = 5 analyses) exposed along Cold Spring Creek (**Figure 2-1**; Plate 1; **Table 6-1**; Appendix). The distribution of unit **Qh4cs** in a high narrow ridge extending from the upper east flank of Mount Hood, suggests emplacement during a time of thick glacier cover. Unit **Qhcwl** is overlain locally by thick till of an end moraine of Suttle Lake advance (**Qgst**); the unit appears to overlie the andesite of Cold Spring-Polallie divide (**Qh4cp**). Unit **Qh4cs** has normal magnetic polarity and is assigned a Middle Pleistocene age on the basis of stratigraphic position in a sequence of andesites on the east flank of Mount Hood that range in age from 150 to 200 ka (Scott and Gardner, 2017).

Qh4cp **andesite of Cold Spring-Polallie divide (Middle Pleistocene)—**Andesite lava flows (SiO_2 = 60.75 to 61.64 weight percent; K_2O = 1.33 to 1.38 weight percent; *n* = 4 analyses) forming the divide between Polallie Creek and North Fork Cold Spring Creek (**Figure 2-1**; Plate 1; **Table 6-1**; Appendix). The divide emerges as a narrow ridge of platy andesite at about 2,146 m (7,040 ft) on the east flank of Mount Hood that widens to the east into a broader ridge. The maximum exposed thickness of unit **Qh4cp** is about 120 m (394 ft). Ridge-top distribution of unit **Qh4cp** suggests that lava flows were emplaced during time of extensive glacier cover. Unit **Qh4cp** appears to underlie the andesite of Cold Spring Creek (**Qh4cs**) and is overlain locally by thick deposits of the till of Suttle Lake advance (**Qgst**). Outcrops are characterized by vertical tabular to blocky jointing, weathering to massive, subround boulders. Typical hand samples of the andesite are speckled light gray (N7) with 3 to 5 percent (vol.) seriate, fresh clear to chalky white (N9), euhedral blocky plagioclase microphenocrysts and phenocrysts to 8 mm (0.3 in) and 3 to 5 percent (vol.) fresh black iridescent (N1) to greenish black (5GY2/1) euhedral prismatic pyroxene microphenocrysts (clinopyroxene > orthopyroxene) <1 mm (0.04 in), contained within a fine-grained vesicular holocrystalline groundmass. Unit **Qh4cp** has normal magnetic polarity and is assigned a Middle Pleistocene age on the basis of stratigraphic position in 150 to 200-ka andesites on the east flank Mount Hood and a K-Ar age of 180 ± 16 ka (whole rock; sample 940707-1; Scott and Gardner, 2017) (Plate 1; **Table 5-1**; Appendix).

Qh4lb **andesite of Lamberson Butte (Middle Pleistocene)—**Sequence of andesite lava flows (SiO_2 = 61.6 to 61.7 weight percent; K_2O = 1.37 weight percent; *n* = 2 analyses) forming the divide between the valleys of Newton Creek and Cold Spring Creek (**Figure 2-1**; Plate 1; **Table 6-1**; Appendix). Distribution of unit **Qh4lb** west of the map area suggests that Newton Creek canyon probably contained a thick glacier at the time of emplacement. Unit **Qh4lb** is overlain by diamicts of the Polallie eruptive period (**Qh2pc**) and till of the Suttle Lake advance (unit **Qgst**). Maximum exposed thickness of unit **Qh4lb** is 200 m (656 ft) along the north side of Newton Creek canyon, west of the map area. Unit **Qh4lb** has normal magnetic polarity and is assigned a Middle Pleistocene age on the basis of stratigraphic position in 150 to 200-ka andesites on the east flank Mount Hood (Scott and Gardner, 2017).

Qh4gc **andesite of lower Gnarl Ridge and North Fork Cold Spring Creek (Middle Pleistocene)—**Sequence of andesite lava flows exposed on the north side of North Fork Cold Spring Creek, in the southwestern part of the map area (**Figure 2-1**; Plate 1). Unit **Qh4gc** is likely correlative to lavas on Gnarl Ridge, which have a reported K-Ar age of 238 ka (Scott and Gardner, 2017). Unit **Qh4gc** has normal magnetic polarity and is assigned a Middle Pleistocene age on the basis of the K-Ar age and stratigraphic position beneath 150 to 200-ka andesites on the east flank Mount Hood.

Qh4tj **andesite of Tilly Jane Creek (Middle Pleistocene)—**Andesite lava flows (SiO_2 = 58.84 to 59.75 weight percent, K_2O = 1.13 to 1.37 weight percent; *n* = 11 analyses) forming the ridge between lower Tilly Jane Creek and East Fork Hood River; unit **Qh4tj** includes a small exposure on the north wall of Polallie Creek that is overlain by the basaltic andesite and andesite of Cloud Cap (**Qr4cc**) and younger surficial deposits (**Figure 2-1**; Plate 1; **Table 6-1**; Appendix). Well exposed cliff-forming outcrops weather out as triangular prisms, suggesting poorly developed platy jointing. Typical hand samples are medium gray (N5), containing >5 percent (vol.) seriate, clear to chalky white (N9) plagioclase microphenocrysts ≤1 mm (0.04 in), sparse plagioclase phenocrysts ≤3 mm (0.1

in), <1 percent (vol.) dusky red (5R 3/4) iddingsitized olivine ≤1 mm (0.04 in), and scattered greenish black (5GY2/1) clinopyroxene and orthopyroxene microphenocrysts, contained within a fine-grained holocrystalline groundmass. Unit **Qh4tj** has normal magnetic polarity and is assigned a Middle Pleistocene age on the basis of stratigraphic position and a K-Ar age of 475 ± 14 ka (whole rock; sample 931029-6; Scott and Gardner, 2017) (Plate 1; **Table 5-1**; Appendix).

Qhcgr **diamict of Griswell Creek (Middle or lower Pleistocene)—**Poorly-exposed, well-weathered, clay-rich diamict, with clasts chiefly of porphyritic andesite. Most vuggy clasts can be cut by a shovel, while denser clasts are punky. Many clasts display evidence of hydrothermal alteration. Unit **Qhcgr** forms a rolling surface that lies about 20 to 25 m (65.6 to 82 ft) above the surface of lahar deposits of Whiskey Creek (**Qhcwl**) (Plate 1); unit **Qhcgr** deposits are often hard to discern if they are in section or remnants of younger fills. A strong argillic B-horizon formed in the deposit, is now buried by colluvium and fine-grained Pleistocene ash. Unit **Qhcgr** is probably a deposit of a debris avalanche or a related lahar. Unit **Qhcgr** is undated; assigned a Middle to early Pleistocene age on the basis of stratigraphic position and degree of weathering.

Qhcu **undifferentiated clastic deposits of Mount Hood (Pleistocene)—**Undifferentiated small exposures of clastic deposits, not correlated with other mapped units. Exposures are often hard to discern if they are in section or remnants of younger fills (Plate 1).

6.3.1.2 Products of pre-Mount Hood composite volcano

Qphd **pre-Mount Hood andesite of Doe Creek (lower Pleistocene)—**Andesite lava flow (SiO_2 = 60.83 weight percent, K_2O = 1.38 weight percent; *n* = 1 analysis) exposed in a small rock quarry along Cloud Cap Road (**Figure 2-1**; Plate 1; **Table 6-1**; Appendix). The mapped extent of unit **Qphd** is approximate owing to few outcrops and a thick mantle of till and Late Pleistocene and Holocene ash deposits. The quarry exposure along Cloud Cap Road has tabular to platy subvertical jointing grading up to a blocky jointed upper surface. The thickness of unit **Qphd** is unknown. Typical hand samples of the andesite are medium gray (N5) and distinctively speckled, containing 20 to 30 percent (vol.) fresh clear to chalky white (N9), euhedral blocky plagioclase phenocrysts 1 to 3 mm (0.04 to 0.1 in), 3 to 5 percent (vol.) fresh black (N1) iridescent, euhedral prismatic pyroxene phenocrysts (clinopyroxene > orthopyroxene) ≤3 mm (0.1 in), 10 percent (vol.) euhedral prismatic plagioclase and pyroxene microphenocrysts <1 mm (0.04 in), and 2 to 3 percent (vol.) plagioclase-pyroxene glomerocrysts ≤2 mm (0.08 in), contained within a very fine-grained holocrystalline groundmass. Unit **Qphd** has normal magnetic polarity and is assigned an early Pleistocene age on the basis of stratigraphic position and a K-Ar age of age of 931 ± 15 ka (whole rock; sample 91T-84; Scott and Gardner, 2017) (Plate 1; **Table 5-1**).

Qphe **pre-Mount Hood andesite of Elk Mountain (lower Pleistocene)—**Andesite lava flow (SiO_2 = 59.7 to 60.77 weight percent, K_2O = 1.2 to 1.26 weight percent; *n* = 4 analyses), forming a topographically distinctive cliff-forming bench at an elevation from 1,531 to 1,664 m (5,023 to 5,458 ft), along the south face of Elk Mountain (**Figure 2-1**; Plate 1; **Table 6-1**; Appendix). Unit **Qphe** is chemically similar to underlying unit **Qphm**, but is distinguished on the basis of relatively higher TiO_2 (1.11 to 1.12 weight percent), FeO* (6.06 to 6.63 weight percent), K_2O (1.40 to 1.52 weight percent), and Zr (169 to 190 ppm) (Plate 1; **Table 6-1**; Appendix). Map pattern indicates unit **Qphe** was

emplaced as an intracanyon lava flow adjacent to <3.5 Ma Pliocene and early Pleistocene lavas forming the south part of Bluegrass Ridge. Unit **Qphe** now forms inverted high topography capped by glacial debris (**Qgot**) near the summit of Elk Mountain. Outcrops are characterized by vertical platy to tabular jointing. Maximum thickness of unit **Qphe** is ~132 m (435 ft). Typical hand samples of the andesite are light bluish gray (5B 7/1) to medium bluish gray (5B 5/1), containing 3 to 5 percent (vol.) fresh clear, euhedral blocky to prismatic, seriate plagioclase microphenocrysts and phenocrysts from 1 to 5 mm (0.04 to 0.2 in), 1 percent (vol.) black (N1) pyroxene (clinopyroxene = orthopyroxene) microphenocrysts <1 mm (0.04 in), 3 to 5 percent (vol.) plagioclase-pyroxene glomerocrysts ≤5 mm (0.2 in), and sparse fine-grained subround xenoliths ≤1 cm (0.4 in), contained within a fine-grained holocrystalline groundmass. The rock contains trace amounts of hornblende. Unit **Qphe** has reversed-polarity magnetization and is assigned an early Pleistocene age on the basis of stratigraphic position above the 1.5 Ma pre-Mount Hood andesite of Elk Meadows Trail (**Qphm**).

Qphm **pre-Mount Hood andesite of Elk Meadows Trail (lower Pleistocene)—**Andesite lava flow (SiO_2 = 58.65 to 59.53 weight percent, K_2O = 1.4 to 1.52 weight percent; *n* = 3 analysis) forming a narrow discontinuous southeast-dipping bench at about 1,463 to 1,524 m (4,800 to 5,000 ft) elevation along the southern slope of Elk Mountain, north of Newton Creek (**Figure 2-1**; Plate 1; **Table 6-1**; Appendix). Unit **Qphm** is chemically similar to overlying unit **Qphe** but is distinguished on the basis of relatively lower TiO_2 (0.86 to 0.88 weight percent), FeO* (5.63 to 5.99 weight percent), K_2O (1.20 to 1.26 weight percent), and Zr (144 to 154 ppm) (Plate 1; **Table 6-1**; Appendix). Map pattern indicates unit **Qphm** was emplaced as an intracanyon lava flow adjacent to <3.5 Ma Pliocene and early Pleistocene lavas forming the south part of Bluegrass Ridge. Outcrops typically have vertical to horizontal, platy to tabular jointing. Typical thickness of unit **Qphm** in outcrop is <18 m (55 ft), but distribution of float on slopes and lidar interpretation suggests the unit may be up to 98 m thick (320 ft). Typical hand samples of the andesite are light gray (N7) to light bluish gray (5B 7/1), containing 1 percent (vol.) fresh clear, euhedral prismatic plagioclase phenocrysts ≤2 mm (0.08 in), 3 percent (vol.) fresh black (N1), euhedral prismatic pyroxene phenocrysts (clinopyroxene > orthopyroxene) ≤4 mm (0.2 in), and 10 to 15 percent (vol.) euhedral prismatic plagioclase and pyroxene microphenocrysts <1 mm (0.04 in), contained within a fine-grained holocrystalline groundmass. Unit **Qphm** has reversed-polarity magnetization and is assigned an early Pleistocene age on the basis of stratigraphic position and a K-Ar age of age of 1.5 Ma reported by Scott and Gardner (2017).

6.3.1.3 Products of regional Quaternary volcanoes

Qr1pk **andesite of Parkdale (Holocene)—**Andesite lava flow (SiO_2 = 58.27 to 58.69 weight percent; K_2O = 0.85 to 0.90 weight percent; *n* = 9 analyses [5 outside map area]) up to 1.25 km wide (0.8 mi), exposed along Middle Fork Hood River (**Figure 2-1**; Plate 1; **Table 6-2**; Appendix; Darr, 2006; McClaughry and others, 2012). The Parkdale flow (**Qr1pk**) extends for a distance of ~6.5 km (4 mi) north from a vent area lying ~12 km (7.5 mi) north-northeast of the Mount Hood summit (**Figure 2-1**; Wise, 1969; Sherrod and Scott, 1995). Unit **Qr1pk** is composed of multiple lobes of steep-sided blocky lava, characterized by prominent inset levees and steep margins about 50 m (164 ft) high. The top and sides of the Parkdale flow (**Qr1pk**) is largely unvegetated. Maximum thickness of unit **Qr1pk** is ~75 m (246 ft). The Parkdale lava (**Qr1pk**) flowed across a relatively flat

surface underlain by the lahar deposits of Whiskey Creek (**Qhcwl**; ~38 to 120 ka) and younger lahar and pyroclastic deposits of the Polallie eruptive episode (**Qh2pc**; ~30 to 15 ka). The flow completely filled a channel occupied by Middle Fork Hood River, which subsequently incised a new channel along the west margin of the lava. Springs emerge from the base of the unit along the north and northeast flow margins. Typical hand samples of the lava are medium dark gray (N4), containing ~3 to 5 percent (vol.) fresh clear, seriate plagioclase phenocrysts 1 to 5 mm (0.04 to 0.2 in) across, ~1 percent (vol.) black (N1) hypersthene phenocrysts 1 to 3 mm (0.04 to 0.1 in) across, and ~1 percent (vol.) plagioclase-hypersthene glomerocrysts ≤8 mm (0.3 in), distributed within a fine-grained, locally diktytaxitic holocrystalline groundmass.

Unit **Qr1pk** has normal magnetic polarity and is assigned a Holocene age on the basis of a radiocarbon age of 6,890 ± 130 yr and a calibrated radiocarbon age of 7,510 to 7,970 yr (2-σ uncertainty) obtained from charcoal directly beneath the lava (Harris, 1973). Tephra from the ~7.7 ka eruption of Mount Mazama, that formed Crater Lake (Bacon and Lanphere, 2006), is between 5 and 10 cm thick (0.2 and 0.4 in) on Mount Hood but is not evident on the Parkdale flow **(Qr1pk**) surface. The absence of the Mazama tephra on the Parkdale flow **(Qr1pk**) surface may suggest eruption of this lava followed the climatic eruption that formed Crater Lake. Alternatively, the Mazama tephra may be absent in this area, due to stripping of deposits by wind or natural filtering of the ash down through the blocky and open framework of the lava flow.

Table 6-2. Select XRF geochemical analyses for regional Quaternary lavas in the Dog River–Badger Lake area (part 1 of 2).

Sample	PD-05-03	940523-3	RCS 92-H446	51 DRBLJ 19	178 DFWJ 15	89a MCB-DRJ 18	JM DR 13-31	RC98-198	252 DRBLJ 19	RC13-498-71
Geographic Area	Upper Hood River Valley	East Fork	Brooks Meadow	Shellrock Butte	Mill Creek Buttes	East Fork	Brooks Meadow	Cooks Meadow	Lookout Mountain	Cooks Meadow
Formation	Regional volcano	Regional volcano	Regional volcano	Regional volcano	Regional volcano	Regional volcano	Regional volcano	Regional volcano	Regional volcano	Regional volcano
Map Unit	Qr1pk	Qr4cc	Qrab	Qras	Qr5dr	Qrai	Qrba	Qrbw	Qrbhp	Qrbc
UTM N (NAD 83)	5038436	5035485	5030887	5035643	5032481	5037045	5029114	5028423	5022651	5029726
UTM E (NAD 83)	607629	610995	614577	614867	614681	612470	616079	615318	614409	615868
Age (Ma, ka)	~7.7 ka	~424	1.18 Ma	na	1.87 Ma	1.83 Ma	na	na	na	na
Map No.	G620	G570	G431	G579	G490	G595	G393	G358	G186	G411
Oxides, weight percent										
SiO_2	58.35	55.38	58.13	60.29	57.16	56.58	50.77	53.22	52.34	51.60
Al_2O_3	18.32	18.56	18.04	17.90	18.14	18.65	18.68	17.85	18.58	17.61
TiO_2	1.15	1.27	1.12	0.78	1.22	1.26	1.99	1.74	1.51	1.70
FeO*	6.49	7.60	6.93	5.54	6.79	6.77	10.39	8.90	8.47	9.54
MnO	0.11	0.12	0.12	0.09	0.11	0.12	0.16	0.14	0.14	0.15
CaO	6.69	7.38	5.86	6.48	7.52	7.75	7.81	7.77	8.52	8.33
MgO	3.40	4.53	3.61	3.74	3.73	3.16	5.92	5.03	5.75	6.04
K_2O	0.85	0.72	1.57	1.03	1.14	1.69	0.58	1.09	0.86	0.96
Na_2O	4.37	4.16	4.25	3.98	3.93	3.74	3.30	3.88	3.55	3.71
P_2O_5	0.27	0.27	0.37	0.16	0.26	0.29	0.41	0.38	0.29	0.37
LOI	na	na	na	0.88	na	0.85	0.26	na	na	na
Total_I	99.73	na	na	98.80	99.29	98.60	98.19	na	99.38	99.92
Trace Elements, parts per million										
Ni	32	52	23	48	39	25	48	70	79	98
Cr	47	80	26	76	48	30	59	80	82	121
Sc	16	na	18	15	18	18	18	19	20	21
V	116	na	124	104	166	155	163	169	174	176
Ba	291	222	618	240	338	379	348	298	256	287
Rb	10	7	17	16	19	21	17	12	9	9
Sr	649	621	1045	533	790	758	786	604	805	657
Zr	145	126	210	150	160	171	158	180	127	165
Y	18	16	20	17	21	22	23	28	20	23
Nb	9.0	7.8	14.4	7.8	9.1	11.3	8.6	17.5	10.8	15.5
Ga	21	na	23	21	19	21	20	19	19	18
Cu	40	53	41	40	48	44	50	58	17	59
Zn	87	84	83	66	69	68	73	105	78	95
Pb	5	na	7	3	4	6	5	4	3	3
La	13	38	38	15	20	23	18	29	14	19
Ce	33	20	86	28	44	51	45	40	34	44
Th	1	na	6	2	3	4	4	1	2	1
Nd	17	na	na	16	27	26	26	na	17	25
U	na	na	na	1	na	1	1	na	1	0

Major element determinations have been normalized to a 100-percent total on a volatile-free basis and recalculated with total iron expressed as FeO*; nd - no data or element not analyzed; na - not applicable or no information. LOI, Loss on Ignition; Total_I, original analytical total.

Table 6-2, continued. Select XRF geochemical analyses for the Gunsight Butte volcanics in the Dog River–Badger Lake area (part 2 of 2).

Sample	S92-H269	110-WISE	339 DRBLJ 19	RC01-130	RC-DS197	RC13-498-70	74 MCB-DRJ 17
Geographic Area	Dog River	East Fork	Lookout Mountain	Lookout Mountain	Horkelia Meadow	Dog River	S. Fork Mill Creek
Formation	Regional volcano	Regional volcano	Regional volcano	Regional volcano	Regional volcano	Regional volcano	Regional volcano
Map Unit	Qrbb	Qrbb	Qrbp	Qrbi	Qrbh	Qrbu	QTbk
UTM N (NAD 83)	5031022	5032151	5022475	5022230	5027452	5032353	5031009
UTM E (NAD 83)	612245	613725	614601	614765	614218	612124	615955
Age (Ma, ka)	2.06 Ma	2.26 Ma	~2.35 Ma	na	2.52 Ma	na	na
Map No.	G443	G478	G184	G175	G328	G485	G442
Oxides, weight percent							
SiO_2	54.78	53.60	50.74	53.73	51.38	52.81	50.50
Al_2O_3	18.02	18.34	17.18	18.51	16.79	17.43	17.27
TiO_2	1.16	1.22	1.86	1.19	1.42	1.78	1.95
FeO*	6.71	7.73	10.57	8.47	7.45	10.14	10.83
MnO	0.11	0.12	0.17	0.13	0.13	0.15	0.17
CaO	8.75	8.92	8.43	8.12	9.51	7.81	9.55
MgO	5.77	5.57	6.32	4.85	8.19	4.46	5.51
K_2O	0.86	0.86	0.82	0.86	1.13	1.01	0.55
Na_2O	3.53	3.33	3.54	3.94	3.57	4.09	3.42
P_2O_5	0.31	0.30	0.37	0.20	0.44	0.31	0.25
LOI	na	na	0.00	na	na	na	0.06
Total_I	na	na	99.34	na	na	100.62	99.54
Trace Elements, parts per million							
Ni	95	na	94	54	156	27	64
Cr	134	na	144	38	256	20	136
Sc	0	na	24	20	20	21	26
V	157	na	196	153	204	200	228
Ba	325	na	246	178	552	252	237
Rb	10	na	9	10	21	17	5
Sr	906	na	516	559	924	536	530
Zr	147	na	155	135	209	168	122
Y	16	na	26	19	21	24	28
Nb	9	na	14.0	9.9	10.3	13.2	10.7
Ga	na	na	20	21	17	22	22
Cu	55	na	42	37	47	37	41
Zn	68	na	97	88	80	104	98
Pb	na	na	2	2	na	3	3
La	na	na	17	12	28	20	16
Ce	na	na	35	26	90	39	31
Th	na	na	1	2	5	3	2
Nd	na	na	21	16	na	18	21
U	na	na	2	2	na	1	2

Major element determinations have been normalized to a 100-percent total on a volatile-free basis and recalculated with total iron expressed as FeO*; nd - no data or element not analyzed; na - not applicable or no information. LOI, Loss on Ignition; Total_I, original analytical total.

Qr4cc **basaltic andesite and andesite of Cloud Cap (Middle Pleistocene)—**Sequence of basaltic andesite (SiO_2 = 55.34 to 55.87; K_2O = 0.63 to 0.72 weight percent; *n* = 10 analyses) and andesite lava flows (SiO_2 = 57.60 to 58.67 weight percent; K_2O = 0.87 to 1.02 weight percent; *n* = 13 analyses) forming a broad slope of a shield volcano on the northeast flank of Mount Hood, north of Polallie Creek (**Figure 2-1**; Plate 1; **Table 6-2**; Appendix). Distal samples tend to have lower silica content than those exposed nearer to the vent area (<56 weight percent SiO_2). **Qr4cc** lava flows funneled down valleys between high terrain formed by the 931 ka andesite of Doe Creek (**Qphd**), 475 ka andesite of Tilly Jane (**Qh4tj**), 2.5 Ma High-TiO_2 basalt and basaltic andesite (**QTbt**), and other units to form three distal tongues down ancestral valleys of Polallie Creek and northward along East Fork Hood River (total length 8.3 km [5.2 mi]); Tilly Jane Creek and northward along East Fork (12.3 km [7.6 mi]); and Crystal Springs Creek terminating at present-day Cooper Spur Road (8.4 km [5.2 mi]) (**Figure 2-1**; Plate 1). The maximum exposed thickness of unit **Qr4cc** on the east side of Eliot Branch, west of the map area, is about 120 to 140 m (393 to 459 ft); the Eliot Branch section comprises more than 10 separate lava flows with thick intervening breccias (Scott and Gardner, 2017). Distal outcrops of unit **Qr4cc** along East Fork Hood River expose two lava flows, totaling about 50 m (164 ft) of thickness; these flows display fans of narrow-columned lava, consistent with rapid cooling, probably against a paleo-valley wall, as lava ponded in the ancestral East Fork valley. The vent area for unit **Qr4cc** is not exposed, but must lie within 5 km (2.5 mi) of the summit of Mount Hood, near Cloud Cap Inn (**Figure 2-1**). Typical hand samples of basaltic andesite are medium dark gray (N4) and speckled with 10 to 15 percent (vol.) clear to chalky white (N9), euhedral, seriate plagioclase microphenocrysts <1 mm (0.04 in) and 2 to 3 percent (vol.) fresh iridescent to iddingsitized, subhedral olivine <1 mm (0.04 in), contained within a fine-grained holocrystalline groundmass. Typical hand samples of andesite are medium bluish gray (5B 5/1) aphyric to very sparsely microphyric with <1 percent (vol.) plagioclase, orthopyroxene, and olivine, contained within a mottled fine-grained holocrystalline groundmass. Unit **Qr4cc** is assigned a Middle Pleistocene age on the basis of stratigraphic position and K-Ar ages of 590 ± 30 ka (Keith and others, 1985) and 424 ± 19 ka (Scott and Gardner, 2017) from samples west of the map area. The younger age is more consistent with mapped stratigraphic relationships.

Qrab **microdiorite of Brooks Meadow (lower Pleistocene)**—Singular microdiorite dome (SiO_2 = 58.13 weight percent; K_2O = 1.57 weight percent; *n* = 1 analysis) cropping out between Dog River and Cooks Meadow (**Figure 2-1**; Plate 1; **Table 6-2**; Appendix). Outcrops are characterized by meter-scale blocky jointing; the unit weathers to meter-scale tabular blocks. Typical hand samples of the microdiorite are light brownish gray (5YR 6/1), speckled with 3 to 5 percent (vol.) clear to chalky white (N9), euhedral, seriate plagioclase microphenocrysts and phenocrysts ≤4 mm (0.1 to 0.2 in), and 5 to 10 percent (vol.) dark gray (N2) to dark reddish brown (10R 3/4), euhedral blocky to acicular, seriate hornblende microphenocrysts and phenocrysts ≤8 mm (0.3 in), distributed within a fine- to medium-grained holocrystalline groundmass. Salt- and pepper-patterned plagioclase-hornblende inclusions, as large as 12 cm (4.7 in), are common. Unit **Qrab** is assigned an early Pleistocene age on the basis of stratigraphic position and an $^{40}Ar/^{39}Ar$ plateau age of 1.18 ± 0.01 Ma (groundmass; sample 51 MCB-DRJ 17) (Plate 1; **Table 5-1**; Appendix). A $^{40}Ar/^{39}Ar$ plateau age on amphibole from the same sample is 1.91 ± 0.22 Ma (amphibole; sample 51 MCB-DRJ 17) (Plate 1; **Table 5-1**; Appendix). The microdiorite intrudes vent deposits (**Qrbv**) related to the eruption of the 1.87 Ma basaltic andesite of Dog River (**Qr5dr**) (Plate 1).

Qras **microdiorite of Shellrock Mountain (lower Pleistocene)—**Singular microdiorite dome (SiO_2 = 60.13 to 62.17 weight percent; K_2O = 1.03 to 1.43, *n* = 3 analyses) forming Shellrock Mountain along the Cat Creek thrust fault, north of Mill Creek Buttes (**Figure 2-1**; Plate 1; **Table 6-2**; Appendix). Outcrops in the north face of the mountain consist of precipitous cliff-forming, north-inclined layers (sills?), tens of meters thick marked by distinct columnar jointing. The summit of the mountain is marked by spine-forming, vertically tabular to platy jointed outcrops. Thickness of the **Qras** dome exceeds 305 m (1,000 ft). Shellrock Mountain is flanked by extensive active talus cones (**Qt**), originating from summit outcrops. Typical hand samples of the microdiorite are yellowish gray (5Y 8/1), containing 5 to 7 percent (vol.) clear to chalky white (N9), subhedral to anhedral, prismatic to blocky, seriate plagioclase microphenocrysts and phenocrysts ≤3 mm (0.1 in) and 5 to 7 percent (vol.) fresh grayish black (N2) iridescent, dark reddish brown (10R 3/4), euhedral to subhedral, prismatic to needle-like hornblende microphenocrysts and phenocrysts ≤4 mm (0.2 in), contained within an equigranular medium-grained holocrystalline groundmass. The rock includes sparsely scattered, subround, medium bluish gray (5B 5/1) microporphyritic inclusions. Unit **Qras** has reversed magnetic polarity. Sherrod and Scott (1995) considered Shellrock Mountain to be of Miocene or Pliocene age. Unit **Qras** is here assigned an early Pleistocene age on the basis of chemistry, minerology, non-altered appearance, and geomorphic expression similar to the isotopically dated 1.18 Ma dome at Brooks Meadow (**Qrab**). Taken together, the Shellrock Mountain dome (**Qras**), Brooks Meadow dome (**Qrab**), and several other mafic vents (**Qrbv**) farther south to Lookout Mountain, form a conspicuous north-south belt of Quaternary volcanic centers situated along the Dog River-Mill Creek divide (**Figure 2-1**; Plate 1).

Qrbv **basalt and basaltic andesite vents (lower Pleistocene)—**Basalt or basaltic andesite cinders, scoria, agglutinate, or near-vent flows forming high buttes along the east side of the map area. Vents are oriented in a north-south belt extending from Lookout Mountain on the south to Mill Creek Buttes on the north (**Figure 2-1**; Plate 1). The unit is assigned an early Pleistocene age on the basis of stratigraphic position and correlation to dated lava flows. Unit **Qrbv** vent deposits, from north to south, mark eruptive centers for the 1.87 Ma basaltic andesite of Dog River (**Qr5dr**), the basaltic andesite of High Prairie (**Qrbhp**), and the 2.06/2.26 Ma basaltic andesite of Blue Bucket Spring (**Figure 2-1**; Plate 1).

Qrai **basaltic andesite intrusive rocks (lower Pleistocene)—**N.20°E. to N.30°E.-striking basaltic andesite dike (SiO_2 = 56.28 to 56.90 weight percent; K_2O = 1.43 to 1.69 weight percent; *n* = 4 analyses) intruding Grande Ronde Basalt (**Tgsb**, **Tgww**) and fault breccia (**QTfb**) along East Fork Hood River in the northern part of the map area (**Figure 2-1**; Plate 1; **Table 6-2**; Appendix). Ledge- to spire-forming outcrops are distinguished by prominent horizontal columnar joint sets, with irregular to hexagonal columns up to 1 m (3.3 ft) across. Dike boundaries are irregular, defined by ≤50-cm-thick (20 in) zones of vertically oriented vesicular bands. The dike ranges between 30 and 50 m wide (98.4 and 164 ft). Typical hand samples of the basaltic andesite are dark gray (N3) with ~20 percent (vol.) clear to chalky light gray (N7), euhedral to subhedral, blocky to prismatic, plagioclase microphenocrysts and phenocrysts ≤5 mm (0.2 in), ≤1 percent (vol.) subhedral olivine microphenocrysts ≤1 mm (0.04 in), and rare subangular to subrounded andesite xenoliths ≤1 cm (0.4 in), distributed within a fine-grained holocrystalline groundmass. Unit **Qrai** also includes a tens of meters high, spire-forming, N.30°W.- to N.50°W.-striking basaltic andesite (SiO_2 = 56.99 weight percent; K_2O = 1.16 weight percent; *n* = 1 analysis) dike exposed in the draw between

Shellrock Mountain and Puppy Creek in the northeast part of the map area (**Figure 2-1**; Plate 1). The dike outcrop is approximately 15 m wide (49 ft), protruding through older Dalles Formation volcaniclastic rocks (**Tmdl**). The dike outcrop is bordered by fragmental breccia composed of blocks of dike rock floating in a matrix of angular gravel and coarse palagonitic sand. Typical hand samples of the dike are similar to the dike along East Fork Hood River. Both dikes are similar in lithologic appearance and composition to the basaltic andesite of Dog River (**Qr5dr**), and may be similar in age to that lava flow. Unit **Qrai** is assigned an early Pleistocene age on the basis of stratigraphic position and a $^{40}Ar/^{39}Ar$ plateau age of 1.83 ± 0.02 Ma (groundmass; sample 89a MCB-DRJ 18) for the dike exposed along East Fork Hood River (**Figure 2-1**; Plate 1; **Table 5-1**; Appendix). Bela (1982) reported a similar K-Ar age of 2.1 ± 0.1 Ma (whole rock; Bela-19) for this outcrop.

Qr5dr **basaltic andesite of Dog River (lower Pleistocene)—**Basaltic andesite lava flow (SiO_2 = 55.88 to 57.56 weight percent; K_2O = 1.08 to 1.24 weight percent; *n* = 20 analyses [6 outside map area]) exposed along the Mill Creek-Dog River divide and beneath the 424-ka basaltic andesite and andesite of Cloud Cap (**Qr4cc**) in abandoned quarry exposures along OR Highway 35 (**Figure 2-1**; Plate 1; **Table 6-2**; Appendix). The basaltic andesite of Dog River (**Qr5dr**) was erupted from an extant cinder cone-capped fissure located south of Mill Creek Buttes, along the Dog River-Mill Creek divide at an altitude of 1,391 m (4,565 ft) (**Figure 2-1**; Plate 1). South of Mill Creek Buttes the lava flow (**Qr5dr**) descended into the South Fork Mill Creek drainage and flowed northeast as an intracanyon lava ~25 km (15.5 mi) to Oak Flat, southwest of The Dalles (**Figure 2-1**; Plate 1). Unit **Qr5dr** lava flows also moved northwest into the Hood River graben and ancestral valley of East Fork Hood River (Plate 1). Roadcuts and outcrops are characterized by a massive rounded form, by broad blocky meter-scale columns, or intervals of thick platy or slabby jointing. The flow typically weathers to subrounded boulders up to 0.5 m (1.6 ft) across or thick, angular slabs up to 2 m (6.6 ft) across. Maximum thickness of unit **Qr5dr** between East Fork Hood River and Dog River is 134 m (440 ft) (**Figure 2-1**; Plate 1). Typical hand samples of the basaltic andesite are medium gray (N5), containing 15 to 25 percent (vol.) chalky light gray (N7), distinctly resorbed, euhedral to subhedral, blocky to prismatic, seriate plagioclase microphenocrysts and phenocrysts ≤5 mm (0.2 in), <1 percent (vol.) subhedral olivine microphenocrysts ≤1 mm (0.04 in), <1 percent (vol.) subhedral to anhedral, blocky- to lath-shaped, clinopyroxene microphenocrysts <1 mm (0.04 in), and rare subangular to subrounded andesite xenoliths ≤1 cm (0.4 in), distributed within a fine-grained hypocrystalline groundmass. Unit **Qr5dr** has normal magnetic polarity and is assigned an early Pleistocene age on the basis of stratigraphic position and isotopic ages. A groundmass sample yielded an $^{40}Ar^{39}Ar$ plateau age of 1.87 ± 0.01 Ma and a total fusion age of 1.88 ± 0.01 Ma (groundmass; sample 178 DFWJ 15); a younger $^{40}Ar^{39}Ar$ plateau age of 1.51 ± 0.08 Ma was determined for plagioclase separates from the same sample (Plate 1; **Table 5-1**; Appendix). A K-Ar age of 1.7 ± 0.4 Ma (whole-rock, sample JA85023) was reported for this unit by Anderson (1987) for a sample collected along South Fork Mill Creek (northeast of the map area). The reader should note that the original reported location for sample JA85023 was inadvertently transposed with sample JA85022, with a reported K-Ar age of 3.7 Ma (J.L. Anderson, written commun., 1998, to R.M. Conrey; Appendix). The 3.7 Ma age belongs to the older trachydacite of Fivemile Creek (**Tpdv**).

Qrbhp **basaltic andesite of High Prairie (lower Pleistocene)—**Basaltic andesite lava flows (SiO_2 = 52.10 to 52.65 weight percent; K_2O = 0.83 to 0.94 weight percent; Sr = 805 to 892 ppm; *n* = 9 analyses) mapped between a vent (**Qrbv**) at the summit of Lookout Mountain, north into the uppermost reaches of Dog River (**Figure 2-1**; Plate 1; **Table 6-2**; Appendix). The unit includes distal basaltic andesite lobes characterized by slightly higher silica (SiO_2 = 53.96 to 54.88) and lesser strontium (Sr = 631 to 679) (*n* = 2 analyses) extending north to Bottle Prairie and the upper parts of Puppy Creek (**Figure 2-1**; Plate 1). Outcrops consist of multiple flow lobes of massive to subhorizontal platy- to tabular- and blocky-jointed lava, separated by intervening horizons of sintered, moderate red brown-oxidized (5YR3/4) flow breccia. On Lookout Mountain, flow cores are characterized by ~5 percent (vol.) conspicuous white-black speckled, subrounded plagioclase-pyroxene micro-gabbro inclusions (SiO_2 = 46.02 weight percent; K_2O = 0.17 weight percent; *n* = 1 analyses) ≤10 cm (4 in) across (**Figure 2-1**; Plate 1). Maximum thickness of unit **Qrbhp** beneath Lookout Mountain is ≤140 m (460 ft); thickness of the unit along Puppy Creek is ≤23 m (75 ft). Typical hand samples of the basaltic andesite are medium light gray (N6) and medium gray (N5) to medium bluish gray (5B 5/1), containing 3 to 8 percent (vol.), fresh clear to chalky white (N9), anhedral to subhedral, blocky, seriate plagioclase (commonly resorbed) microphenocrysts and phenocrysts ≤5 mm (0.2 in), 2 to 3 percent (vol.) waxy, subhedral blocky, seriate iddingsitized olivine microphenocrysts and phenocrysts 1 to 2 mm (0.04 to 0.08 in), 3 percent (vol.) grayish black (N2) subhedral blocky clinopyroxene phenocrysts 1 to 3 mm (0.04 to 0.1 in; locally megacrystic to 1 cm [2.5 in]), and 2 percent (vol.) plagioclase-pyroxene micro-gabbro inclusions, contained within a mottled fine-grained holocrystalline groundmass. Extensive active talus sheets (**Qt**) originate from this flow on Lookout Mountain, extending downslope for distances of 500 m (1,640 ft) (**Figure 2-1**; Plate 1). Unit **Qrbhp** has reversed magnetic polarity and is assigned an early Pleistocene age on the basis of stratigraphic position above the 2.35 Ma basalt of Bennett Pass Road (**Qrbp**). Along Puppy Creek, unit **Qrbhp** is characterized by an intracanyon geomorphic setting lying above the 2.06 Ma basaltic andesite of Blue Bucket Springs (**Qrbb**) and underlying the 1.87 Ma basaltic andesite of Dog River (**Qr5dr**) (**Figure 2-1**; Plate 1).

Qrba **basalt of Agnes Spring (lower Pleistocene)—**Basaltic lava flow (SiO_2 = 50.76 weight percent; K_2O = 0.58 weight percent; *n* = 1 analyses) exposed only in roadcuts between Brooks Meadow and Bottle Prairie in the east-central part of the map area (**Figure 2-1**; Plate 1; **Table 6-2**; Appendix). Outcrops of the basalt are massive to blocky jointed. Typical hand samples of the basalt are medium light gray (N6), aphyric to sparsely olivine phyric, containing 3 to 5 percent (vol.) subhedral fresh to iddingsitized olivine microphenocrysts ≤1 mm (0.04 in) distributed within a mottled, locally diktytaxitic, fine-grained holocrystalline groundmass. Magnetic polarity is not known. Unit **Qrba** is assigned an early Pleistocene age on the basis of stratigraphic position above the 2.35 Ma basalt of Bennett Pass Road (**Qrbp**) (Plate 1).

Qrbw **basaltic andesite of Ward Creek (lower Pleistocene)—**Basaltic andesite (SiO_2 = 52.29 to 53.24 weight percent; K_2O = 0.99 to 1.09 weight percent; *n* = 6 analyses [3 outside map area]) exposed in roadcuts between Brooks Meadow and Bottle Prairie in the east-central part of the map area (**Figure 2-1**; Plate 1; **Table 6-2**; Appendix). Flows vented from the upper part of Ward Creek and flowed at least 9 km (5.6 mi) downslope to the northeast, extending into upper reaches of both the middle and south forks of Fivemile Creek (**Figure 2-1**; Plate 1). Limited roadcut exposures are characterized by intervals of poorly-developed columnar jointing and platy to tabular jointing.

Unit **Qrbw** weathers to a landscape mantled by subrounded boulders up to 1 m (3.28 ft) across. Thickness of unit **Qrbw** is ~20 to 30 m (66 to 98 ft). Typical hand samples of the basaltic andesite are light gray (N7) to medium light gray (N6) and aphyric to microporphyritic or very sparsely porphyritic, containing <1 percent (vol.) clear, euhedral prismatic, seriate trachytic plagioclase microphenocrysts and phenocrysts ≤2 mm (0.08 in) (rarely with phenocrysts up to 5 mm [0.2 in]) and < 1 percent (vol.) subhedral seriate olivine microphenocrysts ≤1 mm (0.04 in) across, distributed within a mottled, locally diktytaxitic, fine-grained holocrystalline groundmass. Unit **Qrbw** has normal magnetic polarity and is assigned an early Pleistocene age on the basis of stratigraphic position above the 2.35 Ma basalt of Bennett Pass Road (**Qrbp**) (Plate 1).

Qrbc **basalt of Cooks Meadow (lower Pleistocene)—**Basaltic lava flow (SiO_2 = 51.60 to 52.91 weight percent; K_2O = 0.93 to 0.97 weight percent; *n* = 4 analyses) exposed in roadcuts along Brooks Meadow Road in the east-central part of the map area (**Figure 2-1**; Plate 1; **Table 6-2**; Appendix). The flow can be discontinuously traced ~5 km (3.1 mi) to the northwest of Cooks Meadow into the ridge divide between Dog River and Puppy Creek (**Figure 2-1**; Plate 1). Outcrops are characterized by blocky jointing. Maximum thickness of unit **Qrbc** in the map area is ≤49 m (160 ft). Typical hand samples of the basalt are medium light gray (N7) to medium light gray (N6), microporphyritic or very sparsely porphyritic to microporphyritic, containing <1 to 5 percent (vol.) chalky white (N9), subhedral blocky, seriate plagioclase microphenocrysts and phenocrysts ≤3 mm [0.1 in], 2 to 3 percent (vol.) grayish black (N2) subhedral blocky clinopyroxene ≤3 mm [0.2 in], 1 to 2 percent (vol.) subhedral olivine microphenocrysts ≤1 mm (0.04 in), and 3 to 5 percent (vol.) plagioclase-clinopyroxene glomerocrysts ≤7 mm (0.3 in), distributed within a fine-grained holocrystalline groundmass. The basalt has indeterminate magnetic polarity and is assigned an early Pleistocene age on the basis of stratigraphic position. Unit **Qrbc** overlies the 2.06 Ma basaltic andesite of Blue Bucket Springs (**Qrbb**) and underlies the 1.87 Ma basaltic andesite of Dog River (**Qr5dr**) on the east side of Dog River canyon (**Figure 2-1**; Plate 1).

Qrbb **basaltic andesite of Blue Bucket Springs (lower Pleistocene)—**Basaltic andesite lava flow (SiO_2 = 53.6 to 54.96 weight percent; K_2O = 0.93 to 0.97 weight percent; *n* = 8 analyses) extending from a vent (**Qrbv**) at Blue Bucket Springs, north to the middle-lower reaches of Dog River (**Figure 2-1**; Plate 1; **Table 6-2**; Appendix). Correlative, cliff-forming outcrops of the lava are found directly above Polallie Campground along East Fork Hood River (**Figure 2-1**; Plate 1). Outcrops are typically massive or characterized by blocky jointing. Maximum thickness of unit **Qrbb** along Dog River is ≤91 m (300 ft). Typical hand samples of the basaltic andesite are medium light gray (N6), containing 3 to 5 percent (vol.), fresh clear to chalky white (N9), subhedral to euhedral, blocky to prismatic, seriate plagioclase microphenocrysts and phenocrysts ≤5 mm (0.2 in), 2 to 3 percent (vol.) fresh black (N1), subhedral to euhedral blocky, seriate olivine microphenocrysts and phenocrysts ≤3 mm (0.1 in), and 1 to 2 percent (vol.) plagioclase-olivine glomerocrysts ≤5 mm (0.2 in), distributed within a mottled, fine-grained holocrystalline groundmass of plagioclase and intergranular olivine. Unit **Qrbb** has reversed magnetic polarity and is assigned an early Pleistocene age on the basis of stratigraphic position and K-Ar ages of 2.06 ± 0.08 (whole rock; sample S92-H265; Conrey and others, 1996) and 2.26 ± 0.08 Ma (whole rock; S92-H269; Conrey and others, 1996) (Plate 1; **Table 5-1**; Appendix).

Qrbp **basalt of Bennett Pass Road (lower Pleistocene)—**Basaltic lava flow (SiO_2 = 50.01 to 51.90 weight percent; K_2O = 0.78 to 0.96 weight percent; *n* = 5 analyses) exposed directly beneath unit **Qrbhp** along Lookout Mountain-Bennett Pass Road and at Bottle Prairie (**Figure 2-1**; Plate 1; **Table 6-2**; Appendix). From Bottle Prairie (**Figure 2-1**; Plate 1), unit **Qrbhp** extends eastward as intracanyon lava for ~10.5 km (6.5 mi) to the mouth of Hesslan Canyon (east of map area). The unit forms bold, ledge-forming massive outcrops or is marked by broad blocky meter-scale columns or intervals of subvertical to vertical platy jointing. Unit **Qrbp** generally weathers to subangular plates 0.25 to 1 m (0.8 to 3.3 ft) across. Vesicle cylinders are common; the upper parts of the unit are characterized by zones of stretched vesicles up to several cm across. Maximum thickness of unit **Qrbp** beneath Lookout Mountain is ≤47 m (154 ft) (**Figure 2-1**; Plate 1); flow thickness exceeds 32 m (105 ft) in Hesslan Canyon, east of the map area. Typical hand samples of the basalt are light gray (N7) to medium dark gray (N4), aphyric to sparsely microporphyritic, containing ≤1 percent (vol.) clear, subhedral to anhedral, prismatic, seriate plagioclase microphenocrysts ≤1 mm (0.04 in) and 2 to 3 percent, fresh dark greenish yellow (10Y 6/6), subhedral olivine microphenocrysts and phenocrysts ≤3 mm (0.1 in), contained in a fine-grained holocrystalline groundmass. Unit **Qrbp** has reversed magnetic polarity and is assigned an early Pleistocene age on the basis of stratigraphic position, intracanyon geomorphic setting, and a K-Ar age of 2.35 ± 0.03 Ma (whole rock; S92-H271a/Wise-104; Conrey and others, 1996) for outcrops at Lookout Mountain (**Figure 2-1**; Plate 1; **Table 5-1**; Appendix).

Qrbi **gabbro norite intrusion (lower Pleistocene)—**Gabbro norite intrusion (SiO_2 = 53.72 weight percent; K_2O = 0.85 weight percent; *n* = 1 analysis) striking ~N.63°E. beneath Lookout Mountain andesite (units **QTal2**, **QTal3**) and basaltic andesite lava flows (**Qrbhp**) along Lookout Mountain-Bennett Pass Road (**Figure 2-1**; Plate 1; **Table 6-2**; Appendix). The unit is heavily mantled by extensive active talus (**Qt**) aprons, but exposed outcrops are characterized by subvertical, platy to tabular jointing. Typical hand samples of the gabbro norite are light olive gray (5Y 5/2), containing 1 to 2 percent (vol.), fresh clear to chalky white (N9), subhedral to euhedral, blocky, seriate plagioclase phenocrysts ≤8 mm (0.3 in) and 1 to 2 percent (vol.) grayish black (N2), subhedral to euhedral, blocky to prismatic clinopyroxene ≤8 mm (0.3 in), contained within a fine- to medium-grained equigranular holocrystalline groundmass. Trace amounts of olivine are present. Unit **Qrbi** has reversed magnetic polarity and is assigned an early Pleistocene age on the basis of stratigraphic position; the unit may be the subvolcanic feeder for vents and overlying flows of unit **Qrbhp** (Plate 1).

Qrbh **basalt of Horkelia Meadow (lower Pleistocene or upper Pliocene)—**Basaltic lava flow (SiO_2 = 51.37 weight percent; K_2O = 1.12 weight percent; *n* = 1 analysis) very poorly exposed beneath the basaltic andesite of Blue Bucket Springs (**Qrbb**) and above flows of the andesite of Lookout Mountain (units **QTal2**, **QTal3**) at Horkelia Meadow (**Figure 2-1**; Plate 1; **Table 6-2**; Appendix). Outcrops of unit **Qrbh** are rare; the unit is recognized by extensive monolithologic float scattered along Lookout Mountain Road and the adjacent forest floor (**Figure 2-1**; Plate 1). Typical hand samples of the basalt are medium gray (N5), conspicuously olivine microporphyritic and porphyritic with 3 to 4 percent (vol.), fresh dark greenish yellow (10Y 6/6), subhedral blocky, seriate olivine microphenocrysts and phenocrysts ≤7 mm (0.3 in) and 1 to 2 percent (vol.) grayish black (N2), subhedral blocky to prismatic, seriate clinopyroxene ≤4 mm (0.2 in), contained within a fine-grained holocrystalline groundmass. Magnetic polarity of the unit is indeterminate due to

lack of coherent outcrops. Unit **Qrbh** is assigned an early Pleistocene or upper Pliocene age on the basis of stratigraphic position and a K-Ar age of 2.52 ± 0.13 Ma (whole rock; sample S91-H197; Conrey and others, 1996) obtained from an outcrop on NF Road 4410-630, near Horkelia Meadow (**Figure 2-1**; Plate 1; **Table 5-1**; Appendix).

Qrbu **basalt, undifferentiated (lower Pleistocene or upper Pliocene [?])—**Basaltic lava flows (SiO_2 = 51.8 to 52.8 weight percent; K_2O = 1.01 to 1.07 weight percent; *n* = 2 analyses) unconformably (angular) overlying the ~8 Ma Dalles Formation, dacite of East Fork (**Tmde**) and lying beneath the 1.87 Ma basaltic andesite of Dog River (**Qr5dr**) between the East Fork Hood River and lower Dog River (**Figure 2-1**; Plate 1; **Table 6-2**; Appendix). A broader correlation of the unit beyond the area of lower Dog River is not possible on the basis of current mapping. Unit **Qrbu** is assigned a late Pliocene (?) or early Pleistocene age on the basis of stratigraphic position directly below the 1.87 Ma basaltic andesite of Dog River (**Qr5dr**) and above 2.6 to 2.4 Ma High-TiO_2 basalt and basaltic andesite flows (**QTbt**) (Plate 1).

Qr5ll **basalt and basaltic andesite of Laurance Lake (lower Pleistocene [?] or upper Pliocene [?])—**Basalt and basaltic andesite lava flows exposed south and west of Volmer Ditch in the northwest part of the map area (**Figure 2-1**; Plate 1). Unit **Qr5ll** is traceable west and upslope as one or two lava flows of slightly porphyritic basalt and basaltic andesite capping a prominent escarpment north of Laurance Lake; the probable vent area lies at the western end of the escarpment at Vista Ridge (**Figure 2-1**; Sherrod and Scott, 1995). Typical hand samples of unit **Qr5ll**, west of the map area, contain 1 percent (vol.) phenocrysts of olivine 1 to 2 mm across (0.04 to 0.08 in), 1 to 2 percent (vol.) clinopyroxene 1 to 2 mm across (0.04 to 0.08 in), and ~1 percent (vol.) microphenocrysts of amphibole <1 mm across (0.04 in) (Sherrod and Scott, 1995). No geochemical data were obtained for this unit in the map area; the unit is correlated with the more widespread unit north of Laurance Lake on the basis of lithology, geomorphic setting of the unit as an intracanyon lava, and apparent stratigraphic position. Mapped distribution of the lava flow in the Dog River–Badger Lake area, suggests unit **Qr5ll** lies stratigraphically above and is inset as an intracanyon lava into older late Miocene rocks of the Dalles Formation (**Tmdl**). Unit **Qr5ll** has reversed magnetic polarity and is assigned a late Pliocene (?) or early Pleistocene (?) age on the basis of stratigraphic position.

QTbk **glomeroporphyritic basalt of Knebal Springs (lower Pleistocene [?] or upper Pliocene [?])—**Basaltic lava flow (SiO_2 = 50.38 to 50.88 weight percent; K_2O = 0.58 to 0.64 weight percent; *n* = 5 analyses [3 outside map area]) exposed above the trachydacite of Fivemile Creek (**Tpdv**), north of Brooks Meadow in the east-central part of the map area (**Figure 2-1**; Plate 1; **Table 6-2**; Appendix). Unit **QTbk** extends east of the map area ~3.3 km (2.0 mi) to the vicinity of Knebal Springs (**Figure 2-1**). Good outcrops of unit **QTbk** are rare; flows are typically exposed as piles of meter-scale boulders and slabs across the forest floor. Limited exposures are characterized by intervals of platy to tabular jointing. The maximum thickness of unit **QTbk** in the map area is ~ 58 m (190 ft). Typical hand samples of the basalt are light gray (N7) to medium light gray (N6) and abundantly plagioclase and olivine phyric, containing 5 to 10 percent (vol.) chalky white (N9) to clear, euhedral, prismatic, seriate plagioclase microphenocrysts and phenocrysts ≤8 mm (0.3 in) and 5 to 10 percent (vol.) variably altered, fresh dark greenish yellow (10Y 6/6), subhedral, blocky, seriate iddingsitized olivine microphenocrysts and phenocrysts ≤5 mm across (0.2 in), distributed within a diktytaxitic, fine-grained holocrystalline groundmass. Unit **QTbk** has reversed

magnetic polarity and is assigned a late Pliocene (?) or early Pleistocene (?) age on the basis of stratigraphic position. The basalt of Knebal Springs (**QTbk**) sits directly upon the 3.69 Ma trachydacite of Fivemile Creek (**Tpdv**) and predates the 1.87 Ma basaltic andesite of Dog River (**Qr5dr**) (Plate 1).

Disconformity

6.3.2 Lower Pleistocene and Pliocene volcanic and sedimentary rocks of the late High Cascades

6.3.2.1 Badger Butte volcanics

Qbba **basaltic andesite (lower Pleistocene)—**Basaltic andesite lava flow (SiO_2 = 54.37 to 54.83 weight percent; K_2O = 0.78 to 0.80 weight percent; *n* = 2 analyses) capping the narrow ridge extending north from Gunsight Butte; unit **Qbba** also underlies a small knob north of Gumjuwac Saddle (**Figure 2-1**; Plate 1; **Table 6-3**; Appendix). Unit **Qbba** typically crops out as ledges characterized by blocky jointing. Thickness of unit **Qbba** is ≤30 m (100 ft). Typical hand samples of the basaltic andesite are medium bluish gray (5B 5/1), containing 15 to 20 percent (vol.) clear to chalky white (N9) or grayish yellow (5Y 8/4), subhedral to anhedral, prismatic to blocky, seriate plagioclase microphenocrysts and phenocrysts ≤5 mm (0.2 in), 3 to 4 percent (vol.) grayish black (N2), euhedral to subhedral, prismatic needle-like pyroxene microphenocrysts and phenocrysts ≤2 mm (0.08 in) (orthopyroxene ≥ clinopyroxene), <1 percent (vol.) brownish black (5YR 2/1) iridescent, subhedral to anhedral, seriate olivine microphenocrysts ≤1 mm (0.04 in), and ≤1 percent (vol.) plagioclase-pyroxene glomerocrysts ≤3 mm (0.1 in), distributed within a very fine-grained hypocrystalline to holohyaline groundmass. The rock contains ≤1 percent (vol.) subround microdiorite inclusions ranging from 5 mm to 2 cm (0.2 to 0.8 in) across. Unit **Qbba** has reversed magnetic polarity and is assigned an early Pleistocene age on the basis of stratigraphic position above 2.44 Ma andesite of unit **Qbla** (Plate 1).

Table 6-3. Select XRF geochemical analyses for the Badger Butte volcanics in the Dog River–Badger Lake area.

Sample	RC01-126/84 DRBLJ 19	107 DRBLJ 19	KS57
Geographic Area	Gunsight Butte	Gunsight Butte	Gunsight Butte
Formation	Badger Butte volcanics	Badger Butte volcanics	Badger Butte volcanics
Map Unit	Qbba	Qbua	Qbla
UTM N (NAD 83)	5017915	5020186	5019735
UTM E (NAD 83)	611574	612949	612891
Age (Ma)	2.44 Ma	nd	nd
Map No.	G39	G89	G85
Oxides, weight percent			
SiO_2	59.06	57.75	54.38
Al_2O_3	17.11	17.69	19.60
TiO_2	1.15	1.11	1.40
FeO*	6.83	6.84	7.46
MnO	0.11	0.11	0.14
CaO	6.29	6.97	8.92
MgO	3.48	3.99	3.31
K_2O	1.62	1.47	0.79
Na_2O	4.08	3.85	3.75
P_2O_5	0.26	0.23	0.26
LOI	na	0.16	na
Total_I	na	99.37	na
Trace Elements, parts per million			
Ni	52	41	17
Cr	53	45	23
Sc	15	17	19
V	132	152	154
Ba	412	347	206
Rb	29	23	8
Sr	636	720	705
Zr	202	177	142
Y	24	19	21
Nb	13.5	9.5	8.4
Ga	20	19	17
Cu	29	34	10
Zn	77	73	73
Pb	5	5	5
La	25	17	0
Ce	49	43	43
Th	4	3	4
Nd	27	23	na
U	2	3	na

Major element determinations have been normalized to a 100-percent total on a volatile-free basis and recalculated with total iron expressed as FeO*; nd - no data or element not analyzed; na - not applicable or no information. LOI, Loss on Ignition; Total_I, original analytical total.

Qbua **andesite (lower Pleistocene)—**Andesite lava flow (SiO2 = 56.93 to 57.81 weight percent; K2O = 1.24 to 1.48 weight percent; n = 6 analyses) forming a narrow ridge between Gunsight Butte and Jack Springs (**Figure 2-1**; Plate 1; **Table 6-3**; Appendix). Unit **Qbua** crops out as extensive cliffs marked by vertical to subvertical, tabular to platy jointing. Many outcrops are frost heaved and flanked by extensive active talus cones (**Qt**). Thickness of unit **Qbua** is ≤91 m (300 ft) at Gunsight Butte (**Figure 2-1**; Plate 1). Typical hand samples of the andesite are medium bluish gray (5B 5/1) to medium light gray (N6), containing 3 to 5 percent (vol.) clear to chalky white (N9), euhedral, prismatic, seriate plagioclase microphenocrysts and phenocrysts ≤5 mm (0.2 in), 3 to 5 percent (vol.) grayish black (N2), euhedral to subhedral, prismatic needle-like to blocky, seriate pyroxene microphenocrysts and phenocrysts ≤3 mm (0.1 in) (orthopyroxene ≥ clinopyroxene), <1 percent (vol.) brownish black (5YR 2/1) iridescent, anhedral, seriate olivine microphenocrysts <1 mm (0.04 in), and ≤1 percent (vol.) plagioclase-pyroxene glomerocrysts ≤3 mm (0.1 in), distributed within a fine-grained hypocrystalline groundmass. Unit **Qbua** has reversed magnetic polarity and is assigned an early Pleistocene age on the basis of stratigraphic position above the 2.44 Ma andesite of Gunsight Butte (**Qbla**) (Plate 1).

Qbla **andesite (lower Pleistocene)—**Andesite lava flow (SiO_2 = 58.75 to 59.26 weight percent; K_2O = 1.45 to 1.65 weight percent; *n* = 11 analyses) capping the ridge south of Gunsight Butte (**Figure 2-1**; Plate 1; **Table 6-3**; Appendix). Unit **Qbla** crops out as ledges and knobs, characterized by blocky to horizontal tabular jointing in lower parts and thin platy jointing in upper parts. Outcrops weather to meter-scale slabs and subround boulders. Thickness of unit **Qbla** is ≤35 m (115 ft) south of Gunsight Butte (**Figure 2-1**; Plate 1). Typical hand samples of the andesite are medium bluish gray (5B 5/1), containing 5 to 7 percent (vol.) clear to chalky white (N9), euhedral, prismatic to blocky, seriate plagioclase microphenocrysts and phenocrysts ≤4 mm (0.1 in), ≤1 percent (vol.) grayish black (N2), subhedral to anhedral, blocky, seriate pyroxene microphenocrysts and phenocrysts ≤4 mm (0.1 in) (orthopyroxene ≥ clinopyroxene), trace amounts of olivine, and ≤1 percent (vol.) plagioclase-pyroxene glomerocrysts ≤7 mm (0.3 in), distributed within a fine-grained holocrystalline groundmass. Unit **Qbla** has reversed magnetic polarity and is assigned an early Pleistocene age on the basis of stratigraphic position and isotopic ages. A groundmass sample yielded an $^{40}Ar/^{39}Ar$ plateau age of 2.44 ± 0.02 Ma and a total fusion age of 2.60 ± 0.04 Ma (groundmass; sample RC01-126/84 DRBLJ); a younger $^{40}Ar/^{39}Ar$ plateau age of 2.10 ± 0.09 Ma was determined for plagioclase separates from the same sample (Plate 1; **Table 5-1**; Appendix). Correlative lava flows mapped as the andesite of Badger Butte east of the map area by Sherrod and Scott (1995) have a similar reported K-Ar age of 2.1 ± 0.4 Ma (whole rock; sample W-55; Wise, 1969).

6.3.2.2 Lookout Mountain volcanics

Bluegrass Ridge area

QTai **andesite intrusive rocks (lower Pleistocene)—**Andesite dike (SiO_2 = 59.07 to 59.92 weight percent; K_2O = 1.63 to 1.70 weight percent; *n* = 2 analyses) cropping out for ~1.4 km (0.8 mi) from south to north across Elk Mountain, at the southern end of Bluegrass Ridge (**Figure 2-1**; Plate 1; **Table**

6-4; Appendix). Along its length, the dike is ≤50 m thick (168 ft), striking N.15°E. to N.30°W. and dipping steeply to the west. Outcrops are characterized by blocky jointing and well-developed horizontal columnar joint sets oriented perpendicular to dike margins. Typical hand samples of the andesite are medium gray (N5), containing 2 to 3 percent (vol.) clear, euhedral to subhedral, blocky to prismatic, seriate plagioclase microphenocrysts and phenocrysts ≤3 mm (0.1 in), 2 to 3 percent (vol.) fresh grayish black (N2) to brownish black (5YR 2/1), subhedral to euhedral, blocky to prismatic, seriate hornblende microphenocrysts and phenocrysts ≤3 mm (0.1 in), distributed within a fine-grained holocrystalline groundmass. Unit **QTai** has normal magnetic polarity and is assigned an early Pleistocene age on the basis of stratigraphic position crosscutting <2.36 Ma andesite flows of **QTab4** (Plate 1). Unit **QTai** is similar in chemistry and mineralogy (containing hornblende) to flows of unit **QTab6** capping the northern part of Bluegrass Ridge (**Figure 2-1**; Plate 1).

Table 6-4. Select XRF geochemical analyses for the Lookout Mountain volcanics on Bluegrass Ridge in the Dog River–Badger Lake area.

Sample	413 DRBLJ 19	412 DRBLJ 19	378 MCB-DRJ 17	377 MCB-DRJ 17	376 MCB-DRJ 17	375 MCB-DRJ 17	420 DRBLJ 19	S90-H76	374 MCB-DRJ 17
Geographic Area	Elk Mountain	Elk Mountain	Bluegrass Ridge	Bluegrass Ridge	Bluegrass Ridge	Bluegrass Ridge	Bluegrass Ridge	Bluegrass Ridge	Bluegrass Ridge
Formation	Lookout Mountain volcanics	Lookout Mountain volcanics	Lookout Mountain volcanics	Lookout Mountain volcanics	Lookout Mountain volcanics	Lookout Mountain volcanics	Lookout Mountain volcanics	Lookout Mountain volcanics	Lookout Mountain volcanics
Map Unit	QTai	QTdi	QTab1	QTab2	QTab2	QTab3	QTab4	QTab5	QTab6
UTM N (NAD 83)	5021246	5021244	5025696	5025677	5025654	5025673	5020939	5022221	5025711
UTM E (NAD 83)	609503	609539	611036	610889	610753	610751	609195	609219	610330
Age (Ma)	na	na	na	na	na	2.36 Ma	na	na	na
Map No.	G118	G117	G287	G285	G279	G284	G105	G174	G289
Oxides, weight percent									
SiO_2	59.07	63.86	61.66	58.62	58.80	63.92	61.76	60.49	58.79
Al_2O_3	18.03	16.05	17.32	17.73	17.53	17.25	16.88	17.83	17.55
TiO_2	1.12	1.14	1.02	1.05	1.15	0.76	0.89	0.97	1.15
FeO*	6.24	5.88	5.97	6.47	6.70	5.06	5.70	5.84	6.76
MnO	0.10	0.10	0.10	0.11	0.11	0.09	0.10	0.10	0.12
CaO	6.60	4.49	5.44	6.67	6.54	4.52	5.66	6.00	6.50
MgO	2.86	1.62	2.35	3.61	3.35	2.47	2.76	3.02	3.32
K_2O	1.71	1.78	1.50	1.57	1.51	1.49	1.69	1.42	1.52
Na_2O	4.02	4.85	4.43	3.99	4.07	4.22	4.31	4.12	4.05
P_2O_5	0.26	0.23	0.22	0.20	0.23	0.21	0.25	0.20	0.23
LOI	0.55	0.44	0.17	0.46	0.13	0.24	0.30	na	1.51
Total_I	99.21	99.27	99.34	98.99	99.23	98.82	99.09	na	97.66
Trace Elements, parts per million									
Ni	27	4	21	42	40	26	26	25	41
Cr	23	4	25	43	42	34	37	24	41
Sc	15	16	11	16	15	11	11	na	14
V	128	116	85	132	131	85	99	na	129
Ba	375	386	356	340	370	350	475	330	368
Rb	25	29	37	29	26	21	30	28	25
Sr	686	448	510	567	620	547	736	580	611
Zr	195	206	166	181	190	169	194	176	189
Y	22	25	19	21	21	16	19	na	21
Nb	11.1	11.5	11.7	11.3	11.4	9.4	10.9	na	11.1
Ga	19	21	20	19	20	19	19	na	19
Cu	35	43	23	38	39	17	32	34	65
Zn	68	76	69	67	70	72	69	60	71
Pb	6	8	7	4	4	4	6	na	4
La	22	20	19	21	22	18	22	na	20
Ce	45	43	39	42	46	40	54	61	41
Th	3	4	3	4	4	4	4	na	3
Nd	24	24	19	21	22	19	26	na	24
U	2	3	3	2	2	2	2	61	3

Major element determinations have been normalized to a 100-percent total on a volatile-free basis and recalculated with total iron expressed as FeO*; nd - no data or element not analyzed; na - not applicable or no information. LOI, Loss on Ignition; Total_I, original analytical total.

QTdi **dacite intrusive rocks (lower Pleistocene)—**Dacite intrusion (SiO_2 = 63.14 to 63.86 weight percent; K_2O = 1.73 to 1.78 weight percent; *n* = 2 analyses) of very limited distribution, exposed just east of the summit of Elk Mountain at the southern end of Bluegrass Ridge (**Figure 2-1**; Plate 1; **Table 6-4**; Appendix). The unit crops out as ledges characterized by horizontal platy to blocky jointing. Thickness of unit **QTdi** is unknown. Typical hand samples of the dacite are medium gray (N5), containing 1 to 2 percent (vol.) chalky white (N9) to clear, subhedral to euhedral, blocky to prismatic, seriate plagioclase microphenocrysts and phenocrysts ≤3 mm (0.1 in), <1 percent (vol.) grayish black (N2), subhedral to euhedral, blocky to prismatic, seriate pyroxene microphenocrysts ≤0.5 mm (0.02 in) (orthopyroxene > clinopyroxene), and 1 to 2 percent (vol.) plagioclase-pyroxene glomerocrysts ≤2 mm (0.08 in), contained within a trachytic, very fine-grained hypocrystalline groundmass. Unit **QTdi** has reversed magnetic polarity and is assigned an early Pleistocene age on the basis of stratigraphic position, crosscutting <2.36 Ma andesite flows of **QTab4** (Plate 1). Correlation to other units beyond the outcrop on Bluegrass Ridge is unknown.

QTab6 **andesite of Bluegrass Ridge, flow sequence 6 (lower Pleistocene)—**Andesite lava flow (SiO_2 = 58.79 weight percent; K_2O = 1.51 weight percent; *n* = 1 analysis) exposed across the top of the northern half of Bluegrass Ridge (**Figure 2-1**; Plate 1; **Table 6-4**; Appendix). Exposure of the unit is poor, limited to a ridge cap of tightly packed boulders. The maximum thickness of unit **QTab6** is ~76 m (250 ft). Typical hand samples of the andesite are medium bluish gray (5B 5/1), containing 10 to 15 percent (vol.) chalky white (N9) to clear, subhedral to euhedral, blocky to prismatic, seriate plagioclase microphenocrysts ≤1 mm (0.04 in) and phenocrysts ≤7 mm (0.3 in), 2 to 3 percent (vol.) fresh to corroded grayish black (N2) to brownish black (5YR 2/1), subhedral to euhedral, blocky to prismatic, seriate hornblende microphenocrysts and phenocrysts ≤4 mm (0.2 in), and trace amounts of pyroxene in a fine-grained holocrystalline to hypocrystalline groundmass. Unit **QTab6** is chemically indistinguishable from flows of unit **QTab2**, occurring lower in the Bluegrass Ridge section, but is separated on the basis of minerology (contains hornblende) and stratigraphic position (Plate 1). Unit **QTab6** is similar in chemistry and mineralogy (containing hornblende) to andesite intrusive rocks of unit **QTai** exposed at the southern end of Bluegrass Ridge (**Figure 2-1**; Plate 1). Magnetic polarity of unit **QTab6** is unknown. Unit **QTab6** is assigned an early Pleistocene age on the basis of stratigraphic position above the 2.36 Ma dacite of Bluegrass Ridge (**QTab3**) (Plate 1).

QTab5 **andesite of Bluegrass Ridge, flow sequence 5 (lower Pleistocene)—**Andesite lava flow (SiO_2 = 59.38 to 60.49 weight percent; K_2O = 1.41 to 1.53 weight percent; *n* = 3 analyses) exposed across the top of the southern half of Bluegrass Ridge (**Figure 2-1**; Plate 1; **Table 6-4**; Appendix). Outcrops of unit **QTab5** are platy jointed. Typical hand samples are two-pyroxene andesite with trace amounts of olivine(?). Unit **QTab5** has reversed magnetic polarity and is assigned an early Pleistocene age on the basis of stratigraphic position above the 2.36 Ma dacite of unit **QTab3** (Plate 1). The unit may be approximately equivalent in age to unit **QTab6**.

QTab4 **andesite of Bluegrass Ridge, flow sequence 4 (lower Pleistocene)—**Sequence of andesite lava flows (SiO_2 = 59.52 to 62.76 weight percent; K_2O = 1.65 to 1.80 weight percent; *n* = 5 analyses) underlying Elk Mountain in the southwest part of the map area (**Figure 2-1**; Plate 1; **Table 6-4**; Appendix). The unit includes a downfaulted, lithologically and compositionally similar, ~40 m thick (130 ft), bench-forming andesite lava (SiO_2 = 62.56 weight percent; *n* = 1 analysis) overlying

Pliocene basaltic andesite (**Tpba**) along the Elk Meadows Trail (Plate 1). Unit **QTab4** forms multiple ledges and cliffs characterized by vertical platy jointing. Outcrops contain ~ 5 to 10 percent (vol.) conspicuous subrounded to rounded, equigranular plagioclase-pyroxene inclusions ≤20 cm across (7.9 in). Thickness of the composite **QTab4** flow unit ranges between 61 and 152 m (200 to 500 ft) near the summit of Elk Mountain. Typical hand samples of the andesite are medium gray (N5), containing 2 to 3 percent (vol.) chalky white (N9) to clear, subhedral to euhedral, blocky to prismatic, seriate plagioclase microphenocrysts and phenocrysts ≤4 mm (0.2 in), 2 to 3 percent (vol.) grayish black (N2), subhedral to euhedral, blocky to prismatic, seriate pyroxene microphenocrysts and phenocrysts ≤3 mm (0.1 in) (orthopyroxene > clinopyroxene), and 3 to 5 percent (vol.) fine-grained inclusions contained within a fine-grained holocrystalline groundmass. Unit **QTab4** has reversed magnetic polarity and is assigned an early Pleistocene age on the basis of stratigraphic position above the 2.36 Ma dacite of Bluegrass Ridge (**QTab3**) (Plate 1).

QTab3 **dacite of Bluegrass Ridge, flow sequence 3 (lower Pleistocene)—**Dacite lava flow (SiO_2 = 63.92 weight percent; K_2O = 1.48 weight percent; *n* = 1 analysis) exposed in prominent and extensive cliff forming outcrops on Bluegrass Ridge (**Figure 2-1**; Plate 1; **Table 6-4**; Appendix). Outcrops of the dacite are characterized by tabular to platy jointing. The maximum thickness of unit **QTab3** is ≤46 m (152 ft). Typical hand samples of the dacite are medium gray (N5), containing 2 to 3 percent (vol.) chalky white (N9) to clear, subhedral to euhedral, blocky to prismatic, seriate plagioclase microphenocrysts and phenocrysts ≤7 mm (0.3 in) and 2 to 3 percent (vol.) grayish black (N2), subhedral to euhedral, blocky to prismatic, seriate pyroxene microphenocrysts ≤1 mm (0.04 in) (orthopyroxene > clinopyroxene), contained within a fine-grained holocrystalline groundmass. Unit **QTab3** has reversed magnetic polarity and is assigned an early Pleistocene age on the basis of stratigraphic position and an $^{40}Ar/^{39}Ar$ plateau age of 2.36 Ma ± 0.03 Ma (plagioclase; 375 MCB-DRJ 17) (Plate 1; **Table 5-1**; Appendix).

QTab2 **andesite of Bluegrass Ridge, flow sequence 2 (lower Pleistocene)—**Andesite lava flows (SiO_2 = 58.61 to 59.00 weight percent; K_2O = 1.5 to 1.56 weight percent; *n* = 5 analyses) exposed in prominent and extensive cliff forming outcrops on Bluegrass Ridge (**Figure 2-1**; Plate 1; **Table 6-4**; Appendix). Flows dip northward, extending from the south-central part of Bluegrass Ridge, where the base of the unit lies at an elevation of 1,415 m (4,640 ft) north to Tamanawas Falls, where the base of the unit is at 1,178 m (3,864 ft) (**Figure 2-1**; Plate 1). Bluegrass Ridge andesite flows of unit **QTab2** terminate just south of Tamanawas Falls where they are incised and filled by younger flows of the ~46 ka andesite of Langille Crags (**Qh3lc**) (**Figure 2-1**; Plate 1). Outcrops of unit **QTab2** are characterized by tabular to platy jointing. The maximum thickness of unit **QTab2** is ~ 118 m (386 ft). Typical hand samples of the andesite are medium gray (N5), containing 10 to 15 percent (vol.) chalky white (N9) to clear, subhedral to euhedral, blocky to prismatic, seriate plagioclase microphenocrysts and phenocrysts ≤8 mm (0.3 in), 5 percent (vol.) grayish black (N2), subhedral to euhedral, blocky to prismatic, seriate pyroxene microphenocrysts and phenocrysts ≤4 mm (0.2 in) (orthopyroxene > clinopyroxene), contained within a fine- to medium-grained holocrystalline groundmass. Unit **QTab2** has reversed magnetic polarity and is assigned an early Pleistocene age on the basis of stratigraphic position below the 2.36 Ma dacite of Bluegrass Ridge (**QTab3**) and above 2.63 Ma High-TiO_2 basalt (**QTbt**) (Plate 1). Keith and others (1985) reported K-Ar ages of 1.68 ± 0.06 (whole rock; sample 79TF0004) and 1.88 ± 0.05 Ma (whole rock; sample

79TF0004) for an outcrop that falls within this unit near Tamanawas Falls (**Figure 2-1**; Plate 1; **Table 5-1**; Appendix). Their reported K-Ar ages, appear too young in reference to higher precision $^{40}Ar/^{39}Ar$ ages obtained from the Bluegrass Ridge section.

QTab1 **andesite of Bluegrass Ridge, flow sequence 1 (lower Pleistocene)—**Andesite lava flow (SiO_2 = 61.66 weight percent; K_2O = 1.49 weight percent; *n* = 1 analysis) exposed in extensive cliff forming outcrops on Bluegrass Ridge **Figure 2-1,** Plate 1; **Table 6-4**; Appendix). Flows dip northward from the south-central part of Bluegrass Ridge to Tamanawas Falls on the north. On the south, unit **QTab1** lies above older rhyolite and basaltic andesite (**Tpre**, **Tpba**) at an elevation of 1,325 m (4,345 ft), while the base of the unit lies over High-TiO_2 basalt flows (**QTbt**) near Tamanawas Falls at an elevation of 1,163 m (3,815 ft) (**Figure 2-1**; Plate 1). Outcrops are characterized by tabular to platy jointing. The maximum thickness of unit **QTab1** is 91 m (300 ft). Typical hand samples of the andesite are medium gray (N5), containing 5 to 10 percent (vol.) chalky white (N9) to clear, subhedral to euhedral, blocky to prismatic, seriate plagioclase microphenocrysts and phenocrysts ≤4 mm (0.2 in), 5 percent (vol.) grayish black (N2), subhedral to euhedral, blocky to prismatic, seriate pyroxene microphenocrysts (orthopyroxene > clinopyroxene), ≤1 percent (vol.) plagioclase-pyroxene glomerocrysts ≤1 mm (0.04 in), and ≤2 percent (vol.) fine-grained, subround inclusions ≤1.5 cm (0.6 in), contained within a fine-grained holocrystalline groundmass. Unit **QTab1** has reversed magnetic polarity and is assigned an early Pleistocene age on the basis of stratigraphic position below the 2.36 Ma dacite of Bluegrass Ridge (**QTab3**) and above 2.63 Ma High-TiO_2 basalt (**QTbt**) (Plate 1).

Lookout Mountain area

QTrl **porphyritic rhyolite (lower Pleistocene or upper Pliocene)—**Isolated rhyolite flow or intrusion (SiO_2 = 69.23 weight percent; K_2O = 3.17 weight percent; *n* = 1 analysis) lying above unit **QTal4** andesite, northwest of High Prairie (**Figure 2-1**; Plate 1; **Table 6-5**; Appendix). Outcrops of unit **QTrl** are massive, weathering to boulders up to several meters across. Grus-weathering is characteristic, resulting from a highly porphyritic texture. Typical hand samples are medium dark gray (N4) and abundantly porphyritic with ≤50 percent (vol.) chalky white (N9), euhedral to subhedral, plagioclase phenocrysts ≤1 cm (0.4 in), ≤1 percent fresh brownish black (5YR 2/1), euhedral to subhedral, blocky to prismatic, seriate hornblende microphenocrysts and phenocrysts ≤2 mm (0.8 in), and ≤1 percent (vol.) plagioclase-hornblende glomerocrysts ≤3 mm (0.1 in), contained within a glassy devitrified spherulitic groundmass. Magnetic polarity of unit **QTrl** is unknown. Unit **QTrl** is is assigned a late Pliocene or early Pleistocene age on the basis of stratigraphic position above unit **QTal4** (Plate 1).

QTal4 **andesite of Lookout Mountain, flow sequence 4 (lower Pleistocene or upper Pliocene)—A**ndesite lava flow (SiO_2 = 58.33 to 58.91 weight percent; K_2O = 1.43 to 1.68 weight percent; Zr = 151 to 161 ppm; *n* = 6 analyses) of very limited distribution, exposed in the uppermost reaches of Dog River, northwest of High Prairie (**Figure 2-1**; Plate 1; **Table 6-5**; Appendix). Unit **QTal4** sits directly on **QTal2** flows; flows of **QTal3** are missing in the section in the vicinity of High Prairie (Plate 1). Unit **QTal4** chiefly crops out as knobs or cliffs, marked by platy to blocky jointing. The maximum thickness of unit **QTal4** is 53 m (175 ft). Typical hand samples of the andesite are medium gray (N5), containing 3 to 5 (vol.) percent clear to chalky white (N9), euhedral to subhedral, prismatic to blocky, seriate plagioclase microphenocrysts ≤1 mm (0.04 in) and <1 percent (vol.) phenocrysts ≤6 mm (0.2 in) (commonly resorbed), 2 to 3 percent (vol.) grayish black (N2), subhedral to euhedral, blocky to prismatic, seriate pyroxene microphenocrysts ≤1 mm (0.04 in) (orthopyroxene > clinopyroxene), <1 percent (vol.) pyroxene phenocrysts ≤6 mm (0.2 in), and ≤1 percent (vol.) white (N9) and black (N1) speckled plagioclase-pyroxene glomerocrysts ≤1 cm (0.4 in), contained within a mottled fine-grained holocrystalline groundmass. Unit **QTal4** has reversed magnetic polarity and is assigned a late Pliocene or early Pleistocene age on the basis of stratigraphic position directly below the ~2 Ma basaltic andesite of High Prairie (**Qrbhp**) (Plate 1).

Table 6-5. Select XRF geochemical analyses for the Lookout Mountain volcanics on Lookout Mountain in the Dog River–Badger Lake area.

Sample	123 DRBLJ 19	226 DRBLJ 19	221 DRBLJ 19	RC13-498-54	220 DRBLJ 19	209 DRBLJ 19
Geographic Area	Lookout Mountain	Lookout Mountain	Lookout Mountain	Lookout Mountain	Lookout Mountain	Lookout Mountain
Formation	Lookout Mountain volcanics	Lookout Mountain volcanics	Lookout Mountain volcanics	Lookout Mountain volcanics	Lookout Mountain volcanics	Lookout Mountain volcanics
Map Unit	QTrl	QTal1	QTal2	QTal3	QTal4	QTa
UTM N (NAD 83)	5023952	5023543	5023570	5028487	5023602	5021910
UTM E (NAD 83)	614474	614136	614375	613682	614496	615112
Age (Ma)	na	na	na	na	na	na
Map No.	G234	G224	G227	G367	G230	G155
Oxides, weight percent						
SiO_2	69.23	59.91	61.93	60.58	58.90	56.77
Al_2O_3	16.00	17.40	16.96	17.61	18.11	17.85
TiO_2	0.47	1.00	0.92	1.01	1.09	1.08
FeO*	3.19	6.38	5.78	6.00	6.42	7.60
MnO	0.06	0.10	0.10	0.09	0.10	0.11
CaO	2.57	6.23	5.28	5.89	6.64	7.36
MgO	0.89	3.10	2.60	2.76	3.23	4.06
K_2O	3.17	1.73	2.11	1.75	1.49	1.27
Na_2O	4.32	3.96	4.14	4.14	3.85	3.69
P_2O_5	0.10	0.18	0.18	0.17	0.16	0.16
LOI	1.00	0.33	0.59	na	0.47	0.48
Total_I	98.52	99.31	99.28	98.55	98.99	98.83
Trace Elements, parts per million						
Ni	6	30	29	20	18	42
Cr	9	35	29	19	30	54
Sc	6	15	13	13	16	18
V	34	119	97	111	127	138
Ba	619	348	416	343	313	269
Rb	50	37	48	38	31	26
Sr	271	585	488	545	593	540
Zr	258	189	213	185	161	153
Y	22	20	24	20	19	21
Nb	13.3	10.1	11.6	10.6	8.3	7.6
Ga	19	19	20	20	20	19
Cu	10	31	24	31	29	37
Zn	54	66	64	66	70	73
Pb	12	5	5	4	5	3
La	29	25	28	24	22	15
Ce	62	43	52	46	40	35
Th	10	5	6	6	5	2
Nd	22	22	25	22	21	21
U	3	1	2	1	2	1

Major element determinations have been normalized to a 100-percent total on a volatile-free basis and recalculated with total iron expressed as FeO*; nd - no data or element not analyzed; na - not applicable or no information. LOI, Loss on Ignition; Total_I, original analytical total.

QTal3 **andesite of Lookout Mountain, flow sequence 3 (lower Pleistocene or upper Pliocene)—**Andesite lava flows (SiO_2 = 58.76 to 61.05 weight percent; K_2O = 1.64 to 1.83 weight percent; Zr = 171 to 215 ppm; *n* = 15 analyses) overlying inclusion-rich lavas of unit **Tpdf** northwest of Lookout Mountain (**Figure 2-1**; Plate 1; **Table 6-5**; Appendix). **QTal3** flows underlie the 2.5 Ma basalt of Horkelia Meadows (**Qrbh**) near Powder Springs, and are found in outcrops above Brooks Meadow Road, downfaulted across the Powder Springs fault (**Figure 2-1**; Plate 1). The unit forms extensive ledge- and cliff-forming outcrops with blocky, platy, and tabular jointing. The maximum thickness of unit **QTal3** is 35 m (115 ft). Typical hand samples of the andesite are medium dark gray (N4), with 3 to 5 percent (vol.) clear to chalky white (N9), euhedral to subhedral, prismatic to blocky, seriate plagioclase microphenocrysts and phenocrysts 2 to 4 mm (0.08 to 0.04 in), 1 to 2 percent (vol.) grayish black (N2), subhedral to euhedral, blocky to prismatic, seriate pyroxene microphenocrysts ≤1 mm (0.04 in) (orthopyroxene > clinopyroxene), and 1 to 2 percent (vol.) plagioclase-pyroxene glomerocrysts ≤1 cm (0.4 in), contained within a fine- to medium-grained holocrystalline groundmass. Unit **QTal3** has reversed magnetic polarity and is assigned a late Pliocene or early Pleistocene age on the basis of stratigraphic position (Plate 1).

QTal2 **andesite of Lookout Mountain, flow sequence 2 (lower Pleistocene or upper Pliocene)—**Andesite lava flows (SiO_2 = 60.78 to 62.34 weight percent; K_2O = 1.95 to 2.23 weight percent; Zr = 201 to 257 ppm; *n* = 27 analyses) exposed northwest of Lookout Mountain and west of Horkelia Meadow (**Figure 2-1**; Plate 1; **Table 6-5**; Appendix). Unit **QTal2** includes a chemically similar, north-south striking dike daylighting through extensive colluvial deposits in the head of Culvert Creek (**Figure 2-1**; Plate 1). Unit **QTal2** is distinguished from other flow sequences in the Lookout Mountain volcanics by stratigraphic position and characteristically higher contents of silica, potassium, and zirconium (**Table 6-5**; Appendix). The unit forms extensive ledge- and cliff-forming outcrops with blocky, platy, and tabular jointing. Maximum thickness of unit **QTal2** is 122 m (400 ft). Typical hand samples of the andesite are medium dark gray (N4), with 5 to 10 percent (vol.) clear to chalky white (N9), euhedral to subhedral, prismatic to blocky seriate plagioclase microphenocrysts and phenocrysts from 5 mm to 1 cm (0.2 to 0.4 in), 1 to 2 percent (vol.) grayish black (N2), subhedral to euhedral, blocky to prismatic, seriate pyroxene microphenocrysts and phenocrysts ≤4 mm (0.2 in) (orthopyroxene > clinopyroxene), and ≤1 percent (vol.) plagioclase-pyroxene glomerocrysts ≤1 cm (0.4 in), contained within a fine- to medium-grained crystalline groundmass. Unit **QTal2** has reversed magnetic polarity and is assigned a late Pliocene or early Pleistocene age on the basis of stratigraphic position (Plate 1). North of Tumble Creek, flows forming part of unit **QTal2**, directly overlie 2.6 to 2.4 Ma High-TiO_2 lavas (**QTbt**); unit **QTal2** sits directly below the 2.35 Ma basalt of Bennett Pass Road (**Qrbp**) on the west slope of Lookout Mountain and the 2.52 Ma basalt of Horkelia Meadow (**Qrbh**), west of Horkelia Meadow (**Figure 2-1**; Plate 1).

QTal1 **andesite of Lookout Mountain, flow sequence 1 (lower Pleistocene or upper Pliocene)—**Andesite lava flow (SiO_2 = 59.90 to 60.52 weight percent; K_2O = 1.72 to 1.74 weight percent; Zr = 185 to 188 ppm; *n* = 2 analyses) exposed beneath unit **QTal2**, northwest of Lookout Mountain and west of Horkelia Meadow (**Figure 2-1**; Plate 1; **Table 6-5**; Appendix). Outcrops are characterized by thick intervals of platy to tabular jointing. The unit is ~100 m (300 ft) thick northwest of High Prairie (**Figure 2-1**; Plate 1). Typical hand samples of the andesite are medium dark gray (N4) to medium bluish gray (5B 5/1) and pale blue (5B 6/2), with 5 to 10 percent (vol.) clear to chalky

white (N9), euhedral to subhedral, prismatic to blocky, seriate plagioclase microphenocrysts and phenocrysts 2 to 4 mm (0.08 to 0.1 in), 2 percent (vol.) grayish black (N2), subhedral to euhedral, blocky to prismatic, seriate pyroxene microphenocrysts and phenocrysts ≤2 mm (0.08 in) (orthopyroxene > clinopyroxene), and ≤1 percent (vol.) plagioclase-pyroxene glomerocrysts ≤1 cm (0.4 in), contained within a fine-grained holocrystalline groundmass. Unit **QTal1** has normal magnetic polarity and is assigned a late Pliocene or early Pleistocene age on the basis of stratigraphic position above the ~3.02 Ma dacite of Fifteenmile Creek (**Tpdf**) and below the 2.35 Ma basalt of Bennett Pass Road (**Qrbp**) (Plate 1).

QTa **andesite (lower Pleistocene or upper Pliocene)—**Andesite lava flow (SiO_2 = 56.77 to 57.20 weight percent; K_2O = 1.18 to 1.27 weight percent; *n* =2 analyses) exposed at the base of the Lookout Mountain volcanic sequence (**Figure 2-1**; Plate 1; **Table 6-5**; Appendix). The unit forms a small outcrop on Lookout Mountain, west of the Powder Springs fault (**Figure 2-1**; Plate 1). A poorly-exposed outcrop of unit **QTa** is also present on the Lookout Mountain Trail, ~0.5 km (0.3 mi) southeast of Senecal Spring. The andesite (**QTa**) crops out as ledges characterized by blocky jointing. Typical hand samples of the andesite are medium gray (N5), with 1 to 2 percent (vol.) clear, euhedral, prismatic, seriate plagioclase phenocrysts to 2 to 4 mm (0.08 to 0.1 in), 1 percent grayish black (N2), subhedral to euhedral, blocky to prismatic, seriate pyroxene microphenocrysts ≤0.5 mm (0.02 in), and ≤1 percent (vol.) plagioclase-pyroxene glomerocrysts ≤4 mm (0.1 in), contained in a fine-grained holocrystalline to hypocrystalline groundmass. Unit **QTa** has reversed magnetic polarity and is assigned a late Pliocene or early Pleistocene age on the basis of stratigraphic position above the 3.14 Ma andesite and dacite flows of Senecal Spring (**Tpds**).

6.3.2.3 Lower Pleistocene and Pliocene volcanic rocks along East Fork Hood River

QTbt **High-TiO_2 basalt and basaltic andesite (lower Pleistocene and/or upper Pliocene [?])—**Sequence of high-TiO_2 basalt and basaltic andesite lavas (TiO_2 = 1.94 to 2.37 weight percent) occurring at a similar stratigraphic position in three geographic areas, including: 1) Bluegrass Ridge; 2) Tumble Creek and Dog River drainages; and 3) Tilly Jane Creek (**Figure 2-1**; Plate 1; **Table 6-6**; Appendix). Typical hand samples of High-TiO_2 basalt are medium gray (N5) aphyric to plagioclase microporphyritic with 1 percent (vol.) fresh clear, seriate plagioclase microphenocrysts ≤1 mm (0.04 in) and ≤1 to 2 percent (vol.), fresh to waxy altered moderate greenish yellow (10Y 7/4) subhedral blocky, seriate olivine microphenocrysts ≤1 mm (0.04 in), contained within a fine-grained crystalline groundmass. Rocks contain sparse larger phenocrysts of plagioclase and olivine ≤4 mm (0.2 in). Isotopic ages ranging between 2.6 and 2.4 Ma indicate emplacement close to the Quaternary-Pliocene boundary.

- Bluegrass Ridge hosts a horizon of High-TiO_2 basaltic lava flows (SiO_2 = 50.22 to 50.99 weight percent; TiO_2 = 2.12 to 2.22 weight percent; K_2O = 1.03 to 1.22 weight percent; *n* =2 analyses) exposed at the base of the Lookout Mountain volcanics (**Figure 2-1**; **Table 6-6**; Plate 1; Appendix). These flows have reversed magnetic polarity and an $^{40}Ar/^{39}Ar$ plateau age of 2.63 ± 0.01 Ma (groundmass; sample 380 MCB-DRJ 17) (**Table 5-1**; Appendix).
- High-TiO_2 basaltic lava flows (SiO_2 = 49.06 to 52.20 weight percent; TiO_2 = 1.94 to 2.37 weight percent; K_2O = 0.96 to 1.43 weight percent; *n* =5 analyses) are exposed above Tumble Creek and along the middle reaches of Dog River (**Figure 2-1**; Plate 1; **Table 6-6**; Appendix).

Outcrops are massive or characterized by blocky jointing and thin vesicular flow lobes. These flows have reversed magnetic polarity. The section exposed north of Tumble Creek, includes at its base, a lower TiO_2 and K_2O basaltic lava (SiO_2 = 50.62 weight percent; TiO_2 = 1.63 weight percent; K_2O = 0.64 weight percent; *n* = 1 analysis) relative to other flows in the unit (**Figure 2-1**; Plate 1; Appendix). This flow is similar in character and composition to those exposed in the Tilly Jane section along Glacier Ditch (Plate 1). A channelized lava overlying a fluvial boulder gravel deposit along Brooks Meadow Road, just south of Tumble Creek, has a K-Ar age of 2.43 ± 0.14 Ma (whole rock; sample S91-H47; Conrey and others, 1996) (**Figure 2-1**; Plate 1; **Table 5-1**; Appendix).

- Tilly Jane exposures include a group of four separate, and not necessarily genetically related lava flows of chiefly basalt and basaltic andesite (**Figure 2-1**; Plate 1; Scott and Gardner, 2017; basalt of Tilly Jane): 1) Basaltic lava flows (SiO_2 = 50.68 to 50.93 weight percent; TiO_2 = 2.00 to 2.07 weight percent; K_2O = 1.00 to 1.04 weight percent; *n* =6 analyses) form a broad upland between Tilly Jane Creek and Weygandt Canyon (**Figure 2-1**; Plate 1; **Table 6-6**; Appendix). These lava flows have reversed magnetic polarity and a K-Ar age of 2.5 ±0.026 Ma (whole rock; sample 940616-1; Scott and Gardner, 2017) (**Table 5-1**; Appendix); 2) An underlying basaltic andesite lava flow (SiO_2 = 53.06 weight percent; TiO_2 = 2.28 weight percent; K_2O = 0.84 weight percent; *n* = 1 analysis) is little exposed in the bed of Tilly Jane Creek (**Figure 2-1**; Plate 1; Appendix); 3) A talus comprising blocks of basalt lava (SiO_2 = 51.23 weight percent; TiO_2 = 1.49 weight percent; K_2O = 0.55 weight percent; *n* = 1 analysis) is poorly exposed along Glacier Ditch on the southeast side of Evans Creek valley but must be in place nearby (**Figure 2-1**; Plate 1; Appendix); it has lower TiO_2 and K_2O than subunit 1 flows between Tilly Jane Creek and Weygandt Canyon; 4) A deeply weathered basalt breccia with areas of potentially intact lava (SiO_2 = 51.81 weight percent; TiO_2 = 1.43 weight percent; K_2O = 0.24 weight percent; *n* = 1 analysis) exposed along Cooper Spur Road is chemically similar to (3) (**Figure 2-1**; Plate 1; Appendix). Subunits 2 to 4 are undated; no in-place lava for determining magnetic polarity.

Table 6-6. Select XRF geochemical analyses for early Pleistocene and Pliocene volcanics in the Dog River–Badger Lake area (part 1 of 3).

Sample	RC-DS47	940616-1	380 MCB-DRJ 17	299 MCB-DRJ 17	230 DRBLJ 19	236 DRBLJ 19	196A DRBLJ 19	196B DRBLJ 19	176 DRBLJ 19	177 DRBLJ 19
Geographic Area	Brooks Meadow Road	Tilly Jane Creek	Bluegrass Ridge	Brooks Meadow Road	Lookout Mountain	Lookout Mountain	Culvert Creek	Culvert Creek	Lookout Mountain	Lookout Mountain
Formation	Pliocene Pleist. volcanics	Pliocene Pleist. volcanics	Pliocene Pleist. volcanics	Pliocene Pleist. volcanics	Pliocene Pleist. volcanics	Pliocene Pleist. volcanics	Pliocene Pleist. volcanics	Pliocene Pleist. volcanics	Pliocene Pleist. volcanics	Pliocene Pleist. volcanics
Map Unit	QTbt	QTbt	QTbt	QTat	QTpi	QTpi	Tpdf	Tpdf (inclus.)	Tpds	Tpds
UTM N (NAD 83)	5027895	5031352	5025723	5027835	5023235	5023255	5024935	5024935	5021984	5021965
UTM E (NAD 83)	612670	609425	611173	612618	613967	613826	614211	614211	615280	615274
Age (Ma)	2.43 Ma	2.5 Ma	2.63 Ma	~2.7 Ma	na	na	~3 Ma	na	~3.14 Ma	na
Map No.	G339	G461	G290	G335	G213	G217	G263	G264	G162	G160
Oxides, weight percent										
SiO_2	50.42	50.82	50.22	62.13	63.82	57.54	63.14	54.55	62.79	64.75
Al_2O_3	16.85	17.55	16.74	17.60	16.78	17.77	16.62	18.94	17.48	16.73
TiO_2	1.95	2.08	2.12	0.94	0.91	1.42	0.89	1.35	0.93	0.80
FeO*	9.77	10.44	10.94	5.26	5.27	7.53	5.62	8.79	5.59	4.78
MnO	0.15	0.16	0.17	0.09	0.07	0.12	0.09	0.14	0.09	0.09
CaO	8.38	8.12	8.11	5.57	4.60	6.77	4.80	7.42	4.46	4.20
MgO	7.21	5.40	5.92	2.09	1.69	3.23	2.13	4.07	2.19	1.64
K_2O	1.00	1.01	1.22	1.78	2.28	1.44	2.27	1.18	2.19	2.53
Na_2O	3.85	3.95	4.03	4.35	4.39	3.92	4.27	3.34	4.09	4.31
P_2O_5	0.42	0.47	0.53	0.19	0.18	0.27	0.18	0.23	0.19	0.17
LOI	na	na	na	0.04	0.43	0.93	0.75	2.29	1.20	0.63
Total_I	na	na	99.55	99.54	99.33	98.69	98.77	97.17	98.50	99.17
Trace Elements, parts per million										
Ni	122	42	91	13	12	18	10	14	12	10
Cr	208	47	140	14	12	34	19	35	14	9
Sc	24	0	21	11	12	16	13	25	13	11
V	200	0	163	94	90	140	96	188	100	80
Ba	319	255	256	376	426	300	460	307	467	474
Rb	8	12	16	24	50	20	55	21	48	57
Sr	546	560	514	633	467	602	434	595	440	417
Zr	162	210	239	188	224	181	222	126	246	266
Y	25	28	31	17	21	21	21	18	22	25
Nb	19.1	16.0	22.8	9.9	11.7	11.3	11.1	6.7	12.9	13.6
Ga	19	0	20	20	19	21	20	20	21	20
Cu	46	41	37	27	27	33	31	45	28	23
Zn	91	74	104	73	62	82	61	79	67	62
Pb	1	0	3	6	6	5	5	3	6	6
La	8	0	24	18	24	17	26	12	25	30
Ce	44	43	49	40	49	38	50	36	49	57
Th	4	0	2	4	6	2	7	2	6	7
Nd	na	na	27	22	22	22	23	18	23	27
U	na	na	2	3	2	2	3	1	3	3

Major element determinations have been normalized to a 100-percent total on a volatile-free basis and recalculated with total iron expressed as FeO*; nd - no data or element not analyzed; na - not applicable or no information. LOI, Loss on Ignition; Total_I, original analytical total. Sample 600 MCBJ 16 is located outside the study area, in the Fivemile Butte 7.5' quadrangle.

Table 6-6, continued. Select XRF geochemical analyses for Pliocene and early Pleistocene volcanics in the Dog River–Badger Lake area. (part 2 of 3).

Sample	296 DRBLJ 19	326 DRBLJ 19	404 DRBLJ 19	S90-H66	431 MCB-DRJ 17	301 MCB-DRJ 17	708 MCBJ 16	RC14na/ 22 DRBLJ 19	RC14-8	55 DRBLJ 19	302 MCB-DRJ 17
Geographic Area	Lookout Mt.	Lookout Mt.	Elk Mt.	Bluegr. Ridge	Culvert Creek	Brooks Meadow Road	Fret Creek	Culvert Creek	Culvert Creek	Brooks Meadow Road	Brooks Meadow Road
Formation	Pliocene Pleist. volcanics	Pliocene Pleist. volcanics	Pliocene Pleist. volcanics	Pliocene Pleist. volcanics	Pliocene Pleist. volcanics	Pliocene Pleist. volcanics	Pliocene Pleist. volcanics	Pliocene Pleist. volcanics	Pliocene Pleist. volcanics	Pliocene Pleist. volcanics	Pliocene Pleist. volcanics
Map Unit	Tprd	Tpat	Tpre	Tpba	Tprc	Tpbb	Tpaf	Tpdc	Tpda	Tpbe	Tpbc
UTM N (NAD 83)	5021779	5021547	5021632	5023124	5025630	5027543	5021419	5025306	5025456	5026928	5026769
UTM E (NAD 83)	614416	614291	609087	610424	613318	612664	616270	613074	612927	612421	612565
Age (Ma)	na	na	na	na	na	na	na	3.77 Ma	na	na	na
Map No.	G145	G136	G138	G205	G278	G301	G130	G269	G275	G315	G308
Oxides, weight percent											
SiO_2	70.89	58.94	69.66	54.66	71.09	53.95	59.83	66.46	61.19	54.07	51.83
Al_2O_3	14.94	16.59	15.87	18.32	14.91	19.24	17.27	15.81	17.71	17.40	17.90
TiO_2	0.44	1.74	0.53	1.19	0.42	1.19	1.01	0.76	1.23	1.62	1.50
FeO*	3.47	7.56	3.19	7.59	3.02	8.50	6.22	4.77	5.87	9.28	9.11
MnO	0.04	0.12	0.07	0.12	0.05	0.13	0.11	0.07	0.05	0.15	0.14
CaO	1.57	6.29	2.35	8.46	1.75	7.87	6.26	2.92	5.32	7.48	9.74
MgO	0.10	2.61	0.37	5.17	0.44	4.16	3.36	0.91	1.48	4.79	5.51
K_2O	3.24	2.05	2.87	0.76	3.39	0.84	1.76	3.02	2.23	1.20	0.87
Na_2O	5.23	3.74	4.95	3.51	4.86	3.93	3.98	5.04	4.53	3.69	3.21
P_2O_5	0.09	0.36	0.13	0.23	0.08	0.19	0.20	0.24	0.38	0.32	0.21
LOI	1.09	1.36	0.80	na	0.56	0.37	0.20	na	na	0.73	na
Total_I	98.45	98.05	99.04	na	98.86	99.29	99.07	98.39	97.80	98.96	99.59
Trace Elements, parts per million											
Ni	1	6	1	80	4	42	43	2	8	65	59
Cr	2	15	3	67	4	31	45	1	7	74	113
Sc	10	18	6	na	5	18	15	10	13	21	26
V	8	145	15	na	17	145	122	33	87	158	194
Ba	639	440	600	305	588	206	378	620	464	338	182
Rb	74	51	55	na	76	10	37	67	57	23	12
Sr	202	442	319	650	190	572	595	270	457	478	524
Zr	402	227	292	160	322	147	186	407	277	202	119
Y	40	28	30	na	26	19	21	52	38	29	21
Nb	25.6	21.2	18.0	na	16.6	8.8	9.7	26.3	19.8	15.7	7.8
Ga	20	20	19	na	20	21	21	23	22	20	19
Cu	5	24	3	43	10	36	36	13	35	38	48
Zn	74	89	59	77	48	87	71	92	80	96	80
Pb	10	6	7	na	9	3	6	9	5	4	4
La	39	26	37	na	34	13	24	40	33	20	13
Ce	70	55	64	34	58	24	43	75	67	43	24
Th	9	6	7	na	10	2	5	8	7	3	2
Nd	36	28	31	na	27	18	23	37	38	26	15
U	3	3	2	na	3	2	3	2	1	2	2

Major element determinations have been normalized to a 100-percent total on a volatile-free basis and recalculated with total iron expressed as FeO*; nd - no data or element not analyzed; na - not applicable or no information. LOI, Loss on Ignition; Total_I, original analytical total.

Table 6-6, continued. Select XRF geochemical analyses for Pliocene and early Pleistocene volcanics in the Dog River–Badger Lake area. (part 3 of 3).

Sample	300 DRBLJ 19	247 DRBLJ 19	130 MCB-DRJ 18	450 MCBJ 16	142 DRBLJ 19	275 DRBLJ 19	366 DRBLJ 19	320 DRBLJ 19	30 MCB-DRJ 18	184 MCB-DRJ 17
Geographic Area	Engineers Creek	Engineers Creek	Brooks Meadow Road	South Fork Fivemile Creek	Culvert Creek	Engineers Creek	Engineers Creek	Hellroaring Creek	Rimrock	Rimrock
Formation	Pliocene Pleist. volcanics	Pliocene Pleist. volcanics	Pliocene Pleist. volcanics	Pliocene Pleist. volcanics	Pliocene Pleist. volcanics	Pliocene Pleist. volcanics	Pliocene Pleist. volcanics	Pliocene Pleist. volcanics	Pliocene Pleist. volcanics	Pliocene Pleist. volcanics
Map Unit	Tpdd (clast)	Tpal	Tpdv	Tpdv	Tpbl	Tpde	Tprn	Tpdu	Tpbr	Tpbr
UTM N (NAD 83)	5021847	5023566	5026413	5031668	5024457	5023153	5023481	5022360	5038487	5038579
UTM E (NAD 83)	614100	613405	612627	616418	612968	613240	613054	612458	614712	615311
Age (Ma)	na	na	~3.69 Ma	~3.69 Ma	na	na	na	na	na	4.19 Ma
Map No.	G153	G226	G303	G472	G244	G206	G218	G181	G622	G627
Oxides, weight percent										
SiO_2	68.72	63.09	65.93	65.89	51.58	67.54	75.72	65.64	52.81	52.75
Al_2O_3	15.03	17.04	15.33	15.12	18.17	15.90	13.28	16.02	16.70	16.39
TiO_2	0.57	0.83	0.95	0.94	1.48	0.65	0.09	1.11	2.07	1.69
FeO*	4.55	4.86	5.99	6.81	9.19	4.03	1.57	7.02	10.46	9.42
MnO	0.14	0.08	0.09	0.05	0.15	0.06	0.02	0.13	0.17	0.15
CaO	1.91	5.27	3.00	2.57	10.13	3.02	0.78	2.05	7.89	8.46
MgO	0.40	2.17	0.73	0.52	5.50	1.18	0.01	0.82	5.74	6.55
K_2O	3.12	2.21	2.79	2.99	0.62	2.92	4.51	2.72	0.75	0.95
Na_2O	5.41	4.29	4.89	4.79	2.96	4.56	4.00	4.20	3.04	3.26
P_2O_5	0.14	0.15	0.28	0.28	0.21	0.14	0.01	0.30	0.38	0.38
LOI	1.01	1.53	1.17	1.55	2.19	1.51	0.59	2.47	2.11	0.45
Total_I	98.59	98.11	98.16	97.68	97.24	97.92	98.99	97.30	97.54	99.15
Trace Elements, parts per million										
Ni	0	20	1	2	51	4	2	6	85	74
Cr	3	18	2	1	110	6	2	8	196	174
Sc	10	12	12	11	26	8	3	13	25	25
V	10	84	34	21	191	51	2	65	191	200
Ba	617	396	595	594	187	521	726	548	357	407
Rb	68	49	68	70	17	69	118	65	9	16
Sr	195	424	299	254	523	291	66	250	530	703
Zr	428	208	359	399	114	267	160	361	174	197
Y	44	22	50	47	20	23	37	55	30	30
Nb	29.9	10.5	24.8	27.8	7.4	12.9	22.1	24.5	12.6	11.4
Ga	22	20	21	22	19	19	18	22	20	19
Cu	8	25	15	22	41	12	6	18	40	42
Zn	90	59	97	106	80	57	40	100	107	101
Pb	7	7	9	9	2	10	13	7	4	5
La	36	26	57	54	8	27	39	45	23	28
Ce	77	44	73	67	27	55	72	76	43	61
Th	9	6	8	8	1	9	13	8	2	4
Nd	36	19	52	48	16	25	27	42	25	35
U	4	3	3	2	2	3	4	4	2	2

Major element determinations have been normalized to a 100-percent total on a volatile-free basis and recalculated with total iron expressed as FeO*; nd - no data or element not analyzed; na - not applicable or no information. LOI, Loss on Ignition; Total_I, original analytical total.

QTat **andesite of Tumble Creek (lower Pleistocene or upper Pliocene)—**Andesite lava flow (SiO_2 = 60.06 to 62.12 weight percent; *n* = 9 analyses) overlying the ~8 to 7 Ma dacite of East Fork (**Tmde**) in extensive cliff-forming outcrops along the east canyon wall of East Fork Hood River in the vicinity of Tumble Creek (**Figure 2-1**; Plate 1; **Table 6-6**; Appendix). Outcrops of unit **QTat** along East Fork Hood River are characterized by columnar jointing, with well-developed hexagonal columns tens of meters high. Zones within the flow show horizontal to subvertical platy or tabular jointing. The unit forms ~60-m-high (197 ft) cliffs east of Sherwood campground along OR Highway 35 (**Figure 2-1**; Plate 1). The maximum thickness of unit **QTat** along East Fork Hood River is ~230 m (755 ft). Typical hand samples of the andesite are medium gray (N5), with 5 to 10 percent (vol.) clear to chalky white (N9), subhedral to euhedral, blocky to prismatic, seriate plagioclase microphenocrysts ≤1 mm (0.04 in) and phenocrysts 2 to 4 mm (0.08 to 0.1 in), scant black (N1) amphibole phenocrysts ≤2 mm (0.08 in), and trace amounts of fresh moderate yellow green (5GY 7/4) olivine ≤1 mm (0.04 in) in a very fine-grained holocrystalline groundmass. The andesite lacks pyroxene phenocrysts, which distinguishes it from the overlying andesite flows of the Lookout Mountain volcanic sequence (**QTal1**–**QTal4**). Unit **QTat** is assigned a late Pliocene or early Pleistocene age on the basis of stratigraphic position and a K-Ar age of 2.74 ± 0.3 Ma (whole rock; sample 79SWCOO10A; Keith and others, 1985) (Plate 1; **Table 5-1;** Appendix). Bela (1982) reported a similar K-Ar age of 2.7 ± 0.2 Ma (whole rock; Bela-18) for this unit from the same locality.

QTpi **intrusive rocks (lower Pleistocene or upper Pliocene)—**Andesite (SiO_2 = 57.57 to 57.97 weight percent; K_2O = 1.43 to 1.75 weight percent; *n* =2 analyses) and dacite (SiO_2 = 62.47 to 63.81 weight percent; K_2O = 1.81 to 2.27 weight percent; *n* = 3 analyses) forming a small intrusive complex downslope and west of High Prairie (**Figure 2-1**; Plate 1; **Table 6-6**; Appendix). The complex includes an array of meter-scale dikes and domes of andesite and dacite composition. Dacitic rocks are light gray (N7) with ~2 percent (vol.), fresh black (N1) to brownish black (5YR 2/1) iridescent, euhedral, needle-like hornblende phenocrysts ≤3 mm (0.1 in) and ~1 percent (vol.), clear, euhedral, blocky plagioclase phenocrysts ≤3 mm (0.1 in) in a vesicular holocrystalline groundmass. Andesitic variants include 1) a dark gray (N6) aphyric to very sparsely microporphyritic andesite with ~1 percent (vol.) clear, euhedral, prismatic plagioclase microphenocrysts in a very fine-grained holocrystalline groundmass marked by plagioclase microlites; and 2) a yellowish gray, aphyric microdiorite. Unit **QTpi** rocks have reversed magnetic polarity and are assigned a late Pliocene or early Pleistocene age on the basis of stratigraphic position. Intrusions crosscut ~3.02 Ma flows of unit **Tpdf** and are overlain by 2.7 to 2.35 Ma flows of unit **QTal1** (Plate 1).

Tpdf **dacite of Fifteenmile Creek (upper Pliocene)—**Flow-on-flow-succession of dacite lava flows (SiO_2 = 62.55 to 66.26 weight percent; K_2O = 2.01 to 3.01 weight percent; *n* = 19 analyses) exposed between Fret Creek northwest to Culvert Creek in the southeast part of the map area (**Figure 2-1**; Plate 1; **Table 6-6**; Appendix). Unit **Tpdf** is mapped from the headwaters of Fret Creek east into the Middle Columbia Basin for ~14 km (8.7 mi) as a single intracanyon dacite lava flow (SiO_2 = 62.55 to 64.14 weight percent; K_2O = 2.01 to 2.31 weight percent; *n* = 9 analyses outside map area) now represented as inverted topography along the south side of Fifteenmile Creek (**Figure 2-1**; Plate 1; McClaughry and others, in press; J.D. McClaughry, unpublished geologic mapping). Several prominent N.15°E.- to N.25°E.-striking dikes mapped as part of unit **Tpdf** in the upper

parts of Culvert Creek mark the vent area (**Figure 2-1**; Plate 1). The dacite typically crops out as precipitous cliffs marked by meter-scale columnar-jointing; columns are often characterized by internal, horizontal platy joint sets. Cliffs of unit **Tpdf** weather to meter-scale, subrounded boulders and angular slabs, forming extensive talus slopes (**Qt**). Irregularly shaped gabbro-norite inclusions (SiO_2 = 53.85 to 57.77 weight percent; K_2O = 0.72 to 1.88 weight percent; *n* = 7 analyses), ranging from centimeters to several meters across, are a conspicuous and distinguishing feature of this unit throughout its outcrop distribution (**Table 6-6**; Appendix). Concentration of inclusions ranges from ~5 to ≤50 percent (vol.). The preferential weathering out of fine-grained inclusions leads to distinctive cavernous weathering at some localities. The maximum composite thickness unit **Tpdf** in the map area is ~162 m (530 ft) (Plate 1). Typical hand samples of the host dacite are medium light gray (N6), medium dark gray (N4), light bluish gray (5B 7/1), to medium bluish gray (5B 5/1), with 10 to 20 percent (vol.) clear to chalky white (N9), euhedral to subhedral, prismatic to blocky, seriate plagioclase microphenocrysts and phenocrysts ≤1 cm (0.4 in), 2 to 3 percent (vol.) grayish black (N2), euhedral to subhedral, blocky to prismatic pyroxene microphenocrysts and phenocrysts ≤3 mm (0.1 in) (orthopyroxene > clinopyroxene), and ~2 percent (vol.) plagioclase-pyroxene glomerocrysts ≤6 mm (0.2 in), distributed within a very fine-grained holocrystalline to hypocrystalline groundmass. Gabbro-norite inclusions are medium light gray (N6) to pale yellowish brown (10YR 6/2) and equigranular, with a mottled medium-grained holocrystalline groundmass of plagioclase and pyroxene (clinopyroxene + orthopyroxene). The unit directly underlies the base of the Lookout Mountain volcanic sequence, east of East Fork Hood River (**Figure 2-1**; Plate 1). Unit **Tpdf** has normal magnetic polarity and is assigned a late Pliocene age on the basis of stratigraphic position directly above the 3.77 Ma porphyritic trachydacite of Culvert Creek (**Tpdc**) and the 3.14 Ma andesite and dacite of Senecal Spring (**Tpds**); the unit is older than the 2.52 Ma basalt of Horkelia Meadow (**Qrbh**) and the 2.35 Ma basalt of Bennett Pass Road (**Qrbp**) (Plate 1). Intracanyon lava forming part of unit **Tpdf** in the Wolf Run 7.5′ quadrangle, east of the map area, has an $^{40}Ar/^{39}Ar$ plateau age of 3.02 ± 0.02 Ma (groundmass; sample 146 DFWJ 15; McClaughry and others, in press). A K-Ar age of 2.86 ± 0.06 Ma (whole rock; sample RCS88-25) was reported by Gray and others (1996) within unit **Tpdf** for a sample collected from Cold Point, ~4 km (2.5 mi) east of upper Fret Creek (**Figure 2-1**).

Tpds **andesite and dacite of Senecal Spring (upper Pliocene)—**Andesite and dacite lava flows of limited distribution forming Lookout Mountain and underlying High Prairie in the southeastern part of the map area (**Figure 2-1**; Plate 1). The unit consists of at least two bench-forming flows, an upper andesite lava (SiO_2 = 61.08 to 62.79 weight percent; K_2O = 2.01 to 2.19 weight percent; *n* = 2 analyses) and a lower dacite lava (SiO_2 = 64.62 to 64.80 weight percent; K_2O = 2.37 to 2.52 weight percent; *n* = 3 analyses) (Plate 1; **Table 6-6**; Appendix). Outcrops of both lavas show poorly developed vertical columns marked by horizontal platy cross jointing. Crystallinity of the flows leads to grus-type weathering. Unit **Tpds** is downfaulted on the west by the north-northwest-trending Powder Springs fault (**Figure 2-1**; Plate 1). Typical hand samples of the andesite and dacite flows are medium gray (N5) to medium bluish gray (5B 5/1) medium dark gray (N4), with 5 to 10 percent (vol.) clear to chalky white (N9), euhedral to subhedral, prismatic to blocky, seriate plagioclase microphenocrysts and phenocrysts ≤ 7 mm (0.3 in), 3 to 5 percent (vol.) grayish black (N2), euhedral to subhedral, blocky to prismatic pyroxene microphenocrysts ≤ 1 mm (0.04 in) (orthopyroxene >> clinopyroxene), and 2 to 3 percent (vol.) plagioclase-pyroxene

glomerocrysts ≤ 5 mm (0.2 in), distributed within a very fine-grained holocrystalline to hypocrystalline groundmass. Upper **Tpds** andesite flows have normal magnetic polarity, while lower **Tpds** dacite flows have reversed magnetic polarity. Unit **Tpds** is assigned a late Pliocene age on the basis of stratigraphic position and a whole-rock K-Ar age of 3.14 ± 0.2 Ma reported by Wise (1969) (Plate 1; **Table 5-1**; Appendix).

Tprd **rhyolite and volcaniclastic rocks (upper Pliocene)—**Rhyolite lava flow (SiO_2 = 70.89 to 70.96 weight percent; K_2O = 3.21 to 3.23 weight percent; *n* = 2 analyses) interbedded with pumiceous volcaniclastic rocks along Lookout Mountain-Bennett Pass Road, west of Lookout Mountain (**Figure 2-1**; Plate 1; **Table 6-6**; Appendix). The unit includes a several meter-thick section of massive to crudely bedded yellowish gray (5Y 8/1), poorly sorted lithic- and pumice-rich volcaniclastic rock, including thin horizons of air-fall tuff and ash-flow tuff beds ≤2 m (6.6 ft) thick. The rhyolite lava is flow banded, contains cm-scale irregular bands of vesicles, and is blocky to platy jointed. A medium dark gray (N4) to dusky red (5R 3/4) autobreccia, composed of highly vesiculated clasts of rhyolite, is associated with the flow where it contacts intervening layers of volcaniclastic rock. Breccia fragments occur as feathered lenses and isolated pods, partially to completely enclosed in volcaniclastic strata (similar to pillows). Typical hand samples of the rhyolite are medium dark gray (N4), aphyric to sparsely microporphyritic, containing ≤1 percent (vol.) clear to chalky white (N9), euhedral, prismatic plagioclase microphenocrysts ≤1mm (0.04 in), distributed within a hypocrystalline groundmass. Unit **Tprd** has reversed magnetic polarity and is assigned a late Pliocene age on the basis of stratigraphic position beneath the 3.14 Ma andesite and dacite of Senecal Spring (**Tpds**) and above the 3.69 Ma trachydacite of Fivemile Creek (**Tpdv**) (Plate 1).

Tpat **andesite (upper Pliocene)—**Andesite lava flow (SiO_2 = 58.92 weight percent; K_2O = 2.05 weight percent; *n* = 1 analysis) of very limited distribution, cropping out beneath unit **Tprd** and interbedded with unit **Tpdd** breccia along Lookout Mountain-Bennett Pass Road, west of Lookout Mountain (**Figure 2-1**; Plate 1; **Table 6-6**; Appendix). Outcrops are characterized by hackly jointing. Thickness of unit **Tpat** is ~20 m (65 ft). Typical hand samples of the andesite are grayish black (N2) and sparsely microporphyritic to porphyritic containing ≤2 percent (vol.), clear to chalky white (N9), subhedral to euhedral, prismatic to blocky, seriate trachytic plagioclase microphenocrysts and phenocryst ≤3 mm (0.1 in), ≤1 percent (vol.) grayish black (N2), euhedral to subhedral, blocky to prismatic clinopyroxene microphenocrysts ≤1 mm (0.04 in), and <1 percent (vol.) plagioclase-pyroxene glomerocrysts ≤3 mm (0.1 in), contained in a hypohyalline groundmass. Unit **Tpat** has reversed magnetic polarity and is assigned a late Pliocene age on the basis of stratigraphic position beneath the 3.14 Ma andesite and dacite of Senecal Spring (**Tpds**) and above the 3.69 Ma trachydacite of Fivemile Creek (**Tpdv) (**Plate 1).

Tpre **rhyolite of Elk Mountain (upper Pliocene)—**Rhyolite lava flow (SiO_2 = 69.66 to 70.53 weight percent; K_2O = 2.87 to 3.04 weight percent; *n* = 3 analyses) exposed over a distance of 1.8 km (1.5 mi), along the southern part of Bluegrass Ridge, north of Elk Mountain (**Figure 2-1**; Plate 1; **Table 6-6**; Appendix). Precipitous cliff- and knob-forming outcrops are characterized by thin subhorizontal platy to tabular jointing. Thickness of unit **Tpre** is ≤105 m (345 ft). Typical hand samples are light bluish gray (5B 7/1) to medium bluish gray (5B 5/1) and aphyric to very sparsely microporphyritic and porphyritic, with ≤1 percent (vol.), clear euhedral to subhedral,

prismatic, seriate plagioclase microphenocrysts and phenocrysts ≤3 mm (0.1 in) and <1 percent (vol.) grayish black (N2), blocky orthopyroxene microphenocrysts <1 mm (0.04 in), contained within a foliated, mottled very fine-grained holocrystalline groundmass. Unit **Tpre** has reversed magnetic polarity and is assigned a late Pliocene age on the basis of stratigraphic position beneath two-pyroxene andesite flows of unit **QTab4** and above the dacite of Engineers Creek (**Tpde**) (Plate 1). Unit **Tpre** is chemically similar to porphyritic rhyolite of unit **Tprc**, but lacks the abundant plagioclase phenocrysts characterizing unit **Tprc**.

Tpba **basaltic andesite of Bluegrass Ridge (upper Pliocene)—**Basaltic andesite lava flows and vent deposits (SiO_2 = 54.34 to 54.99 weight percent; K_2O = 0.75 to 1.20 weight percent; *n* = 5 analyses) exposed along the southern terminus and east slope of Bluegrass Ridge (**Figure 2-1**; Plate 1; **Table 6-6**; Appendix). Vent deposits are characterized by poorly sorted, dusky red (5R 3/4) oxidized cinders (1 to 10 cm [0.4 to 4 in]) and dense lava blocks (≤0.5 m [1.6 ft]), with intervening thin vesicular lava flows 1 to 3 m thick (3.3 to 9 ft). Exposures on the east side of Bluegrass Ridge consist of vesicular, 2 to 4 m thick (6.6 to 13.2 ft), pyroxene-bearing basaltic andesite lava flows separated by ≤1-m-thick (3.3 ft) zones of intervening flow breccia. Basaltic andesite flows tend to be rubbly and blocky weathering, unlike overlying platy andesites capping Bluegrass Ridge (**QTab1**-**QTab6**) (**Figure 2-1**; Plate 1). Minor white (N9) zeolite, calcite, clays, and dark yellowish orange (10YR 6/6) Fe-staining is common across many vesicles and voids. The unit includes a 3- to 4-m-wide (10 to 13 ft) dike, too small to map, just east of the summit of Elk Mountain (sample G126; **Figure 2-1**; Plate 1; Appendix). Typical hand samples of the basaltic andesite are dark gray (N3), containing 2 to 3 to ≤10 percent (vol.), clear, subhedral to anhedral, prismatic to blocky, seriate plagioclase microphenocrysts ≤1 mm (0.04 in), ≤1 percent (vol.) waxy, moderate brown (5YR 3/4), subhedral blocky, seriate iddingsitized olivine microphenocrysts and phenocrysts ≤5 mm (0.02 in), ≤1 percent (vol.) grayish black (N2) subhedral, blocky pyroxene microphenocrysts ≤1 mm (0.04 in) (orthopyroxene = clinopyroxene), and ≤ percent plagioclase-pyroxene microglomerocrysts ≤1 mm (0.1 in), distributed within a fine-grained holocrystalline groundmass. Basaltic andesite lavas (**Tpba**) on the south end of Bluegrass Ridge have reversed magnetic polarity; polarity of thin basaltic andesite lavas (**Tpba**) on the east side of Bluegrass Ridge is unknown (**Figure 2-1**; Plate 1). Unit **Tpba** is assigned a late Pliocene age on the basis of stratigraphic position beneath 2.36 Ma two-pyroxene andesite and dacite flows (**QTab3**) and above the dacite of Pocket Creek (**Tpml**) (Plate 1).

Tptb **tuff breccia (upper Pliocene)—**Volcaniclastic tuff breccia exposed beneath 2.63 Ma lava flows of unit **QTbt** and above ~3 Ma porphyritic rhyolite of unit **Tprc** along Bluegrass Ridge (**Figure 2-1**; Plate 1). Contains clasts of fresh pyroxene andesite.

Tprc **porphyritic rhyolite of Culvert Creek (upper Pliocene)—**Rhyolite lava flow (SiO_2 = 71.02 to 72.94 weight percent; K_2O = 3.38 to 3.74 weight percent; *n* = 7 analyses) exposed in prominent cliff- and hoodoo-forming outcrops in the vicinity of Culvert Creek, east of East Fork Hood River (**Figure 2-1**; Plate 1; **Table 6-6**; Appendix). The unit is also exposed near the base of Bluegrass Ridge, west of East Fork Hood River (**Figure 2-1**; Plate 1). Outcrops of unit **Tprc** are typically massive and are distinguished by the following characteristics: 1) grus-weathering resulting from a highly porphyritic texture; 2) Fe-staining appearing as a dark yellowish orange (10YR 6/6) wash on many surfaces; and 3) sparsely distributed, subround pale yellowish brown (10YR 6/2) gabbro-

norite inclusions, ranging from 1 cm (0.4 in) to ≤10 cm (4 in) across. The rhyolite is ≤152 m (500 ft) thick along Culvert Creek and ≤137 m (450 ft) on Bluegrass Ridge (**Figure 2-1**; Plate 1). Typical hand samples of the rhyolite are medium bluish gray (5B 5/1) and abundantly porphyritic, with 20 to 30 percent (vol.) chalky white (N9), euhedral to subhedral plagioclase phenocrysts ≤1 cm (0.4 in), <1 percent (vol.) grayish black (N2) euhedral to subhedral, blocky to prismatic, seriate pyroxene microphenocrysts ≤1 mm (0.04 in) (orthopyroxene + clinopyroxene), and ≤3 percent (vol.) plagioclase-pyroxene glomerocrysts ≤3 mm (0.1 in), contained within a fresh very fine-grained holocrystalline to hypocrystalline groundmass. Unit **Tprc** has reversed magnetic polarity and is assigned a late Pliocene age on the basis of stratigraphic position directly above the 3.77 Ma porphyritic trachydacite of Culvert Creek (**Tpdc**) and below 2.63 Ma High-TiO_2 basalt (**QTbt**) on Bluegrass Ridge (**Figure 2-1**; Plate 1).

Tpbb **basaltic andesite (upper Pliocene)—**Basaltic andesite lava flow (SiO_2 = 53.65 to 53.95 weight percent; K_2O = 0.83 to 0.84 weight percent; *n* = 2 analyses) discontinuously exposed between Culvert Creek and Brooks Meadow Road in the central part of the map area (**Figure 2-1**; Plate 1; **Table 6-6**; Appendix). Outcrops of unit **Tpbb** are blocky jointed. The maximum thickness of unit **Tpbb** is 30 m (100 ft). Typical hand samples of the basaltic andesite are light gray (N7) to medium light gray (N6) and abundantly plagioclase phyric, containing 5 to 10 percent (vol.) chalky white (N9) to clear, euhedral to subhedral, prismatic, seriate plagioclase microphenocrysts and phenocrysts ≤6 mm (0.2 in) and 3 to 4 percent (vol.) variably altered to fresh dark greenish yellow (10Y 6/6), subhedral blocky-shaped, seriate iddingsitized olivine microphenocrysts ≤1 mm (0.04 in), distributed within a diktytaxitic, fine-grained inequigranular holocrystalline groundmass. Unit **Tpbb** has normal magnetic polarity and is assigned a late Pliocene age on the basis of stratigraphic position directly above the 3.77 Ma porphyritic trachydacite of Culvert Creek (**Tpdc**) and below the 2.52 Ma basalt of Horkelia Meadow (**Qrbh**) (Plate 1). Bela (1982) showed a K-Ar age of 2.7 ± 0.2 Ma along Brooks Meadow Road that may have been obtained from this unit, but location data are imprecise (**Table 5-1**; Appendix).

Tpaf **andesite of Fret Creek (upper Pliocene)—**Andesite lava flow (SiO_2 = 59.83 to 60.13 weight percent; K_2O = 1.73 to 1.93 weight percent; *n* = 5 analyses) forming a thick sequence beneath unit **Tpds** across the broad glacial cirque forming upper Fifteenmile Creek in the southeast part of the map area (**Figure 2-1**; Plate 1; **Table 6-5**; Appendix). Unit **Tpaf** flows are mapped eastward from the Dog River–Badger Lake area to the vicinity of Fifteenmile Campground and Cold Spring, ~5 km (3 mi) east of Senecal Spring (**Figure 2-1;** J.D. McClaughry, unpublished geologic mapping). Unit **Tpaf** also includes prominent bench-forming outcrops west of Horkelia Meadow and those poorly exposed between Brooks Meadow Road and OR Highway 35 (sample G316; **Figure 2-1**; Plate 1). Outcrops of unit **Tpaf** are characterized by thick intervals of platy to tabular jointing; more typically the unit is exposed as piles of meter-scale boulders and slabs scattered across the forest floor. The unit has an apparent thickness exceeding 300 m (984 ft) in upper Fifteenmile Creek (**Figure 2-1**; Plate 1). Typical hand samples of the andesite are medium dark gray (N4) to medium bluish gray (5B 5/1) and pale blue (5B 6/2), containing 5 to 10 percent (vol.) clear to chalky white (N9), euhedral to subhedral, prismatic to blocky, seriate plagioclase microphenocrysts and phenocrysts 2 to 4 mm (0.08 to 0.1 in), 2 percent (vol.) grayish black (N2), subhedral to euhedral, blocky to prismatic, seriate pyroxene microphenocrysts and phenocrysts ≤2 mm (0.08 in) (orthopyroxene > clinopyroxene), and ≤1 percent (vol.) plagioclase-pyroxene glomerocrysts ≤1

cm (0.4 in), contained within a fine-grained holocrystalline groundmass. Unit **Tpaf** has normal magnetic polarity and is assigned a late Pliocene age on the basis of stratigraphic position below the ~3.02 Ma dacite of Fifteenmile Creek (**Tpdf**) and the 3.14 Ma andesite and dacite flows of Senecal Spring (**Tpds**) in the southeastern part of the map area; outcrops between the East Fork Hood River and Brooks Meadow Road overlie the 3.77 Ma porphyritic trachydacite of Culvert Creek (**Tpdc**) (**Figure 2-1**; Plate 1).

Tpdc **porphyritic trachydacite of Culvert Creek (upper Pliocene)—**Trachydacite lava flow (SiO_2 = 65.15 to 67.94 weight percent; K_2O = 2.99 to 3.63 weight percent; *n* = 5 analyses) exposed in the vicinity of Culvert Creek, east of East Fork Hood River, and near the base of Bluegrass Ridge, west of East Fork Hood River (**Figure 2-1**; Plate 1; **Table 6-6**; Appendix). Unit **Tpdc** typically crops out as ledges and precipitous cliffs characterized by horizontal to subhorizontal platy jointing. Outcrops contain sparsely distributed, subround pale yellowish brown (10YR 6/2) gabbro-norite inclusions ≤1 cm (0.4 in) across. The trachydacite is ≤73 m (240 ft) thick along Culvert Creek and Bluegrass Ridge (**Figure 2-1**; Plate 1). Typical hand samples of the trachydacite are medium dark gray (N4) and abundantly porphyritic with 15 percent (vol.) clear to chalky white (N9) and grayish yellow (5Y 8/4), euhedral to subhedral, seriate, trachytic plagioclase microphenocrysts and phenocrysts ≤5 mm (0.2 in), <1 percent (vol.) corroded euhedral to subhedral, blocky to prismatic, seriate clinopyroxene microphenocrysts ≤1 mm (0.04 in), and ≤3 percent (vol.) plagioclase-pyroxene glomerocrysts ≤3 mm (0.1 in), contained within a very fine-grained holocrystalline to hypocrystalline groundmass. Unit **Tpdc** has reversed magnetic polarity and is assigned a late Pliocene age on the basis of stratigraphic position and isotopic ages. A groundmass sample yielded an $^{40}Ar/^{39}Ar$ plateau age of 3.77 ± 0.02 Ma and a total fusion age of 3.64 ± 0.05 Ma (groundmass; sample RC14-9/22 DRBLJ 19); an $^{40}Ar/^{39}Ar$ plateau age of 3.68 ± 0.07 Ma was determined for plagioclase separates from the same sample (Plate 1; **Table 5-1**; Appendix). The reported groundmass total fusion and plagioclase plateau ages are more consistent with stratigraphic position of unit **Tpdc** above unit **Tpdv**, which has an $^{40}Ar/^{39}Ar$ plateau age of 3.69 ± 0.01 Ma obtained from outcrops along Fivemile Creek, east of the Hood River graben.

Tpda **trachyandesite (upper Pliocene)—**Trachyandesite lava flow (SiO_2 = 61.2 weight percent; K_2O = 2.21 weight percent; *n* = 1 analysis) exposed in several roadcuts along abandoned NF Road 740, east of Little John Sno-Park (**Figure 2-1**; Plate 1; **Table 6-6**; Appendix). Outcrops are blocky to platy jointed (**Figure 2-1**; Plate 1). Unit **Tpda** directly overlies a dusky red-oxidized (5R 3/4) flow top of plagioclase-phyric basaltic lava and vent deposits that are part of underlying unit **Tpbc**. Maximum thickness of unit **Tpda** is 26 m (85 ft) thick. Typical hand samples of the trachyandesite are medium gray (N5) to medium dark gray (N4) and microporphyritic to porphyritic with 2 to 3 percent (vol.) grayish yellow (5Y 8/4), euhedral to subhedral seriate, trachytic plagioclase microphenocrysts and phenocrysts ≤3 mm (0.1 in), 2 to 3 percent (vol.) grayish black (N2), euhedral to subhedral, blocky to prismatic, seriate corroded clinopyroxene microphenocrysts and phenocrysts ≤3 mm (0.1 in), and ≤3 percent (vol.) plagioclase-pyroxene glomerocrysts ≤3 mm (0.1 in), contained within a very fine-grained holocrystalline to hypocrystalline groundmass. Unit **Tpda** has reversed magnetic polarity and is assigned a late Pliocene age on the basis of stratigraphic position below the 3.77 Ma porphyritic trachydacite of Culvert Creek (**Tpdc**) and above the 3.69 Ma trachydacite of Fivemile Creek (**Tpdv**) (Plate 1).

Tpbe **basaltic andesite (upper Pliocene)—**Basaltic andesite lava flow (SiO_2 = 54.06 weight percent; K_2O = 1.20 weight percent; *n* = 1 analysis) little exposed between Brooks Meadow Road and OR Highway 35, west of Horkelia Meadow (sample G315; **Figure 2-1**; **Table 6-6**; Plate 1; Appendix). A broader correlation of the unit beyond the area of Brooks Meadow Road is not possible on the basis of current mapping. Outcrops are blocky jointed and highly vesicular. Typical hand samples of the basaltic andesite are dark gray (N3), containing 2 to 3 percent (vol.) subhedral blocky, seriate iddingsitized olivine microphenocrysts ≤1 mm (0.04 in), ≤1 percent (vol.) clear, subhedral to anhedral, prismatic to blocky, seriate plagioclase microphenocrysts ≤1 mm (0.04 in), and ≤1 percent (vol.) grayish black (N2) (vol.) subhedral, blocky pyroxene microphenocrysts ≤1 mm (0.04 in) (orthopyroxene = clinopyroxene), distributed within a fine-grained holocrystalline groundmass. Unit **Tpbe** has reversed magnetic polarity and is assigned a late Pliocene age on the basis of stratigraphic position below the 3.77 Ma porphyritic trachydacite of Culvert Creek (**Tpdc**) and above the 3.69 Ma trachydacite of Fivemile Creek (**Tpdv**) (Plate 1).

Tpbc **basalt (upper Pliocene)—**Basaltic lava flow (SiO_2 = 51.89 to 51.83 weight percent; K_2O = 0.79 to 0.88 weight percent; *n* = 4 analyses) cropping out between Culvert Creek and Brooks Meadow Road in the central part of the map area (**Figure 2-1**; Plate 1; **Table 6-6**; Appendix). Outcrops are blocky jointed; north of Culvert creek the lava flow has an irregular flow base of dusky red-oxidized (5R 3/4) autobreccia. The maximum thickness of unit **Tpbc** is 48 m (158 ft). Typical hand samples of the basalt are light gray (N7) to medium light gray (N6) and plagioclase phyric, containing 10 to 15 percent (vol.) clear to chalky white (N9), euhedral to subhedral, prismatic, seriate plagioclase microphenocrysts and phenocrysts ≤7 mm (0.3 in), 2 to 3 percent (vol.) variably altered to fresh dark greenish yellow (10Y 6/6), subhedral, blocky, seriate iddingsitized olivine microphenocrysts ≤1 mm (0.04 in), and <1 percent (vol.) grayish black (N2) euhedral to subhedral, blocky to prismatic, seriate clinopyroxene microphenocrysts ≤1 mm (0.04 in), distributed within a very fine-grained holocrystalline to hypocrystalline groundmass. Unit **Tpbc** has reversed magnetic polarity and is assigned a late Pliocene age on the basis of stratigraphic position below the ~3.7 Ma porphyritic trachydacite of Culvert Creek (**Tpdc**) and above the 3.69 Ma trachydacite of Fivemile Creek (**Tpdv**).

Tpdd **tuff breccia of Engineers Creek (lower Pliocene)—**Sequence of very poorly sorted boulder breccia beds exposed in numerous ledge-forming outcrops in the headwaters of Engineers Creek, west of Lookout Mountain (**Figure 2-1**; Plate 1). The breccia is composed of highly angular, texturally similar-appearing clasts of dense to highly vesiculated, grayish black (N2) plagioclase-phyric glassy andesite to rhyolite. Deposits are clast-supported and massive to faintly stratified, with a dusky red (5R 3/4) oxidized to grayish yellow (5Y 8/4) matrix. Most clasts are ≤10 cm (4 in) across, but deposits occasionally contain outsized blocks ranging from 10 cm (4 in) to several meters across. Clasts sampled from the breccia include andesite to rhyolite and trachydacite chemical compositions (SiO_2 = 63.53 to 69.43 weight percent; K_2O = 2.29 to 3.12 weight percent; *n* = 5 analyses) with relatively high amounts of niobium (Nb = 19.6 to 29.9 ppm) and zirconium (Zr = 194 to 430 ppm) (**Table 6-6**; Appendix). The base of the unit, exposed north of Hellroaring Creek, consists of ~10 m (32.8 ft) of massive to thin-bedded, planar-stratified to trough (?) cross-stratified sandstone, poorly sorted pebbly sandstone with angular- to subrounded-volcanic lithics, and silicified sandstone (**Figure 2-1**; Plate 1). The uppermost exposures of unit **Tpdd,** poorly exposed along Lookout Mountain-Bennett Pass Road, are deeply weathered, moderate

yellow (5Y 7/6), well-sorted feldspathic fine-grained pebbly sandstone (**Figure 2-1**; Plate 1). Thickness of unit **Tpdd** may be as much as 275 m (902 ft); the map pattern suggests that unit **Tpdd** fills a broad southeast directed paleochannel. Unit **Tpdd** is assigned an early Pliocene age on the basis of stratigraphic position below the ~3.02 Ma dacite Fifteenmile Creek (**Tpdf**) and the 3.14 Ma andesite and dacite of Senecal Spring (**Tpds**); the unit lies above the undated dacite of Engineers Creek (**Tpde**) (Plate 1). Unit **Tpdd** is interpreted to be correlative to identical-looking and time-equivalent ~3.7 Ma trachyandesite- and trachydacite-clast boulder breccia filling a broad channel between upper Fifteenmile Creek, Friend, and Dufur in the eastern part of the Middle Columbia Basin (east of map area; McClaughry and others, in press; **Figure 5-6**). A single clast from the breccia deposit collected near Dufur has an $^{40}Ar/^{39}Ar$ plateau age of 3.71 ± 0.02 Ma (plagioclase; sample 265 DFWJ 14; McClaughry and others, in press).

Tpal **andesite and dacite of Lunch Creek (lower Pliocene)—**Flow-on-flow succession of andesite and dacite lava flows (SiO_2 = 62.23 to 63.23 weight percent; K_2O = 2.08 to 2.22 weight percent; *n* = 4 analyses) exposed between Engineers Creek and Little John Sno-Park, east of the East Fork Hood River (**Figure 2-1**; Plate 1; **Table 6-6**; Appendix). The unit crops out as several cliff-forming benches, marked by internal platy jointing. **Tpal** flows are locally separated by poorly sorted, porphyritic, dacite-clast boulder breccia. The maximum thickness of unit **Tpal** is 106 m (350 ft) near Engineers Creek (**Figure 2-1**; Plate 1). Typical hand samples are medium gray (N5) to medium dark gray (N4) and microporphyritic to porphyritic, with 5 to 10 percent (vol.) grayish yellow (5Y 8/4), euhedral to subhedral, seriate plagioclase microphenocrysts and phenocrysts ≤7 mm (0.3 in) and 1 to 2 percent (vol.) grayish black (N2), euhedral to subhedral, blocky to prismatic, seriate corroded pyroxene microphenocrysts ≤1 mm (0.04 in) (orthopyroxene > clinopyroxene), contained within a fine-grained holocrystalline groundmass. The lowest flow in unit **Tpal** has normal magnetic polarity, while upper flows have reversed magnetic polarity. Unit **Tpal** is assigned an early Pliocene age on the basis of stratigraphic position below the ~3.7 Ma porphyritic trachydacite of Culvert Creek (**Tpdc**) and above the 3.69 Ma dacite of Fivemile Creek (**Tpdv**) (Plate 1).

Tpdv **trachydacite of Fivemile Creek (lower Pliocene)—**Trachydacite lava flow (SiO_2 = 64.09 to 66.07 weight percent; K_2O = 2.76 to 3.36 weight percent; Nb = 24.8 to 31 ppm; Zr = 356 to 421 ppm; *n* = 20 analyses [16 outside map area]) present in two locations in the map area (**Table 6-6**; Appendix). The unit is exposed 1) as a flow in stratigraphic section at an elevation of ~ 1,097 m (3,600 ft) between Engineers Creek and Brooks Meadow Road and in the base of Bluegrass Ridge, and 2) as an intracanyon lava cropping out at 1,291 m (4,234 ft) elevation on the south side of South Fork Fivemile Creek, 2 km (1.2 mi) south of Mill Creek Buttes (**Figure 2-1**; Plate 1). Intracanyon unit **Tpdv** lava flows extend east of the map area ~24 km (15 mi) down the main fork of Fivemile Creek (east of map area; **Figure 5-6**). Outcrops of the unit are marked by massive to meter-scale columnar-joints and irregular zones of horizontal platy jointing. Thickness of unit **Tpdv** ranges between 38 and 76 m (125 and 250 ft) in the map area. Typical hand samples of the trachydacite are dark gray (N3), containing 1 to 2 percent (vol.) clear, subhedral to anhedral, prismatic to blocky, seriate plagioclase microphenocrysts and phenocrysts ≤3 mm (0.1 in), ~1 percent (vol.) grayish black (N2) (vol.) euhedral to subhedral, prismatic- to lath-shaped pyroxene microphenocrysts ≤1 mm (0.04 in) (orthopyroxene ≥ clinopyroxene), and ≤1 percent (vol.) plagioclase-pyroxene microglomerocrysts ≤1 mm (0.1 in), distributed within a very fine-grained

holocrystalline to hypocrystalline groundmass. Unit **Tpdv** has reversed magnetic polarity and is assigned an early Pliocene age on the basis of stratigraphic position and an $^{40}Ar/^{39}Ar$ plateau age of 3.69 ± 0.02 Ma (groundmass; sample 173 DFWJ 15; McClaughry and others, in press) and an older K-Ar age of 3.7 ± 0.2 Ma (whole rock; sample JA85022; Anderson, 1987) determined on outcrops in Fivemile Canyon east of the map area (**Figure 5-6**).

Tpbl **basalt (lower Pliocene)—**Basaltic lava flow (SiO_2 = 51.57 weight percent; K_2O = 0.62 weight percent; *n* = 1 analysis) of very limited distribution, exposed beneath the dacite of Fivemile Creek (**Tpdv**) and above the dacite of East Fork (**Tmde**), 1 km (0.6 mi) southeast of Little John Sno-Park (**Figure 2-1**; Plate 1; **Table 6-6**; Appendix). Outcrops are characterized by cm-scale horizontal platy jointing. Thickness of unit **Tpbl** is ~40 m (131 ft). Typical hand samples of the basalt are dark gray (N3), containing 1 to 2 percent (vol.) clear to grayish yellow (5Y 8/4), subhedral to anhedral, prismatic, seriate plagioclase microphenocrysts and phenocrysts ≤2 mm (0.8 in) and 1 to 2 percent (vol.) grayish black (N2), euhedral to subhedral, blocky to prismatic, seriate clinopyroxene microphenocrysts ≤2 mm (0.08 in), distributed within a fine-grained holocrystalline groundmass. Unit **Tpbl** has reversed magnetic polarity and is assigned an early Pliocene age on the basis of stratigraphic position directly beneath the 3.69 Ma trachydacite of Fivemile Creek (**Tpdv**) (Plate 1).

Tpde **dacite of Engineers Creek (lower Pliocene)—**Dacite domes, dikes, and lava flows (SiO_2 = 65.47 to 67.77 weight percent; K_2O = 2.74 to 3.25 weight percent; *n* = 10 analyses) exposed along Engineers Creek east of East Fork Hood River (**Figure 2-1**; Plate 1; **Table 6-6**; Appendix). Unit **Tpde** typically appears as distinctive cliffs and spires, characterized by thin platy jointing or columnar jointing. Grus-weathering is characteristic, resulting from a highly porphyritic texture. Sparsely distributed (≤3 to 5 percent), pale yellowish brown (10YR 6/2), subround, boulder-sized gabbro-norite inclusions ≤30 cm (12 in) across are present in outcrops, north of Engineers Creek (**Figure 2-1**; Plate 1). Inclusions are often completely weathered out, leaving large cavities in the outcrop. Dark yellowish orange (10YR 6/6) Fe-staining is pervasive through outcrops along both strands of the Hellroaring Creek thrust fault zone (**Figure 2-1**; Plate 1); locally, Fe-stained rocks are associated with pods of chalcedonic quartz. Typical hand samples of the dacite are medium bluish gray (5B 5/1) to medium gray (N5) and light gray (N7), microporphyritic to porphyritic, with 2 to 10 percent (vol.) clear to chalky white (N9) and grayish yellow (5Y 8/4), euhedral to subhedral, seriate plagioclase microphenocrysts and phenocrysts ≤5 mm (0.2 in), 1 to 3 percent (vol.) grayish black (N2), euhedral to subhedral, blocky to prismatic, seriate pyroxene microphenocrysts ≤1 mm (0.04 in) (orthopyroxene >> clinopyroxene), and 2 to 5 percent (vol.) plagioclase-pyroxene glomerocrysts ≤2 mm (0.08 in), contained within a fine-grained holocrystalline to hypocrystalline groundmass. Most outcrops of unit **Tpde** have reversed magnetic polarity, although some outcrops measured are normal. Unit **Tpde** is assigned an early Pliocene age on the basis of stratigraphic position beneath the 3.69 Ma trachydacite of Fivemile Creek (**Tpdv**) and a thrust-fault contact relationship with 5.37 Ma hypabyssal intrusion (**Tmdei**) along Hellroaring Creek (**Figure 2-1**; Plate 1).

Tprn **rhyolite of Engineers Creek (lower Pliocene)—**Rhyolite lava flows and tuff (SiO_2 = 75.39 to 76.3 weight percent; K_20 = 4.18 to 5.27 weight percent; *n* = 5 analyses) exposed along Engineers Creek, east of East Fork Hood River (**Figure 2-1**; Plate 1; **Table 6-6**; Appendix). Unit **Tprn** is chiefly

composed of ledge-forming, massive pale red purple (5RP 6/2) to medium gray (N4), flow-banded, spherulitic stony rhyolite and autobreccia, with local areas of white (N9) to very light gray (N8) crystal-vitric tuff. Flow outcrops in unit **Tprn**, are massive to vertically flow foliated, and display platy, blocky, or hackly jointing. The rhyolite is mostly altered and devitrified, but locally retains relatively fresh perlitic obsidian zones. Outcrops along the lower part of NF Road 640 consist of yellowish gray (5Y 8/1) to light greenish gray (5G 8/1), celadonitic clay-altered (replaces glass), 10- to 50-cm-thick (4 to 19.7 in) beds of lithic tuff breccia, lithic lapilli tuff, air-fall (?) tuff, and tuffaceous sandstone. Lithic tuff breccia includes subangular, intermediate to silicic composition clasts, chiefly 1 to 2 cm (0.4 to 0.8 in) across. Locally clasts are up to 30 cm (11.8 in) across. Unit thickness may exceed 140 m (460 ft). Typical hand samples of the rhyolite are grayish blue (5PB 5/2) to pale red purple (5RP 6/2) with 2 to 3 percent (vol.) clear to chalky white (N9), subhedral, blocky plagioclase microphenocrysts ≤1mm (0.04 in) and trace amounts of grayish black (N2), euhedral to subhedral, seriate biotite microphenocrysts <1 mm (0.4 in), contained within a completely devitrified, spherulitic to axiolitic groundmass of intergrown feldspar and quartz. Unit **Tprn** has reversed magnetic polarity and is assigned an early Pliocene age on the basis of stratigraphic position beneath the 3.69 Ma trachydacite of Fivemile Creek (**Tpdv**) (Plate 1).

Tpdu **trachydacite (lower Pliocene)—**Trachydacite lava flow or intrusion (SiO_2 = 65.63 weight percent; K_2O = 2.71 weight percent; Nb = 24.5 ppm; Zr = 361 ppm; *n* = 1 analysis) very poorly exposed beneath rhyolite of unit **Tprn** between Hellroaring and Engineers Creek (**Figure 2-1**; Plate 1; **Table 6-6**; Appendix). A single small outcrop of the unit, found in the base of an abandoned NF road and cut bank, has platy to blocky jointing. Thickness of the unit is unknown. Typical hand samples of the trachydacite are pale olive (10Y 6/2), with 5 to 10 percent (vol.) chalky white (N9), subhedral, blocky, seriate plagioclase microphenocrysts and phenocrysts ≤ 2 to 4 mm (0.08 to 0.1 in), and 2 to 3 percent (vol.) plagioclase-pyroxene glomerocrysts ≤ 4 mm (0.1 in) in a medium-grained holocrystalline groundmass. Moderate yellow (5Y 7/6) clay staining is common as a surface wash and in some vesicles on hand samples. Unit **Tpdu** has normal magnetic polarity and is assigned a late Pliocene age on the basis of stratigraphic position. The chemical composition of unit **Tpdu** is identical to the trachydacite of Fivemile Creek (**Tpdv**), but the unit is texturally dissimilar and appears stratigraphically older (Plate 1).

Tpbr **basalt and basaltic andesite of Rimrock Creek (lower Pliocene)—**Flow-on-flow succession of basaltic and basaltic andesite lavas (SiO_2 = 51.22 to 53.33 weight percent; K_2O = 0.51 to 0.95 weight percent; *n* = 10 analyses) exposed in cliff-forming outcrops in the headwaters of Rimrock Creek, in the northeast part of the map area (**Figure 2-1**; Plate 1; **Table 6-6**; Appendix). Stratigraphically older flows are high-TiO_2, high FeO* basalt and basaltic andesite (TiO_2 = 1.99 to 2.07 weight percent; FeO* = 9.50 to 10.68 weight percent; *n* = 4 analysis) (**Table 6-6**; Appendix). Stratigraphically younger flows have relatively less amounts of TiO_2 and FeO* (TiO_2 = 1.65 to 1.90 weight percent; FeO* = 8.74 to 9.99 weight percent; *n* = 4 analysis) (**Table 6-6**; Appendix). Unit **Tpbr** crops out as cliffs and ledges, composed of thinly stacked, massive to blocky- and platy-jointed, flow lobes bounded by vesicular flow tops and bottoms. Flow lobes are separated by intervening horizons of dusky red (5R 3/4) interflow breccia. Composite thickness of unit **Tpbr** is 152 m (500 ft). Typical hand samples of the basalt and basaltic andesite are light gray (N7) to medium light gray (N6) and olivine phyric, containing 3 to 5 percent (vol.), variably altered, very

dark red (5R 2/6) to fresh dark greenish yellow (10Y 6/6), euhedral to subhedral, blocky, seriate iddingsitized olivine microphenocrysts and phenocrysts ≤4 mm (0.1 in), distributed within a fine-grained holocrystalline groundmass. Unit **Tpbr** has reversed magnetic polarity and is assigned an early Pliocene age on the basis of stratigraphic position and a $^{40}Ar/^{39}Ar$ plateau age of 4.19 ± 0.01 Ma (groundmass, sample 184 MCB-DRJ 17) (Plate 1; **Table 5-1**; Appendix).

Disconformity

6.3.3 Lower Pliocene and upper Miocene volcanic and sedimentary rocks of the early High Cascades

6.3.3.1 Gunsight Butte volcanics

Tpag **andesite of Gumjuwac Saddle (lower Pliocene)—**Flow-on-flow sequence of andesite lavas (SiO_2 = 57.00 to 59.26 weight percent; K_2O = 1.47 to 1.74 weight percent; *n* = 12 analyses) extending from Gumjuwac Saddle on the north to Badger Lake on the south (**Figure 2-1**; Plate 1; **Table 6-7**; Appendix). Unit **Tpag** crops out as extensive cliffs characterized by blocky jointing. The unit weathers to large meter-scale boulders and angular tabular plates. Many outcrops are frost heaved and flanked by extensive active talus cones (**Qt**). Springs emit from the boundaries between individual flows. Thickness of unit **Tpag** is ≤137 m (450 ft) at Gumjuwac Saddle; the unit thins to the south where the flow sequence is ≤58 m (190 ft) west of Badger Lake (**Figure 2-1**; Plate 1). Typical hand samples of the andesite are light gray (N7), containing ≤2 percent (vol.) clear, euhedral, prismatic to blocky, seriate plagioclase microphenocrysts and phenocrysts ≤3 mm (0.1 in), ≤2 percent (vol.) grayish black (N3), subhedral to anhedral, blocky, seriate pyroxene microphenocrysts and phenocrysts ≤4 mm (0.1 in) (orthopyroxene ≥ clinopyroxene), trace amounts of olivine, and ≤1 percent (vol.) plagioclase-pyroxene glomerocrysts ≤5 mm (0.2 in), distributed within a fine-grained holocrystalline groundmass. Unit **Tpag** has reversed magnetic polarity and is assigned an early Pliocene age on the basis of stratigraphic position and a K-Ar age of 4.25 ± 0.6 Ma (whole-rock; Wise-49; Wise, 1969) (Plate 1; **Table 5-1**; Appendix).

Tpms **dacite (lower Pliocene)—**Dacite lava flow (SiO_2 = 67.19 to 67.36 weight percent; K_2O = 2.37 to 2.40 weight percent; *n* = 2 analyses) exposed along the narrow ridgeline running from Gunsight Butte to the south end of the map area (**Figure 2-1**; Plate 1; **Table 6-7**; Appendix). Outcrops are characterized by bold meter-scale blocky jointing with horizontal zones of stretched flattened vesicles or intervals of thin cm-scale horizontal platy jointing. Many outcrops are frost heaved and flanked by extensive active talus cones (**Qt**). Thickness of unit **Tpms** is ≤91 m (300 ft). Typical hand samples of the dacite are medium bluish gray (5B 5/1), containing 5 to 10 percent (vol.) clear to chalky white (N9), euhedral, prismatic to blocky, seriate plagioclase microphenocrysts and phenocrysts ≤3 mm (0.1 in) and 1 to 2 percent (vol.) grayish black (N2) to brownish black (5YR 2/1), subhedral to anhedral, blocky, seriate pyroxene microphenocrysts ≤1 mm (0.1 in) (orthopyroxene ≥ clinopyroxene), distributed within a flow-banded, vesicular, holohyaline groundmass. Unit **Tpms** has reversed magnetic polarity and is assigned an early Pliocene age on the basis of stratigraphic position below the 4.25 Ma andesite of Gumjuwac Saddle (**Tpag**) (Plate 1).

Table 6-7. Select XRF geochemical analyses for Gunsight Butte volcanics in the Dog River–Badger Lake area (part 1 of 2).

Sample	RC01-125	77 DRBLJ 19	95 DRBLJ 19	65 DRBLJ 19	68 DRBLJ 19	97 DRBLJ 19	98 DRBLJ 19	103 DRBLJ 19	319 DRBLJ 19	284 DRBLJ 19
Geographic Area	Gunsight Butte	Gunsight Butte	Gunsight Butte	Pocket Creek	Pocket Creek	Gunsight Butte	Gunsight Butte	Gunsight Butte	Hellroaring Creek	Gunsight Butte
Formation	Gunsight Butte volcanics	Gunsight Butte volcanics	Gunsight Butte volcanics	Gunsight Butte volcanics	Gunsight Butte volcanics	Gunsight Butte volcanics	Gunsight Butte volcanics	Gunsight Butte volcanics	Gunsight Butte volcanics	Gunsight Butte Volcanics
Map Unit	Tpag	Tpms	Tpmj	Tpmp	Tpmc	Tpmb3	Tpmb2	Tpmb1	Tpmh	Tpmn
UTM N (NAD 83)	5018432	5016997	5018065	5015435	5015536	5018073	5018182	5018664	5022109	5019678
UTM E (NAD 83)	611977	611225	611452	610257	610470	611422	611391	611479	612533	611950
Age (Ma)	4.25 Ma	nd	nd	nd	nd	nd	nd	nd	nd	nd
Map No.	G58	G27	G50	G2	G4	G51	G54	G63	G170	G82
Oxides, weight percent										
SiO_2	58.55	67.20	60.54	60.19	61.23	55.12	56.74	55.88	56.77	59.99
Al_2O_3	17.54	16.30	17.38	18.25	17.58	17.47	17.86	17.31	16.91	17.86
TiO_2	1.06	0.72	0.94	0.87	0.86	1.32	1.05	1.29	1.03	0.96
FeO*	6.29	4.05	5.78	5.75	5.85	7.49	6.62	7.72	6.73	6.05
MnO	0.12	0.08	0.10	0.11	0.10	0.13	0.12	0.13	0.11	0.11
CaO	6.68	3.44	5.83	6.82	5.92	7.87	7.63	7.21	7.34	6.27
MgO	3.74	0.96	3.12	2.96	2.69	4.93	4.71	4.91	5.04	3.07
K_2O	1.69	2.38	1.93	0.93	1.44	1.42	1.33	1.44	1.88	1.25
Na_2O	4.11	4.69	4.17	3.92	4.14	3.97	3.75	3.82	3.81	4.26
P_2O_5	0.22	0.18	0.20	0.20	0.19	0.28	0.18	0.29	0.38	0.18
LOI	na	0.69	0.13	0.10	0.23	0.00	0.00	0.32	0.19	0.30
Total_I	na	98.97	99.53	99.67	99.29	99.35	99.41	99.05	99.10	99.06
Trace Elements, parts per million										
Ni	46	6	32	10	13	48	50	57	82	34
Cr	54	7	31	20	20	86	66	93	112	31
Sc	18	9	14	14	13	21	20	16	17	15
V	137	54	114	111	104	163	164	149	150	124
Ba	393	485	422	219	337	349	282	392	571	300
Rb	27	42	32	8	21	21	22	24	26	22
Sr	651	397	632	1018	622	699	621	731	1003	574
Zr	193	256	208	135	181	174	152	158	187	154
Y	24	24	21	16	21	21	20	20	18	19
Nb	12.5	14.1	11.3	6.0	9.8	14.9	10.0	12.1	7.9	8.2
Ga	20	19	18	21	19	19	20	19	20	20
Cu	27	28	34	17	29	39	36	37	47	35
Zn	76	53	69	65	64	71	68	74	77	65
Pb	8	8	7	2	5	5	5	7	8	5
La	24	29	22	16	20	21	17	25	40	17
Ce	45	52	52	32	43	48	38	50	86	43
Th	4	5	5	1	3	4	3	4	9	2
Nd	22	26	25	18	21	23	19	26	44	20
U	1	1	3	0	1	2	1	1	3	2

Major element determinations have been normalized to a 100-percent total on a volatile-free basis and recalculated with total iron expressed as FeO*; nd - no data or element not analyzed; na - not applicable or no information. LOI, Loss on Ignition; Total_I, original analytical total.

Table 6-7, continued. Select XRF geochemical analyses for the Gunsight Butte volcanics in the Dog River–Badger Lake area (part 2 of 2).

Sample	423 DRBLJ 19	104 DRBLJ 19	286 DRBLJ 19	59 DRBLJ 19	58 DRBLJ 19	445A DRBLJ 19	285 DRBLJ 19	427 DRBLJ 19	435C DRBLJ 19	435B DRBLJ 19
Geographic Area	Bluegrass Ridge	Gunsight Butte	Gunsight Butte	Pocket Creek	Pocket Creek	Pocket Creek	Gunsight Butte	Bluegrass Ridge	Bluegrass Ridge	Bluegrass Ridge
Formation	Gunsight Butte Volcanics	Gunsight Butte Volcanics	Gunsight Butte Volcanics	Gunsight Butte Volcanics	Gunsight Butte Volcanics	Gunsight Butte Volcanics	Gunsight Butte Volcanics	Gunsight Butte Volcanics	Gunsight Butte Volcanics	Gunsight Butte Volcanics
Map Unit	Tpmn	Tpmd	Tpma	Tpmi	Tpmu	Tpmt	Tpml	Tpml	Tpmv (clast)	Tpmv (clast)
UTM N (NAD 83)	5020732	5018782	5019741	5016763	5017359	5017893	5019683	5020456	5020784	5020784
UTM E (NAD 83)	609239	611494	611825	609267	608809	609148	611870	609282	609864	609864
Age (Ma)	nd	nd	nd	nd	nd	nd	nd	nd	nd	nd
Map No.	G97	G65	G86	G24	G29	G38	G83	G90	G99	G98
Oxides, weight percent										
SiO_2	59.55	64.34	62.40	59.47	66.26	65.25	67.46	67.58	63.49	61.77
Al_2O_3	18.05	16.77	16.74	17.56	16.63	17.15	16.08	15.73	17.50	17.79
TiO_2	0.99	0.83	1.08	1.02	0.61	0.63	0.71	0.68	0.72	0.80
FeO*	6.16	4.90	5.87	6.25	4.00	4.17	4.01	4.25	4.56	5.18
MnO	0.10	0.09	0.10	0.10	0.04	0.08	0.09	0.05	0.08	0.09
CaO	6.43	4.44	4.67	6.33	4.13	4.63	3.23	3.64	5.48	5.93
MgO	3.12	1.89	2.10	3.76	1.71	1.80	0.94	1.13	2.48	2.80
K_2O	1.18	1.88	1.94	1.39	1.92	1.60	2.24	2.41	2.01	1.80
Na_2O	4.23	4.65	4.84	3.91	4.55	4.53	5.08	4.35	3.53	3.67
P_2O_5	0.17	0.21	0.25	0.20	0.15	0.16	0.17	0.18	0.14	0.16
LOI	0.15	0.33	0.70	1.56	2.20	1.03	0.67	1.08	1.71	1.29
Total_I	99.61	99.12	98.87	98.23	97.29	98.67	98.81	98.67	98.11	98.56
Trace Elements, parts per million										
Ni	33	15	12	34	10	16	1	8	30	32
Cr	27	17	9	40	12	13	3	7	32	29
Sc	16	10	10	13	8	8	9	7	11	11
V	125	79	87	134	57	92	51	56	77	93
Ba	302	482	441	300	374	370	458	468	323	307
Rb	16	30	29	22	35	26	36	49	44	39
Sr	592	511	560	625	446	510	379	384	546	551
Zr	159	223	208	171	179	178	232	236	137	136
Y	19	20	23	19	16	15	25	21	16	17
Nb	9.0	12.8	14.2	9.1	10.2	9.8	12.1	13.0	7.1	6.7
Ga	20	19	20	19	18	18	19	18	20	19
Cu	33	26	17	35	24	20	8	25	27	32
Zn	66	64	70	66	49	53	55	59	59	64
Pb	4	7	5	5	7	7	6	6	7	5
La	18	24	23	15	16	19	26	23	15	12
Ce	37	56	48	39	32	31	41	49	33	32
Th	3	4	4	3	4	4	4	6	4	3
Nd	17	26	24	19	14	15	25	23	15	16
U	1	2	2	2	2	2	2	2	2	1

Major element determinations have been normalized to a 100-percent total on a volatile-free basis and recalculated with total iron expressed as FeO*; nd - no data or element not analyzed; na - not applicable or no information. LOI, Loss on Ignition; Total_I, original analytical total.

Tpmj **andesite (lower Pliocene)—**Sequence of andesite lava flows (SiO_2 = 58.39 to 61.51 weight percent; K_2O = 1.70 to 2.05 weight percent; *n* = 6 analyses) exposed along the ridgeline, west of Bennett Pass Road in the south part of the map area (**Figure 2-1**; Plate 1; **Table 6-7**; Appendix). Unit **Tpmj** crops out as extensive precipitous cliffs of blocky-jointed lava in west-facing slopes; the unit weathers to meter scale boulders. Thickness of unit **Tpmj** is ≤30 m (100 ft). Typical hand samples of the andesite are medium light gray (N6), containing 5 to 10 percent (vol.) clear, euhedral, prismatic to blocky, seriate plagioclase microphenocrysts and phenocrysts ≤3 mm (0.1 in), ≤1 percent (vol.) grayish black (N3), subhedral to anhedral, blocky, seriate pyroxene microphenocrysts and phenocrysts ≤2 mm (0.08 in) (orthopyroxene ≥ clinopyroxene), ≤1 percent (vol.) brownish black (5YR 2/1) iridescent, subhedral to anhedral, seriate olivine microphenocrysts ≤1 mm (0.04 in), and 1 to 3 percent (vol.) plagioclase-pyroxene glomerocrysts ≤5 mm (0.2 in), distributed within a fine-grained holocrystalline to hypocrystalline groundmass. Unit **Tpmj** has reversed magnetic polarity and is assigned an early Pliocene age on the basis of stratigraphic position below the 4.25 Ma andesite of Gumjuwac Saddle (**Tpag**) (Plate 1).

Tpmp **andesite (lower Pliocene)—**Andesite lava (SiO_2 = 60.18 to 60.65 weight percent; K_2O = 0.92 to 1.04 weight percent; *n* = 4 analyses) capping the ridge in the southernmost part of the map area (**Figure 2-1**; Plate 1; **Table 6-7**; Appendix). Outcrops have blocky to subvertical tabular jointing. Unit **Tpmp** is flanked downslope by extensive active talus cones (**Qt**). Thickness of unit **Tpmp** is ≤41 m (134 ft). Typical hand samples of the andesite are light gray (N6) and aphyric to very sparsely microporphyritic, containing <1 percent (vol.) clear, euhedral, prismatic to blocky, seriate plagioclase microphenocrysts ≤1 mm (0.04 in) and rare outsized plagioclase phenocrysts ≤7 mm (0.3 in), ≤1 percent (vol.) grayish black (N3), subhedral to anhedral, blocky, seriate pyroxene microphenocrysts and phenocrysts ≤4 mm (0.1 in) (orthopyroxene ≥ clinopyroxene), trace brownish black (5YR 2/1) iridescent, subhedral to anhedral, seriate olivine phenocrysts <1 mm (0.04 in), and <1 percent (vol.) plagioclase-pyroxene glomerocrysts <1 mm (0.04 in), distributed within a fine-grained holocrystalline to hypocrystalline groundmass. Unit **Tpmp** has reversed magnetic polarity and is assigned an early Pliocene age on the basis of stratigraphic position below the 4.25 Ma andesite of Gumjuwac Saddle (**Tpag**) (Plate 1).

Tpmc **andesite (lower Pliocene)—**Andesite lava flows exposed in the upper part of Pocket Creek in the southern part of the map area (**Figure 2-1**; Plate 1). The lower part of the unit contains lower-silica flows (SiO_2 = 58.27 to 59.23 weight percent; K_2O = 1.35 to 1.37 weight percent; *n* = 3 analyses); the upper part of the unit is characterized by higher-silica flows (SiO_2 = 61.22 to 61.56 weight percent; K_2O = 1.43 to 1.49 weight percent; *n* = 3 analyses) (**Figure 2-1**; Plate 1; **Table 6-7**; Appendix). Unit **Tpmc** crops out as knobs and ledges marked by blocky or platy jointing. Thickness of the unit is ≤98 m (320 ft). Typical hand samples of the upper flow are medium blue gray (5B 5/1) and microporphyritic, containing 3 to 5 percent (vol.) clear, euhedral, prismatic to blocky, seriate plagioclase microphenocrysts ≤5 mm (0.2 in), ≤1 percent (vol.) grayish black (N3), subhedral to anhedral, blocky, seriate pyroxene microphenocrysts <1 mm (0.04 in) (orthopyroxene ≥ clinopyroxene), trace brownish black (5YR 2/1) iridescent, subhedral to anhedral, seriate olivine phenocrysts <1 mm (0.04 in), and ≤2 percent plagioclase-pyroxene glomerocrysts ≤2.2 cm (0.9 in) distributed within a fine- to medium-grained holocrystalline groundmass. Typical hand samples of the lower flow are light gray (N7) and microporphyritic, containing 3 to 5 percent (vol.) clear, euhedral, prismatic to blocky, seriate plagioclase

microphenocrysts ≤5 mm (0.2 in), ≤3 percent (vol.) grayish black (N3), subhedral to anhedral, blocky, seriate pyroxene microphenocrysts <4 mm (0.1 in) (orthopyroxene ≥ clinopyroxene), and trace brownish black (5YR 2/1) iridescent, subhedral to anhedral, seriate olivine phenocrysts <1 mm (0.04 in), distributed within a fine- to medium-grained holocrystalline groundmass. Unit **Tpmc** has reversed magnetic polarity and is assigned an early Pliocene age on the basis of stratigraphic position (Plate 1).

Tpmb3 **basaltic andesite, upper flows (lower Pliocene)—**Basaltic andesite lava flow (SiO_2 = 54.70 to 55.11 weight percent; K_2O = 1.39 to 1.41 weight percent; *n* = 2 analyses) of restricted distribution, exposed in the west slope of Gunsight Butte (**Figure 2-1**; Plate 1; **Table 6-7**; Appendix). Outcrops are either massive or blocky jointed. Thickness of unit **Tpmb3** is ≤38 m (125 ft). Typical hand samples of the basaltic andesite are medium gray (N5), containing 2 to 3 percent (vol.) clear, euhedral, prismatic to blocky, seriate plagioclase microphenocrysts ≤3 mm (0.1 in), ≤2 percent (vol.) grayish black (N3), subhedral to anhedral, blocky, seriate pyroxene microphenocrysts ≤3 mm (0.1 in) (orthopyroxene ≥ clinopyroxene), and ≤1 percent (vol.) brownish black (5YR 2/1) iridescent, subhedral to anhedral, seriate olivine phenocrysts ≤1 mm (0.04 in), distributed within a vesicular fine-grained holocrystalline to hypocrystalline groundmass. Unit **Tpmb3** has reversed magnetic polarity and is assigned an early Pliocene age on the basis of stratigraphic position below the 4.25 Ma andesite of Gumjuwac Saddle (**Tpag**) (Plate 1).

Tpmb2 **basaltic andesite, middle flows (lower Pliocene)—**Basaltic andesite lava (SiO_2 = 56.32 to 56.74 weight percent; K_2O = 1.33 to 1.34 weight percent; *n* = 2 analyses) exposed the west slope of Gunsight Butte (**Figure 2-1**; Plate 1; **Table 6-7**; Appendix). Unit **Tpmb2** crops out as cliffs, characterized by subvertical to vertical platy to tabular jointing; the unit weathers into large angular blocks and is flanked downslope locally by extensive active talus cones (**Qt**). Thickness of unit **Tpmb2** ranges between 30 and 91 m (100 and 300 ft). Typical hand samples of the basaltic andesite are medium gray (N5), containing 2 to 3 percent (vol.) clear, euhedral, prismatic to blocky, seriate plagioclase microphenocrysts and phenocrysts ≤3 mm (0.1 in), 2 to 3 percent (vol.) grayish black (N3), subhedral to anhedral, blocky, seriate pyroxene microphenocrysts and phenocrysts ≤3 mm (0.1 in) (orthopyroxene ≥ clinopyroxene), ≤1 percent brownish black (5YR 2/1) iridescent, subhedral to anhedral, seriate olivine microphenocrysts ≤1 mm (0.04 in), and 2 to 3 percent (vol.) plagioclase-pyroxene glomerocrysts ≤1.5 cm (0.6 in), distributed within a vesicular, fine-grained holocrystalline to hypocrystalline groundmass. Unit **Tpmb2** has reversed magnetic polarity and is assigned an early Pliocene age on the basis of stratigraphic position below the 4.25 Ma andesite of Gumjuwac Saddle (**Tpag**) and above the 5.37 Ma microdiorite of East Fork (**Tmdei**) (Plate 1).

Tpmb1 **basaltic andesite, lower flows (lower Pliocene)—**Basaltic andesite lava (SiO_2 = 55.82 to 56.46 weight percent; K_2O = 1.22 to 1.50 weight percent; *n* = 6 analyses) exposed beneath unit **Tpmb2** in slopes west of Gunsight Butte (**Figure 2-1**; Plate 1; **Table 6-7**; Appendix). Unit **Tpmb1** extends south to the head of Pocket Creek, where the flow underlies the andesite of unit **Tpmc** (**Figure 2-1**; Plate 1). Cliff-forming outcrops are characterized by blocky jointing; the unit weathers to meter scale, angular blocks and is locally flanked downslope by extensive active talus cones (**Qt**). Thickness of **Tpmb1** unit is ≤80 m (262 ft). Typical hand samples of the basaltic andesite are dark gray (N3) to medium gray (N5), speckled with 5 percent (vol.) clear, euhedral,

prismatic to blocky, seriate plagioclase microphenocrysts ≤3 mm (0.1 in), 2 to 3 percent (vol.) grayish black (N3) to brownish black (5YR 2/1), subhedral to anhedral, blocky, seriate pyroxene microphenocrysts ≤3 mm (0.1 in) (orthopyroxene ≥ clinopyroxene), and ≤1 percent brownish black (5YR 2/1) iridescent, subhedral to anhedral, seriate olivine phenocrysts ≤1 mm (0.04 in), distributed within a fine-grained hypocrystalline to holohyaline groundmass. Unit **Tpmb1** has indeterminate magnetic polarity and is assigned an early Pliocene age on the basis of stratigraphic position below the 4.25 Ma andesite of Gumjuwac Saddle (**Tpag**) and above the 5.37 Ma microdiorite of East Fork (**Tmdei**) (Plate 1).

Tpmh **basaltic andesite, undifferentiated (lower Pliocene)—**Basaltic andesite lava (SiO_2 = 56.76 weight percent; K_2O = 1.88 weight percent; *n* = 1 analyses) poorly exposed in the Hellroaring Creek thrust fault zone (**Figure 2-1**; Plate 1; **Table 6-7**; Appendix). Unit **Tpmh** crops out as ledges marked by blocky jointing. Thickness of unit **Tpmh** is unknown. Typical hand samples of the basaltic andesite are medium gray (N5), speckled with 2 to 3 percent (vol.) clear to chalky white (N9), euhedral, prismatic to blocky, seriate plagioclase microphenocrysts and phenocrysts ≤4 mm (0.2 in), ≤1 percent (vol.) grayish black (N3) to brownish black (5YR 2/1), subhedral to anhedral, blocky, seriate pyroxene microphenocrysts ≤1 mm (0.04 in) (orthopyroxene ≥ clinopyroxene), and <1 percent (vol.) grayish yellow (5YR 2/1), subhedral, seriate olivine microphenocrysts ≤0.5 mm (0.02 in), distributed within a fine-grained hypocrystalline to holohyaline groundmass. Unit **Tpmh** has indeterminate magnetic polarity and is assigned an early Pliocene age on the basis of apparent stratigraphic position below the rhyolite of Engineers Creek (**Tprn**); units underlying unit **Tpmh** basaltic andesite are unknown (Plate 1). Apparent stratigraphic position, lithology, and geochemical composition suggest a permissible correlation with the basaltic andesite flow sequence underlying Gunsight Butte (**Tpmb1**, **Tpmb2**, **Tpmb3**) (**Figure 2-1**; Plate 1).

Tpmn **andesite (lower Pliocene)—**Andesite lava flow (SiO_2 = 59.99 weight percent; K_2O = 1.24 weight percent; *n* = 2 analyses) exposed beneath unit **Tpmb1** in slopes west of Gunsight Butte and in a small flow remnant on the southeast mid-slope of Elk Mountain (**Figure 2-1**; Plate 1; **Table 6-7**; Appendix). Unit **Tpmn** crops out as ledges characterized by blocky jointing. Thickness of unit **Tpmn** is ≤32 m (105 ft). Typical hand samples of the andesite are medium dark gray (N4), with 2 percent (vol.) clear, euhedral, prismatic to blocky, seriate plagioclase microphenocrysts ≤1 mm (0.04 in), <1 percent (vol.) grayish black (N3) to brownish black (5YR 2/1), subhedral to anhedral, blocky, seriate pyroxene microphenocrysts ≤1 mm (0.1 in) (orthopyroxene ≥ clinopyroxene), ≤1 percent (vol.) plagioclase-pyroxene glomerocrysts ≤1.5 cm (0.6 in), and trace amounts of brownish black (5YR 2/1) iridescent, subhedral to anhedral, seriate olivine phenocrysts ≤1 mm (0.04 in), distributed within a mottled fine-grained holocrystalline groundmass. Unit **Tpmn** has reversed magnetic polarity and is assigned an early Pliocene age on the basis of stratigraphic position below the 4.25 Ma andesite of Gumjuwac Saddle (**Tpag**) and above the 5.37 Ma microdiorite of East Fork (**Tmdei**) (Plate 1).

Tpmd **dacite (lower Pliocene)—**Dacite lava flow (SiO_2 = 62.34 to 64.34 weight percent; K_2O = 1.79 to 1.88 weight percent; *n* = 4 analyses) exposed beneath unit **Tpmn** in slopes west of Gunsight Butte (**Figure 2-1**; Plate 1; **Table 6-7**; Appendix). Unit **Tpmd** extends south to the head of Pocket Creek, where it underlies basaltic andesite of unit **Tpmb1** (**Figure 2-1**; Plate 1). Unit **Tpmd** typically crops out as precipitous cliffs marked by meter-scale blocky jointing; the upper parts of unit **Tpmd**

are characterized by hackly jointing and vesicle-rich zones. Irregularly shaped gabbro-norite inclusions, ≤15 cm (6 in) across, are locally a conspicuous and distinguishing feature of this unit. The concentration of inclusions at outcrops ranges from ~5 to ≤10 percent (vol.). The preferential weathering out of fine-grained inclusions from outcrops leads to distinctive cavernous weathering at some localities. Thickness of unit **Tpmd** is ~ 80 m (261 ft) near Pocket Creek; the unit thins to the north, where it is <41 m (135 ft) in the slopes west of Gunsight Butte. Typical hand samples of the dacite are medium light gray (N6) to medium blue gray (5B 5/1), speckled with 5 to 10 percent (vol.) clear, euhedral, prismatic to blocky, seriate plagioclase microphenocrysts and phenocrysts ≤3 mm (0.1 in), 1 to 2 percent (vol.) grayish black (N3) to brownish black (5YR 2/1), subhedral to anhedral, blocky, seriate pyroxene microphenocrysts ≤1 mm (0.1 in) (orthopyroxene ≥ clinopyroxene), ≤1 percent (vol.) plagioclase-pyroxene glomerocrysts ≤3 mm (0.1 in), and trace amounts of brownish black (5YR 2/1) iridescent olivine, distributed within a mottled fine-grained holocrystalline to hypocrystalline groundmass. Unit **Tpmd** has reversed magnetic polarity and is assigned an early Pliocene age on the basis of stratigraphic position below the 4.25 Ma andesite of Gumjuwac Saddle (**Tpag**) and above the 5.37 Ma microdiorite of East Fork (**Tmdei**) (Plate 1).

Tpmi **andesite dikes (lower Pliocene)—**East-west- to N.70°W.-striking andesite dikes (SiO_2 = 58.32 to 59.78 weight percent; K_2O = 1.39 to 1.52 weight percent; *n* = 3 analyses) exposed as prominent vertical spires along Bennett Pass Road in the southern part of the map area (**Figure 2-1**; Plate 1; **Table 6-7**; Appendix). Dikes are up to 14 m wide (45 ft), intruding the tuff breccia of Bennett Pass Road (**Tpmt**) (**Figure 2-1**; Plate 1). Outcrops of unit **Tpmi** are marked by tabular jointing and well-developed horizontal columns perpendicular to dike margins. Typical hand samples of the andesite are medium light gray (N6) to yellowish gray (5Y 8/1), with 2 to 3 percent (vol.) clear, euhedral, prismatic to blocky, seriate plagioclase microphenocrysts and phenocrysts ≤3 mm (0.1 in), 1 to 2 percent (vol.) fresh grayish black (N3) to brownish black (5YR 2/1), subhedral to anhedral, blocky, seriate pyroxene microphenocrysts and phenocrysts ≤2 mm (0.08 in) (orthopyroxene ≥ clinopyroxene), and ≤1 percent (vol.) plagioclase-pyroxene glomerocrysts ≤3 mm (0.1 in), distributed within a fine-grained holocrystalline groundmass. Unit **Tpmi** has reversed magnetic polarity and is assigned an early Pliocene age on the basis of stratigraphic position (Plate 1). Outcrops on Bennett Pass Road may be similar in age to 5.26 ± 0.44 Ma dikes that cut the lower part of Gunsight Mountain volcanics, along NF Road 48, ~3 km (1.8 mi) west-southwest of the Dog River-Badger Lake area (Sherrod and Scott, 1995) (**Figure 2-1**; Plate 1).

Tpmu **dacite of Bennett Pass Road (lower Pliocene)—**Dacite lava flows (SiO_2 = 65.13 to 66.92 weight percent; K_2O = 1.73 to 2.04 weight percent; *n* = 6 analyses) exposed between Bennett Pass Road and East Fork Hood River in the southwest part of the map area (**Figure 2-1**; Plate 1; **Table 6-7**; Appendix). Map pattern indicates the unit is interbedded between units **Tpmb1** and **Tpml** (Plate 1). Lava flows forming unit **Tpmu** are typically poorly exposed; outcrops found are characterized by blocky jointing. Unit **Tpmu** is similar in lithology and chemical composition to dacite clasts (SiO_2 = 65.25 weight percent; K_2O = 1.59 weight percent; *n* =1 analyses) in the underlying tuff breccia of Bennett Pass Road (**Tpmt**) (Plate 1). Maximum thickness of the unit **Tpmu** flow sequence is >215 m (705 ft). Typical hand samples of the dacite are medium gray (N5), with 5 to 10 percent (vol.) chalky white (N9), euhedral, prismatic to blocky, seriate plagioclase microphenocrysts and phenocrysts ≤3 mm (0.1 in), 1 to 2 percent (vol.) altered brownish black (5YR 2/1), euhedral to

subhedral, prismatic, seriate hornblende microphenocrysts and phenocrysts ≤5 mm (0.2 in), ≤1 percent (vol.) plagioclase-hornblende glomerocrysts ≤3 mm (0.1 in), and trace amounts of pyroxene, distributed within a fine-grained holocrystalline groundmass. Unit **Tpmu** has reversed magnetic polarity and is assigned an early Pliocene age on the basis of stratigraphic position (Plate 1). The presence of hornblende distinguishes unit **Tpmu** from the greater part of the Gunsight Butte volcanic sequence.

Tpmt **tuff breccia of Bennett Pass Road (lower Pliocene)—**Dacite-clast tuff breccia exposed above the dacite of Bennett Pass Road (**Tpmu**) (Plate 1). A single clast from the unit has a dacitic chemical composition (SiO_2 = 65.25 weight percent; K_2O = 1.59 weight percent; *n* = 1 analysis) (**Table 6-7**; Appendix). Thickness of unit **Tpmt** breccia is >134 m (440 ft) west of Pocket Creek (**Figure 2-1**; Plate 1). Map pattern indicates unit **Tpmt** is interbedded between units **Tpmb1** and **Tpml** (Plate 1). Tuff breccia of unit **Tpmt** is typically very poorly sorted, clast supported, and apparently monolithologic, containing angular pebble- to boulder-sized clasts of hornblende- and plagioclase-phyric dacite in a tuffaceous matrix of similar composition to the clasts. Typical clasts are light gray (N7), with 2 to 3 percent (vol.) chalky white (N9), euhedral, prismatic to blocky, seriate plagioclase microphenocrysts and phenocrysts ≤3 mm (0.1 in), 1 to 2 percent (vol.) fresh black (N1) to brownish black (5YR 2/1) iridescent, euhedral to subhedral, prismatic, seriate hornblende microphenocrysts and phenocrysts ≤3 mm (0.1 in), ≤1 percent (vol.) fresh black (N1) euhedral to subhedral, prismatic, seriate pyroxene microphenocrysts ≤0.05 mm (0.02 in) (orthopyroxene ≥ clinopyroxene), and ≤1 percent (vol.) plagioclase-hornblende-pyroxene glomerocrysts ≤3 mm (0.1 in), distributed within a mottled, fine-grained hypocrystalline groundmass. Unit **Tpmt** is assigned an early Pliocene age on the basis of stratigraphic position (Plate 1). Tuff breccia (**Tpmt**) is intruded by andesite dikes of unit **Tpmi** west of Pocket Creek (**Figure 2-1**; Plate 1).

Tpml **dacite of Pocket Creek (lower Pliocene)—**Dacite lava flows (SiO_2 = 64.26 to 68.35 weight percent; K_2O = 2.00 to 2.41 weight percent; *n* = 9 analyses) exposed beneath units **Tpmn** and **Tpmd** in slopes west of Gunsight Butte (**Figure 2-1**; Plate 1; **Table 6-7**; Appendix). Unit **Tpml** extends south to the head of Pocket Creek, where flows underlie unit **Tpmd**; the unit also forms remarkable cliff-forming flow-on-flow exposures along the southeast part of Bluegrass Ridge (**Figure 2-1**; Plate 1). Outcrops are marked by blocky to tabular jointing. Maximum thickness of unit **Tpml** is ~245 m (804 ft) on Bluegrass Ridge; the unit thins to ≤121 m (400 ft) near Pocket Creek and to <37 m (121 ft) in the slopes west of Gunsight Butte (**Figure 2-1**; Plate 1). Typical hand samples of the dacite are medium gray (N5) to medium blue gray (5B 5/1) with 1 to 2 percent (vol.) clear, euhedral, prismatic to blocky, seriate plagioclase microphenocrysts and phenocrysts ≤4 mm (0.1 in), ≤1 percent (vol.) grayish black (N3) to brownish black (5YR 2/1), subhedral to anhedral, blocky, seriate pyroxene microphenocrysts ≤0.5 mm (0.02 in) (orthopyroxene ≥ clinopyroxene), and 1 to 2 percent (vol.) plagioclase-pyroxene glomerocrysts ≤3 mm (0.1 in), distributed within a mottled trachytic fine-grained holocrystalline groundmass. Unit **Tpml** has reversed magnetic polarity and is assigned an early Pliocene age on the basis of stratigraphic position below the 4.25 Ma andesite of Gumjuwac Saddle (**Tpag**) and above the ~8 to 7 Ma andesite and dacite of East Fork (**Tmde**) (Plate 1).

Tpma **andesite (lower Pliocene)—**Andesite lava flow (SiO_2 = 60.22 to 62.39 weight percent; K_2O = 1.67 to 1.93 weight percent; *n* = 7 analyses) exposed beneath unit **Tpml** in slopes west of Gunsight Butte and above unit **Tmdei**, southwest of Lookout Mountain (**Figure 2-1**; Plate 1; **Table 6-7**; Appendix). Unit **Tpma** crops out as bold cliffs marked by meter-scale columnar jointing and subhorizontal platy jointing. The stratigraphically lowest flows, exposed west of Gunsight Butte, contain 2 to 3 percent conspicuous subround gabbro-norite inclusions ≤5 cm (2 in) across (**Figure 2-1**; Plate 1). Andesite exposed in the area closer to the Hellroaring Creek thrust fault is characterized by moderate reddish brown (10R 4/6) Fe-staining on fractures and a similar discoloration of plagioclase (Plate 1). Thickness of unit **Tpma** is ≤70 m (228 ft) west of Gunsight Butte. Typical hand samples of the andesite are medium dark gray (N4) to medium light gray (N6) with 2 to 3 percent (vol.) clear, euhedral, prismatic to blocky, seriate plagioclase microphenocrysts and phenocrysts ≤4 mm (0.1 in), 1 to 2 percent (vol.) grayish black (N3) to brownish black (5YR 2/1), subhedral to anhedral, blocky, seriate pyroxene microphenocrysts ≤0.5 mm (0.02 in) (orthopyroxene ≥ clinopyroxene) and rare outsized phenocrysts ≤5 mm (0.2 in), and 1 to 2 percent (vol.) plagioclase-pyroxene glomerocrysts ≤3 mm (0.1 in), distributed within a mottled trachytic fine-grained holocrystalline to hypocrystalline groundmass. Unit **Tpma** has reversed magnetic polarity and is assigned an early Pliocene age on the basis of stratigraphic position below the 4.25 Ma andesite of Gumjuwac Saddle (**Tpag**) and above the 5.37 Ma microdiorite of East Fork (**Tmdei**) (Plate 1).

Tpmv **Gunsight Butte volcanics, undivided (lower Pliocene or upper Miocene [?])—**Volcaniclastic rocks forming the base of the Gunsight Butte volcanics east of East Fork Hood River and along the south end of Bluegrass Ridge (**Figure 2-1**; Plate 1). Unit **Tpmv** directly overlies the andesite and dacite of East Fork (**Tmde**) near the base of Bluegrass Ridge (**Figure 2-1**; Plate 1). Exposures at the base of Bluegrass Ridge form high-standing ribs and cliffs composed of poorly sorted, clast to matrix supported, boulder-rich tuff breccia (**Figure 2-1**; Plate 1). Unit **Tpmv** is poorly exposed east of the East Fork Hood River, where it is largely buried by extensive colluvium (**Qc**). Clasts are comprised almost entirely of grayish black (N2), glassy to highly vesiculated, plagioclase microporphyritic andesite contained within a whitish (N9) tuffaceous matrix. Clasts analyzed from the unit include andesite (SiO_2 = 61.77 weight percent; K_2O = 1.80 weight percent; *n* = 1 analysis) and dacite (SiO_2 = 63.48 weight percent; K_2O = 2.01 weight percent; *n* = 1 analysis) (**Table 6-7**; Appendix). Unit **Tpmv** is assigned an early Pliocene or late Miocene age on the basis of stratigraphic position below the 4.25 Ma andesite of Gumjuwac Saddle (**Tpag**) and above the ~8 to 7 Ma andesite and dacite of East Fork (**Tmde**) (Plate 1).

Disconformity to nonconformity

6.3.3.2 Dalles Formation

Tmdl **Dalles Formation, undivided (lower Pliocene [?] and upper Miocene)—**Moderately- to well-indurated, pale yellowish brown (10YR 6/2), medium gray (N5) to very light gray (N8) boulder conglomerate and breccia, fluvial conglomerate and sandstone, tuffaceous siltstone, and pumice-, ash-, and lithic-tuff, broadly exposed above the CRBG in the Hood River graben escarpment in the northeast part of the Dog River–Badger Lake area (Plate 1, cross section A-A′). Unit **Tmdl** includes late Miocene(?) tuff breccia, conglomerate, and sandstone poorly exposed at lower elevations along Volmer Ditch and Cooper Spur Road at Crystal Spring Creek in the Upper Hood

River Valley (**Figure 2-1**; Plate 1). Upper Hood River Valley exposures were previously mapped as "Dalles Formation" by Wise (1969) and "Volcaniclastic Rocks of Middle Fork" by Sherrod and Scott (1995). Collectively, unit **Tmdl** is stratigraphically equivalent to volcaniclastic strata forming a widespread arc-adjacent apron mapped between East Fork Hood River and far eastern parts of the Middle Columbia Basin (e.g., Deschutes River, Biggs; **Figure 5-6**; Madin and McClaughry, 2019; McClaughry and others, in press; J.D. McClaughry, unpublished geologic mapping).

A majority of beds within unit **Tmdl** are often thin, discontinuous, lithologically indistinct, and occur at a scale too small to map separately and are therefore grouped here. Breccia beds are typically well-exposed, forming erosion-resistant ledges along canyon walls. Tuff breccia exposures north of Shellrock Mountain, containing hornblende-porphyritic mega-blocks, crop out as deeply-eroded fins and hoodoos (**Figure 2-1**; Plate 1). Where breccia beds are deeply weathered, surfaces are commonly mantled by meter-scale boulders intermixed with coarse-grained sandy soils. Breccia is typically matrix-supported with localized clast-supported areas. The deposits range from monolithologic to heterolithologic, dominated by a variety of medium light gray (N6) to pale blue (5B 6/2) and pale purple (5P 6/2), subrounded to subangular clasts of plagioclase and two-pyroxene (± hornblende) andesite and dacite. Clasts are typically enclosed in a matrix composed of volcanic lithics, pumice, partly altered volcanic glass, and plagioclase and pyroxene crystals. Locally, breccia is interbedded with massive to planar stratified sandstone and pebble conglomerate deposited by hyperconcentrated flood-flows, tuff deposited by pyroclastic flows and falls, and lenticular bedded, massive to trough- and planar-cross bedded pebble- to cobble-rich conglomerate, pebbly sandstone, and sandstone and massive to laminated tuffaceous siltstone deposited in fluvial environments. Thickness of unit **Tmdl** in the Dog River–Badger Lake area is ≤412 m (1,350 ft). Unit **Tmdl** is assigned a late Miocene and early Pliocene age, ranging between 8.8 and ~5 Ma on the basis of stratigraphic position, numerous isotopic ages in the Middle Columbia Basin, and vertebrate and leaf fossils. Equivalent to the Dalles Formation as defined by Condon (1874).

Tmdei **microdiorite of East Fork (lower Pliocene [?] or upper Miocene)—**Microdiorite (SiO_2 = 63.57 weight percent, K_2O = 1.20 to 1.32; *n* = 2 analyses) exposed as an upthrown block along the south side of the Hellroaring Creek thrust fault in the southeast part of the map area (**Figure 2-1**; Plate 1; **Table 6-8**; Appendix). Unit **Tmdei** forms a distinctly faceted slope along the Lookout Mountain-Gumjuwac Saddle Trail up to an elevation of 1,505 m (4,935 ft) (**Figure 2-1**; Plate 1); the unit is there unconformably overlain by younger flows of the ~5.37 to 4.25 Ma Gunsight Butte volcanics (**Tpml**; **Tpmn**; **Tpmb1**; **Tpmb2**; **Tpag**) (Plate 1). Microdiorite overlies and intrudes Columbia River Basalt below 1,160 m (3,800 ft) elevation. Outcrops of the main microdiorite mass are characteristically blocky-jointed; platy or columnar jointing is absent. Thickness of the microdiorite is ≥ 350 m (1,150 ft). Typical hand samples of the microdiorite are medium dark gray (N4) to pale blue green (5BG 7/2), containing 2 to 3 percent (vol.) clear to chalky white (N9), subhedral to anhedral, prismatic to blocky, seriate plagioclase microphenocrysts and phenocrysts ≤ 4 mm (0.1 in), and 2 to 3 percent (vol.) grayish black (N2) to grayish olive (10Y 4/2) euhedral to subhedral, prismatic to blocky seriate pyroxene microphenocrysts and phenocrysts ≤4 mm (0.1 in) (orthopyroxene ≥ clinopyroxene) in an equigranular, consertal medium-grained crystalline groundmass of plagioclase and pyroxene. Localized propylitic alteration has altered pyroxenes to chlorite and epidote.

Quarry exposures just south of the Lookout Mountain-Gumjuwac Saddle trailhead, along OR Highway 35, reveal two flows of NW-dipping CRBG invaded by several yellowish gray (5Y 8/1) to dark yellowish orange (10YR 6/6) microdiorite sills and dikes, up to several meters in thickness (**Figure 2-1**; Plate 1). Dikes and sills are propylitically altered and sulfidized, containing ~10 to 15 percent (vol.) or greater visible disseminated pyrite. Microdiorite is characterized by a fine groundmass, now altered to chlorite and epidote, where original pyroxenes have gone to a grayish olive (10Y 4/2) clay. CRBG lavas in the quarry are characterized by traces of disseminated pyrite coating fractures and numerous amygdules infilled by white (N9) zeolite and calcite. Geochemical analyses of CRBG samples in the quarry and on the periphery of the intrusion are altered, with low original analytical totals <95.0 (TotalInitial) and high Loss on Ignition (LOI = 4.94 to 6.68 weight percent) (Appendix). Alteration is associated with relict feeder zones to the upper mass of the intrusion, which itself is locally propylitically altered, but not pyritized.

The microdiorite of East Fork (**Tmdei**) is indistinguishable in chemical composition and mineralogy to andesite and dacite of East Fork lava flows (**Tmde**), exposed just south of Culvert Creek (SiO_2 = 63.22 to 63.40 weight percent, K_2O = 1.20 to 1.27; n = 2 analyses, Plate 1 map no. G255 and G256; **Table 6-8**; Appendix). Interpreted as a hypabyssal intrusion and/or dome complex. Unit **Tmdei** has reversed magnetic polarity and is assigned a late Miocene or early Pliocene age on the basis of stratigraphic position and isotopic ages. A groundmass sample yielded an $^{40}Ar^{39}Ar$ plateau age of 5.37 ± 0.06 Ma and a total fusion age of 4.90 ± 0.04 Ma (groundmass; sample 34 DRBLJ 19); an older late Miocene $^{40}Ar^{39}Ar$ plateau age of 8.78 ± 0.29 Ma was determined for plagioclase separates from the same sample (Plate 1; **Table 5-1**; Appendix).

Tmda **plagioclase-microporphyritic dacite of Surveyors Ridge Road (upper Miocene)—**Dacite lava flow (SiO_2 = 63.33 to 63.76 weight percent; K_2O = 1.20 to 1.24, Sr = 506 to 568 ppm; *n* = 4 analyses) showing in two small outcrop exposures on the west and northeast flanks of Mill Creek Buttes (**Figure 2-1**; Plate 1; **Table 6-8**; Appendix). Outcrops are characterized by vertical banding and blocky or tabular jointing. Thickness of unit **Tmda** is ≤53 m (175 ft). Typical hand samples of the dacite are medium dark gray (N4), containing ~10 to 20 percent (vol.), euhedral to subhedral, blocky to prismatic, equigranular plagioclase microphenocrysts ≤1 mm (0.04 in) and 5 to 7 percent (vol.) black (N1) to brownish black (5YR 2/1), euhedral to subhedral, blocky to prismatic, seriate pyroxene microphenocrysts and phenocrysts ≤2 mm (0.08), contained within an equigranular medium-grained holocrystalline groundmass. Brownish gray (5YR 4/1) clay is present as staining on internal fractures. Unit **Tmda** has normal magnetic polarity and is assigned a late Miocene age on the basis of stratigraphic position above the ~8 to 7 Ma andesite and dacite of East Fork (**Tmde**) and ~6.2 Ma hornblende-phyric dacite of Surveyors Ridge (**Tmdy**) (Plate 1).

Table 6-8. Select XRF geochemical analyses for the Dalles Formation in the Dog River–Badger Lake area (part 1 of 2).

Sample	34 DRBLJ 19	445 MCBJ 16	129 MCB-DRJ 17	396 MCB-DRJ 17	215 MCB-DRJ 18	660 MCBJ 16	671 MCBJ 16	440 MCBJ 16
Geographic Area	Lookout Mt. Trail	Mill Creek Buttes	Mill Creek Buttes	East Fork	East Fork	Mill Creek Buttes	Mill Creek Buttes	Mill Creek Buttes
Formation	Dalles Formation	Dalles Formation	Dalles Formation	Dalles Formation	Dalles Formation	Dalles Formation	Dalles Formation	Dalles Formation
Map Unit	Tmdei	Tmda	Tmdy	Tmde	Tmde	Tmdm	Tmdh	Tmdi
UTM N (NAD 83)	5021158	5033328	5034006	5031053	5032689	5033208	5033950	5033752
UTM E (NAD 83)	612500	614767	614419	612118	611352	616253	617250	615440
Age (Ma)	5.37 Ma	nd	~6.2 Ma	~7.15 Ma	~8.18 Ma	6.83 Ma	nd	~7.5 Ma
Map No.	G111	G515	G547	G445	G492	G509	G545	G533
Oxides, weight percent								
SiO_2	63.58	63.76	64.81	65.19	63.82	64.94	64.08	63.03
Al_2O_3	17.24	17.00	17.14	17.10	17.23	17.17	16.73	17.24
TiO_2	0.72	0.71	0.68	0.69	0.68	0.67	0.73	0.74
FeO*	5.03	4.82	4.38	4.99	4.84	3.99	4.24	4.90
MnO	0.08	0.08	0.08	0.08	0.08	0.06	0.08	0.09
CaO	5.82	5.57	5.53	4.36	5.31	5.79	6.35	6.06
MgO	2.34	2.57	1.98	1.90	2.26	2.40	2.72	3.00
K_2O	1.20	1.20	1.29	1.56	1.37	0.84	0.89	0.93
Na_2O	3.86	4.13	3.96	3.99	4.26	4.00	3.99	3.87
P_2O_5	0.14	0.15	0.16	0.14	0.15	0.15	0.19	0.14
LOI	3.24	0.64	0.46	1.44	0.48	0.88	0.47	0.55
Total_I	96.21	98.82	98.79	98.22	98.91	98.56	98.81	98.94
Trace Elements, parts per million								
Ni	17	33	18	18	22	22	40	38
Cr	29	49	24	33	38	35	57	54
Sc	12	11	9	10	11	10	11	13
V	85	92	71	75	85	73	82	93
Ba	303	318	273	384	317	190	228	223
Rb	24	22	28	35	30	15	17	20
Sr	415	507	665	386	419	935	1028	775
Zr	155	148	146	149	149	126	138	126
Y	16	14	14	13	14	10	12	14
Nb	8.9	8.5	7.4	9.4	8.2	5.0	5.9	5.8
Ga	19	20	20	20	19	19	20	20
Cu	28	21	29	27	19	25	28	36
Zn	62	67	74	65	59	53	52	58
Pb	7	5	11	6	4	5	5	4
La	16	17	15	17	16	11	17	13
Ce	36	37	30	37	32	25	34	27
Th	4	3	4	4	3	2	3	2
Nd	17	17	16	18	16	14	18	15
U	2	2	1	2	2	1	1	2

Major element determinations have been normalized to a 100-percent total on a volatile-free basis and recalculated with total iron expressed as FeO*; nd - no data or element not analyzed; na - not applicable or no information. LOI, Loss on Ignition; Total_I, original analytical total.

Table 6-8, continued. Select XRF geochemical analyses for the Dalles Formation in the Dog River–Badger Lake area. (part 2 of 2).

Sample	RC13-498-72	160 DRBLJ 19	155 DRBLJ 19	339 MCB-DRJ 17	61a MCB-DRJ 18	39 MCB-DRJ 18
Geographic Area	Bottle Prairie	Bottle Prairie	Eightmile Creek	Dog River	Rimrock CR.	Rimrock CR.
Formation	Dalles Formation	Dalles Formation	Dalles Formation	Dalles Formation	Dalles Formation	Dalles Formation
Map Unit	Tmdf	Tmdv	Tmdw	Tmdp	Tmdc	Tmdr
UTM N (NAD 83)	5027993	5026830	5024383	5033700	5037023	5037428
UTM E (NAD 83)	616803	616878	617060	611547	613408	613950
Age (Ma)	nd	~7.71 Ma	~7.91 Ma	nd	nd	nd
Map No.	G345	G311	G242	G531	G592	G604
Oxides, weight percent						
SiO_2	63.28	62.79	63.49	64.69	57.47	60.50
Al_2O_3	17.46	17.23	16.64	17.19	18.05	17.88
TiO_2	0.71	0.84	0.97	0.72	1.04	0.92
FeO*	5.11	5.09	5.67	4.57	7.29	6.25
MnO	0.08	0.08	0.14	0.07	0.12	0.11
CaO	5.62	6.09	4.17	5.74	7.19	6.30
MgO	2.19	2.60	1.88	1.87	4.08	3.88
K_2O	1.08	1.18	2.80	1.04	0.84	0.98
Na_2O	4.29	3.87	4.04	3.96	3.76	3.07
P_2O_5	0.18	0.23	0.20	0.15	0.18	0.11
LOI	nd	0.93	0.99	1.58	0.85	0.11
Total_I	99.79	98.56	98.34	98.02	98.90	94.58
Trace Elements, parts per million						
Ni	21	21	16	21	44	59
Cr	39	24	18	33	82	115
Sc	11	11	12	11	19	16
V	80	98	91	100	156	109
Ba	309	273	520	224	221	249
Rb	18	25	68	11	16	22
Sr	480	1142	352	767	429	384
Zr	161	167	317	137	128	157
Y	14	14	31	14	18	18
Nb	10.1	7.7	15.9	6.7	7.6	6.7
Ga	21	19	20	20	21	18
Cu	23	30	26	23	25	63
Zn	77	59	71	54	78	62
Pb	3	4	9	5	3	5
La	15	26	35	14	13	12
Ce	35	57	66	28	30	28
Th	2	4	8	2	2	2
Nd	19	26	32	17	14	16
U	1	3	4	2	2	2

Major element determinations have been normalized to a 100-percent total on a volatile-free basis and recalculated with total iron expressed as FeO*; nd - no data or element not analyzed; na - not applicable or no information. LOI, Loss on Ignition; Total_I, original analytical total.

Tmdy **hornblende-porphyritic dacite of Surveyors Ridge Road (upper Miocene)—**Dacite (SiO_2 = 63.45 to 65.01 weight percent; K_2O = 1.19 to 1.31, Sr = 473 to 665 ppm; *n* = 4 analyses) exposed on the western edge of Mill Creek Buttes (**Figure 2-1**; Plate 1; **Table 6-8**; Appendix). Outcrops are characterized by subhorizontal blocky to tabular jointing. Thickness of unit **Tmdy** is ≤30 m (100 ft). Typical hand samples of the dacite are light gray (N7) to pinkish gray (5YR 8/1), with ≤10 percent (vol.) black (N1) to brownish black (5YR 2/1) iridescent, euhedral to subhedral, blocky to prismatic needle-like, seriate hornblende phenocrysts ≤4 mm (0.2 in), ≤20 percent (vol.) clear to chalky light gray (N7), euhedral to subhedral, prismatic to blocky, seriate plagioclase microphenocrysts ≤1 mm (0.04 in), and ≤1 percent (vol.) plagioclase-hornblende glomerocrysts ≤3 mm (0.1 in), contained within a vesicular, consertal medium-grained holocrystalline groundmass of plagioclase and hornblende. Unit **Tmdy** has reversed magnetic polarity and is assigned a late Miocene age on the basis of stratigraphic position above the ~8 to 7 Ma andesite and dacite of East Fork (**Tmde**) and a K-Ar age of 6.2 ± 1.3 Ma (whole rock, sample PH-MCB-1; P.E. Hammond in Fiebelkorn and others, 1983) (Plate 1; **Table 5-1**; Appendix).

Tmde **andesite and dacite of East Fork (upper Miocene)—**Andesite and dacite lava flows (SiO_2 = 59.45 to 65.68 weight percent, avg = 62.86 weight percent; K_2O = 0.99 to 1.65, avg = 1.27 weight percent; *n* = 53 analyses, [3 outside map area]) exposed extensively in the northeast part of the map area between Mill Creek Buttes and Gibson Prairie and along East Fork Hood River through the central part of the map area (**Figure 2-1**; Plate 1; **Table 6-8**; Appendix). The unit includes multiple porphyritic lava flow sequences, interfingering with Dalles Formation volcaniclastic rocks (**Tmdl**) at variable stratigraphic intervals. Outcrops of unit **Tmde** are commonly characterized by meter scale, poorly developed columnar joint sets or intervals of platy jointing. Along OR Highways 35, the unit includes thick intervals of autobreccia between flows (**Figure 2-1**; Plate 1). Outcrops often weather to meter scale, subrounded boulders, forming extensive talus slopes (**Qt**) beneath ridge-capping outcrops. Unit **Tmde** ranges in thickness from ≤33 m (100 ft) for individual flows to composite ridge-capping sections ≤215 m (705 ft). Typical hand samples of the andesite and dacite are grayish blue (5PB 5/2) to medium bluish gray (5B 5/1), containing 10 to 20 percent (vol.) clear to chalky white (N9), subhedral to anhedral, prismatic to blocky, seriate plagioclase microphenocrysts and phenocrysts ≤6 mm (0.2 in), and 1 to 2 percent (vol.) grayish black (N2) euhedral to subhedral, prismatic to blocky seriate pyroxene microphenocrysts and phenocrysts ≤4 mm (0.1 in) (orthopyroxene ≥ clinopyroxene), contained within in a very fine-grained holocrystalline to hypocrystalline groundmass. Rare andesitic or dacitic rock fragments <2 mm (0.08 in) across are also present. Unit **Tmde** has both normal and reversed magnetic polarity flows and is assigned a late Miocene age on the basis of stratigraphic position and whole-rock K-Ar ages of 7.15 ± 0.8 Ma (whole rock; sample 40-Wise; Wise, 1969) on cliff-forming outcrops northeast of Polallie Campground and 8.18 ± 0.06 (whole rock; sample 79EF0016A; Keith and others, 1985) for a roadcut along OR Highway 35 (**Figure 2-1**; Plate 1; **Table 5-1**; Appendix). The andesite and dacite of East Fork (**Tmde**) is chemically indistinguishable from the microdiorite of East Fork (**Tmdei**) (**Table 6-8**; Appendix).

Mill Creek Buttes

Hornblende-phyric dacite and microdiorite exposed across Mill Creek Buttes in the headwaters of South Fork of Mill Creek (**Figure 2-1**; Plate 1). Relative to other units in the Dalles Formation, Mill Creek Buttes rocks have lower potassium (K_2O = 0.75 to 1.08 weight percent) and higher strontium (Sr = 748 to 1047

ppm) (**Table 6-8**; Appendix). Isotopic ages obtained on Mill Creek Buttes indicate that rocks range in age from ~7.5 to 6 Ma (**Table 5-1**; Appendix). The absence of vesicular zones between units, great apparent thickness, and high-standing topography of Mill Creek Buttes likely indicates emplacement as a late Miocene dome complex.

Tmdm **plagioclase- and hornblende-porphyritic dacite of Mill Creek Buttes (upper Miocene)—**Microdiorite (SiO_2 = 64.75 to 64.94 weight percent; K_2O = 0.83 to 0.94, Sr = 831 to 934 ppm; *n* = 4 analyses) exposed in two small areas capping the southern and eastern points of Mill Creek Buttes (**Figure 2-1**; Plate 1; **Table 6-8**; Appendix). Unit **Tmdm** crops out as spires, knobs, and ledges characterized by vertical platy to tabular jointing. Thickness of unit **Tmdm** is ≤46 m (150 ft). Typical hand samples of the dacite are light gray (N7) to very light gray (N8), with 20 to 30 percent (vol.) clear to chalky light gray (N7), prismatic to blocky, seriate plagioclase microphenocrysts ≤1 mm (0.04 in), ≤10 percent (vol.) black (N1) to brownish black (5YR 2/1) iridescent, euhedral to subhedral, blocky to prismatic needle-like, seriate hornblende phenocrysts ≤4 mm (0.2 in), and ≤1 percent (vol.) plagioclase-hornblende glomerocrysts ≤3 mm (0.1 in), contained within a fine-grained holocrystalline groundmass. Unit **Tmdm** has normal magnetic polarity and is assigned a late Miocene age on the basis of stratigraphic position and an $^{40}Ar/^{39}Ar$ plateau age of 6.83 ± 0.01 Ma (groundmass; sample 660 MCBJ 16) (Plate 1; **Table 5-1**; Appendix). The mapped distribution and character of unit **Tmdm** has characteristics similar to a late stage lava forming a carapace across earlier domes.

Tmdh **hornblende-porphyritic microdiorite of Mill Creek Buttes (upper Miocene)—**Microdiorite (SiO_2 = 63.64 to 65.13 weight percent; K_2O = 0.75 to 0.95, Sr = 778 to 1047 ppm; *n* = 7 analyses) forming most of the eastern and southern flanks of Mill Creek Buttes (**Figure 2-1**; Plate 1; **Table 6-8**; Appendix). Outcrops of unit **Tmdh** are characterized by intervals of tabular to vertical platy jointing; the weathered unit forms land surfaces covered with angular plates or subangular blocks <0.5 m (1.6 ft) across. Thickness of unit **Tmdh** is ≤130 m (600 ft). Typical hand samples of the microdiorite are medium light gray (N6), containing 3 to 10 percent (vol.) black (N1) to brownish black (5YR 2/1) iridescent, fresh to corroded, subhedral to anhedral, prismatic- to lath-shaped, seriate hornblende phenocrysts ≤5 up to ≤1.5 cm (0.2 to 0.6 in), <1 percent (vol.) clear, prismatic to blocky, seriate plagioclase microphenocrysts ≤1 mm (0.04 in), and <1 percent (vol.) plagioclase-hornblende glomerocrysts ≤1 mm (0.04 in), distributed within a fine- to medium-grained holocrystalline groundmass. Unit **Tmdh** has reversed magnetic polarity and is assigned a late Miocene age on the basis of stratigraphic position relative to the 6.83 Ma microdiorite of unit **Tmdm** (Plate 1).

Tmdi **hornblende-porphyritic microdiorite of Mill Creek Buttes Lookout (upper Miocene)—**Microdiorite (SiO_2 = 63.02 to 64.82 weight percent; K_2O = 0.9 to 1.08, Sr = 748 to 895 ppm; *n* = 6 analyses) forming the main core of the northern part of Mill Creek Buttes (**Figure 2-1**; Plate 1; **Table 6-8**; Appendix). Outcrops are

characterized by tabular to platy jointing; the weathered unit forms meter-scale slabs. Unit **Tmdi** includes areas of poorly sorted, matrix-supported autobreccia with angular clasts ranging in size from 5 cm up to 40 cm (2 to 15.8 in) across in a very coarse-grained sandstone matrix. Breccia clasts are monolithologic hornblende-phyric microdiorite, identical to the main mass of the unit. Thickness of unit **Tmdi** is unknown. Typical hand samples of the microdiorite are very light gray (N8) to light greenish gray (5GY 8/1), containing 15 percent (vol.) black (N1) to brownish black (5YR 2/1) iridescent, subhedral to anhedral, prismatic- to lath-shaped, seriate hornblende microphenocrysts ≤1 mm (0.04 mm) and 5 to 10 percent (vol.) corroded hornblende phenocrysts ≤1.5 cm (0.6 in), <1 percent (vol.) clear, prismatic to blocky, seriate plagioclase microphenocrysts ≤1 mm (0.04 in), and <1 percent (vol.) plagioclase-hornblende glomerocrysts ≤1 mm (0.04 in), distributed within an equigranular medium-grained holocrystalline groundmass. Unit **Tmdi** has reversed magnetic polarity and is assigned a late Miocene age on the basis of stratigraphic position and a K-Ar age of 7.5 ± 0.4 Ma (whole rock; sample HD-64; Hull and Riccio, 1979) (Plate 1; **Table 5-1**; Appendix). The unit is intrusive into clastic rocks of unit **Tmdl** and is overlain by the andesite and dacite of East Fork (**Tmde**).

Tmdf **dacite of Fivemile Butte, upper flow (upper Miocene)—**Dacite lava flow (SiO_2 = 63.28 to 63.72 weight percent; K_2O = 1.07 to 1.09, *n* = 5 analyses, [3 outside map area]) exposed in a down-on-the west fault block on the north side of Bottle Prairie (**Figure 2-1**; Plate 1; **Table 6-8**; Appendix). The flow extends east of the map area for ~ 8.4 km (5.2 mi), forming a narrow ridge capping Fivemile Butte and continuing east to Joes Point (**Figure 2-1**; Plate 1). Roadcuts, quarry exposures, and outcrops of the dacite are characterized by intervals of vertical to subvertical tabular to platy jointing. Unit **Tmdf** weathers to subangular fragments <0.5 m (1.6 ft) across. Thickness of unit **Tmdf** in the map area is ≤40 m (130 ft). Typical hand samples of the dacite are light gray (N7) to medium bluish gray (5B 5/1), containing 2 to 3 percent (vol.) clear to chalky white (N9), euhedral, prismatic, seriate plagioclase microphenocrysts and phenocrysts 1 to 4 mm (0.04 to 0.2 in) across and up to 1 cm (0.4 in) long, ≤1 percent (vol.) dark gray (N2) rod-like orthopyroxene phenocrysts ≤4 mm (0.2 in), and ~1 percent (vol.) plagioclase-pyroxene glomerocrysts ≤1 cm (0.4 in), distributed within a fine-grained holocrystalline groundmass. Unit **Tmdf** has both normal and reversed magnetic polarity outcrops, and is assigned a late Miocene age on the basis of stratigraphic position directly above the 7.71 Ma lower flows and domes of the dacite of Fivemile Butte (**Tmdv**). Equivalent, in part, to the andesite of Fivemile Butte unit Tafv unit of Sherrod and Scott (1995).

Tmdv **dacite of Fivemile Butte, lower flows and domes (upper Miocene)—**Sequence of dacite lava flows and/or domes (SiO_2 = 62.78 to 64.70 weight percent; 1.17 to 1.48 weight percent K_2O, *n* = 15 analyses, [9 outside map area]) exposed extensively across the upper reaches of Dog River (**Figure 2-1**; Plate 1; **Table 6-8**; Appendix). One outcrop within unit **Tmdv** between Perry Point and Fivemile Butte, analyzed and dated by Gray and others (1996), has distinctively higher K_2O than the rest of the unit (2.12 weight percent). The unit forms the ridgeline of Perry Point and Fivemile Butte, extending ~10.2 km (6.3 mi) east to Hesslan Canyon (east of map area) as a narrow intracanyon flow (**Figure 2-1**; Plate 1). Roadcuts and outcrops are characterized by a

massive rounded form, by broad blocky meter-scale columns, or intervals of vertical platy jointing. Outcrops weather to meter scale, subrounded boulders and angular plates, forming extensive talus slopes beneath cliffs. Thickness of unit **Tmdv** in the map area is ≥305 m (1,000 ft) (Plate 1). Typical hand samples of the dacite are medium gray (N5) to medium dark gray (N4), containing ~3 to 5 percent (vol.), clear to chalky light gray (N7), euhedral, prismatic to blocky, seriate plagioclase microphenocrysts and phenocrysts ≤1 cm (0.4 in) long and ≤1 percent (vol.) fresh grayish black (N2) pyroxene microphenocrysts and phenocrysts ≤2 mm (0.08 in) (orthopyroxene ≥ clinopyroxene), distributed within a very fine-grained holocrystalline to hypocrystalline groundmass. The dacite has both normal and reversed magnetic polarity outcrops. Unit **Tmdv** is assigned a late Miocene age on the basis of stratigraphic position and a K-Ar age of 7.71 ± 0.17 Ma (plagioclase; sample RC S88-23) obtained by Gray and others (1996) for an outcrop in the saddle between Perry Point and Fivemile Butte (east of map area; **Figure 2-1**). The dacite of Fivemile Butte (**Tmdv**) is interpreted to be younger than the dacite of Wolf Run (**Tmdw**), on the basis of isotopic ages; no outcrops exposing the contact between the two units are known in the map area or adjacent Fivemile Butte 7.5′ quadrangle.

Tmdw **dacite of Wolf Run (upper Miocene)—**Dacite lava flow (SiO_2 = 63.49 to 65.11 weight percent; K_2O = 2.76 to 2.96, *n* = 10 analyses, 9 outside map area) poorly exposed in an erosional window beneath younger Quaternary lava (**Qrbhp**) and glacial deposits (**Qgot**), northeast of High Prairie (**Figure 2-1**; Plate 1; **Table 6-8**; Appendix). The unit has a distinct and unique chemical composition for a lava flow of Dalles Formation age, with higher K_2O (> 2.5 weight percent) and higher amounts of niobium (15.7 to 17.6 ppm) and zirconium (319 to 341 ppm) (**Table 6-8**; Appendix). The chemically distinct lava forms an important stratigraphic marker in the Middle Columbia Basin, extending ~24 km (15 mi) northeast of the map area to the intersection of Wolf Run and Eightmile Creek (**Figure 5-6**), as a topographically inverted intracanyon flow overlying volcaniclastic rocks in the Dalles Formation (**Tmdl**). A vent area for the lava has not been determined and no outcrops of unit **Tmdw** are known west of the single exposure in the map area. Thickness of unit **Tmdw** in the map area is ≤105 m (345 ft). Typical hand samples of the dacite are medium gray (N5) to medium dark gray (N4), containing 20 to 30 percent (vol.) clear to chalky white (N9), subhedral to anhedral, prismatic to blocky seriate plagioclase microphenocrysts and phenocrysts ≤5 mm (0.2 in), ≤1 percent (vol.) grayish black (N2), euhedral to subhedral, prismatic pyroxene microphenocrysts and phenocrysts ≤2 mm (0.08 in) (orthopyroxene ≥ clinopyroxene), and <1 percent (vol.) plagioclase-pyroxene glomerocrysts ≤3 mm (0.1 in), contained within a very fine-grained holocrystalline to hypocrystalline groundmass. Unit **Tmdw** has normal magnetic polarity and is assigned a late Miocene age on the basis of stratigraphic position and an $^{40}Ar/^{39}Ar$ plateau age of 7.91± 0.08 Ma (plagioclase; sample 291 DFWJ 14) for a sample collected from outcrops at the intersection of Wolf Run and Eightmile Creek (northeast of the map area; **Figure 5-6**; McClaughry and others, in press). Bunker and others (1982) and Bela (1982) reported a comparable K-Ar age of 8.2 ± 0.8 Ma (whole rock; sample 103-WB) collected from this unit just to the east of the map area near Camp Baldwin (**Figure 2-1**).

Tmdp **hornblende-porphyritic dacite of Puppy Creek (upper Miocene)—**Hornblende-porphyritic dacite flows and intrusions (SiO_2 = 63.36 to 66.72 weight percent; 1.04 to 1.44 weight percent K_2O; *n* = 15 analyses) exposed in a northwest-trending, fault-bound zone between East Fork Hood River on the west and Puppy Creek on the east (**Figure 2-1**; Plate 1; **Table 6-8**; Appendix). The unit is

also exposed in stratigraphic section, in fault-bound blocks north of the Cat Creek thrust fault (Plate 1). Unit **Tmdp** typically crops out as ridges and knobs with vertical blocky jointing; platy jointing is uncommon. Zones of fragmental breccia and hornblende-porphyritic dacite-clast tuff breccia are included in the unit. Thickness of unit **Tmdp** is unknown. Typical hand samples in the unit are of two varieties: 1) light gray (N7) to very light gray (N8) porphyritic dacite with 10 to 20 percent (vol.) fresh black (N1), iridescent euhedral to subhedral, blocky to needle-like prismatic, seriate hornblende microphenocrysts ≤1 mm (0.04 in) and phenocrysts ranging from 4 mm to 1 cm (0.2 to 0.4 in) and 2 to 3 percent (vol.) chalky white (N9) block plagioclase microphenocrysts ≤1 mm (0.04 in), contained within a fine to medium-grained holocrystalline groundmass. Cores to both plagioclase and hornblende are commonly corroded.; and 2) light gray (N7) to very light gray (N8) and pinkish gray (5YR 8/1) sparsely porphyritic dacite with 2 to 3 percent (vol.) blocky grayish black (N2) hornblende phenocrysts from 3 mm to 1 cm (0.1 to 0.4 in), contained within an equigranular, consertal medium-grained holocrystalline groundmass. Unit **Tmdp** has both normal and reversed magnetic polarity outcrops and is assigned a late Miocene age on the basis of apparent stratigraphic position (Plate 1).

Tmdc **andesite (upper Miocene)—**Andesite and andesite breccia (SiO_2 = 57.47 weight percent; K_2O = 0.83; *n* = 1 analysis) exposed above the tuff of Rimrock (**Tmdr**) (**Figure 2-1**; Plate 1; **Table 6-8**; Appendix). Outcrops are characterized by massive to blocky jointed dense lava over a poorly sorted basal autobreccia. Flow breccia is dusky red (5R 3/4) oxidized, consisting of poorly sorted, closely packed autoclasts, ranging from several cm to ≤30 cm (11.8 in) across. Thickness of unit **Tmdc** is ≤15 m (50 ft) in the map area. Typical hand samples of the andesite are medium gray (N5) and aphyric to sparsely microporphyritic with ≤1 percent (vol.) clear, blocky plagioclase and dark gray (N2) pyroxene microphenocrysts ≤1 mm (0.04 in) contained within a mottled fine-grained holocrystalline groundmass. Flow-breccia clasts are medium light gray (N6) and abundantly microporphyritic with 5 to 10 percent (vol.) chalky white, blocky plagioclase microphenocrysts ≤1 mm (0.04 in). Unit **Tmdc** has reversed magnetic polarity and is assigned a late Miocene age on the basis of stratigraphic position (Plate 1).

Tmdr **tuff of Rim Rock (upper Miocene)—**Andesitic tuff (SiO_2 = 59.76 to 62.00 weight percent; 0.72 to 1.19 weight percent K_2O; *n* = 8 analyses) exposed in a southeast-dipping stratigraphic section of Dalles Formation between Rimrock Creek and the Cat Creek thrust fault in the northern part of the map area (**Figure 2-1**; Plate 1; **Table 6-8**; Appendix). The unit consists of four to five cooling units, cropping out as distinct benches. Outcrops are commonly massive, with horizons of polygonal jointing. Welded horizons contain pumice fiamme ≤6 cm (2.4 in). Thickness of the unit is ≤ 90 m (295 ft) in the map area. Landslides (**Qls**) are associated with dip slopes unit **Tmdr**. Typical hand samples of the tuff are medium light gray (N6), well-sorted crystal tuff with 1 to 2 percent (vol.) broken clear plagioclase ≤3 mm (0.1 in), dark gray (N2) to dark reddish brown (10R 3/4) hornblende crystals 1 to 3 mm (0.04 to 0.1 in), ≤1 percent (vol.) plagioclase-hornblende glomerocrysts ≤5 mm, <1 percent (vol.) to more than 5 percent (vol.) scattered chalky white (N9) plagioclase-hornblende-phyric pumices ≤1 cm (0.4 in), and occasional perlite fragments ≤1 cm (0.4 in) contained within a fine-grained crystal-vitric groundmass of plagioclase and hornblende. Unit **Tmdr** has reversed magnetic polarity and is assigned a late Miocene age on the basis of stratigraphic position near the base of the Dalles Formation (Plate 1).

Angular unconformity to disconformity

6.3.4 Middle and Lower Miocene volcanic rocks

6.3.4.1 Columbia River Basalt Group

6.3.4.2 Wanapum Basalt

The Wanapum Basalt in the Dog River–Badger Lake area consists of lavas assigned to the Frenchman Springs Member. Composite thickness of the Wanapum Basalt in the map area is ~95 m (312 ft) (Plate 1).

6.3.4.3 Frenchman Springs Member

Frenchman Springs lavas are distinguished from other CRBG units by large, widely scattered to locally abundant plagioclase phenocrysts and high titanium contents (~2.9 to 3.06 weight percent) (Beeson and others, 1985, 1989; Martin and others, 2013). The Frenchman Springs Member is subdivided in the map area into:

Twfs **Basalt of Sentinel Gap (middle or lower Miocene)—**High-titanium, aphyric to sparsely plagioclase-phyric basalt and basaltic andesite (SiO_2 = 51. 83 to 52.53 weight percent; TiO_2 = 2.99 to 3.17 weight percent; *n* = 4 analyses) lying stratigraphically beneath the Dalles Formation (**Tmdl**) and above the Basalt of Sand Hollow (**Twfh**) in a faulted, southeast-dipping stratigraphic section in the northeast part of the map area (**Figure 2-1**; Plate 1; **Table 6-9**; Appendix). Unit **Twfs** is not exposed in the map area south of Rimrock Creek (**Figure 2-1**; Plate 1). Sentinel Gap lavas (**Twfs**) are distinguished from the underlying Basalt of Sand Hollow (**Twfh**) on the basis of relatively higher amounts of titanium (avg = TiO_2 = 3.09 weight percent) and phosphorous (avg = P_2O_5 = 0.63 weight percent) and lesser amounts of chrome (avg = Cr = 14 ppm) (*n* = 71 analyses in Middle Columbia Basin; Madin and McClaughry; McClaughry and others, in press; J.D. McClaughry, unpublished geologic mapping). Good outcrops of unit **Twfs** are typically characterized by well-defined colonnade jointing and/or platy jointing. Where the upper parts of unit **Twfs** are exposed, outcrops have 0.2- to 2 m thick (0.7 to 6.6 ft) vesicular flow lobes. Thickness of unit **Twfs** in the map area ranges between 5 m (16.5 ft) and 43 m (141 ft), thickening to the north and east (Plate 1). Typical hand samples of the basalt are medium dark gray (N4) to dark gray (N2), aphyric to very sparsely porphyritic, with <1 percent (vol.) clear to pale yellowish orange (10YR 8/6), euhedral to subhedral, prismatic- to lath-shaped and blocky, seriate plagioclase microphenocrysts and phenocrysts ≤7 mm (0.3 in) (~1 phenocryst/m^2) and <2 percent (vol.) grayish black (N2) clinopyroxene microphenocrysts, enclosed within a fine-grained holocrystalline to hypocrystalline groundmass of plagioclase, intergranular clinopyroxene, Fe-Ti oxides, and intersertal glass. The Basalt of Sentinel Gap (**Twfs**) has normal magnetic polarity and an early to middle Miocene age bracketed by U/Pb dates of 15.895 ± 0.019 Ma for ash between the overlying Basalt of Rosalia and Basalt of Lolo (Priest Rapids Member), and 16.066 ± 0.04 Ma for ash between the older Basalt of Ginkgo and the Sentinel Bluffs Member **(Tgsb)** (Kasbohm and Schoene, 2018). Unit **Twfs** is equivalent to the Sentinel Gap flows of Mackin (1961) and Beeson and others (1985), and flows of Union Gap of Powell (1982).

Twfh **Basalt of Sand Hollow (middle or lower Miocene)—**High-titanium, aphyric to sparsely plagioclase-phyric basalt and basaltic andesite (SiO_2 = 51.54 to 52.36 weight percent; TiO_2 = 2.82 to 2.99 weight percent; *n* = 13 analyses) lying stratigraphically beneath the Basalt of Sentinel Gap (**Twfs**) and above the Sentinel Bluffs Member (**Tgsb**) in a faulted, southeast-dipping stratigraphic section north of the Cat Creek thrust fault, in the northern part of the map area (**Figure 2-1**; Plate 1; **Table 6-9**; Appendix). Sand Hollow flows (**Twfh**) also crop out in creek and quarry exposures south of the Hellroaring Creek thrust fault in the southern part of the map area (**Figure 2-1**; Plate 1). Unit **Twfh** lavas are distinguished from other Frenchman Springs units on the basis of sparsely distributed plagioclase phenocrysts and relatively lower amounts of titanium (avg = TiO_2 = 2.97 weight percent) and phosphorous (avg = P_2O_5 = 0.56 weight percent) and higher amounts of chrome (avg = Cr = 38 ppm) (*n* = 156 analyses in Middle Columbia Basin, Madin and McClaughry, 2019; McClaughry and others, in press; J.D. McClaughry, unpublished geologic mapping). Outcrops are characterized by a well-developed platy to blocky colonnade jointing. Where unit **Twfh** is weathered, slopes underlain by the basalt are mantled by subrounded boulders, generally <1.5 m (4.9 ft) in diameter. Typical hand samples of the basalt are pale blue (5B 6/2) to medium dark gray (N4), aphyric to very sparsely porphyritic, with <1 percent (vol.) clear to pale yellowish orange (10YR 8/6), euhedral to subhedral, prismatic- to lath-shaped and blocky, seriate plagioclase microphenocrysts and phenocrysts ≤1 cm (0.6 in) (~1 phenocryst/m^2), <2 percent (vol.) grayish black (N2) clinopyroxene microphenocrysts, and trace olivine microphenocrysts ≤0.5 (0.02 in) mm across, enclosed within a fine-grained hypocrystalline groundmass of plagioclase, intergranular clinopyroxene, Fe-Ti oxides, and intersertal glass. The uppermost part of the Basalt of Sand Hollow (**Twfh**) may contain as much as 3 to 5 percent, pale yellowish orange (10YR 8/6) plagioclase phenocrysts and glomerocrysts ≤2 cm (0.8 in). The Basalt of Sand Hollow (**Twfh**) has normal magnetic polarity and an early to middle Miocene age bracketed by U/Pb dates of 15.895 ± 0.019 Ma for ash between the overlying Basalt of Rosalia and Basalt of Lolo (Priest Rapids Member), and 16.066 ± 0.04 Ma for ash between the older Basalt of Ginkgo and the Sentinel Bluffs Member **(Tgsb) (**Kasbohm and Schoene, 2018). Unit **Twfh** is equivalent to the Sand Hollow flows of Mackin (1961) and Beeson and others (1985) and the Kelly Hollow flow of Powell (1982).

Disconformity — Vantage Member of the Ellensburg Formation

Table 6-9. Select XRF geochemical analyses for the Columbia River Basalt and Ancestral Cascades volcanics in the Dog River–Badger Lake area.

Sample	6 MCB-DRJ 18	7 MCBJ-DRJ 18	9 MCB-DRJ 18	10 MCB-DRJ 18	12 MCB-DRJ 18	13 MCB-DRJ 18	1111-3-1
Geographic Area	Yellowjacket Cr.	Yellowjacket Cr.	Yellowjacket Cr.	Yellowjacket Cr.	Yellowjacket Cr.	Yellowjacket Cr.	Smullin Road
Formation	Wanapum Basalt	Wanapum Basalt	Wanapum Basalt	Grande Ronde Basalt	Grande Ronde Basalt	Grande Ronde Basalt	Ancestral Cascades
Map Unit	Twfs	Twfh	Twfh	Tgsb	Tgsb	Tgww	Toav
UTM N (NAD 83)	5039267	5039300	5039232	5039269	5039304	5039375	5042057
UTM E (NAD 83)	614656	614596	614479	614442	614167	613899	613126
Age (Ma)	~15.9 Ma	~15.9 Ma	~15.9 Ma	~16.1 Ma	~16.1 Ma	~16.1 Ma	26.29 Ma
Map No.	G642	G644	G639	G643	G646	G647	na
Oxides, weight percent							
SiO_2	52.49	51.93	51.92	54.42	54.09	56.54	57.4
Al_2O_3	13.09	13.39	13.39	14.56	14.32	13.81	17.24
TiO_2	2.99	2.99	2.99	1.79	1.89	2.12	1.31
FeO*	14.46	14.19	14.25	11.16	11.66	11.68	8.92
MnO	0.22	0.21	0.22	0.19	0.19	0.20	0.17
CaO	7.84	8.17	8.36	8.80	8.84	7.12	6.79
MgO	3.95	4.46	4.22	4.81	4.89	3.44	2.65
K_2O	1.38	1.29	1.26	1.16	0.98	1.80	1.45
Na_2O	2.90	2.81	2.80	2.80	2.86	2.92	3.78
P_2O_5	0.67	0.56	0.59	0.31	0.28	0.36	0.3
LOI	0.89	1.16	1.69	0.86	1.31	1.36	5.3
Total_I	98.18	98.15	97.77	98.63	98.31	97.93	na
Trace Elements, parts per million							
Ni	15	17	17	13	16	4	23
Cr	12	39	38	39	36	3	45
Sc	35	37	37	36	38	33	26
V	384	413	414	310	322	336	152
Ba	641	557	563	542	453	677	420
Rb	28	31	30	26	21	49	36
Sr	301	301	308	319	314	326	307
Zr	201	176	176	153	148	182	277
Y	46	40	40	41	33	38	43.2
Nb	16	14	14	11	11	13	15.9
Ga	21	21	21	19	21	22	19.9
Cu	22	29	27	28	30	10	78
Zn	144	137	134	114	115	131	90
Pb	9	7	7	6	6	10	10
La	30	26	23	29	18	27	28
Ce	68	57	59	41	40	57	56
Th	4	4	5	4	4	7	3.6
Nd	39	32	31	30	23	29	1.7
U	3	3	3	3	1	2	27

Major element determinations have been normalized to a 100-percent total on a volatile-free basis and recalculated with total iron expressed as FeO*; nd - no data or element not analyzed; na - not applicable or no information. LOI, Loss on Ignition; Total_I, original analytical total.

6.3.4.1 Grande Ronde Basalt

Grande Ronde lavas are generally monotonously fine-grained, aphyric, and petrographically non-distinctive. Chemical compositions also have a relatively narrow range. Grande Ronde lavas are distinguished from the overlying Wanapum Basalt by the absence of large plagioclase phenocrysts and glomerocrysts, and significantly less titanium contents (Hooper, 2000; Tolan and others, 2009b). Composite thickness of the Grande Ronde Basalt in the map area exceeds 450 m (1,476 ft) (Plate 1).

6.3.4.1.1 *Normal-polarity (N2) magnetostratigraphic unit*

The N2 magnetostratigraphic unit is the youngest Grande Ronde Basalt magnetostratigraphic unit, and is subdivided in the map area into the following units:

Tgsb **Sentinel Bluffs Member (lower Miocene)—**Aphyric basaltic andesite lavas (SiO_2 = 53.78 to 55.02 weight percent; TiO_2 =1.79 to 2.01 weight percent; *n* = 9 analyses) exposed beneath the Frenchman Springs Member (**Twfh**, **Twfs**) and above the Winter Water Member (**Tgww**) in a faulted, southeast-dipping stratigraphic section north of the Cat Creek thrust fault, in the northern part of the map area (**Figure 2-1**; Plate 1; **Table 6-9**; Appendix**)**. The Sentinel Bluffs Member(**Tgsb**) also crops out just east of Gumjuwac Saddle, in the headwaters of Gumjuwac Creek (outside map area; **Figure 2-1**). The Sentinel Bluffs Member (**Tgsb**) is distinguished from other members of the Grande Ronde Basalt on the basis of lithology and higher contents of magnesium (avg = MgO = 4.99 weight percent; 139 analyses in Middle Columbia Basin; Madin and McClaughry, 2019; McClaughry and others, in press; J.D. McClaughry, unpublished geologic mapping). Unit **Tgsb** is composed of thin lava flow lobes, generally <5 to 20 m thick (16.4 to 65.6 ft), that have well-developed vesicular flow tops and basal flow breccia. Flow interiors are typically characterized by massive meter-scale colonnade jointing with lesser hackly entablatures. The Sentinel Bluffs Member (**Tgsb**) is generally more resistant to erosion than other CRBG flows in the area, tending to form cliffs and steep slopes. Thickness of the Sentinel Bluffs Member (**Tgsb**) in the map area is ~130 m (426 ft) (Plate 1). Typical hand samples of the basalt are medium light gray (N6) to medium gray (N5), aphyric to very sparsely microporphyritic, containing ≤2 percent (vol.) clear, euhedral, prismatic to blocky, plagioclase microphenocrysts distributed within an equigranular, fine-grained diktytaxitic hypocrystalline groundmass of plagioclase, intergranular clinopyroxene, minor opaques, and intersertal glass. Trace amounts of olivine microphenocrysts may also be present in some flows. The Sentinel Bluffs Member (**Tgsb**) has normal magnetic polarity and is assigned an early Miocene age bracketed by U/Pb dates of 16.066 ± 0.04 Ma for ash from the overlying Vantage Horizon and 16.254 ± 0.034 Ma for ash between the Wapshilla Ridge and Meyer Ridge Members of the underlying R2 magnetostratigraphic unit (Kasbohm and Schoene, 2018). Unit **Tgsb** is equivalent to the high-MgO flows of Wright and others (1973), the Sentinel Bluffs unit of Reidel and others (1989), and the Sentinel Bluffs Member of Reidel and Tolan (2013).

Tgww **Winter Water Member (lower Miocene)**—Aphyric to sparsely plagioclase-phyric basaltic andesite lavas (SiO_2 = 56.11 to 56.87 weight percent; TiO_2 =2.08 to 2.11 weight percent; *n* = 3 analyses) exposed beneath the Sentinel Bluffs Member (**Tgsb**) and above the Ortley member (**Tgo**) in a faulted, southeast-dipping stratigraphic section north of the Cat Creek thrust fault, in the northern part of the map area (**Figure 2-1**; Plate 1; **Table 6-9**; Appendix). Winter Water flows (**Tgww**) are also exposed east of Gumjuwac Saddle in the headwaters of Gumjuwac Creek (east of map area;

Figure 2-1). Unit **Tgww** is chemically distinguished from the underlying Ortley member (**Tgo**) by higher amounts of titanium (avg = TiO_2 = 2.10 weight percent) and from the overlying Sentinel Bluffs Member (**Tgsb**) by lesser amounts of MgO (avg = MgO = 3.43 weight percent) (*n* = 38 analyses in the Middle Columbia Basin; McClaughry and others, in press; J.D. McClaughry, unpublished geologic mapping). Outcrops of unit **Tgww** are typically hackly jointed, and are composed of irregular, narrow (5 to 15 cm [2 to 5.9 in] wide) columns that extend across horizontal, vesicle-rich bands. Talus slopes beneath **Tgww** outcrops are typically composed of medium gray (N5) to brownish gray (5YR 4/1), angular, equidimensional fragments up to 10 cm (3.9 in) in diameter. The composite thickness of the unit in the map area is ~95 m (311 ft) (Plate 1). Typical hand samples of the basaltic andesite are medium dark gray (N4) to dark gray (N2), aphyric to very sparsely microporphyritic and glomeroporphyritic, containing ≤1 percent (vol.) clear, euhedral, prismatic, plagioclase microphenocrysts and v-shaped or radial, spoked glomerocrysts ≤2 mm (0.02 in) across, distributed within a very fine-grained hypocrystalline groundmass of plagioclase, intergranular clinopyroxene, Fe-Ti oxides, and intersertal glass. Conspicuous plagioclase phenocrysts and glomerocrysts are diagnostic field characteristics, which distinguishes this unit from other lavas in the N2 magnetostratigraphic unit (Reidel and others, 1989; Wells, personal communication, 2011). The Winter Water Member (**Tgww**) has normal magnetic polarity and is assigned an early Miocene age on the basis of stratigraphic position below the ~16.1 Ma Sentinel Bluffs Member (**Tgsb**) and above the ~16.2 Ma Wapshilla Ridge Member of the underlying R2 magnetostratigraphic unit (Kasbohm and Schoene, 2018). Unit **Tgww** is equivalent to the Winter Water flow of Powell (1978), the Winter Water unit of Reidel and others (1989), and the Winter Water Member of Reidel and Tolan (2013).

Tgo **Ortley member (lower Miocene)**—Aphyric, iron-rich basaltic andesite inferred to be exposed directly beneath the Winter Water Member (**Tgww**), north of Rimrock Creek (Figure 2-1; Plate 1). Areas mapped as the Ortley member (**Tgo**) were not visited as part this study, but are projected into the map area on the basis of earlier work in the Upper Hood River Valley by McClaughry and others (2012). The Ortley member has normal magnetic polarity and is assigned an early Miocene age on the basis of stratigraphic position below the ~16.1 Ma Sentinel Bluffs Member (**Tgsb**) and above the ~16.2 Ma Wapshilla Ridge Member of the R2 magnetostratigraphic unit (Kasbohm and Schoene, 2018). Unit **Tgo** is equivalent to the low-MgO flows of Wright and others (1973), the Ortley unit of Reidel and others (1989), and the Ortley member of Reidel and Tolan (2013).

6.3.4.1.2 *Reversed-polarity (R2) magnetostratigraphic unit*

The R2 magnetostratigraphic unit is the most aerially extensive Grande Ronde Basalt magneto-stratigraphic unit, and is subdivided in the map area into the following units:

Tggc **Grouse Creek member (lower Miocene)**—Aphyric, iron-rich basaltic andesite inferred to be exposed directly beneath the Ortley member (**Tgo**), north of Rimrock Creek (Figure 2-1; Plate 1). Areas mapped as the Grouse Creek member (**Tggc**) were not visited as part this study but are projected into the area on the basis of earlier work in the Upper Hood River Valley by McClaughry and others (2012). The Grouse Creek member (**Tggc**) has transitional reversed magnetic polarity and can be recognized by a steep magnetic inclination (-85°) (Wells and others, 2009). The Grouse Creek member (**Tggc**) is assigned an early Miocene age on the basis of stratigraphic position below the ~16.1 Ma Sentinel Bluffs Member (**Tgsb**) and above the ~16.2 Ma of the underlying Wapshilla

Ridge Member in the R2 magnetostratigraphic unit (Kasbohm and Schoene, 2018). Unit **Tggc** is equivalent to the Grouse Creek flows of Ross (1978), the Grouse Creek unit of Reidel and others (1989), and the Grouse Creek member of Reidel and Tolan (2013).

Unconformity

6.3.5 Oligocene volcanic rocks

Toav **Oligocene volcanic rocks, undivided (upper Oligocene) (cross section only)—**Volcanic rocks inferred to be present below the CRBG in the map area. In the Smullin Road area, 2 km (1.2 mi) north of the map area, abundantly plagioclase-phyric andesite (SiO_2 = 57.40 weight percent; 1.45 weight percent K_2O; *n* = 1 analysis) is exposed at 595 m (1,950 ft) elevation below the Grouse Creek member (**Tggc**) (**Figure 2-1**; Plate 1; **Table 6-9**; Appendix). Isotopic dating of the plagioclase-phyric andesite from the Smullin Road area has returned a $^{40}Ar/^{39}Ar$ integrated age of 26.29 ± 0.03 Ma (groundmass; sample 1111-3-1) (**Figure 2-1**; **Table 5-1**; Appendix)

6.3.6 Other rocks

QTfb **fault breccia (Pleistocene [?] to upper Miocene [?])—**Extensive zones of chaotically brecciated and disturbed rock, cross-cutting CRBG in the northern part of the map area (Plate 1). The most notable areas mapped as fault breccia occur along East Fork Hood River along the Hood River fault zone. Zones of fault breccia are up to 35 m wide (114 ft). Outcrops of fault breccia typically stand high as erosion-resistant hoodoos surrounded by areas of loosely consolidated talus mixtures of angular rock fragments and soils. Fragments weathering from both outcrops and hand samples are typically in the size range of the ¾″ minus gravel fraction. Typical hand samples from unit **QTfb** are intensely damaged/brecciated, being crosscut by a number of irregularly oriented fractures leading to a poorly defined, but pervasive fissility. The intersection of numerous foliation planes forms a pencil-like cleavage, where the rock easily breaks into irregularly faceted and smoothly curved interfering surfaces. Fault breccia is assigned a middle Miocene to Quaternary age on the basis of displacement of units with variable stratigraphic age; the Hood River fault zone displaces units as young as early Pleistocene (Plate 1).

7.0 STRUCTURE

Geologic structure in the Dog River–Badger Lake area is defined by the mapped distribution of geologic units, faults, topographic lineaments (as observed in 1-m lidar DEMs and 10-m DEMs), folds, and structural orientations (Plate 1; Appendix). Primary structural features (e.g., slickensides or fault breccia) were not observed in the field. The faults and fault zones shown on Plate 1 are recognized and mapped on the basis of offset geologic contacts, missing units, and topographic lineaments as indicators of possible movement.

The great thickness of relatively competent, brittle volcanic rocks of the CRBG and younger Cascade Range volcanic rocks results in a structural style that varies significantly in extensional and compressional regimes. Broad to narrow folds and locally steep dips are associated with propagating thrust and tear faults and define zones where shortening has been accommodated. In contrast, zones of extension are characterized by missing units and little changed or back-rotated bedding at varying elevations.

Several regional structural elements converge in the Hood River area, including the Yakima Fold Belt and the High Cascades graben (**Figure 5-2**; see discussion in Section 5 of this report). The salient structural features defining the southern part of the Hood River graben in the Dog River–Badger Lake area are 1) thrust faults and 2) north-northwest-striking faults. Complex interplay of these structures since the late Miocene has resulted in the development of a prominent fault-segmented, topographically high escarpment of early Pliocene to late Miocene and older rocks east of East Fork Hood River. West of the escarpment, the southern part of the Hood River graben is infilled by a deeply eroded and dissected, faulted section of Pliocene and early Pleistocene volcanic rocks. Post-500 ka Mount Hood flows and clastic rocks are not obviously faulted, concealing all evidence for older regional-scale faulting in the western part of the map area.

7.1.1 Thrust faults

Cat Creek fault – The Cat Creek fault is a high-angle, up-on-the-south, thrust or reverse fault, paralleling Cat Creek in the northeast part of the map area (**Figure 2-1**, **Figure 7-1**; Plate 1). The western edge of the bedrock-mapped fault terminates against north-south trending strands of the Hood River fault zone, whereas the eastern tip terminates at the north-south- to northwest-striking Gibson Prairie fault (Plate 1). Three-point solutions on the irregular mapped fault trace along Cat Creek indicate a variable N.80°W. to east-west-striking and steep ~65° to 75°S.-dipping fault.

The most extensive exposures of CRBG occur in the northern part of the Dog River–Badger Lake area, north of the Cat Creek fault, where these rocks are exposed in several complex fault blocks (**Figure 7-1**; Plate 1). Relatively planar CRBG flow horizons in this area strike ~N.43°E. to N.87°E., dipping 10° to 17°SE. Strike of CRBG beds varies for outcrops bounded within northwest-striking fault zones; flows within fault zones have fault-parallel strikes, ~N.37°W. to N.66°W., dipping 14° to 23°SW. Overlying Dalles Formation units (Tmdp, Tmdl, Tmde) exposed in the footwall of the Cat Creek fault form a steeply dipping rollover monocline where beds are oriented ~N.65°E., dipping >20° to 30° SE.

The amount of apparent up-on-the-south vertical offset of the upper part of the early to middle Miocene CRBG across the Cat Creek fault is estimated at ~609 m (2,000 ft) on the basis of projection of those units into a geologic cross section oriented north-south through Shellrock Mountain. Apparent vertical offset of the overlying late Miocene andesite and dacite of East Fork is less, estimated at ~457 m (1,500 ft). The location of the Cat Creek fault is spatially associated with lower Pleistocene microdiorite intrusives (**Qras**) forming Shellrock Mountain (**Figure 2-1**, **Figure 7-1**; Plate 1). Intrusive rocks forming

Shellrock Mountain (**Qras**) were likely injected as dikes along the fault plane and may have later been beheaded and exhumed from depth by relative offset along the Cat Creek fault.

The Cat Creek fault appears to lie generally along trend with the Mill Creek Ridge anticline, an asymmetric box fold in the CRBG and Dalles Formation, mapped along the North Fork Mill Creek, ~10 km (6.2 mi) northeast of Gibson Prairie (J.D. McClaughry, unpublished geologic mapping). At the deepest levels of exposure, along the North Fork Mill Creek, the Mill Creek Ridge anticline is broken by a major blind to emergent thrust fault, offsetting the anticline in a reverse, up-on-the-south sense (**Figure 5-3**). The North Fork Mill Creek thrust fault is characterized by extensive zones of chaotically brecciated and disturbed CRBG rock. The mapped distribution of fault breccia, combined with cross-section interpretation in the southern part of the Ketchum Reservoir 7.5' quadrangle (**Figure 1-2**), indicates a width (thickness) of the zone >100 m (328 ft). Vertical offset of distinctive flow units of the CRBG along the thrust fault is estimated to range between 75 and 100 m (246 and 328 ft). The North Fork Mill Creek thrust fault zone is offset by or terminates into the northwest-southeast-trending Mill Creek Ridge fault zone in the southern part of the Ketchum Reservoir 7.5' quadrangle (**Figure 1-2**, **Figure 5-3**; J.D. McClaughry, unpublished geologic mapping; **Figure 1-2**). Both the Mill Creek Ridge anticline and North Fork Mill Creek thrust fault zone are separated from the Cat Creek fault by the north-south-striking Gibson Prairie fault (**Figure 5-3**; Plate 1).

Figure 7-1. View looking east from McIntosh Drive in the Upper Hood River Valley in the northern part of the Dog River–Badger Lake area (45.48992, -121.60380 WGS84 geographic coordinates; 609099mE, 5038324mN WGS84 UTM Zone 10 coordinates). The eastern Hood River graben escarpment in this area exposes a complexly faulted section of early to middle Miocene Columbia River Basalt overlain by late Miocene Dalles Formation and younger Pliocene basaltic lavas. Photographer is standing on poorly exposed Dalles Formation (Tmdl) at this location. Deeper in the subsurface are down-faulted Columbia River Basalt lavas equivalent to those exposed high on the Hood River graben escarpment. Labels: CRBG – Columbia River Basalt Group; D – relative down on fault; U – relative up on fault; arrow on fault show direction of relative horizontal slip. Photo credit: Jason McClaughry, 2018.

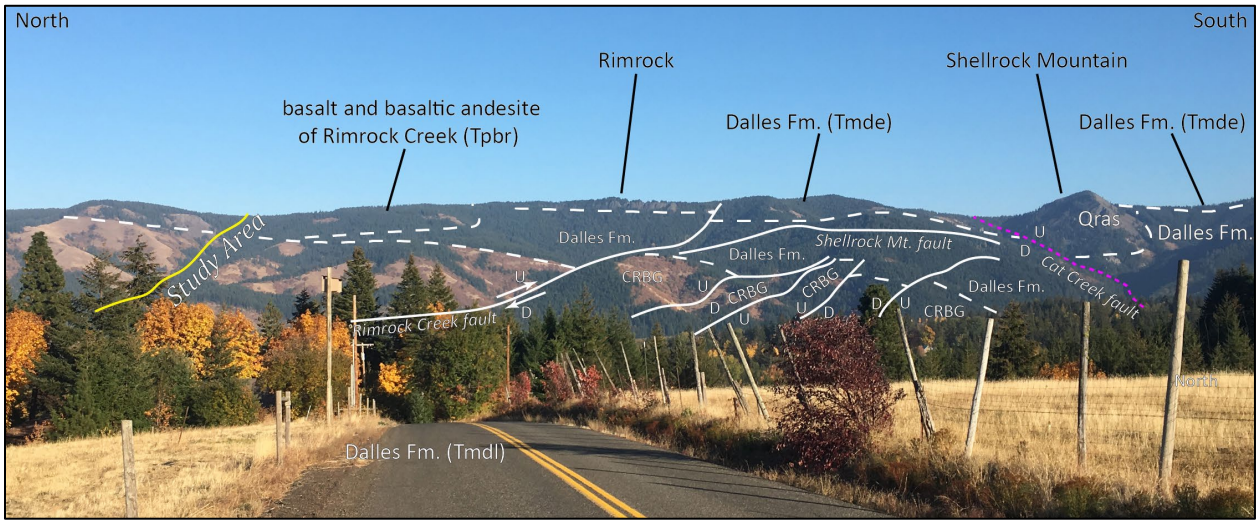

Shellrock Mountain fault – The Shellrock Mountain fault is a down-on-the-west normal fault, northwest of Shellrock Mountain (Plate 1). The northern tip of the Shellrock Mountain fault terminates against the Rimrock Creek fault, while the southern tip terminates at the Cat Creek fault (**Figure 2-1**, **Figure 7-1; Plate** 1). A three-point solution on the mapped fault trace suggests a ~N.15°W.-striking and vertical to ~80°SW. dipping fault plane. The fault offsets a southeast-dipping stratigraphic section of CRBG and Dalles Formation with ~61 to 70 m (200 to 230 ft) down-on-the west apparent vertical offset.

Rimrock Creek fault – The Rimrock Creek fault is an ~4-km-long (2.5 mi), northwest-trending, down-on-the-southwest, right-lateral oblique-slip fault mapped along Rimrock Creek in the northern part of the map area (**Figure 2-1**; **Figure 7-1**; Plate 1). A three-point solution on the mapped fault trace suggests an ~N.50°W.-striking and ~75°SW.-dipping fault. The fault terminates at the north-striking Gibson Prairie fault and offsets a southeast-dipping stratigraphic section of CRBG and Dalles Formation (Plate 1). Latest age of movement on the fault appears to post-date emplacement of the ~8 to 7 Ma andesite and dacite of East Fork (**Tmde**).

Inferred concealed thrust fault – Younger than 500 ka products from Mount Hood volcano (**Qhcwl, Qhcgr**, **Qr4cc**) and glacial debris (**Qgst**) may conceal an additional ~east-west-striking thrust fault beneath the Upper Hood River Valley (**Figure 7-3**; Plate 1). The trace of a thrust fault is inferred beneath the area of the Parkdale lava vent (**Qr1pk**), connecting into and paralleling the Clear Branch Middle Fork Hood River, west of the map area (**Figure 2-1**; Plate 1). Observations suggesting the possibility of a buried thrust fault beneath the Upper Hood River Valley include 1) a topographic high of Dalles Formation (**Tmdl**) in the very northwest corner of the Dog River–Badger Lake area (e.g., Volmer Ditch, Mcintosh Road), which is onlapped by younger late Pliocene and early Pleistocene intracanyon lava flows of the basalt and basaltic andesite of Laurence Lake (**Qr5ll**); 2) a conspicuous east-west-oriented, ~245-m-high (800 ft), escarpment of Dalles Formation capped by unit **Qr5ll** lava flows, running north of and parallel to the Clear Branch Middle Fork Hood River that buttresses <500 ka Mount Hood eruptive products to the south (Sherrod and Scott, 1995); and 3) the location of the Parkdale lava vent (**Qr1pk**) in line with the east-west trend of the prominent escarpment running on the north side of Clear Branch (**Figure 2-1**; Plate 1). The inferred concealed thrust fault lies along strike of the Cat Creek thrust fault, mapped east of East Fork Hood River (**Figure 2-1**; Plate 1), but displays an apparent reversal in offset, likely with an up-on-the-north sense of vertical displacement.

Hellroaring Creek fault – The Hellroaring Creek fault is a complex thrust fault zone located along Hellroaring Creek and underlying Bluegrass Ridge in the southern part of the map area (**Figure 2-1**; **Figure 7-2**; Plate 1). Sherrod and Scott (1995) showed this east-southeast-oriented fault as a major regional up-on-the south thrust, continuing for ~15 km (9.5 mi) beyond and east-southeast of the map area, to Tygh Creek and Hootnany Point. Just east of the map area, the thrust juxtaposes older CRBG against younger Dalles Formation. In the Dog River–Badger Lake area, the fault zone consists of at least two mapped strands (**Figure 7-2**; Plate 1). Three-point solutions on the southern mapped fault trace suggest a variable east-west to N.50°W.-striking and ~30°SW.-dipping fault plane. The northern strand in the Hellroaring Creek fault zone has a similar orientation, striking N.45°W. and dipping ~40°SW. East of East Fork Hood River, the main southern strand of the Hellroaring Creek fault places late Miocene or early Pliocene (5.37 Ma) Dalles Formation intrusive rocks (**Tmdei**) and older ~16 Ma CRBG (**Twfh**) against younger Pliocene rhyolite (**Tprn**), dacite (**Tpde**), and tuff breccia (**Tpdd**). The northern strand cuts similarly across Pliocene rocks between Hellroaring and Engineers Creek (**Figure 2-1**; **Figure 7-2**; Plate 1). Vertical

up-on-the-south separation of the upper contact of the CRBG in the upper part of Gumjuwac Creek is at least 238 m (780 ft); the top of the CRBG in the hanging wall of the Hellroaring Creek fault in uppermost Gumjuwac Creek at Gumjuwac Saddle is at an elevation of 1,586 m (5,202 ft), while the top of the CRBG in the footwall of the Hellroaring Creek fault is at an elevation of 1,348 m (4,420 ft), 1.8 km (1.1 mi) southeast of Gumjuwac Saddle (D.R. Sherrod, unpublished geologic mapping 1991 to 1995; Sherrod and Scott, 1995).

Rocks exposed in the vicinity of both strands are altered and associated with pervasive Fe-staining; chalcedonic quartz is locally found as float across outcrops in the Hellroaring Creek fault zone. West of East Fork Hood River, a concealed fault trace likely projects into the base of Bluegrass Ridge, where late Miocene or early Pliocene Gunsight Butte volcanics (**Tpmv**) are juxtaposed against late Pliocene rhyolite (**Tprc**) (**Figure 2-1**; Plate 1).

Mine Creek fault –The Mine Creek fault is an ~N.85°E.-striking and ~75°NW.-dipping reverse fault paralleling the Hellroaring Creek fault, striking along Mine Creek east through Gumjuwac Saddle (**Figure 2-1**; **Figure 7-2**; Plate 1). The eastern edge of the mapped fault terminates against the north-south trending Gumjuwac Saddle fault, whereas the western tip is inferred to terminate at the north-south-trending East Fork Hood River fault (Plate 1). The fault juxtaposes late Miocene or early Pliocene (5.37 Ma) Dalles Formation intrusive rocks (**Tmdei**) and older ~16 Ma Columbia River Basalt (**Twfh**) against younger rocks of the oldest part of the late Miocene and early Pliocene Gunsight Butte volcanics (**Tpmv**; **Tpma**). North of the Mine Creek fault, unit **Tpma** is exposed up to an elevation of 1,503 m (4,930 ft); south of the fault, unit **Tpma** flows are exposed at lower elevations near 1,378 m (4,520 ft). Vertical up-on-the-south separation of unit **Tpma** across the Mine Creek fault is ~125 m (410 ft). The mapped distribution of Gunsight Butte volcanic flows (**Tpml**; **Tpmn**; **Tpmb1**; **Tpmb2**; **Tpag**) younger than unit **Tpma**, indicates these flows onlap older rocks of unit **Tmdei** and are not themselves cross cut by the Mine Creek fault, thus constraining timing of latest offset along the Mine Creek fault to the early Pliocene between emplacement of unit **Tpma** and unit **Tpml**.

Exposure of late Miocene or early Pliocene Dalles Formation microdiorite (**Tmdei**) and early to middle Miocene Columbia River Basalt (**Twfh**) is restricted to this part of the map area, bounded on the north by the Hellroaring Creek thrust fault and on the south by the Mine Creek fault (**Figure 7-2**; Plate 1). This map association suggests that this fault-bounded region is a pop-up block situated between the main Hellroaring Creek thrust fault and the antithetic Mine Creek reverse fault. This fault geometry indicates that this system of structures has accommodated north-vergent crustal shortening from the late Miocene into the Pliocene.

Figure 7-2. View looking east across the East Fork Hood River Valley, looking from a point near the southern end of Bluegrass Ridge (45.33969, -121.60851 WGS84 geographic coordinates; 609020mE, 5021628mN WGS84 UTM Zone 10 coordinates). The central high point on the horizon is Lookout Mountain. North of Lookout Mountain, the ridge is underlain by a section of early Pleistocene and Pliocene volcanics and regional Quaternary lavas. South of Lookout Mountain, across two strands of the Hellroaring Creek thrust fault, the ridgeline is underlain by older middle to early Miocene Columbia River Basalt Group (CRBG) lavas, late Miocene or early Pliocene Dalles Formation intrusive rocks (Tmdei), lava flows forming the late Miocene to early Pliocene Gunsight Butte volcanics (GV). The East Fork Hood River runs south to north (right to left) through the valley. Labels: CRBG – Columbia River Basalt Group; EFV – East Fork Hood River valley; GB – Gunsight Butte; GS – Gumjuwac Saddle; GV – Gunsight Butte volcanics; HCT – Hellroaring Creek thrust fault; LM – Lookout Mountain; PV – Pliocene volcanics; Tmdei – Dalles Formation microdiorite; U – relative motion up on fault; D – relative motion down on fault. Photo credit: Jason McClaughry, 2019.

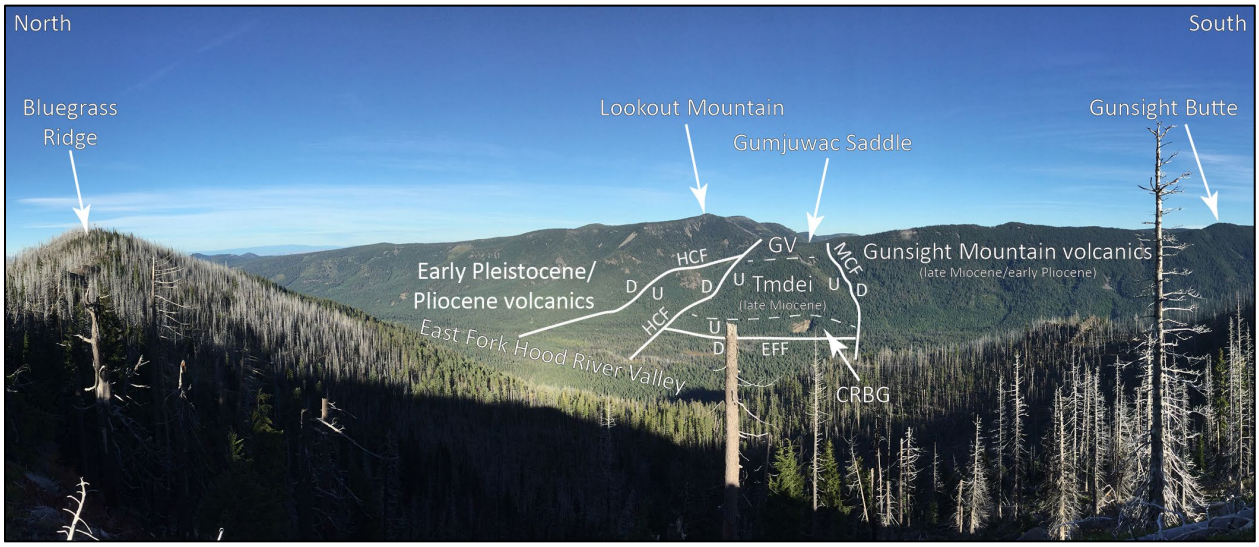

Gumjuwac Saddle fault – The Hellroaring Creek fault is associated with several northwest-trending reverse faults. Three-point problems on these faults indicate traces striking ~N.20°W. and dipping ~70°NE. As much as 530 m (1,738 ft) of up-on-the-east displacement of a north-northeast trending anticline is likely along the strand extending from Hellroaring Creek, south to Gumjuwac Saddle (**Figure 2-1**; Plate 1, cross section C-C′). East of the fault and Gumjuwac Saddle, N.28°W.-striking and 13°-NE.-dipping Grande Ronde basalt flows (**Tgsb**; **Tgww**) are exposed up to an elevation of 1,566 m (5,135 ft). West of the fault, younger, N.20°E.-striking and 19°-NW.-dipping Wanapum Basalt flows (**Twfh**) are present in quarry exposures near river level of the East Fork at an elevation of 1,112 m (3,650 ft). Older Grande Ronde basalt flows (**Tgsb**; **Tgww**) must therefore lie below river level of East Fork Hood River in the vicinity of Horsethief Meadows (**Figure 2-1**; Plate 1, cross section C-C′). Vertical, up-on-the-east separation of CRBG units across the Gumjuwac Saddle Fault is ≥400 m (1312 ft).

East Fork Hood River fault – Wise (1969) and Swanson and others (1981) both portrayed a concealed north-south-trending down-on-the-west normal(?) fault paralleling the East Fork Hood River from the mouth of Engineers Creek south past the mouth of Mine Creek (**Figure 2-1**; Plate 1). We concur with the presence of the fault and interpret this entirely concealed structure as an east-dipping reverse fault paralleling the Gumjuwac Saddle fault, south of the Hellroaring Creek thrust fault. CRBG flows, striking N.20°E. and dipping 19°NW. are exposed in a quarry just to the southeast of Horsethief Meadows on the

east side of the inferred fault (**Figure 2-1**; Plate 1). The fault is interpreted to cut and offset the NW.-dipping CRBG, placing CRBG units below present river level of East Fork Hood River, west of the fault. Cross section interpretation suggests reverse offset across the fault could be at least 50 m (164 ft) **(Figure 2-1**; Plate 1, cross section C-C′). The latest age of movement on the fault postdates the late Miocene or early Pliocene Dalles Formation (**Tmdei**).

7.1.2 North-northwest-striking faults cutting the Hood River graben escarpment

7.1.2.1 North-northwest trending faults in the northern part of the Dog River–Badger Lake area

Gibson Prairie fault **–** The Gibson Prairie fault is a >5-km-long (3.2 mi) north-south-striking normal fault, paralleling the West Fork Neal Creek drainage to the north and mapped south through Gibson Prairie to Mill Creek Buttes (**Figure 2-1**; Plate 1**;** cross section A-A′). A three-point solution on the mapped fault trace suggests an ~N.5˚W.-striking and ~45˚SW.-dipping fault plane. The southern end of the Gibson Prairie fault terminates or steps to the southwest along the northeast-striking Alder Creek fault (Plate 1).

East of the Gibson Prairie fault, the CRBG and overlying Dalles Formation (**Tmdl**) are exposed along the upper reaches of the North Fork Mill Creek, forming the core to the Mill Creek Ridge anticline (east of the map area, **Figure 2-1**; J.D. McClaughry, unpublished geologic mapping). The Mill Creek Ridge anticline is a northeast plunging, N.50˚E.- to N.60˚E.-striking upright and asymmetric box fold. At the deepest levels of exposure the Mill Creek Ridge anticline is offset by a major blind to emergent thrust fault, offsetting the anticlinal structure in a reverse, up-on-the-south sense. The western extent of the Mill Creek Ridge anticline may terminate in the subsurface against the Gibson Prairie fault.

Projection of the southeast-dipping CRBG-Dalles contact west from Mill Creek Ridge to Gibson Prairie places the CRBG-Dalles contact at an elevation of 1,136 m (3,726 ft) in the shallow subsurface just east of the Gibson Prairie fault (**Figure 2-1**; Plate 1, cross section A-A′; J.D. McClaughry, unpublished geologic mapping). Detailed geologic mapping of CRBG flows, southeast–dipping orientation of CRBG flows (N.64˚E., 12˚SE.), and cross section interpretation (Plate 1, cross section A-A′), indicates the CRBG-Dalles contact lies at an elevation of ~727 m (2,380 ft) in the subsurface just west of the Gibson Prairie fault. Down-on-the-west normal vertical offset of the CRBG-Dalles contact along the Gibson Prairie fault is therefore estimated to be ~410 m (1,346 ft).

Alder Creek fault – The Alder Creek fault is a N.45˚E.-striking, high-angle fault cutting ~8 to 7 Ma Dalles Formation units **Tmdi** and **Tmde** across the central part of Mill Creek Buttes (**Figure 2-1**; Plate 1). The southern end of the Gibson Prairie fault terminates or steps to the southwest along the northeast-trending Alder Creek fault (Plate 1). Map pattern suggests that a down-on-the-northwest normal sense of offset across the Alder Creek fault is probable.

7.1.2.2 Dog River-Mill Creek Divide fault zone

The Dog River-Mill Creek Divide fault zone (DRMF), is a 3- to 4-km-wide (1.8 to 2.5 mi) broad zone of parallel north-northwest-striking normal faults, including from east to west the Puppy Creek, Ward Creek, Dog River, and Powder Springs faults. These faults collectively define part of the the eastern margin of the Hood River graben in the Dog River–Badger Lake area (**Figure 7-3**; Plate 1). Mapped fault traces in the DRMF are ≥15 km long (9 mi) and consistently show a west-side-down component of vertical offset of late Miocene Dalles Formation and younger Pliocene and early Pleistocene volcanic rocks. The faults terminate at their northern ends at a northeast-stepping segment of the Hood River fault zone, where East Fork Hood River locally bends into parallelism with this normal fault (Plate 1). These north-northwest-striking

faults are also intersected and offset by the northeast-trending High Prairie normal fault in the southeast part of the map area (Plate 1). Although these faults, cutting the Hood River graben escarpment are rarely exposed, stratigraphic evidence strongly suggests a significant down-on-the-west, normal displacement component. Parallelism with regional strike-slip faults in the Yakima Fold Belt (**Figure 5-3**), suggests that right-lateral strike-slip or oblique-slip may be also be an important component of offset along these faults. Map pattern locally suggests right-lateral offset along several strands (e.g., Puppy Creek and Ward Creek faults), but no direct evidence for lateral movement (e.g., slickenlines) across these faults was found.

Elevation differences between exposures of Dalles Formation units (**Tmdv, Tmde**) across the Puppy Creek, Ward Creek, Dog River, and Powder Springs faults, require vertical down-on-the-west displacement ≥580 m (1,902 ft). Late Miocene Dalles Formation dacite flows and domes (**Tmdv**) are widely exposed in the upper reaches of Dog River at elevations up to ~1,585 m (5,383 ft). At the mouth of Tumble Creek, along East Fork Hood River stratigraphically equivalent **Tmde** flows are exposed up to an elevation of ~ 976 m (3,200 ft).

Figure 7-3. View looking southwest across the southern part of the Hood River graben toward Middle Pleistocene to Holocene Mount Hood volcano. Yellow dashed line is the western extent of the map area. Dashed white lines are faults; magenta dashed line is an inferred concealed thrust fault presumed to underlie the Upper Hood River Valley. Middle ground is the curving trace of East Fork Hood River and OR Highway 35 (elevation 640 m [2,100 ft]). Person at the right of the photograph is standing on high topography (elevation 1,265 m [4,150 ft]) in the east part of the Dog River 7.5′ quadrangle, underlain by late Miocene lavas in the Dalles Formation (Tmde) (45.477876, -121.53106 WGS84 geographic coordinates; 614808mE, 5037088mN WGS84 UTM Zone 10 coordinates). From the East Fork to Mount Hood, low topography, formed by the down-faulted Hood River graben is largely infilled by < 1 m.y. old Pre-Hood lavas and < 500 k.y. old Mount Hood lavas and clastic rocks. Labels: OR 35 – Oregon Highway 35; EF – East Fork Hood River; LL – Laurance Lake; PV – Parkdale vent; Tmdl – Dalles Formation, undivided; QTbt – High-TiO_2 basalt and basaltic andesite; Qr5dr – basaltic andesite of Dog River; D – relative down on fault; U – relative up on fault; arrow on fault show direction of relative horizontal slip. Photo credit: Carlie Duda, 2018.

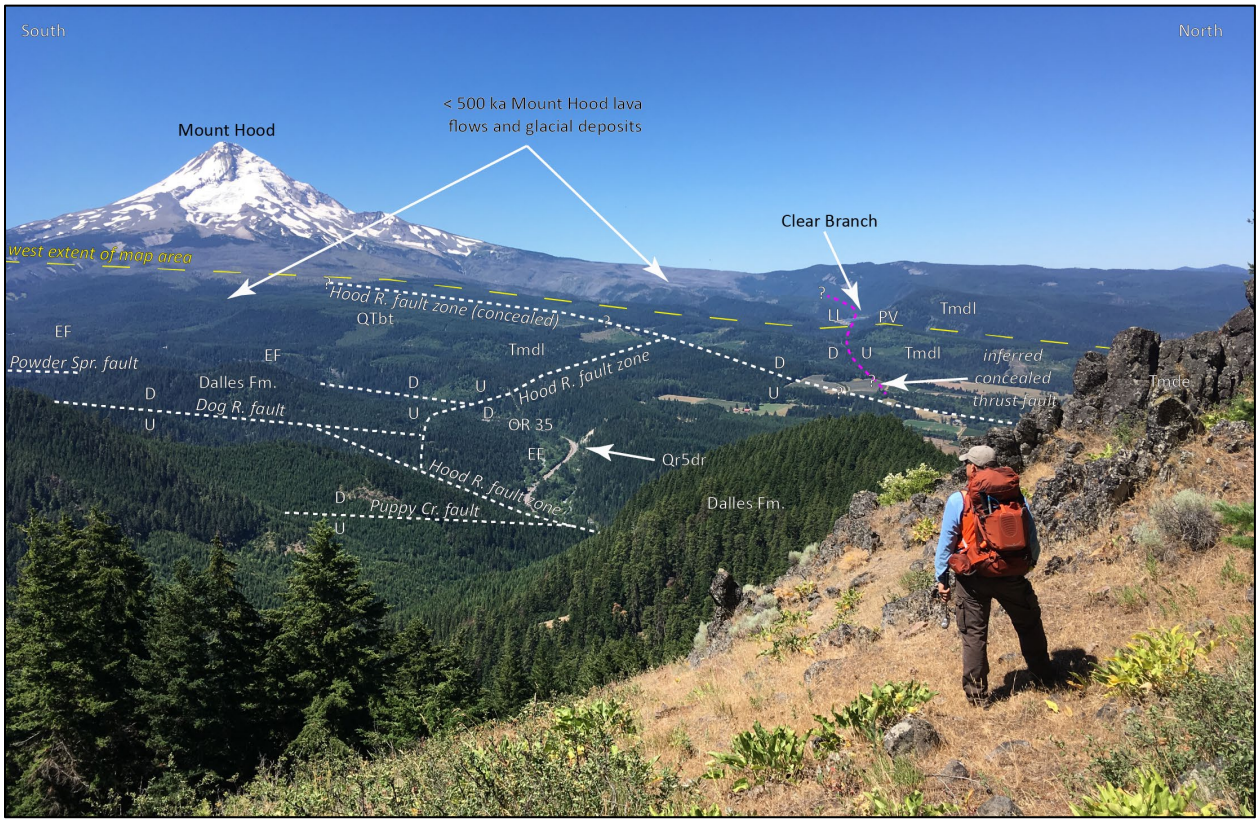

Puppy Creek fault – The Puppy Creek fault is a north-northwest-striking normal fault mapped for a length of ~9.3 km (5.8 mi) from OR Highway 35 on the northwest to Bottle Prairie on the southeast (**Figure 2-1**, **Figure 7-3**; Plate 1, cross section B-B′). Geologic mapping in the adjacent Fivemile Butte and Flag Point 7.5′ quadrangles indicates the fault continues for an additional ~14.5 km (9.0 mi) southeast of the map area (J.D. McClaughry, unpublished geologic mapping). Three-point solutions for the fault suggest an ~N.20°W.-striking and ~60° to 70°SW.-dipping fault plane through the quadrangle. At the faults northern extent, along lower Puppy Creek, the fault juxtaposes undivided Dalles Formation clastic rocks (**Tmdl**) on the northeast with hornblende-porphyritic dacite (**Tmdp**) on the southwest (**Figure 2-1**, **Figure 7-3**; Plate 1). Vertical offset of Dalles Formation units along lower Puppy Creek is >120 m (393 ft). Farther southeast, the fault offsets Quaternary basaltic lavas, including the ~2 Ma basalt of Cooks Meadow (**Qrbc**), in an apparent right-lateral oblique-slip sense with down-on-the west vertical offset. Vertical offset of the basalt

of Cooks Meadow (**Qrbc**) is ~ 30 m (100 ft), while right-lateral offset is ~100 m (328 ft). Southwest of Mill Creek Buttes, the fault forms a prominent lineament cutting across colluvium-mantled slopes (**Qc**) on the west side of the Dog River-Mill Creek divide before running beneath the cinder cone vent (**Qrbv**) for the 1.87 Ma basaltic andesite of Dog River (**Qr5dr**) (**Figure 2-1**; Plate 1). Southeast of this cinder-cone (**Qrbv**), the fault bifurcates into two strands, forming a small graben (**Figure 2-1**; Plate 1, cross section B-B′). The fault does not appear to offset the basaltic andesite of Dog River (**Qr5dr**) vertically; the base elevation for the vent area north of Brooks Meadow, and the highest elevation flow outcrops on either side of Dog River are indistinguishable. Thus, the latest age of fault slip recognized along the Puppy Creek fault is constrained between ~2.06 and 1.87 Ma.

Ward Creek fault – The Ward Creek fault is a northwest-striking, down-on-the-southwest normal fault cutting the Dalles Formation (**Tmdl**, **Tmdv**) along Ward Creek in the east-central part of the Dog River–Badger Lake area (**Figure 2-1**; Plate 1, cross section B-B′). A three-point solution for the fault suggests an ~N.17°W.-striking and ~75°SW.-dipping fault trace. Apparent down-on-the-southwest vertical separation of the **Tmdv/Tmdl** contact is ~91 m (300 ft) (Plate 1, cross section B-B′). Map pattern does not indicate fault activity extending into the Quaternary.

Dog River fault – The Dog River fault is a north-northwest-striking normal fault mapped for a length of ~9.3 km (5.8 mi) from OR Highway 35 on the northwest to High Prairie on the southeast (**Figure 2-1**, **Figure 7-3**; Plate 1 cross section B-B′). Three-point solutions for the fault suggest a steep west-dipping fault plane striking ~N.15°W. and dipping ~45° to 60°SW. In the lower reaches of Dog River, the fault accommodated down-on-the-west offset and eastward tilting of Dalles Formation rocks (**Tmdp**; **Tmde**). West of Horkelia Meadow, vertical, down-on-the-west offset of the dacite of Fivemile Butte (**Tmdv**) is on the order of 137 m (450 ft) (Plate 1). Latest age of faulting along the Dog River fault may be early Pleistocene, as 2.6 to 2.4 Ma High-TiO_2 basaltic lavas (**QTbt**) are offset by ~25 m (80 ft) in the lower reaches of Dog River. The Dog River fault forms a notable structural boundary of the Hood River graben as <3.69 Ma to ~2.5 Ma lavas are, for the most part, only present west of the structure (**Figure 5-4d,e**).

Powder Springs fault – The Powder Springs fault is a north-northwest-striking normal fault mapped for a length of ~14 km (8.8 mi) from OR Highway 35 on the northwest to High Prairie on the southeast (**Figure 2-1**, **Figure 7-3**; Plate 1). A three-point solution for the fault, as it crosses Tumble Creek (**Figure 2-1**; Plate 1, cross section B-B′), suggests a steep west-dipping fault plane striking ~N.12°W. and dipping ~60° to 70°SW. Along East Fork Hood River, the fault juxtaposes an eastward tilted section of 8 to 7 Ma hornblende-phyric dacite (**Tmdp**) and andesite and dacite flows of East Fork (**Tmde**) (**Figure 2-1**; Plate 1). East of Tumble Creek apparent vertical down-on-the-west offset of the ~3 Ma andesite of Fret Creek (**Tpaf**) and latest Pliocene or earliest Pleistocene Lookout Mountain lavas (**QTal2**, **QTal3**) is ≤256 m (840 ft). The 3.14 Ma andesite and dacite of Senecal Spring (**Tpas**) is offset ~290 m (950 ft) in a vertical, down-on-the-west sense along the southern strand of the Powder Springs fault (Plate 1). Vertical, down-on-the west offset of the 3.02 Ma dacite of Fifteenmile Creek (**Tpdf**) across the Powder Springs fault is less at ~45 m (150). The age of latest fault movement post-dates the 1.87 Ma basaltic andesite of Dog River (**Qr5dr**) (**Figure 2-1**; Plate 1, cross section B-B′). The lower contact of the basaltic andesite of Dog River (**Qr5dr**) is offset vertically by ~25 m (80 ft), with ~40 m (131 ft) of apparent right lateral horizontal offset.

High Prairie fault – The High Prairie fault is a northeast-striking, down-on-the-northwest, normal fault mapped for ~6.5 km (4 mi) between East Fork Hood River and the headwaters of Eightmile Creek (**Figure 2-1**; Plate 1).

The fault intersects and offsets the north-northwest-striking Powder Springs, Ward Creek, and Dog River faults and cuts a stratigraphic section of Pliocene and Quaternary lavas. A three-point solution on the mapped fault trace suggests a ~N.65˚E.-striking and ~50˚NW.-dipping fault plane. The amount of apparent vertical offset across the High Prairie fault is ~15 to 20 m (50 to 66 ft). Latest age of movement on the fault postdates emplacement of the ~2.06 to 1.87 Ma basaltic andesite of High Prairie (**Qrbhp**).

7.1.2.3 North-northwest trending faults in the southern part of the Dog River–Badger Lake area

Gunsight Butte fault – The Gunsight Butte fault is a N.30°W.-striking, down-on-the-northeast normal fault cutting the stratigraphic section of Gunsight Butte volcanics in the southeast part of the map area (Plate 1). The map pattern of the Gunsight Butte fault indicates that it is nearly vertical. Apparent vertical separation of flow units low in the stratigraphic section (below **Tpmd**) is ≤76 m (250 ft); upper parts of the section appear to have less apparent vertical offset of ≤40 m (130 ft). The latest age of faulting along the Gunsight Butte fault postdates the 4.25 Ma andesite of Gumjuwac Saddle (**Tpag**) and 2.44 Ma Badger Butte volcanics andesite (**Qbla**).

Pocket Creek fault zone – The Pocket Creek fault zone is an ~0.6-km-wide (0.4 mi) zone of northwest-striking, vertical to steeply west-dipping normal faults offsetting the Gunsight Butte volcanics south of the East Fork Hood River and the Lookout Mountain volcanics across the southern end of Elk Mountain (**Figure 2-1**; Plate 1). Three-point solutions for multiple fault strands suggest fault plane orientations striking N.25˚W. to N.50˚W. and dipping 70˚ to 85˚SW. The predominant offset is in a down-on-the-southwest sense. The amount of apparent vertical offset along any single strand in the Pocket Creek fault zone south of East Fork Hood River ranges between ~20 to 50 m (65 to 164 ft); offset along the Elk Mountain strand is as much as 140 m (460 ft). Latest age of faulting along the Pocket Creek fault zone postdates Badger Butte volcanics andesite (**Qbla**), while the Elk Mountain strand cuts unit **QTab4**, which is younger than 2.3 Ma.

7.1.3 Hood River fault zone

The Hood River fault was portrayed by Sherrod and Scott (1995) in the Dog River–Badger Lake area as single, inferred down-on-the-west normal fault, striking north-south from Griswell Creek south to the west flank of Bluegrass Ridge (**Figure 2-1**; Plate 1). Our mapping through the Dog River–Badger Lake area indicates the structure is a more complex zone of generally north-south-striking, subparallel normal faults bounding the eastern escarpment of the Hood River graben (Plate 1; **Figure 5-3**). Collectively, these faults form the southern part of the Hood River fault zone mapped along the foot of the eastern escarpment of the Hood River graben for a distance of ~25 km (15 mi) north to Hood River, OR (**Figure 5-3**) (McClaughry and others, 2012). Hood River fault zone structures are largely concealed by <500 Ka products of Mount Hood volcano in the Dog River–Badger Lake area, but the delineation of these faults can be reasonably inferred on the basis of the vertical position and distribution of older units that are variably exposed beneath the younger volcanic cover.

In the northern part of the map area, concealed north-south- to ~N.10°E.-striking strands of the Hood River fault zone accommodated down-on-the-west vertical offset of the southeast-dipping section of CRBG and Dalles Formation west of the Gibson Prairie fault (Plate 1, cross section A-A′). Two concealed

strands, east of East Fork Hood River, offset the southeast-dipping contact between the Basalt of Sentinel Gap (**Twfs**) and older Sentinel Bluffs Member (**Tgsb**) contact from elevations above 930 m (3,050 ft) between Rimrock and Yellowjacket Creek down to 563 m (1,845 ft) along OR Highway 35 (**Figure 2-1**; Plate 1). Cross section interpretation indicates down-on-the-west normal vertical offset along this part of the Hood River fault zone of ~535 m (1,755 ft) (Plate 1, cross section A-A′). We portray one of these north-south fault strands to continue south, paralleling East Fork Hood River to the mouth of Cat Creek, where outcrops are marked by pervasive fault gouge in brittle CRBG rocks (**Figure 2-1**; Plate 1). A 1.83 Ma, N.20°E.- to N.30°E.-striking andesite dike (**Qrai**), cropping out ~0.8 km (0.5 mi) north of the mouth of Cat Creek, intrudes fault breccia (**QTfb**) and thus may limit the upper age of faulting along this strand of the Hood River fault zone (Plate 1). The dike is not visibly present west of East Fork Hood River. It may be buried by younger Polallie deposits (**Qh2pc**), or alternatively was offset in a down-on-the-west sense by later movement on this segment of the Hood River fault zone.

At the mouth of Dog River, the Hood River fault zone takes an ~ 1-km-wide (0.6 mi) southwest step, connecting north-south-trending strands via an ~N.60°E.-striking, ~65°NW.-dipping normal fault paralleling East Fork Hood River (**Figure 2-1**; Plate 1). The 1.87 Ma basaltic andesite of Dog River (**Qr5dr**), which forms a graben escarpment-capping lava flow along the middle reaches of Dog River, is offset in a down-to-the-northwest sense across the northeast-striking fault segment (**Figure 2-1**; Plate 1). Southeast of the fault, the base of northern outcrops of the Dog River flow (**Qr5dr**) lies at an elevation of ~1,137 m (3,728 ft); the flow top is at an elevation of ~1,220 m (4,000 ft). Northwest of the fault, **Qr5dr** outcrops are present in an abandoned quarry at lower elevations northwest of East Fork Hood River (**Figure 2-1**; Plate 1). The base of Dog River flows (**Qr5dr**) exposed in the East Fork Hood River quarry are not exposed; the upper flow contact lies at an elevation of ~703 m (2,306 ft), where it is conformably overlain by the 424-ka basaltic andesite and andesite of Cloud Cap (**Qr4cc**) (Plate 1). Northward projection of the basal gradient of the high outcrops of the escarpment-capping Dog River flows (**Qr5dr**) places the bottom of the Dog River flow at an elevation of ~1,011 m (3,315 ft) and the upper surface at ~1,047 m (3,433 ft) as it intersects the channel of the modern East Fork Hood River. The difference in the projected upper flow surface and the actual upper flow contact in East Fork Hood River quarry exposures is ~344 m (1,127 ft). Lack of lateral continuity and offset between Dog River and East Fork Hood River outcrops is accounted for by 1) paleo-gradient of north-northwest-directed drainages entering the developing Hood River graben during the early Pleistocene, and (2) down-on-the-northwest vertical offset of ~344 m (1,127 ft) along the N.60°E.-striking fault strand paralleling the major northeast-oriented bend in East Fork Hood River.

A western strand of the Hood River fault zone is inferred to parallel Griswell Creek in the Upper Hood River Valley in the northern part of the Dog River–Badger Lake area and further offset the CRBG-Dalles section in a down-on-the-west sense (Sherrod and Scott, 1995; **Figure 2-1**; Plate 1, cross section A-A′). In the Upper Hood River Valley, east of Griswell Creek, the Basalt of Sand Hollow (**Twfh**) and older Sentinel Bluffs Member (**Tgsb**) are exposed in outcrops along OR Highway 35 and in a rock pit on the west bank of East Fork Hood River (see sample G637 on Plate 1). West of Griswell Creek, CRBG units are not exposed where they are concealed by the late Miocene Dalles Formation (**Tmdl**), and younger middle to late Pleistocene products of Mount Hood volcano (**Qhcgr**, **Qhcwl**), and late Pleistocene glacial deposits (**Qgso**, **Qgst**). Vertical down-on-the-west offset along a concealed normal fault paralleling Griswell Creek and subsequent burial by younger deposits explains the notable absence of CRBG outcrops across the Upper Hood River Valley (**Figure 2-1**; Plate 1). East-to-west vertical offset along this buried strand could be on the order of 250 m (800 ft), although little subsurface data are present in this area to confirm the total amount of stratigraphic separation (Plate 1, cross section A-A′). The only constraints are 1) a topographic

high of Dalles Formation (**Tmdl**) exposed between West Fork Evans Creek and the Parkdale lava beds (**Qr1pk**), and 2) a water well sited in the Dalles Formation (**Tmdl**) between the Parkdale lava (**Qr1pk**) and Clear Creek Road that reportedly intersects "basalt" at a depth elevation of 582 m (1,910 ft) (Plate 1). Cumulative down-on-the west vertical offset across the parallel strands of the Gibson Prairie fault and Hood River fault strands in the northern part of the Dog River–Badger Lake area is ~1,220 m (4,000 ft) (Plate 1, cross section A-A′).

Sherrod and Scott (1995) showed the concealed western strand of the Hood River fault (zone) paralleling Griswell Creek and continuing south-southwest to the west side of Bluegrass Ridge. Our mapping suggests the original alignment of the concealed Hood River fault, as inferred by Sherrod and Scott (1995), is likely not permissive in the area between the mouth of Crystal Spring Creek and Tamanawas Falls (**Figure 2-1**; Plate 1). Chemically distinctive and isotopically dated High-TiO_2 lavas of unit **QTbt** (2.6 to 2.4 Ma) are exposed across this originally inferred alignment of the Hood River fault having similar upper elevations in the three main outcrop areas at Bluegrass Ridge (1,171 m [3,840 ft]), north of Tilly Jane Creek (1,177 m [3,861 ft]), and east of East Fork Hood River (1,160 m [3,800 ft]). Appreciable apparent vertical offset between the three exposure areas is not recognized. A southern extension of the Griswell Creek segment of the Hood River fault, more plausibly lies concealed and paralleling the area of Crystal Springs Creek and Wygant Canyon, west of early Pleistocene High-TiO_2 lavas (**QTbt**) in the Tilly Jane Creek area (**Figure 2-1**; Plate 1).

Bluegrass Ridge forms a topographically conspicuous, north-south-trending, linear escarpment east of Mount Hood in the southern part of the Hood River graben (**Figure 2-1**; Plate 1). The >610-m-high (2,000 ft) ridge is underlain by a thick sequence of lavas dating from ~8 Ma (**Tmde**) at the base to ~2 Ma near the top (**QTab5**, **QTab6**). Quaternary lava flows forming the high topography of Bluegrass Ridge up to elevations of 1,870 m (5,700 ft) are not exposed west of Cold Spring Creek at an elevation of ~1,460 m (4,788 ft) (**Figure 2-1**; Plate 1). West of Cold Spring Creek, younger 150 to 200 ka Mount Hood lava flows (**Qh4cp**, **Qh4lb**, **Qh4cs**) and Late Pleistocene glacial deposits (**Qgst**) are banked against the topographic high of Bluegrass Ridge (**Figure 2-1**; Plate 1, cross section C-C′). Map pattern indicates Mount Hood lavas (**Qh4cp**, **Qh4lb**, **Qh4cs**, **Qh3lc**) and glacial ice filled a topographic low, banked against the Bluegrass Ridge fault escarpment, and flowed northward around this topographic high in Late Pleistocene time. Formation of Bluegrass Ridge predates emplacement of 150 to 200 ka Mount Hood lava flows and Late Pleistocene glacial advances. The notable geomorphic expression of Bluegrass Ridge, infilled by much younger lava and glacial deposits on the west, is most plausibly explained by a concealed north-south-striking, down-on-the-west normal fault paralleling Cold Spring Creek along the western edge of the escarpment. Post-early Pleistocene offset along the concealed normal fault strand must be on the order of 250 m (820 ft) or greater.

8.0 ACKNOWLEDGMENTS

This project and publication were supported through the STATEMAP component of the National Cooperative Geologic Mapping Program under cooperative agreement numbers G17AC00210 (2017) and G19AC00160 (2019). Additional funds were provided by the State of Oregon. XRF geochemical analyses were prepared and analyzed by Dr. Ashley Steiner at the GeoAnalytical Lab at Washington State University. New $^{40}Ar/^{39}Ar$ ages were prepared and analyzed by Dr. Dan Miggins at the College of Oceanic and Atmospheric Sciences, Oregon State University, Corvallis (OSU) and Drs. Bill McIntosh and Matt Heizler at the New Mexico Institute of Mining and Technology in Socorro, New Mexico. Field assistance and thought-provoking discussions on the outcrop with Annie McClaughry, Bob Houston, Nancy Calhoun, Jon Franczyk, Robert Welch, and Robert Hairston-Porter are sincerely appreciated. Many of the map interpretations and solutions to the myriad of geologic conundrums in the Dog River–Badger Lake area likewise benefited from frequent concept-chats with Mark Ferns and Bob Houston. David Sherrod (USGS CVO) commented on an earlier version of this manuscript and graciously shared his field notes and field maps from reconnaissance field work conducted in the Mount Hood area between 1991 and 1995. Ian Madin (DOGAMI) digitized and contributed linework for an early version of surficial geology in the Badger Lake area. Informative discussions with participants of a 2019 Geological Society of America field trip through the area significantly added to our knowledge and understanding of the Hood River graben. Larry McCollum, Water Quality Manager, granted access to lands administered by the City of The Dalles Municipal Watershed. Jason McClaughry and Carlie Duda sincerely appreciate the gracious hospitality and support of Claire Sierra and Josiah Dean, and staff at the Historic Balch Hotel in Dufur. Cartography for the map plate was provided by Jon J. Franczyk. Critical and insightful reviews by Scott Bennett (USGS), Clark Niewendorp (DOGAMI, retired), Mark Ferns (DOGAMI, retired), Ian Madin (DOGAMI), and Christina Appleby (DOGAMI) greatly enriched the final manuscript, geologic map, and geodatabase.

9.0 REFERENCES

Allen, J.E., 1966, The Cascade Range volcano-tectonic depression of Oregon, *in* Benson, G.T., ed., Transactions of the Lunar Geological Field Conference, Bend, Oregon, August, 1965: Oregon Department of Geology and Mineral Industries Open-File Report O-1966-01, p. 21–23.

Anderson, J.L., 1987, The structure and ages of deformation of a portion of the southwest Columbia Plateau, Washington and Oregon: Los Angeles, University of Southern California, Ph.D. dissertation, 272 p.

Anderson, J.L., and Tolan. T.L., 1986. Ages of wrench faulting in interridge basins, southwest Columbia Plateau, Washington and Oregon: Geological Society of America Abstracts with Programs, v. 18. 82 p.

Anderson, J.L., and Vogt. B.F., 1987, Intracanyon flows of the Columbia River Basalt Group in the southwestern part of the Columbia Plateau and adjacent Cascade Range, Oregon and Washington, *in* Schuster, J.E. ed., Selected papers on the geology of Washington: Washington Division of Geology and Earth Resources Bulletin 77, p. 249–267.

Anderson, J.L., Tolan, T.L., and Wells., R.E., 2013, Strike-slip faults in the western Columbia River flood basalt province, Oregon and Washington, *in* Reidel, S.P., Camp, V., Ross, M.E., Wolff, J.A., Martin, B.E., Tolan, T.L., and Wells, R.E., eds., The Columbia River Flood Basalt Province: Geological Society of America Special Paper 497, p. 325–347, doi:10.1130/2013.2497(13).

Baksi, A.K., 2013, Timing and duration of volcanism in the Columbia River Basalt Group: A review of existing radiometric data and new constraints on the age of the Steens through Wanapum Basalt extrusion, *in* Reidel, S.P., et al., eds., The Columbia River Flood Basalt Province: Geological Society of America Special Paper 497, p. 67–85, https:// doi .org/10.1130/2013.2497(03).

Baksi, A.K., and Farrar, E., 1990, Evidence for errors in the geomagnetic polarity time-scale at 17-15 Ma: $^{40}Ar/^{39}Ar$ dating of basalt from the Pacific Northwest, USA. Geophysical Research Letters, v. 17, p. 1117–1120.

Bacon, C.R., and Lanphere, M.A., 2006, Eruptive history and geochronology of Mount Mazama and the Crater Lake region, Oregon: Geological Society of America Bulletin, v. 118, p. 1331–1359.

Barry, T. L., Self, S., Kelley, S. P., Reidel, S., Hooper, P., and Widdowson, M., 2010, New $^{40}Ar/^{39}Ar$ dating of the Grande Ronde lavas, Columbia River Basalts, USA: Implications for duration of flood basalt eruption episodes: Lithos, v. 118, p. 213–222.

Barry, T.L., Kelley, S.P., Reidel, S.P., Camp, V.E., Self, S., Jarboe, N.A., Duncan, R.A., and Renne, P.R., 2013, Eruption chronology of the Columbia River Basalt Group, *in* Reidel, S.P., Camp, V.E., Martin, M.E., Ross, M.E., Wolff, J.A., Martin, B.S., Tolan, T.L., and Wells, R.E., eds., Geological Society of America Special Paper 497, p. 45–66, doi:10.1130/2013.2497(02).

Beaulieu, J.D., 1977, Geologic Hazards of Parts of Northern Hood River, Wasco, Sherman Counties, Oregon: Oregon Department of Geology and Mineral Industries Bulletin 91, 95 p. 11 plates, scale 1:62,500.

Beeson, M.H., and Tolan, T.L., 1990, The Columbia River Basalt Group in the Cascade Range: A middle Miocene reference datum for structural analysis: Journal of Geophysical Research, v. 95, p. 19,547–19,559.

Beeson, M. H., Moran, M. R., Anderson, J. L., and Vogt, B. F., 1982, The relationship of the Columbia River Basalt Group to the geothermal potential of Mount Hood area, Oregon, *in* Priest, G. R., and Vogt, B. F., eds., Geology and geothermal resources of the Mount Hood area, Oregon: Oregon Department of Geology and Mineral Industries Special Paper 14, p. 43–46.

Beeson, M.H., Fecht, K.R., Reidel, S.P., and Tolan, T.L., 1985, Regional correlations within the Frenchman Springs Member of the Columbia River Basalt Group: new insights into the middle Miocene tectonics of northwest Oregon: Oregon Geology, v. 47, no. 8, p. 87-96.

Beeson, M.H., Tolan, T,L., and Anderson, J.L., 1989, The Columbia River Basalt Group in western Oregon: Geologic structures and other factors that controlled flow emplacement patterns, *in* Reidel, S. P., and Hooper, P. R., eds., Volcanism and tectonism in the Columbia River Flood-Basalt Province: Geological Society of America Special Paper 239, p. 223-246.

Bela, J. L., 1982, Geologic and neotectonic evaluation of north-central Oregon: The Dalles 1° × 2° quadrangle: Oregon Department of Geology and Mineral Industries GMS 27, 2 plates, scale 1:250,000.

Bennett, S.E.K., Wells, R.E., Streig, A.R., Madin, I.P., and Stelten, M.E., 2019, Oblique slip history of active faults along the western margin of the Hood River graben, North-Central Oregon: Geological Society of America Abstracts with Programs, vol. 51, no. 4, ISSN 0016-7592, doi: 10.1130/abs/2019CD-329235

Bunker, R.C., Farooqui, S.M., and Thorns, RE., 1982, K-Ar dates for volcanic rocks associated with Neogene sedimentary deposits in north-central and northeastern Oregon: Isochron/West, no. 33, p. 21-22.

Burchfiel, B.C., and Stewart, J.H., 1966, "Pull-apart" origin of the central segment of Death Valley, California: Geological Society of America Bulletin, v. 7, p. 439–442 doi: 10.1130/0016-7606(1966)77[439:POOTCS]2.0.CO;2.

Burns, E.R., Morgan, D.S., Lee, K.K., Haynes, J.V., and Conlon, T.D., 2012, Evaluation of long-term water-level declines in basalt aquifers near Mosier, Oregon: U.S. Geological Survey Scientific Investigations Report 2012-5002, 134 p., GIS files. https://pubs.usgs.gov/sir/2012/5002/

Butler, R.F., 1992, Origins of natural remanent magnetism, *in* Paleomagnetism: Magnetic domains to geologic terranes: Blackwell Scientific Publications, p. 31-63.

Buwalda, J. P., 1929, A Neocene erosion surface in central Oregon: Carnegie Institute, Washington, Publication, v. 404, p. 1-10.

Buwalda, J.P., and Moore, B.N., 1929, Age of Dalles Beds and "Satsop" Formation and history of Columbia River gorge (abs.): Geological Society of America Bulletin, v. 40, p. 176-177.

Buwalda, J.P., and Moore, B.N., 1930, The Dalles and Hood River Formations and the Columbia River Gorge: Carnegie Institute, Washington, Publication, v. 404, p. 11-26.

Cameron, K.A., and Pringle, P.T., 1986, Post-glacial lahars of the Sandy River basin, Mount Hood, Oregon: Northwest Science, v. 60, no. 4, p. 225–237.

Cameron, K.A., and Pringle, 1987, A detailed chronology of the most recent major eruptive period at Mount Hood, Oregon: Geological Society of America Bulletin, v. 99, p. 845–851.

Cande, S. C., and Kent, D. V., 1992, A new geomagnetic polarity time scale for the Late Cretaceous and Cenozoic: Journal of Geophysical Research, v. 97, p. 13,917–13,951.

Cannon, C.M., and O'Connor, J.E., 2019, New constraints on the timing of Neogene filling and incision of the Dalles Basin, Oregon and Washington: Geological Society of America Abstracts with Programs. Vol. 51, No. 4, ISSN 0016-7592\doi: 10.1130/abs/2019CD-329350

Cohen, K.M., Finney, S.C., Gibbard, P.L., and Fan, J.-X., 2013 (updated 2015), The ICS International Chronostratigraphic Chart: Episodes 36, p. 199-204. https://stratigraphy.org/ICSchart/Cohen2013_Episodes.pdf

Condon, T., 1874, Preliminary report of the State Geologist to the Legislative Assembly, 8th regular session: Salem, Oregon, 22 p.

Conrey, R.M., Sherrod, D.R., Uto, K., Uchiumi, S., 1996, Potassium-Argon ages from Mount Hood Area of Cascade Range, northern Oregon: Isochron/West, no. 63, p. 10-20.

Conrey, R.M., Sherrod, D.R., Hooper, P.R., Swanson, D.A., 1997, Diverse primitive magmas in the Cascade Arc, northern Oregon and southern Washington: The Canadian Mineralogist, v. 35, p. 367-396.

Conrey, R. M., Taylor, E. M., Donnelly-Nolan, J. M., and Sherrod, D. R., 2002, North-central Oregon Cascades: Exploring petrologic and tectonic intimacy in a propagating intra-arc rift, *in* Moore, G. W., ed., Field guide to geologic processes in Cascadia: Oregon Department of Geology and Mineral Industries Special Paper 36, p. 47–90. https://www.oregongeology.org/pubs/sp/SP-36.pdf

Conrey, R.M., Sherrod, D.R., and McClaughry, J.D., 2019, Reconnaissance summary of High Cascades graben structures in central and northern Oregon: Geological Society of America Abstracts with Programs. Vol. 51, No. 4, ISSN 0016-7592. doi: 10.1130/abs/2019CD-329235

Cope, E.D., 1880, Corrections of the geological maps of Oregon: American Naturalist, v. 14, p. 457-458.

Cox, K. G., Bell, J. D., Pankhurst, R. J., 1979, The interpretation of igneous rocks: London, George Allen and Unwin, 450 p.

Crandell, D.R., 1980, Recent eruptive history of Mount Hood, Oregon, and potential hazards from future eruptions: U.S. Geological Survey Bulletin 1492, 81 p.

Crowell, J.C., 1974, Origin of late Cenozoic basins in southern California: in Dickinson, W.R., ed., Tectonics and Sedimentation: Society of Economic Paleontologists and Mineralogists (SEPM) Special Publication 22, p. 190–204.

Darr, C. M., 2006, Magma chamber processes over the past 475,000 years at Mount Hood, Oregon: insights from crystal zoning and crystal size distribution studies: Corvallis, Oregon State University, M.S. thesis, 141 p.

Dicken, S.N., 1965, Oregon Geography: The People, the Place, and the Time, 4th ed: Ann Arbor, Mich., Edwards Brothers, 147 p.

Duda, C.J.M., McClaughry, J.D., Houston, R.A., and Niewendorp, C.A., 2018, Lidar and Structure from Motion-enhanced geologic mapping, examples from Oregon, *in* Thorleifson, L. H., ed., 2018, Geologic Mapping Forum 2018 Abstracts, Minnesota Geological Survey Open File Report OFR-18-1, 107 p. https://conservancy.umn.edu/handle/11299/194852

Duda, C.J.M., McClaughry, J.D., and Madin, I.P., 2019, Building the modern geologic map in Oregon: a multi-faceted field- and technology-based approach: Geological Society of America Abstracts with Programs. Vol. 51, No. 4, ISSN 0016-7592, doi: 10.1130/abs/2019CD-329552. https://gsa.confex.com/gsa/2019CD/meetingapp.cgi/Paper/329552

Duncan, R.A. and Keller, R.A., 2004, Radiometric ages for basement rocks from the Emperor Seamounts, ODP Leg 197. Geochemistry, Geophysics, Geosystems, v. 5. doi:10.1029/ 2004GC000704.

Farooqui, S.M., Bunker, R.C., Stensland, D.E., and Thoms, R.E., Clayton, D.C., 1981a, Post-Columbia River Basalt Group stratigraphy and map compilation of the Columbia Plateau, Oregon: Oregon Department of Geology and Mineral Industries Open-File Report O-81-10, 79 p, 6 plates, scale 1:250,000. www.oregongeology.org/pubs/ofr/O-81-10.pdf

Farooqui, S.M., Beaulieu, J.D., Bunker, R.C., Stensland, D.E., and Thoms, R.E., 1981b, Post-Columbia River Basalt Group stratigraphy and map compilation of the Columbia Plateau, Oregon: Oregon Department of Geology, v. 43, no.10, p. 131-140. https://www.oregongeology.org/pubs/ofr/O-81-10.pdf

Ferns, M.L., and McClaughry, J.D., 2013, Stratigraphy and volcanic evolution of the middle Miocene La Grande—Owyhee eruptive axis in eastern Oregon, *in* Reidel, S.P., Camp, V., Ross, M.E., Wolff, J.A., Martin, B.E., Tolan, T.L., and Wells, R.E., eds., The Columbia River Flood Basalt Province: Geological Society of America Special Paper 497, p. 401-427, doi:10.1130/2013.2497(16).

Fiebelkorn, R.B., Walker, G.W., MacLeod, N.S., McKee, E.H., and Smith, J.G., 1983, Index to K/Ar age determinations for the state of Oregon: Isochron/West, no. 37, p. 3–60.

Gallino, G.L., and Pierson, T.C., 1985, Polallie Creek debris flow and subsequent dam-break flood of 1980, East Fork Hood River basin, Oregon: U.S. Geological Survey Water-Supply Paper 2273, 22 p.

Gannett, M.W., 1982, A geochemical study of the Rhododendron and the Dalles Formations in the area of Mount Hood, Oregon: Portland, Oregon, Portland State University, M.S. thesis, 70 p.

Geological Society of America Rock-Color Chart Committee, 1991, Rock Color Chart, 7th Printing.

Gillespie, M. R., and Styles, M. T., 1999, BGS rock classification scheme, v. 1, Classification of igneous rocks: British Geological Survey Research Report (2nd ed.), RR99-06, 52 p.

Gradstein, F. M., Ogg, J., and Smith A. (eds.), 2004, A geologic time scale 2004, Cambridge University Press, 589 p.

Gray, L.B., Sherrod, D.R., and Conrey, R.M., 1996, Potassium-Argon ages from the northern Oregon Cascade Range: Isochron/West, no. 63, p. 21-28.

Green, G.L., 1981, Soil survey of Hood River County Area, Oregon: Natural Resources Conservation Service Soil Conservation Survey 629, 66 p. https://www.nrcs.usda.gov/Internet/FSE_MANUSCRIPTS/oregon/hoodriverOR1981/hoodriverOR1981.pdf

Hallsworth, C. R., and Knox, R. W. O'B., 1999, BGS rock classification scheme, v. 3, Classification of sediments and sedimentary rocks: British Geological Survey Research Report 99-03, 44 p.

Harris, B.L., 1973, Genesis, mineralogy, and properties of Parkdale Soils, Oregon: Corvallis, Oregon Oregon State University, Ph.D. thesis, 174 p.

Hildreth, W., 2007, Quaternary magmatism in the Cascades—Geologic perspectives: U.S. Geological Survey Professional Paper 1744, 125 p.

Hooper, P.R., 2000, Chemical discrimination of Columbia River Basalt flows: Geochemistry, Geophysics, and Geosystems, v. 1, no. 1, p. 1-14.

Hull, D.A., investigator, and Riccio, J.F., eds., 1979, Geothermal resource assessment of Mount Hood: Oregon Department of Geology and Mineral Industries Open-File Report O-79-8, 273 p. https://www.oregongeology.org/pubs/ofr/p-OFR.htm

Johnson, A.K., 2011, Dextral shear and north-directed crustal shortening defines the transition between extensional and contractional provinces in north-central Oregon: Corvallis, Oregon State University, M.S. thesis, 77 p., 3 plates, scale 1:24,000. https://ir.library.oregonstate.edu/concern/graduate_thesis_or_dissertations/c534ft276

Johnson, D. M., Hooper, P.R., and Conrey, R. M., 1999, XRF analysis of rocks and minerals for major and trace elements on a single low dilution Li-tetraborate fused bead: Advances in X-ray Analysis, v. 41, p. 843-867. https://s3.wp.wsu.edu/uploads/sites/2191/2017/06/Johnson-Hooper-and-Conrey.pdf

Kasbohm, J., and Schoene, B., 2018, Rapid eruption of the Columbia River flood basalt and correlation with mid-Miocene climate optimum; Science Advances v. 4, no. 9. https://advances.sciencemag.org/content/4/9/eaat8223

Keith, T.E.C., Donnelly-Nolan, J.M., Markman, J.L., and Beeson, M.H., 1985, K-Ar ages of rocks in the Mount Hood area, Oregon: Isochron/West, no. 42, p. 12–16.

Korosec, M.A., 1987, Geologic map of the Hood River quadrangle, Washington and Oregon: Washington Division of Geology and Earth Resources Open File Report 87-6, 41 p., 1 plate, scale 1:100,000. https://ngmdb.usgs.gov/Prodesc/proddesc_30784.htm

Le Bas, M.J., and Streckeisen, A.L., 1991, The IUGS systematics of igneous rocks: London, Journal of the Geological Society, v. 148, p. 825-833.

Le Bas, M.J., Le Maitre, R.W., Streckeisen, A., and Zanettin, B., 1986, A chemical classification of volcanic rocks based on the total alkali-silica diagram: Journal of Petrology, v. 27, part 3, p. 745–750.

Le Maitre, R. W., Bateman, P., Dudek, A., Keller, J., Lemeyre, J., Le Bas, M. J., Sabine, P. A., Schmid, R., Sorenson, H., Streckeisen, A., Wooley, A. R., and Zanettin, B., 1989, A classification of igneous rocks and glossary of terms: Oxford, Blackwell, 193 p.

Le Maitre, R.W. (ed.), Streckeisen, A., Zanettin, B., Le Bas, M.J., Bonin, B., Bateman, P., Bellieni, G., Dudek, A., Efremova, S., Keller, J., Lameyre, J., Sabine, P.A., Schmid, R., Sørensen, H., and Woolley, A.R., 2004, Igneous Rocks: A classification and glossary of terms: Recommendations of the International Union of Geological Sciences, Subcommission on the Systematics of Igneous Rocks, Cambridge University Press, United Kingdom,

Lite, K.E., and Grondin, G.H., 1988, Hydrogeology of the basalt aquifers near Mosier, Oregon: A ground water resource assessment: Oregon Water Resources Department Ground Water Report 33, 119 p., 5 plates, scale 1:24,000. https://www.oregon.gov/owrd/wrdreports/GW_Reports_No_33_1988.pdf

Luttrell, G.W., Hubert, M.L., and Murdock, C.R., 1991, Lexicon of New Formal Geologic Names of the United States 1981-1985: U.S. Geological Survey Bulletin 1565, 376 p. https://pubs.er.usgs.gov/publication/b1565

Lux, D.R., 1982, K-Ar and $^{40}Ar/^{39}Ar$ ages of mid-Tertiary volcanic rocks from the West Cascades Range, Oregon: Isochron/West, no. 33, p. 27–32.

Mackenzie, W.S., Donaldson, C.H., and Guilford, C., 1997, Atlas of igneous rocks and their textures: Addison Wesley Longman Limited, seventh edition, 148 p.

Mackin, J.H., 1961, A stratigraphic section in the Yakima Basalt and Ellensburg Formation in south-central Washington: Washington Division of Mines and Geology Report of Investigations, v. 19, 45 p.

Madin, I.P., and Ma, L., 2012, The Blue Ridge Fault, a newly discovered Holocene fault near Mt. Hood, Oregon: Seismological Research Letters, v. 83, no. 2, p. 374.

Madin, I.P., and McClaughry, J.D., 2019, Geologic map of the Biggs Junction and Rufus 7.5' quadrangles, Wasco and Sherman Counties, Oregon: Oregon Department of Geology and Mineral Industries Geological Map Series GMS 124, 105 p., 1 plate, scale 1:24,000, Esri format geodatabase; shapefiles, metadata; spreadsheet (4 sheets). https://www.oregongeology.org/pubs/gms/p-GMS-124.htm

Madin, I.P., Streig, A.R., Burns, W.J., and Ma, L., 2017, The Mount Hood Fault Zone–Late Quaternary and Holocene Fault Features Newly Mapped with High Resolution Lidar Imagery: U.S. Geological Survey Scientific Investigations Report 2017-5022-G, p. 99-109. https://pubs.er.usgs.gov/publication/sir20175022G

Martin, B.S., Tolan, T,L., and Reidel, S.P., 2013, Revisions to the stratigraphy and distribution of the Frenchman Springs Member, Wanapum Basalt, *in* Reidel, S.P., Camp, V.E., Martin, M.E., Ross, M.E., Wolff, J.A., Martin, B.S., Tolan, T.L., and Wells, R.E., eds., Geological Society of America Special Paper 497, p. 155-180.

McClaughry, J. D., Wiley, T. J., Ferns, M. L., and Madin, I. P., 2010, Digital geologic map of the southern Willamette Valley, Benton, Lane, Linn, Marion, and Polk counties, Oregon: Oregon Department of Geology and Mineral Industries Open-File Report O-2010-03, 116 p., 1 sheet, scale 1:63,360, GIS files.

McClaughry, J.D., Wiley, T.J., Conrey, R.C., Jones, C.B., and Lite, K.E., 2012, Digital geologic map of the Hood River Valley, Hood River and Wasco counties, Oregon: Oregon Department of Geology and Mineral Industries Open-File Report O-12-03, 142 p., 1 plate, scale 1:36,000, Esri ArcGIS geodatabase, GIS files, spreadsheets. https://www.oregongeology.org/pubs/ofr/p-O-12-03.htm

McClaughry, J.D., Herinckx, H.H., Niewendorp, C.A., Duda, C.J.M., and Hackett, J.A., in press, Geology of the Dufur Area, Wasco County, Oregon: Oregon Department of Geology and Mineral Industries Geological Map Series GMS 127, 210 p., 3 plates, scale 1:24,000, Esri format geodatabases; shapefiles, metadata; spreadsheets (16 sheets).

McPhee, D.K., Langenheim, V.E., Wells, R.E., and Blakely, R.J., 2014, Tectonic evolution of the Tualatin basin, northwest Oregon, as revealed by inversion of gravity data: Geosphere, v. 10, no. 2, p. 264-275.

Nelson, A.R., Kelsey, H.M., and Witter, R.C., 2006, Great earthquakes of variable magnitude at the Cascadia subduction zone: Quaternary Research, v. 65, p. 354–365. https://geology.humboldt.edu/documents/kelsey/Nelson_etal_2006.pdf

Newcomb, R.C., 1966, Lithology and eastward extension of The Dalles Formation, Oregon and Washington: U.S. Geological Survey Professional Paper 550-D, p. 059-063. https://pubs.er.usgs.gov/publication/pp550D

Newcomb, R.C., 1969, Effect of tectonic structure on the occurrence of groundwater in the basalt of the Columbia River Group of The Dalles area, Oregon and Washington: U.S. Geological Survey Professional Paper 383-C, 33 p., 1 plate, scale 1:62,500. https://pubs.er.usgs.gov/publication/pp383C

NOAA National Centers for Environmental Information, 2020, Data Tools: 1981-2010 Normals: https://www.ncdc.noaa.gov/cdo-web/datatools/normals

Ogg, J.G., Ogg, G., and Gradstein, F.M. (2008). Concise Geologic Time Scale. Cambridge, University Press, 177 p.

Peck, D.L., Griggs, A.B., Schlicker, H.G., Wells, F.G., and Dole, H.M., 1964, Geology of the central and northern parts of the Western Cascade Range in Oregon: U.S. Geological Survey Professional Paper 449, 56 p, 1 pl., scale 1:250,000. https://pubs.er.usgs.gov/publication/pp449

Phillips, W.M., Korosec, M.A., Schasse, H.W., Anderson, J.L., Hagen, R.A., 1986, K-Ar ages of volcanic rocks in southwest Washington: Isochron/West, v. 47, p. 18–24.

Pierson, T.C., Pringle, P.T., and Cameron, K.A., 2011, Magnitude and timing of downstream channel aggradation and degradation in response to a dome-building eruption at Mount Hood, Oregon: Geological Society of America Bulletin, v. 123, p. 3–20, doi: 10.11 30/B30127.1.

Piper, A.M., 1932, Geology and ground-water resources of The Dalles region, Oregon: U.S. Geological Survey Water-Supply Paper 659-B, p. 107–189, 2 pl., scale 1:62,500. https://pubs.er.usgs.gov/publication/wsp659B

Powell, J.E., 1982, Geology of the Columbia Hills, Klickitat County, Washington: Moscow, University of Idaho M.S. thesis, 56 p, 4 pl.

Powell, L.V., 1978, The structure, stratigraphy, and correlation of Grande Ronde Basalt on Tygh Ridge, Wasco County, Oregon: Moscow, University of Idaho, M.S. thesis, 57 p.

Priest, G.R., 1990, Volcanic and tectonic evolution of the Cascade volcanic arc, central Oregon: Journal of Geophysical Research, v. 95, no. B12, p. 19,583–19,599.

Priest, G.R., Woller, N.M., Black, G.L., and Evans, S.H., 1983, Overview of the geology of the central Oregon Cascade Range, *in* Priest, G.R., and Vogt, B.F., eds., Geology and geothermal resources of the central Oregon Cascade Range: Oregon Department of Geology and Mineral Industries Special Paper 15, 123 p., 3 pl., 1:24,000, 1:62,500. https://www.oregongeology.org/pubs/sp/p-SP.htm

Reidel, S.P., and Campbell, N.P., 1989, Structure of the Yakima Fold Belt, Central Washington, *in* Joseph, N.L. and others eds., Geologic guidebook for Washington and adjacent areas: Washington Division of Geology and Earth Resources Information Circular 86, p. 275-303.

Reidel, S.P., and Tolan, T.L., 2013, Grande Ronde Basalt, Columbia River Basalt Group, *in* Reidel, S.P., Camp, V.E., Martin, M.E., Ross, M.E., Wolff, J.A., Martin, B.S., Tolan, T.L., and Wells, R.E., eds., Geological Society of America Special Paper 497, p. 117-154, doi:10.1130/2013.2497(05).

Reidel, S.P., Tolan, T.L., Hooper, P.R., Beeson, M.H., Fecht, K.R., Bentley, R.D., and Anderson, J.L., 1989, The Grande Ronde Basalt, CRBG; Stratigraphic descriptions and correlations in Washington, Oregon, and Idaho, *in* Reidel, S. P., and Hooper, P. R., eds., Volcanism and tectonism in the Columbia River Flood-Basalt Province: Geological Society of America Special Paper 239, p. 21–53.

Reidel, S.P., Camp, V.E., Tolan, T,L., and Martin, B.S., 2013, The Columbia River flood basalt province: Stratigraphy, aerial extent, volume, and physical volcanology, *in* Reidel, S.P., Camp, V.E., Martin, M.E., Ross, M.E., Wolff, J.A., Martin, B.S., Tolan, T.L., and Wells, R.E., eds., Geological Society of America Special Paper 497, p. 1-43, doi:10.1130/2013.2497(01).

Robertson, S., 1999, BGS rock classification scheme, v. 2, Classification of metamorphic rocks: British Geological Survey Research Report 99-02, 24 p.

Ross, M.E., 1978, Stratigraphy, structure, and petrology of Columbia River Basalt in a portion of the Grande Ronde River –Blue Mountains area of Oregon and Washington: Moscow, University of Idaho, Ph.D. Dissertation, 407 p.

Scott, W.E., 1977, Quaternary glaciation and volcanism, Metolius River area, Oregon: Geological Society of America Bulletin, v. 88, p. 113-124.

Scott, W.E., and Gardner, C.A., 2017, Field-trip guide to Mount Hood, Oregon, highlighting eruptive history and hazards: U.S. Geological Survey Scientific Investigations Report 2017-5022-G, 115 p. https://pubs.er.usgs.gov/publication/sir20175022G

Scott, W.E., Gardner, C.A., Tilling, R.A., and Lanphere, M.A., 2003, Geologic history of Mount Hood volcano, Oregon—A field trip guidebook: State of the Arc Conference (SOTA), Timberline Lodge August 16–20, 40 p. http://wpg.forestry.oregonstate.edu/sites/wpg/files/seminars/mt-hood-field-guide-complete.pdf

Scott, W.E., Gardner, C.A., Sherrod, D.R., Tilling, R.I., Lanphere, M.A., and Conrey, R.M., 1997a, Geologic history of Mount Hood Volcano, Oregon; a field-trip guidebook: U.S. Geological Survey Open-File Report 97-263, 38 p. https://pubs.usgs.gov/of/1997/0263/report.pdf

Scott, W.E., Pierson, T.C., Schilling, S.P., Costa, J.E., Gardner, C.A., Vallance, J.W., and Major, J.J., 1997b, Volcano hazards in the Mount Hood region, Oregon: U.S. Geological Survey Open-File Report 97-89, 14 p. https://pubs.usgs.gov/of/1997/0089/

Shearer, K.J., 2002, The petrogenesis of the andesites in the Badger Creek Wilderness, Mount Hood, Oregon: St. Andrews, Scotland, University of St. Andrews, B.S. thesis, 71 p.

Sherrod, D.R., 2019, Cascade Mountain Range in Oregon (essay): The Oregon Encyclopedia, https://oregonencyclopedia.org/articles/cascade_mountain_range/#.XuAE3UVKhaR

Sherrod, D. R., and Pickthorn, L. G., 1989, Some notes on the Neogene structural evolution of the Cascade Range in Oregon, *in* Muffler, L. J. P., Weaver, C. S., and Blackwell, D. D., eds., Geology, geophysics, and tectonic setting of the Cascade Range: U.S. Geological Survey Open-File Report 89-178, p. 351–368.

Sherrod, D.R., and Scott, W.E., 1995, Preliminary geologic map of the Mount Hood 30- by 60-minute quadrangle, Northern Cascade Range, Oregon: U.S. Geological Survey Open-File Report 95-219, 36 p., scale 1:100,000. https://pubs.usgs.gov/of/1995/of95-219/

Sherrod, D.R., and Smith, J.G., 2000, Geologic map of upper Eocene to Holocene volcanic and related rocks of the Cascade Range, Oregon: U.S. Geological Survey Map I-2569, 17 p., 2 plates, scale 1:500,000. https://pubs.usgs.gov/imap/i-2569/

Smith, G.A., and Taylor, E.M., 1983, The central Oregon High Cascade graben: What? Where? When?: Geothermal Resources Council Transactions, v. 7, p. 275–279.

Smith, G.A., Snee, L.W., and Taylor, E.M., 1987, Stratigraphic, sedimentologic, and petrologic record of late Miocene subsidence of the central Oregon High Cascades: Geology, v. 15, p. 389–392.

Smith, R.A., and Roe, W.P., compilers, 2015, Oregon Geologic Data Compilation [OGDC], release 6 (statewide): Oregon Department of Geology and Mineral Industries Digital Data Series OGDC-6, Esri geodatabase. https://www.oregongeology.org/pubs/dds/p-OGDC-6.htm

Swanson, D.A., Wright, T.L., Hooper, P.R., and Bentley, R.D., 1979, Revisions in stratigraphic nomenclature of the CRBG. U.S. Geological Survey Bulletin 1457-G, 59 p., 1 pl. https://pubs.er.usgs.gov/publication/b1457G

Swanson, D. A., Anderson, J. A., Camp, V. E., Hooper, P. R., Taubeneck, W. H., and Wright, T. L., 1981, Reconnaissance geologic map of the Columbia River Basalt Group, Northern Oregon and Western Idaho: U.S. Geological Survey Open-File Report 81-797, 35 p., 6 pl., scale 1:250,000. https://pubs.er.usgs.gov/publication/ofr81797

Taggart, J.E., 2002, Analytical methods for chemical analysis of geologic and other materials, U.S. Geological Survey: U.S. Geological Survey Open-File Report 02-223, https://pubs.usgs.gov/of/2002/ofr-02-0223/.

Taylor, E.M., 1981, Central High Cascade roadside geology – Bend, Sisters, McKenzie Pass, and Santiam Pass, Oregon, *in* Johnston, D.A., and Donnelly-Nolan, J., eds., Guides to some volcanic terranes in Washington, Idaho, Oregon, and northern California: U.S Geological Survey Circular 838, p. 55–83. https://pubs.er.usgs.gov/publication/cir838

Thouret, J.-C., 2005, The stratigraphy, depositional processes, and environment of the late Pleistocene Polallie-period deposits at Mount Hood volcano, Oregon, USA: Geomorphology, v. 70, p. 12–32, doi:10.1016/j.geomorph.2005.03.008

Tolan, T.L., and Beeson, M.H., 1984, Intracanyon flows of the CRBG in the lower Columbia River Gorge and their relationship to the Troutdale Formation: Geological Society of America Bulletin, v. 95, no. 4, p. 463–477.

Tolan, T.L., and Reidel, S.P., compilers, 1989, Structure map of a portion the Columbia-River Flood-Basalt Province, *in* Reidel, S.P., and Hooper, P. R., eds., Volcanism and tectonism in the Columbia River Flood-Basalt Province: Geological Society of America Special Paper 239, scale 1:576,000, 1 plate.

Tolan, T.L., Reidel, S.P., Beeson, M.H., Anderson, J.L., Fecht, K.R., and Swanson, D.A., 1989, Revisions to the estimates of the areal extent and volume of the Columbia River Basalt Group, *in* Reidel, S. P., and Hooper, P. R., eds., Volcanism and tectonism in the Columbia River Flood-Basalt Province: Geological Society of America Special Paper 239, p. 1–20.

Tolan, T.L., Martin, B.S., Reidel Tolan, T.L., Martin, B.S., Reidel, S.P., Anderson, J.L., Lindsey, K.A., and Burt, W., 2009a, An introduction to the stratigraphy, structural geology, and hydrogeology of the Columbia River flood-basalt province: A primer for the GSA CRBG field trips, *in* O'Connor, J. E., Dorsey, R. J., and Madin, I. P., eds., Volcanoes to vineyards: Geologic field trips through the dynamic landscape of the Pacific Northwest: Geological Society of America Field Guide 15, p. 599–643, doi: 10.1130/2009.fl d015(28).

Tolan, T.L., Martin, B.S., Reidel, S.P., Kauffman, J.D., Garwood, D.L., and Anderson, J.L., 2009b, Stratigraphy and tectonics of the central and eastern portions of the Columbia River Flood-Basalt Province: An overview of our current state of knowledge, *in* O'Connor, J. E., Dorsey, R. J., and Madin, I. P., eds., Volcanoes to Vineyards: Geologic field trips through the dynamic landscape of the Pacific Northwest: Geological Society of America Field Guide 15, p. 645–672, doi: 10.1130/2009.fl d015(29).

U.S. Geological Survey National Cooperative Geologic Mapping Program, 2020, GeMS (Geologic Map Schema)—A standard format for the digital publication of geologic maps: U.S. Geological Survey Techniques and Methods, book 11, chap. B10, 74 p., https://doi.org//10.3133/tm11B10.

Vallance, J.W., 1999, Postglacial lahars and potential hazards in the White Salmon River system on the southwest flank of Mount Adams, Washington: U.S. Geological Survey Bulletin 2161, 49 p.

Venkatakrishnan, R., Bond, J. G., and Kauffman, J. D., 1980, Geological linears of the northern part of the Cascade Range, Oregon: Oregon Department of Geology and Mineral Industries, Special Paper 12, 25 p., 5 pls., scale 1:250,000.

Verplanck, E.P., and Duncan, R.A., 1987, Temporal variations in plate convergence and eruption rates in the Western Cascades Oregon: Tectonics, v. 6, p. 197–209.

Vogt, B.F., 1981, The stratigraphy and structure of the CRBG in the Bull Run Watershed, Oregon: Portland, Portland State University, M.S. thesis, 151 p.

Waters, A.C., 1968, Reconnaissance geologic map of the Dufur quadrangle, Hood River, Sherman, and Wasco Counties, Oregon: U.S. Geological Survey Miscellaneous Geologic Investigations Map I-556, scale 1:125,000. https://pubs.er.usgs.gov/publication/i556

Watters, T.R., 1989, Periodically spaced anticlines of the Columbia Plateau, *in* Reidel, S.P., and Hooper, P.R., eds., Volcanism and tectonism in the Columbia River flood-basalt province: Geological Society of America Special Paper 239, p. 283–292.

Wells, R.E., Simpson, R.W., Bentley, R.D., Beeson, M.H., Mangan, M.T., and Wright, T.L., 1989, Correlation of Miocene flows of the CRBG from the central Columbia River Plateau to the coast of Oregon and Washington, *in* Reidel, S. P., and Hooper, P. R., eds., Volcanism and tectonism in the Columbia River Flood-Basalt Province: Geological Society of America Special Paper 239, p. 113–129.

Wells, R.E., Niem, A.R., Evarts, R.C., and Hagstrum, J.T., 2009, The CRBG –From the Gorge to the sea, *in* O'Connor, J.E., Dorsey, R.J., and Madin, I.P., eds., Volcanoes to vineyards: Geologic field trips through the dynamic landscape of the Pacific Northwest: Geological Society of America Field Guide 15, p. 737–774, doi: 10.1130/2009.fl d015(32).

Wentworth, C.K., 1922, A scale of grade and class terms of clastic sediments: Journal of Geology, v. 30, p. 377–392.

Westby, E.G., 2014, The geology and petrology of enigmatic rhyolites at Graveyard and Gordon Buttes, Mount Hood quadrangle, Oregon: Portland, Portland State University, M.S. thesis, 138 p. https://pdxscholar.library.pdx.edu/open_access_etds/2063/

Williams, D.L., Hull, D.A., Ackerman, H.D., and Beeson, M.H., 1982, The Mount Hood region: Volcanic history, structure, and geothermal potential: Journal of Geophysical Research, v. 87, p. 2767–2781.

Wise, W.S., 1969, Geology and petrology of the Mt. Hood area: A study of High Cascade volcanism: Geological Society of America Bulletin, v. 80, no. 6, p. 969–1006.

Wright, T.L., Maurice, J.G., and Swanson, D.A., 1973, Chemical variation related to the stratigraphy of the Columbia River Basalt: Geological Society of America Bulletin, v. 84, p. 371–386.

Wu, J.E., McClay, K., Whitehorse, P., and Dooley, T., 2009, 4D analogue modeling of transtensional pull-apart basins: Marine and Petroleum Geology, v. 26, p. 1608–1623.

Zakšek, K., Oštir, K., and Kokalj, Ž., 2011, Sky-View Factor as a relief visualization technique: Remote Sensing, v. 3, p. 398–415.

10.0 APPENDIX

This Appendix contains a summary of the geodatabase along with a description of analytical and field methods and the list of attribute fields for spreadsheets (see page iii of this report). The Appendix is divided into two sections:

- Section 10.1 describes the digital databases included with this publication.
- Section 10.2 contains a summary of analytical and field methods. Accompanying tables explain the fields listed in various spreadsheets.

10.1 Geographic Information Systems (GIS) Database

Geodatabase specifications

Digital data created for the Dog River–Badger Lake area is stored in an Esri format geodatabase. The geodatabase structure follows that outlined by the U.S. Geological Survey (USGS) Geologic Map Schema (GeMS), version 2.7 (U.S. Geological Survey National Cooperative Geologic Mapping Program, 2020). The following information describes the overall database structure, the feature classes, and supplemental tables (**Figure 10-1**, **Figure 10-2**, **Figure 10-3**, **Table 10-1**, **Table 10-2**).

The data are stored in a file geodatabase feature dataset (GeologicMap). Accessory file geodatabase tables (DataSources, DescriptionOfMapUnits, GeoMaterialDict, and Glossary) were created by using ArcGIS version 10.7 (SP 1). The GeologicMap feature dataset contains all the spatially oriented data (feature classes) created for the Dog River and northern part of the Badger Lake 7.5′ quadrangles. The file geodatabase tables are used to hold additional geologic attributes. Additional information and complete descriptions of the "GeMS" — Geologic Map Schema (formerly "NCGMP09") can be found at https://ngmdb.usgs.gov/Info/standards/GeMS/#docs.

Figure 10-1. Dog River–Badger Lake area geodatabase feature datasets and data tables.

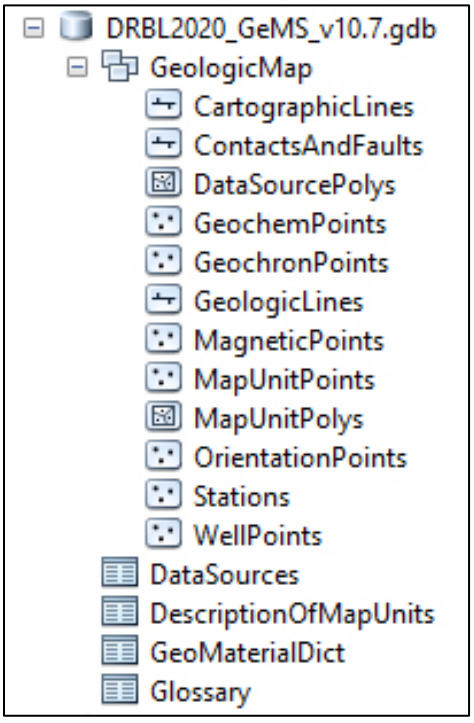

Geodatabase feature class specifications

Each feature class within the GeologicMap feature dataset in the geodatabase contains detailed metadata. Please see the embedded metadata for detailed information such as process descriptions, accuracy specifications, and entity attribute descriptions.

Figure 10-2. Dog River–Badger Lake area geodatabase feature classes.

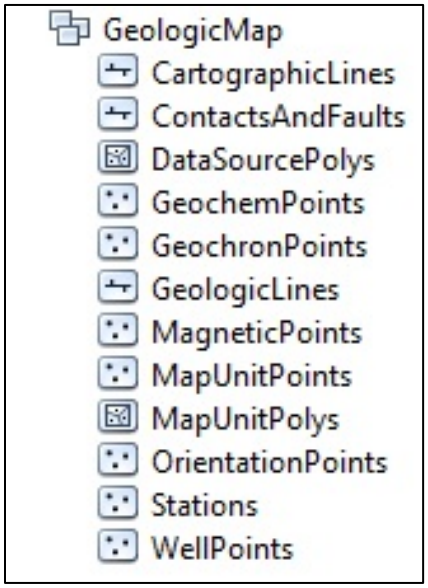

Table 10-1. Feature Class description.

Name	Description
CartographicLines	Vector lines that have no real-world physical existence and do not participate in map-unit topology. The feature class includes cross section lines used for cartography for the quadrangle.
ContactsAndFaults	The vector lines in this feature class contain geologic content including contacts and fault locations used to create the map unit polygon boundaries. The existence and location confidence values for the contacts and faults are provided in the feature class attribute table.
DataSourcePolys	This feature class contains polygons that delineate data sources for all parts of the geologic map. These sources may be a previously published map, new mapping, or mapping with a certain technique. For a map with one data source, for example all new mapping, this feature class contains one polygon that encompasses the map area.
GeochemPoints	This feature class represents point locations where whole-rock samples have been analyzed by X-ray fluorescence (XRF) techniques in the quadrangle. Includes data collected by the authors during this study or compiled from previous studies. These data are also contained in the geochemistry spreadsheet described in more detail below.
GeochronPoints	This feature class represents point locations where $^{40}Ar/^{39}Ar$ isotopic ages have been obtained for rock samples in the map area. Data collected by the authors or compiled during the course of this study. These data are also contained in the geochronology spreadsheet described in more detail below.
GeologicLines	These vector lines represent known fold axis locations in the quadrangle. The existence and location confidence for the fold axes are provided in the feature class attribute table.
MagneticPoints	This feature class represents point locations where measurements of natural remanent magnetization have been obtained for strongly magnetized lavas. Includes data collected by the authors during the course of this study. These data are also contained in the magnetic polarity database described in more detail below.
MapUnitPoints	This feature class represents points used to generate the MapUnitPolys feature class from the ContactsAndFaults feature class.
MapUnitPolys	This polygon feature class represents the geologic map units as defined by the authors.
OrientationPoints	This feature class represents point locations in the quadrangle where structural measurements were made or were compiled from previous studies. These data are also contained in the bedding (strike and dip) spreadsheet described in more detail below.
Stations	This feature class represents point locations in the quadrangle where direct field observations were made or were compiled from previous studies.
WellPoints	This feature class represents point locations of water wells in the quadrangle. Includes data obtained by the authors from the Oregon Department of Water Resources (OWRD). These data are also contained in the Wells Points spreadsheet described in more detail below.

Geodatabase table specifications

Figure 10-3. Dog River–Badger Lake area geodatabase data tables.

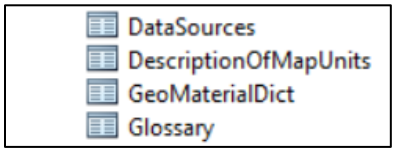

Table Name Description

Table 10-2. Geodatabase tables

Name	Description
DataSources	Data table that contains information about data sources used to compile the geology of the area.
DescriptionOfMapUnits	Data table that captures the content of the Description of Map Units (DMU), or equivalent List of Map Units and associated pamphlet text, included in a geologic map.
GeoMaterialDict	Data table providing definitions and hierarchy for GeoMaterial names prescribed by the GeMS database schema.
Glossary	Data table that contains information about the definitions of terms used in the geodatabase.

Geodatabase Projection Specifications

All spatial data are stored in the Oregon Statewide Lambert Conformal Conic projection. The datum is NAD83 HARN. The linear unit is international feet. See detailed projection parameters below:

Projection: Lambert_Conformal_Conic
False_Easting: 1312335.958005
False_Northing: 0.0
Central_Meridian: -120.5
Standard_Parallel_1: 43.0
Standard_Parallel_2: 45.5
Latitude_Of_Origin: 41.75
Linear Unit: Foot (0.3048)

Geographic Coordinate System: GCS_North_American_1983_HARN
Angular Unit: Degree (0.0174532925199433)
Prime Meridian: Greenwich (0.0)
Datum: D_North_American_1983_HARN
Spheroid: GRS_1980
  Semimajor Axis: 6378137.0
  Semiminor Axis: 6356752.314140356
  Inverse Flattening: 298.257222101

Geologic map

This report is accompanied by a single map plate displaying the surficial and bedrock geology at a scale of 1:24,000 and geologic cross sections (see Plate 1 facsimile below) for the Dog River and northern part of the Badger Lake 7.5′ quadrangles. The map plate was generated from detailed geologic data (scale of 1:8,000 or better) contained in the accompanying Esri format geodatabase. Both bedrock and surficial geologic interpretations can be recovered from the geodatabase and can be used to create a variety of additional thematic maps.

Plate 1. Reproduction of the geologic map of the Dog River and northern part of the Badger Lake 7.5’ quadrangles, Hood River County, Oregon (Plate 1). Plate dimensions are 48 by 52 inches, scale 1;24,000. See digital folder for map plate.

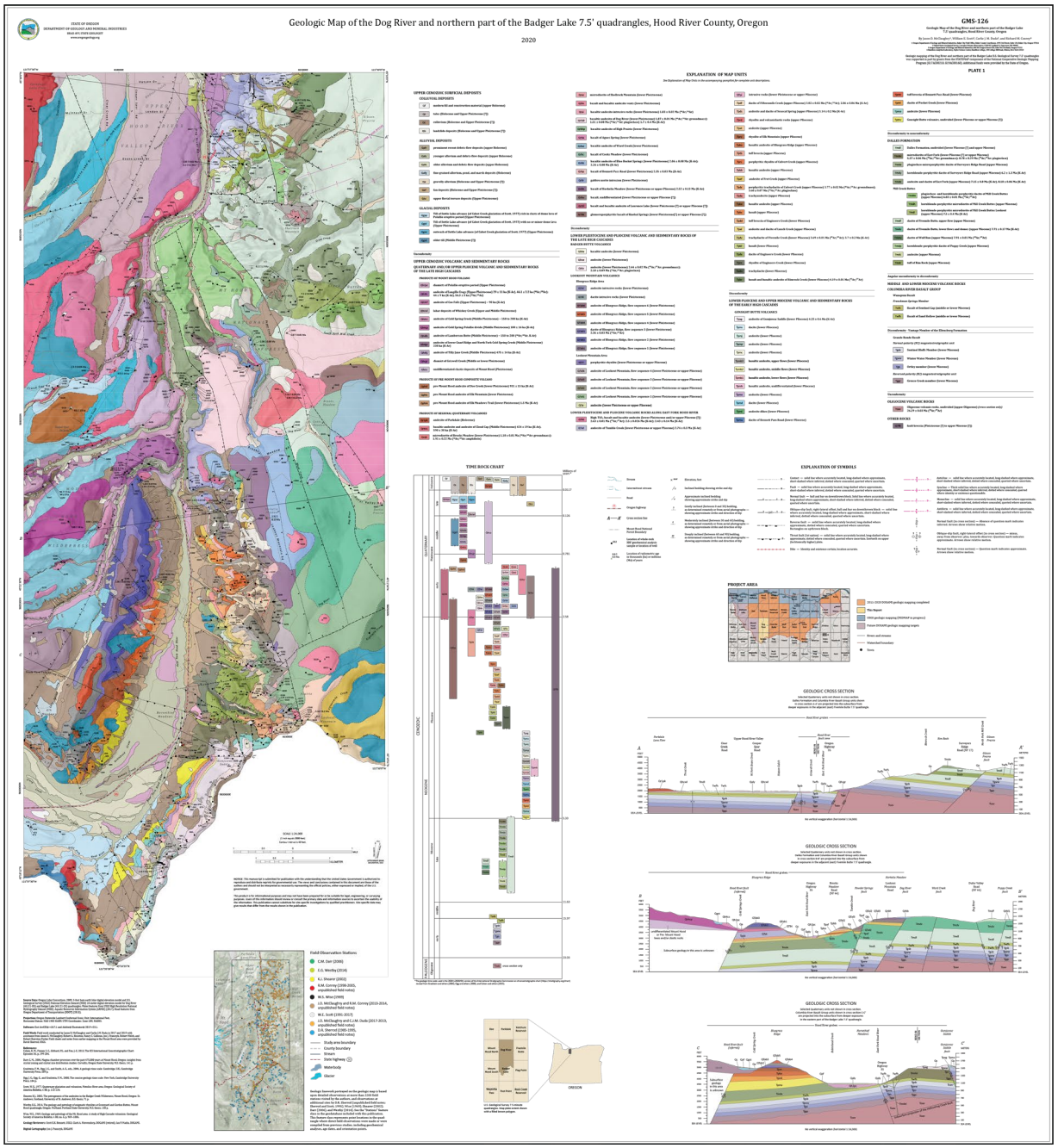

10.2 Methods

Geochemical analytical methods

Geologic mapping in the Dog River–Badger Lake area was supported by 705 X-ray fluorescence (XRF) geochemical analyses of whole-rock samples. Whole-rock geochemical samples were prepared and analyzed by XRF at the Washington State University GeoAnalytical Lab, Pullman, Washington, and at the USGS Geology, Geophysics, and Geochemistry Science Center, Denver, Colorado. Analytical procedures for the Washington State University GeoAnalytical Lab are described by Johnson and others (1999) and are available online at https://environment.wsu.edu/facilities/geoanalytical-lab/technical-notes/; USGS analytical procedures are described by Taggart (2002) and are available online at https://www.usgs.gov/energy-and-minerals/mineral-resources-program/science/analytical-chemistry?qt-science_center_objects=0#qt-science_center_objects. Samples denoted by lab abbreviation WSU were analyzed at the Washington State University; samples denoted by lab abbreviation USGS were analyzed at the U.S. Geological Survey. Descriptive rock unit names for igneous rocks are based on normalized major element analyses plotted on the total alkalis ($Na_2O + K_2O$) versus silica (SiO_2) diagram (TAS) of Le Bas and others (1986), Le Bas and Streckeisen (1991), and Le Maitre and others (1989, 2004). New and compiled XRF-geochemical analyses are included in the geodatabase, in a separate shapefile named DRBL2020_GeochemPoints, and in Microsoft Excel workbook DRBL2020_DATA.xls (sheet DRBL2020_GeochemPoints). **Table 10-3** describes the fields listed in the spreadsheet. The locations of all geochemical samples are given in five coordinate systems: UTM Zone 10 (datum = NAD 27, NAD 83, units = meters), Geographic (datum = NAD 27, NAD 83, units = decimal degrees), and Oregon Lambert (datum = NAD 83, HARN, units = international feet). Notes for spreadsheet: -9 equals no data for numerical fields for analytical data; nd equals no data in text fields; na equals information not applicable for text fields; samples shown with an "R" (e.g., 121 DRBLJ 19R) are a repeat analysis of a single sample.

Table 10-3. Geochemical database spreadsheet columns.

Field	Description
SAMPLE_NO	A unique number identifying the sample – e.g., 21 DRBLJ 19.
Type	The geochemical method used by laboratory that analyzed the sample – e.g., XRF, ICP-MS
FieldSampleID	Unique alpha-numeric id applied to the sample – e.g., 21 DRBLJ 19.
AlternateSampleID	Unique alpha-numeric id applied to the sample – e.g., 21 DRBLJ 19.
Symbol	References a symbol in the GeMS style file – e.g., 31.21.
Label	A unique number assigned to the sample for cartographic purposes – e.g., G1.
LocationConfidenceMeters	Radius in meters of positional uncertainty envelope for the observation locale. Null values not permitted. Recommended value is -9 if value is not otherwise available.
PlotAtScale	Cartographic map scale or larger that the observation or analysis should be plotted at. Value is scale denominator.
Quadrangle	The USGS 7.5' quadrangle in which the sample is located – e.g., Badger Lake.
Elevation	Elevation of data location in feet – e.g., 22.
MapUnit	Map unit from which the analyzed sample was collected – e.g., Tpdv.
MaterialAnalyzed	Type of material analyzed – e.g., whole rock.
TASLithology	Rock name assigned based on the total alkalis ($Na_2O + K_2O$) versus silica (SiO_2) diagram (TAS) of Le Bas and others (1986), Le Bas and Streckeisen (1991), and Le Maitre and others (1989) – e.g., basalt, rhyolite.
MajorElements	SiO_2, Al_2O_3, TiO_2, FeOTotal, MnO, CaO, MgO, K_2O, Na_2O, P_2O_5. In wt. percent.
TraceElements	Ni, Cr, Sc, V, Ba, Rb, Sr, Zr, Y, Nb, Ga, Cu, Zn, Pb, La, Ce, Th, Nd, U, Cs, Co, Hf, Sm, Eu, Yb, Lu. In ppm.
TotalInitial	Original analytical total as reported by the lab.
LossOnIgnition	Value for loss on ignition as reported by the laboratory.
FE2O3	Iron (III) oxide or ferric oxide reported in original analysis.
FeO	Iron (II) oxide or ferrous oxide reported in original analysis.
UTMNorthingNAD27	Meters north in NAD 27 UTM projection, zone 10.
UTMEastingNAD27	Meters east in NAD 27 UTM projection, zone 10.
LatitudeNAD27	Latitude in NAD 27 geographic coordinates.
LongitudeNAD27	Longitude in NAD 27 geographic coordinates.
UTMNorthingNAD83	Meters north in NAD 83 UTM projection, zone 10.
UTMEastingNAD83	Meters east in NAD 83 UTM projection, zone 10.
LatitudeNAD83	Latitude in NAD 83 geographic coordinates.
LongitudeNAD83	Longitude in NAD 83 geographic coordinates.
Northing83HARN	Feet north in Oregon Lambert NAD 83, HARN, international feet.
Easting83HARN	Feet east in Oregon Lambert NAD 83, HARN, international feet.
LocationSourceID	Unique data source from which the data was obtained – e.g., McClJD2020.
AnalysisSourceID	Foreign key to DataSources. Identifies source of analytical data for this sample. Null values not permitted – e.g., WSU.
Notes	Special information about certain samples – e.g., alteration.
GeochemPoints_ID	e.g., GCM01
NOTES	Special information about certain samples – e.g., alteration.

Geochronology

Forty-one isotopic ages are summarized in this report and map, including 16 new $^{40}Ar/^{39}Ar$ ages. Sample preparation and $^{40}Ar/^{39}Ar$ analysis was conducted by Dr. Dan Miggins at the College of Oceanic and Atmospheric Sciences, Oregon State University, Corvallis (OSU). The methodology for $^{40}Ar/^{39}Ar$ geochronology at OSU is summarized on the Web at http://geochronology.coas.oregonstate.edu/ and in Duncan and Keller (2004). One $^{40}Ar/^{39}Ar$ age was determined by Dr. Matt Heizler at the New Mexico Geochronological Research Laboratory (NMGRL) administered by the the New Mexico Bureau of Geology and Mineral Resources at the New Mexico Institute of Mining and Technology in Socorro, New Mexico. The general operational details for the NMGRL can be found at internet site https://geoinfo.nmt.edu/labs/argon/. Original data sheets for new $^{40}Ar/^{39}Ar$ isotopic ages are located in the Appendix. Our map also includes 8 K-Ar and $^{40}Ar/^{39}Ar$ ages of Pliocene and younger lavas, originally published by Scott and others (1997a) and Scott and Gardner (2017). Samples used for K-Ar ages reported by Scott and Gardner (2017) were prepared and analyzed at the U.S. Geological Survey (USGS) laboratory in Menlo Park, California, under the direction of Marvin Lanphere. A few of these samples have been re-dated by higher precision $^{40}Ar/^{39}Ar$ methods and were reported in Scott and Gardner (2017). Additional K-Ar ages in the map area have are compiled from Wise (1969), Hull and Riccio (1979), Bela (1982), P.E. Hammond in Fiebelkorn and others (1983), Keith and others (1985), Sherrod and Scott (1995), and Conrey and others (1996).

Geochronological data are included in the geodatabase, in a separate shapefile named DRBL2020_GeochronPoints, and in Microsoft Excel workbook DRBL2020_DATA.xls (sheet DRBL2020_GeochronPoints). **Table 10-4** describes the fields listed in the spreadsheet. The location of each isotopic age is given in five coordinate systems: UTM Zone 10 (datum = NAD 27, NAD 83, units = meters), Geographic (datum = NAD 27, NAD 83, units = decimal degrees), and Oregon Lambert (datum = NAD 83, HARN, units = international feet). Notes for spreadsheet: -9 equals no data for numerical fields for analytical data; nd equals no data in text fields; na equals information not applicable for text fields.

Table 10-4. Geochronology database spreadsheet columns.

Field	Description
SAMPLE_NO	Unique alpha-numeric id applied to the sample – e.g., 21 DRBLJ 19.
Type	The geochronological method – e.g., $^{40}Ar/^{39}Ar$, K-Ar, radiocarbon, mineral - whole-rock Rb-Sr isochron, etc.) used to estimate the age.
FieldSampleID	Unique alpha-numeric id applied to the sample – e.g., 21 DRBLJ 19.
AlternateSampleID	Unique alpha-numeric id applied to the sample – e.g., 21 DRBLJ 19.
MapUnit	Map unit from which the analyzed sample was collected.
Symbol	References a symbol in the GeMS style file.
Label	Isotopic age of sample with error – e.g., 3.69 ± 0.01 Ma
LocationConfidenceMeters	Radius in meters of positional uncertainty envelope for the observation locale. Null values not permitted. Recommended value is -9 if value is not otherwise available.
PlotAtScale	Cartographic map scale or larger that the observation or analysis should be plotted at. Value is scale denominator.
MaterialAnalyzed	Type of material analyzed – e.g., amphiboles, plagioclase.
NumericAge	Interpreted (preferred) age calculated from geochronological analysis, not necessarily the date calculated from a single set of measurements.
AgePlusError	Plus error in age determination in thousands of years.
AgeMinusError	Minus error in age determination in thousands of years.
AgeUnits	Values = years, Ma, ka, radiocarbon ka, calibrated ka, etc.
UTMNorthingNAD27	Meters north in NAD 27 UTM projection, zone 10.
UTMEastingNAD27	Meters east in NAD 27 UTM projection, zone 10.
LatitudeNAD27	Latitude in NAD 27 geographic coordinates.
LongitudeNAD27	Longitude in NAD 27 geographic coordinates.
UTMNorthingNAD83	Meters north in NAD 83 UTM projection, zone 10.
UTMEastingNAD83	Meters east in NAD 83 UTM projection, zone 10.
LatitudeNAD83	Latitude in NAD 83 geographic coordinates.
LongitudeNAD83	Longitude in NAD 83 geographic coordinates.
Northing83HARN	Feet north in Oregon Lambert NAD 83, HARN, international feet.
Easting83HARN	Feet east in Oregon Lambert NAD 83, HARN, international feet.
StationID	Foreign key to Stations point feature class.
LocationSourceID	Unique data source from which the data was obtained; e.g., McClJD2020.
AnalysisSourceID	Foreign key to DataSources. Identifies source of analytical data for this sample. Null values not permitted – e.g., OSU.
Notes	Special information about certain samples – e.g., alteration.
GeochronPoints_ID	e.g., GCR1

Natural remanent magnetization (magnetic polarity) methods

Field measurements of natural remanent magnetization (the magnetic field of a sample measured when induced magnetic fields are absent or zeroed out by probe; Butler, 1992) were determined from strongly magnetized lavas exposed in the map area during the course of this study in order to distinguish between flow units with normal and reversed magnetic polarity. Magnetic polarity also serves as a check on the permissible age of isotopically-dated samples, when compared to the paleomagnetic time scale of Cande and Kent (1992) (**Figure 10-4**). This method of constraining isotopic ages by magnetic polarity determinations is most effective when the analytical error is less than 0.20 m.y. Larger errors reported for isotopic ages may overlap so many polarity subchrons that no constraint is provided by knowing a samples magnetic polarity. Magnetic polarity values reported were determined using a MEDA, Inc. μMag handheld digital fluxgate magnetometer. The magnetics data are included in the geodatabase, a separate shapefile named DRBL2020_MagneticPoints, and are also provided in a Microsoft Excel workbook DRBL2020_DATA.xls (sheet – DRBL2020_MagneticPoints). **Table 10-5** explains the fields listed in the spreadsheet. The locations of these point data are given in five coordinate systems: UTM Zone 10 (datum = NAD 27, NAD 83, units = meters), Geographic (datum = NAD 27, NAD 83, units = decimal degrees), and Oregon Lambert (datum = NAD 83, HARN, units = international feet).

The natural remanent magnetization (magnetic polarity) of strongly magnetized lavas was determined using the following method:

1. A north-pointing arrow and near horizontal line were drawn on and around (to the extent possible) an approximately fist-sized equidimensional sample that was then removed from the outcrop (**Figure 10-4a).**
2. The magnetometer was placed on the most level ground available in a relatively magnetically clean area (**Figure 10-4b**). The probe was then placed in a fixed position in the horizontal plane and rotated to null the local magnetic field (μMag reads zero). This procedure was done incrementally beginning with minimum range sensitivity (2,000 mG [milliGauss]), increasing the sensitivity (20 mG) and re-rotating the probe until maximum sensitivity was reached. Magnetic polarity was then checked with the north end of a locked compass needle. Total field value will decrease when the compass needle is moved horizontally toward and remains parallel to the probe.
3. The polarity of a sample was determined by placing the oriented sample in a path parallel to the probe. The north-verging line drawn to represent the approximate magnetic pole of the sample was held horizontally (approximately) with the north end facing toward the probe at a distance of at least 10 times farther than the measurement distance. A reading was then determined with the sample absent from the probe. The sample was then moved to a point (typically within 1 to 2 cm) toward the probe in order to cause a change of at least several times greater than the minimum resolution of the magnetometer (**Table 10-5).** A decrease in the total field value indicated normal-polarity (N); an increase in total field value indicated reversed-polarity (R).
4. The sample was then rotated backward (top away from the probe) about a horizontal axis approximately 45° to see if field strength increased as the sample's inclined magnetic field was rotated into parallel with the probe.
5. The polarity of two to ten representative samples from different portions of an outcrop or from different outcrops was determined to verify the repeatability of results. Erratic results, due to re-magnetization resulting from lighting strikes, obscure post-emplacement alteration, or aberrant declination and inclination are reported as indeterminate (I).

Figure 10-4. Procedure for determining natural remanent magnetism of lavas. (a) Ideal sample is selected and oriented in outcrop. North arrow is drawn on upper surface; horizontal lines are drawn around the exposed edges of the sample. Fist-sized sample is then removed. (b) Magnetometer probe is placed in a fixed position in the horizontal plane and rotated to null the local magnetic field. Sample polarity is determined by moving the oriented sample into the path of the probe.

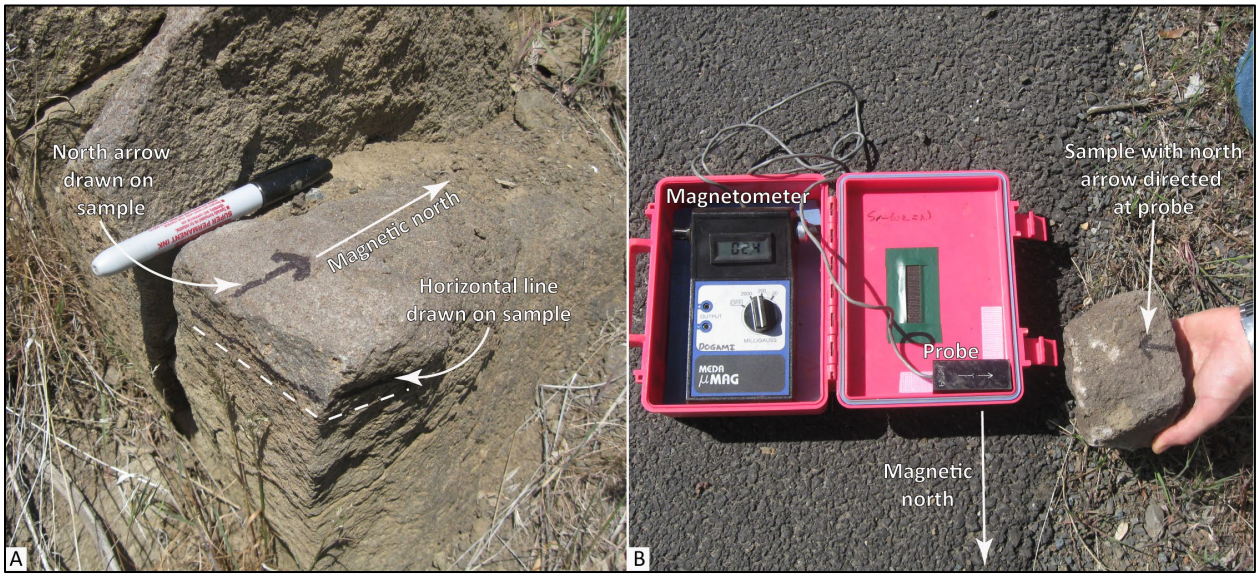

Table 10-5. Magnetic polarity database spreadsheet columns.

Field	Description
Type	The method of measurement – e.g., Digital Portable Fluxgate
FieldSampleID	Unique alpha-numeric id applied to the sample – e.g., 21 DRBLJ 19.
NaturalRemanentMagnetization	Natural remanent magnetization of sample as determined from a portable fluxgate magnetometer. Normal, reversed, indeterminate.
MapUnit	Map unit from which the analyzed sample was collected.
Symbol	References a symbol in the GeMS style file.
Label	<Null>
LocationConfidenceMeters	Radius in meters of positional uncertainty envelope for the observation locale. Null values not permitted. Recommended value is -9 if value is not otherwise available.
PlotAtScale	Cartographic map scale or larger that the observation or analysis should be plotted at. Value is scale denominator.
Quadrangle	The USGS 7.5' quadrangle in which the sample is located – e.g., Badger Lake.
Elevation	Elevation of sample location in feet – e.g., 1928.
UTMNorthingNAD27	Meters north in NAD 27 UTM projection, zone 10.
UTMEastingNAD27	Meters east in NAD 27 UTM projection, zone 10.
LatitudeNAD27	Latitude in NAD 27 geographic coordinates.
LongitudeNAD27	Longitude in NAD 27 geographic coordinates.
UTMNorthingNAD83	Meters north in NAD 83 UTM projection, zone 10.
UTMEastingNAD83	Meters east in NAD 83 UTM projection, zone 10.
LatitudeNAD83	Latitude in NAD 83 geographic coordinates.
LongitudeNAD83	Longitude in NAD 83 geographic coordinates.
Northing83HARN	Feet north in Oregon Lambert NAD 83, HARN, international feet.
Easting83HARN	Feet east in Oregon Lambert NAD 83, HARN, international feet.
LocationSourceID	Unique data source from which the data was obtained; e.g., McClJD2020.
AnalysisSourceID	Foreign key to DataSources. Identifies source of analytical data for this sample. Null values not permitted – e.g., OSU.
Notes	Special information about certain samples – e.g., alteration.
MagneticPoints_ID	e.g., MGP001

Orientation Points

Orientation measurements of inclined bedding and igneous foliation were taken in the Dog River–Badger Lake area during the course of this study by traditional compass and clinometer methods. Additional structural measurements were determined from interpretation of lidar imagery. DOGAMI has developed a routine and model in Esri ArcGIS™ Model Builder to calculate three-point solutions for lidar-derived bedding. The modeling process incorporates the use of 1) a 1-m lidar-derived DEM (digital elevation model); 2) the registration of three non-collinear points picked along the trace of a geological plane or contact discernable from a 1-m lidar DEM; 3) updating these points with their lidar-derived elevation values; and 4) creating a TIN (triangular irregular network) facet of the three points. The aspect of the TIN facet is equivalent to the dip direction, and the slope corresponds to the dip (0 to 90 degrees). The strike is then determined from the dip direction, subtracting or adding 90 degrees on the basis of the right-hand rule (described in below).

The factors influencing the certainty of lidar-derived bedding are the subjectivity of the digitizer and the clarity of the feature presumed to be indicative of bedding. To improve the clarity of lidar visualization, lidar-derived bedding was compiled using both a hillshade and slopeshade image, each at 50 percent transparency, draped over a Sky-View Factor (SVF) image. Sky-View Factor images are enhanced 1-m lidar DEMs, processed using the Sky-View Factor computation tool. The Sky-View Factor computation tool is part of the Relief Visualization Toolbox (RVT), open-source processing software produced by the Institute of Anthropological and Spatial Studies (https://iaps.zrc-sazu.si/en#v) at the Research Centre of the Slovenian Academy of Sciences and Arts (ZRCSAZU), to help visualize raster elevation model datasets. Sky-View visualizes hillshade models using diffuse illumination, overcoming the common problem of direct illumination, which can obscure linear objects that lie parallel to the direction of the light source and saturation of shadow areas. This brings improvements in detection of linear structures because the method exposes edges and holes (Zakšek and others, 2011). DOGAMI's visualization routine, combining a lidar-derived hillshade, slopeshade, and SVF imagery, helps illuminate shadows and amplifies the edges/ridges related to bedding features. Where possible, aerial photography, combined with a contextual knowledge of the geology of the area, was used to verify bedding features interpreted from lidar.

Orientation points are reported in both quadrant format (e.g., N. 30° W., 15° NE.) and azimuthal format using the right-hand rule (e.g., 330°, 15° NE., American convention). Field-measured bedding is coded by its appropriate Federal Geographic Data Committee (FGDC) reference number for geologic map symbolization. The measured point data are included in the geodatabase, in a separate shapefile named DRBL2020_OrientationPoints, and in Microsoft Excel workbook DRBL2020_DATA.xls (sheet DRBL2020_OrientationPoints). **Table 10-6** describes the fields listed in the spreadsheet. The locations of these point data are given in five coordinate systems: UTM Zone 10 (datum = NAD 27, NAD 83, units = meters), Geographic (datum = NAD 27, NAD 83, units = decimal degrees), and Oregon Lambert (datum = NAD 83, HARN, units = international feet). Strike and dip symbols can be properly drawn by the Esri ArcMap product by opening the layer properties, categorizing by type, choosing the appropriate symbol, and rotating the symbol based on the "Strike_Azi" field. (The Advanced button allows you to select the rotation field.) The rotation style should be set to geographic in order to maintain the right-hand rule property. Azimuths are given in true north; an additional clockwise correction of about 1.6 degrees is needed to plot strikes and dips properly on the Oregon Lambert conformal conic projection in this area. Notes for spreadsheet: nd, no data.

Table 10-6. Orientation points database spreadsheet columns.

Field	Description
Type	Type of geologic structure from which feature was determined – e.g., Inclined bedding.
Azimuth	Strike or trend, measured in degrees clockwise from geographic North. Values limited to range 0-360. Use right-hand rule (dip is to right of azimuth direction). Horizontal planar features may have any azimuth – e.g., 20.
Inclination	Dip or plunge, measured in degrees down from horizontal. Values limited to range -90 to 90. Types defined as horizontal (e.g., horizontal bedding) have Inclination = 0. Null values not Data type=float – e.g., 45.
StrikeQuadrant	Strike direction of the inclined plane, stated in a north-directed quadrant format – e.g., N35E.
DipQuadrant	Amount of dip, degrees from horizontal, with direction – e.g., 45SE.
Symbol	References a symbol in the GeMS style file – e.g., 6.40.
Label	Amount of dip, degrees from horizontal – e.g., 45.
LocationConfidenceMeters	Radius in meters of positional uncertainty envelope for the observation locale. Null values not permitted. Recommended value is -9 if value is not otherwise available.
IdentityConfidence	Specifies confidence that observed structure is of the type specified; e.g., 'certain', 'questionable', 'unspecified'.
OrientationConfidenceDegrees	Estimated circular error, in degrees – e.g., 20.
PlotAtScale	Cartographic map scale or larger that the observation or analysis should be plotted at. Value is scale denominator.
Quadrangle	The USGS 7.5' quadrangle in which the sample is located – e.g., Badger Lake.
Elevation	Elevation of data location in feet – e.g., 22.
MapUnit	Map unit from which the analyzed sample was collected.
UTMNorthingNAD27	Meters north in NAD 27 UTM projection, zone 10.
UTMEastingNAD27	Meters east in NAD 27 UTM projection, zone 10.
LatitudeNAD27	Latitude in NAD 27 geographic coordinates.
LongitudeNAD27	Longitude in NAD 27 geographic coordinates.
UTMNorthingNAD83	Meters north in NAD 83 UTM projection, zone 10.
UTMEastingNAD83	Meters east in NAD 83 UTM projection, zone 10.
LatitudeNAD83	Latitude in NAD 83 geographic coordinates.
LongitudeNAD83	Longitude in NAD 83 geographic coordinates.
Northing83HARN	Feet north in Oregon Lambert NAD 83, HARN, international feet.
Easting83HARN	Feet east in Oregon Lambert NAD 83, HARN, international feet.
LocationSourceID	Unique data source from which the data was obtained – e.g., McClJD2020.
OrientationSourceID	Unique data source from which the data was obtained – e.g., McClJD2020.
Notes	Special information about the point – e.g., lidar derived.
OrientationPoints_ID	Primary key – e.g., ORP001.
PTTYPE	e.g., Bedding
RuleID1	Rule ID used for cartographic representation – e.g., 6.40.

Stations

The stations feature class provides locations for observations made by individual contributors to the geologic map. Station locations are obtained from original annotated topographic field sheets, field notebooks, and digitally collected data. **Table 10-7** describes the fields listed in the feature class.

Table 10-7. Stations database spreadsheet columns.

Field	Description
Stations_ID	Unique alpha-numeric id applied to the station.
FieldID	Identifier assigned by person who originally located the station. Commonly a key to a field sheet and (or) field notebook – e.g., 21 DRBLJ 19.
MapUnit	Map unit from which the analyzed sample was collected.
Symbol	References a symbol in the GeMS style file – e.g., 31.21.
Label	A unique number assigned to the location for cartographic purposes– e.g., G1.
PlotAtScale	Cartographic map scale or larger that the observation or analysis should be plotted at. Value is scale denominator.
LocationConfidenceMeters	Radius in meters of positional uncertainty envelope for the observation locale. Null values not permitted. Recommended value is -9 if value is not otherwise available.
LocationMethod	How the location of the station was determined– e.g., Field located by iPad GPS.
Observer	Person responsible for making the original observation.
GPSX	Feet east in Oregon Lambert NAD 83, HARN, international feet
GPSY	Feet north in Oregon Lambert NAD 83, HARN, international feet.
DataSourceID	Foreign key to DataSources table, to track provenance of each data element.– e.g., McClJD2020b.
Notes	Special information about certain samples – e.g., alteration.

Well Points

The well points spreadsheet is derived from written drillers' logs provided by Oregon Department of Water Resources (OWRD). Well logs vary greatly in completeness and accuracy, so the utility of subsurface interpretations based upon these data can be limited. Water well logs compiled and used for interpretation during this study were not field located. The approximate locations were estimated using tax lot maps, street addresses (coordinates obtained from Google Earth™), and aerial photographs to plot locations on the map. The accuracy of the locations ranges widely, from errors of one-half mile possible for wells located only by section and plotted at the section centroid to a few tens of feet for wells located by address or tax lot number on a city lot with bearing and distance from a corner. At each mapped location the number of the well log is indicated. This number can be combined with the first four letters of the county name (e.g., HOOD 5473), to retrieve an image of the well log from the OWRD website.

Point data are included in the geodatabase, in a separate shapefile named DRBL2020_WellPoints, and in Microsoft Excel workbook DRBL2020_DATA.xls (sheet DRBL2020_WellPoints). **Table 10-8** and **Table 10-9** describe the fields listed in the spreadsheet. The locations of water well point data are given in six coordinate systems: UTM Zone 10 (datum = WGS 84, NAD 27, NAD 83, units = meters), Geographic (datum = NAD 27, NAD 83, units = decimal degrees), and Oregon Lambert (datum = NAD 83, HARN, units = international feet).

Lithologies in well intervals listed in the well log spreadsheet can alternate between consolidated and unconsolidated and may be listed as alternating between bedrock and surficial geologic units. This may occur where bedrock units are soft, where paleosols or weak zones lie within bedrock, or where cemented or partly cemented zones alternate with unconsolidated zones in surficial deposits.

Table 10-8. Water well database lithologic abbreviations.

Lithologic abbreviations (alphabetical by group)

UNCONSOLIDATED SURFICIAL UNITS	
Abbreviation	**Description**
a	ash
bd	boulders
c	clay
ch	clay, hard (often logged as claystone but probably not bedrock)
g	gravel
gc	cemented gravel
gs	gravel and sand (also sandy gravel)
m	mud
s	sand
sg	sand and gravel (also gravelly sand)
st	silt
Rock, sedimentary	
bc	breccia
cg	conglomerate
cs	claystone
sh	shale
ss	sandstone
Rock, igneous	
an	andesite
b	basalt
ba	basaltic andesite
cd	cinders
da	dacite
pu	pumice
gr	granite
l	lava
r	rhyolite
sc	scoria
t	tuff
v	volcanic, undivided
vb	volcanic breccia
Other	
af	artificial fill
cl	coal (lignite)
dg	decomposed granite
o	other (drillers unit listed in notes column of spreadsheet)
rk	rock
sl	soil
u	unknown (typically used where a well has been deepened)

Table 10-9. Water well log database spreadsheet columns.

Field	*Description and Example
Type	Type of well located; e.g., well used for domestic-water supply, well used for irrigation-water supply, drill hole for hydrocarbon exploration or exploitation- Showing name and number.
Symbol	References a symbol in the GeMS style file – e.g., 26.1.25.
Label	A unique label identifying the well, if applicable – e.g., Federal 1-10.
IdentityConfidence	Specifies confidence that observed structure is of the type specified; e.g., 'certain', 'questionable', 'unspecified'.
LocationConfidenceMeters	Radius in meters of positional uncertainty envelope for the observation locale. Null values not permitted. Recommended value is -9 if value is not otherwise available.
PlotAtScale	Cartographic map scale or larger that the observation or analysis should be plotted at. Value is scale denominator.
TownshipRangeSection	Two digits for township, two digits for range, and two for section; negative if township is south of Willamette baseline. Exception for township and range if they contain a decimal – e.g., −2132.503.
County	Hood River County – e.g., HOOD.
Grid	Well log number for wells. Wells in Hood River County preceded by acronym HOOD – e.g., HOOD53799.
WellElevation	Wellhead elevation in feet as given by Google Earth™ at corresponding WGS 84 location. e.g., 1978.
LocatedBy	Google Earth™ elevation for cursor location at a given address – e.g., Google. Google Earth™ elevation at house in vicinity of given address – e.g., House. Pad identifying approximate well location, visible in air photo – e.g., Pad. Approximate taxlot centroid or other best guess for well location using a combination of taxlot maps and aerial photographs – e.g., Taxlot. Owner name – e.g., Owner. Address of well listed on Oregon Water Resources Department (OWRD) Startcard. Wells located by Oregon Water Resources Department (OWRD) using handheld GPS – e.g., OWRD. GPS coordinates of wellhead included with well log – e.g., GPS. Approximate quarter-quarter-quarter section centroid – e.g., QQQ. Approximate quarter-quarter-section centroid – e.g., QQ. Approximate quarter-section centroid – e.g., Q. Approximate fit to sketch map included with well log – e.g., map.
Lithology	Best interpretation of driller's log using abbreviations above – e.g., g.
Base	Record base of driller's interval or, if lithology abbreviation would not change, similar intervals, in feet below wellhead – e.g., 17.
Top	Calculated top of driller's interval or similar intervals, in feet below wellhead – e.g., 14.
TopElevation	Calculated elevation at top of driller's interval, or similar intervals, in feet above sea level – e.g., 86.
BaseElevation	Calculated elevation at base of driller's interval, or similar intervals, in feet above sea level – e.g., 83.
BedrockLithology	Lists bedrock lithologies, when encountered, abbreviations listed above – e.g., b.
BedrockElevation	Calculated elevation at which bedrock or soil over bedrock was first encountered, in feet above sea level – e.g., 1924.
TaxLot	Taxlot number. Where it is determined that a taxlot number is used more than once in the section then the appropriate subdivision of the section is indicated in the notes field – e.g., 800.
Color	Color of interval as reported by the well driller – e.g., green.
MapUnit	Geologic unit interpreted in subsurface based on drillers log and designated by map unit label used in accompanying geodatabase. Intervals labeled "suna" (surface unit not applicable) are those where the lithology as interpreted by the original drillers' log do not correspond; also denotes intervals in the subsurface where a precise unit label cannot be applied – e.g., Tb.
Quadrangle	The USGS 7.5' quadrangle in which the sample is located – e.g., Badger Lake.
UTMNorthingWGS84	Meters north in WGS84 UTM projection, zone 10.
UTMEastingWGS84	Meters east in WGS84 UTM projection, zone 10.
UTMNorthingNAD27	Meters north in NAD 27 UTM projection, zone 10.
UTMEastingNAD27	Meters east in NAD 27 UTM projection, zone 10.
LatitudeNAD27	Latitude in NAD 27 geographic coordinates.
LongitudeNAD27	Longitude in NAD 27 geographic coordinates.
UTMNorthingNAD83	Meters north in NAD 83 UTM projection, zone 10.

UTMEastingNAD83	Meters east in NAD 83 UTM projection, zone 10.
LatitudeNAD83	Latitude in NAD 83 geographic coordinates.
LongitudeNAD83	Longitude in NAD 83 geographic coordinates.
Northing83HARN	Feet north in Oregon Lambert NAD 83, HARN, international feet.
Easting83HARN	Feet east in Oregon Lambert NAD 83, HARN, international feet.
LocationSourceID	Unique data source from which the data was obtained – e.g., OWRD2020.
WellSourceID	Unique data source from which the data was obtained – e.g., OWRD2020.
Notes	Notes about the stratigraphic interval as originally described by the well driller or observer.
WellPoints_ID	Primary key – e.g., WLP593
PTTYPE	e.g., Water Well, Oil and Gas.

*Well location given in six coordinate systems calculated by reprojecting original WGS 84 UTM, zone 10 locations.